VDI

K

KUNSTSTOFFTECHNIK

Plastics in Automotive Engineering

KUNSTSTOFFTECHNIK

Plastics in Automotive Engineering

Herausgeber: VDI Wissensforum GmbH
VDI-Gesellschaft Materials Engineering

Bibliographische Information der Deutschen Bibliothek
Die Deutsche Bibliothek verzeichnet diese Publikation in der Deutschen Nationalbibliographie; detaillierte bibliographische Daten sind im Internet unter http://dnb.ddb.de abrufbar.

Bibliographic information published by the Deutsche Bibliothek
(German National Library)
The Deutsche Bibliothek lists this publication in the Deutsche Nationalbibliographie (German National Bibliography); detailed bibliographic data is available via Internet at http://dnb.ddb.de.

Printed in Germany

ISBN 978-3-18-234343-1

Foreword

In current new automotive developments the focus today is on topics such as lightweight design, resource efficiency, user benefits, aesthetic appeal as well as active and passive safety. Engineering plastics, fiber-reinforced composites and hybrid plastics technologies play an important role here as pacesetters.

In many cases, multifunctional tools and automated processing make system solutions possible which are of particular interest from the commercial point of view. New kinds of additive manufacturing processes already have a great potential for making individual, tailored component designs a reality, especially in low-volume production.

Innovations in plastic technologies have a direct influence on future concepts in the automotive field. Multimaterial design, hybrid solutions, flat heating systems for electric vehicles, in-mold laminated parts, laminated exterior components, and also plastic-based luminescent films and background lighting - these all make possible the delivery of customized system solutions in passenger car and commercial vehicle construction and thus in the long term secure international competitiveness in the plastics and automotive industries.

On 9th and 10th March 2016 in Mannheim the Association of German Engineers is hosting the international plastics conference ‘Plastics in Automotive Engineering 2016’. Strategic overview papers from research and the market, technical reports from the passenger car and commercial vehicles sectors concerning plastics innovations, as well as practical reports from the plastics processing sphere deliver detailed information about the state of the art in plastics technology in automotive engineering. A technical exhibition by plastics producers and machine manufacturers as also an accompanying auto show with the latest cars and commercial vehicles allow attendees to discuss technical points at the physical object itself.

We cordially welcome you to Mannheim!

Prof. Dr. Rudolf C. Stauber

Table of Contents

Structure

Simulation

Engine & Technics

Material & Technology

Lightweight Design

Industry 4.0

Plenary Session

Framework Conditions for Plastic Applications

Cost Efficient Lightweight Design

Plastics in the Chassis

Framework Conditions for Plastic Applications

The lightness of design

Potential of lightweight design for structure and surfaces in architecture

Prof. Dr.-Ing. **G. Henn**, Henn GmbH

Abstract

- Monocoque construction as space-creating shell
- Structural framework and surfaces in high-rise construction
- High-rise structures based on minimal surfaces

‘Monocoque construction as space-creating shell’

The Porsche pavilion in motor city Wolfsburg

Lines and curves make the pavilion a dynamic and trimmed sculpture whose characteristics derive from the brand image of the vehicle manufacturer. Uniform, matt stainless steel sheets wrap the body shell seamlessly. In a similar way to monocoque design, which is used in lightweight construction in the automotive and aircraft industries, the space-creating shell of the building takes over the load-bearing function. A total of 620 stainless steel covering sheets with welded-on stiffening ribs were prefabricated in a shipyard in Stralsund and assembled on site.

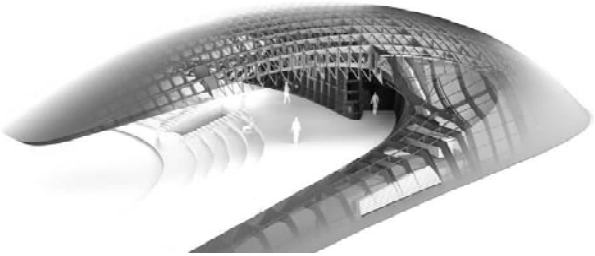

‘Structural framework and surfaces in high-rise construction’
The Haikou Tower, Hainan

The 450 meter high Haikou Tower is to become the heart of the new business district of Haikou, on Hainan island in the South China Sea. The shape and structure of the tower are directly influenced by the spatial requirements of the program. The office space in the lower part should be flexible and generously dimensioned while the hotel rooms in the upper part should give an unobstructed view to the outside. The reinforcing structure clearly shows the connection of program and structural framework. Furthermore, the total height of 450 meters also requires an intelligent, high-performance adaptive façade design which reacts to changes in sunlight depending on the orientation of the façade.

‘High-rise structures based on minimal surfaces’
DRX Design Research Exchange

Minimal surfaces, abundant in the natural world, have an enormous potential for use in the design of high buildings since they integrate structure, material and form. These factors mean that structures based on minimal areas can represent a serious alternative to the usual sustainability concepts.

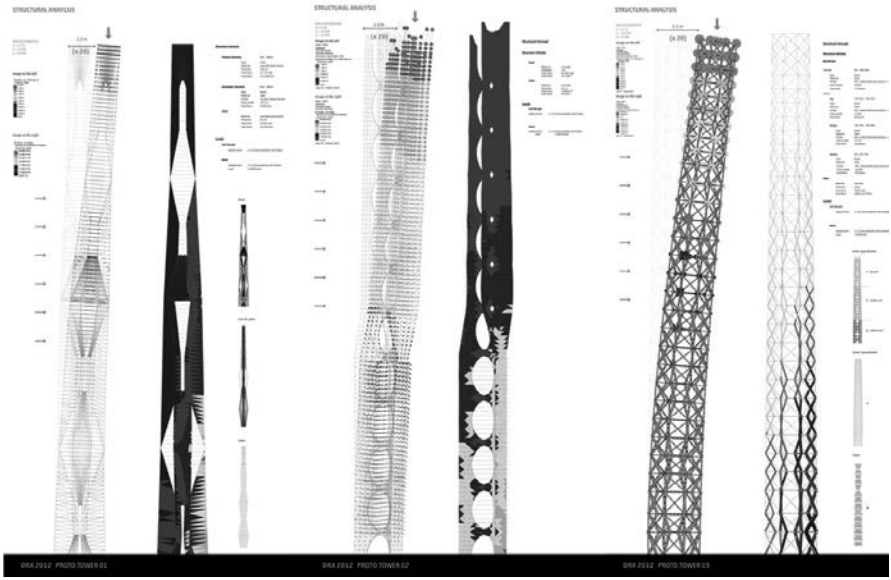

Challenging surfaces and lightweight construction in the instrument panel of the new Volkswagen Tiguan

Dipl.-Wirtsch.-Ing. (TU) **R. Mielke**, Dipl.-Ing. (FH) **P. Dierks**,
Volkswagen AG, Wolfsburg

1 Introduction

The first generation Volkswagen Tiguan is a huge success with over 2.8 million vehicles sold since production started in 2007. According to Volkswagen forecasts the compact SUV segment will continue to expand throughout the world in coming years. There are therefore great expectations of the new Tiguan which was presented to the world public at the IAA in 2015. It is the first SUV in the Volkswagen Group on the modular transverse matrix (MQB) platform. To achieve these ambitious goals, high demands were made of the development of the instrument panel of the new Tiguan. Alongside the aspects of safety, ease of use and quality, this also affected the aspects of surface appearance and lightweight construction with a high level of cost consciousness to be maintained. During the development of the new Tiguan, a number of new technologies and concepts were developed and successfully implemented in series production.

2 Best-in-class surfaces

2.1 Technical grain

Currently, reproductions of real leather – so-called leather grains – dominate in the surface structures of plastic components in the interior of the vehicle. Hide as a natural product has an irregular surface structure. It is therefore insensitive to surface disturbances, such as unevennesses in plastic components. Geometrically oriented surface structures, which are referred to as technical graining, do not have this advantage since their trend is homogeneous. Deviations from the regular structure are perceived more easily by the human eye which means that unevennesses arising from the production process are noticed more quickly. For this reason the oriented surface structure is used only with the very highest development and production accuracy. To underline the existing quality appeal of the instrument panel of the new Volkswagen Tiguan, the front section has now for the first time been given a technical grain as the surface structure.

The dimples on the surface of a golf ball served as the model in selection of the graining. Just as the dimples markedly improve the aerodynamics of a golf ball, so does the technical

graining emphasize the design language of a 'dynamic instrument panel'. In addition, a golf ball embodies not only sportiness, precision and quality but also technical attributes such as robustness, strength and stability. The new Tiguan stands for these properties.

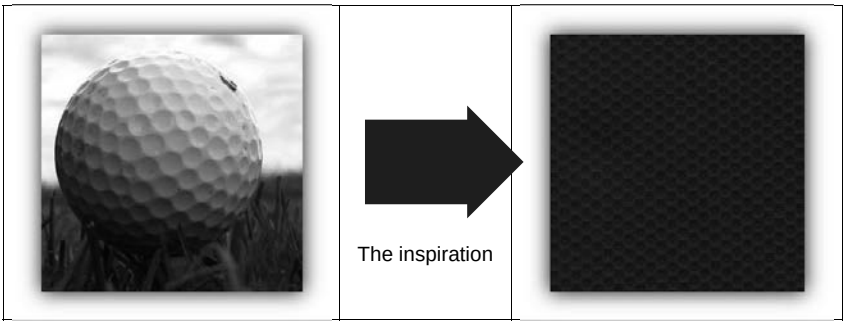

Fig. 1: Inspiration for the graining

2.2 Laser graining

The classic way of reproducing a grained structure on the instrument panel is by means of the so-called leathering model. This is an aid for creating the electroforming shells, the tooling for producing the skin of the instrument panel. Here the model is manually covered with a synthetic leather having the desired grain structure (Figure 2).

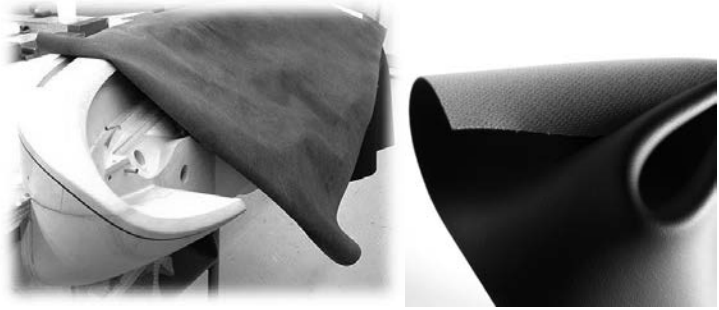

Fig. 2: Covering the leathering model with a sheet of synthetic leather

The master model is prepared via a molding process with a negative. The master model is the reference part and thus the basis for all subsequently generated electroforming shells used in series production of the instrument panel skin (Figure 3).

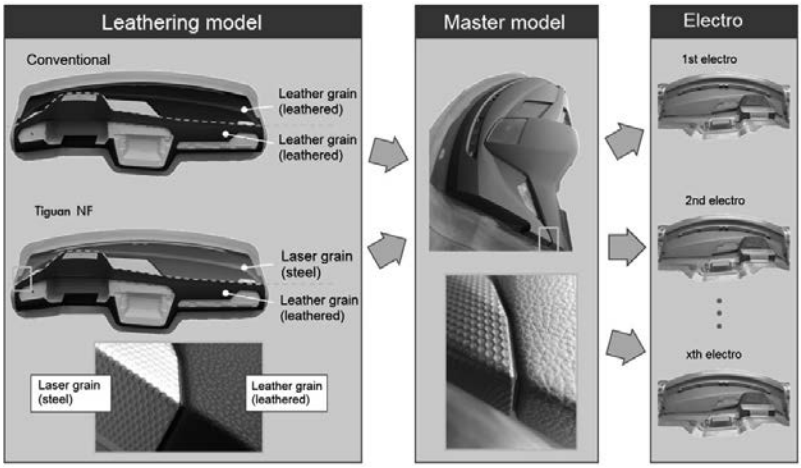

Fig. 3: Process steps with the leathering model up to electroforming

A laser is used to apply the technical graining to the front section of the instrument panel of the new Tiguan. Lasering is not carried out on the component itself nor in the mold but rather on part of the leathering model, the steel core. Here the leathering model was divided into the section covered with a leather grain and the section with the laser grain. The laser grain was cut into the milled steel insert by a five-axis solid-state laser. The insert is later married to the leather-covered part to form the finished leathering model. Since the two grained sections close directly on each other there is no need for the classic graining blank at the parting line. This generates new degrees of freedom in the styling of the transition areas.

Laser graining has several advantages over a classic molded grain.

Mapping process

When the model is leathered off-reel, the graining orientation can only follow the direction of rotation of the reel. It is not possible to make adjustments to a specific design geometry. The result is that unwanted effects such as stretching occur at edges and joints.

With laser graining, on the other hand, adjustments to the contours of the component are possible. This is done with the mapping process. The orientation of the surface structure is designed in the virtual environment before being applied to the steel insert. The precise geometric structure of a technical grain is adjusted and modeled such that it is optimized to individual edges below the threshold of visibility. The aim here is to obtain a harmonious edge line. In the new Tiguan this was done as shown in Figure 4. Another advantage of the mapping process is the possibility of virtual proving with oriented real surface structures.

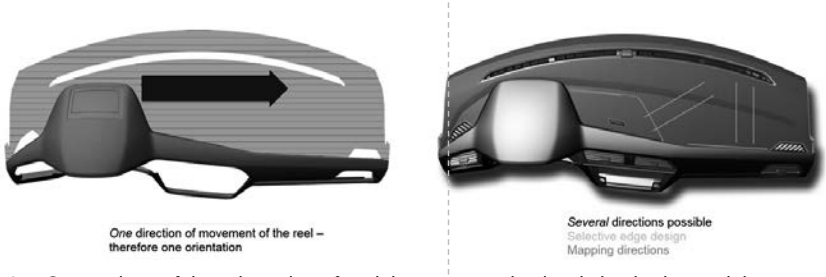

Fig. 4: Comparison of the orientation of graining structure in classic leathering and the mapping process

Flattenings

To avoid sawtooth effects on tight radii, in the laser graining process the grain depth and grain form can be adjusted to the local situation. For example, with convex curves and sharp angles the grain depth can be adjusted steplessly for individual areas without taking depth or character away from the graining (Fig. 5).

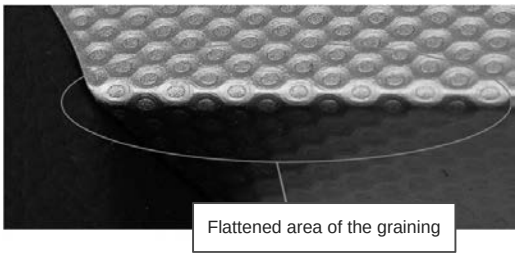

Fig. 5: Grain flattening

Precision

Etched grains work with a low single-figure number of layers during texturizing. Depending on the process, edges are rounded off by the etching. The laser graining process on the other hand does not require any large radii and thus allows for an unimpeded design. The individual structure of the laser grain can be created with distances of 3 µm between the layers. The high double-digit number of such layers makes it possible to give the laser grain a high degree of texturizing precision and a striking surface.

2.3 HUD cover

The new Tiguan is the first compact vehicle of the Volkswagen Group to offer a head-up display (HUD). Important information, such as alerts, driving data and route information, is projected via multiple mirrors into the driver's field of vision in such a way to give an impression that the image is about 2 m in front of the vehicle. This is another important contribution to more safety and more comfort. The last mirror, the projection unit called the combiner, can be lowered into the control panel when not in use. For this, the instrument panel has a motor-driven plastic cover which completely closes off this area, thereby providing protection against dirt and damage. When the HUD is in use, the cover retracts into the scoop in the instrument panel. For this it makes perfect use of the restricted installation space available. The HUD including the movable cover is integrated into the instrument panel architecture while ensuring existing functionalities, such as crash behavior, component stability under all climatic conditions, and passenger-compartment and glazing ventilation, are not impaired. This challenge was mastered without changing the structure of the instrument panel and the components base, air ducts and instrument-panel carrier remain common to the basic variant without the HUD option. The result is a Group module which reduces investment and enables popularization of this new HUD feature even when low numbers are installed in each vehicle project.

A key driver in the development of the cover was the desire for the instrument panel to have a harmonious surface without any disturbing surface projections or recesses when the head-up display is not in use. In addition to the aesthetic advantage, this reduces annoying reflections in the windshield in unfavourable light conditions. For this, the cover size, the width of the external frame and the joint dimensions were optimized. The cover is integrated into the control panel in such a way that the cover is invisible to the driver and the cogency of the design language is thereby underlined.

The head-up display cover consists of the components shown in Figure 6. Motor-driven on one side, an axle transfers force via two gearwheels to two toothed cams, one on each side of the cover. The cover moves with correct aligment since it is driven on both sides and is thus prevented from tilting in the guide tracks. The double-sided drive thus makes minimal expansion joints possible. The two plastic gearwheels and parts of the plastic rack are of involute form. This permits a minimal backlash and minimizes noise when the cover is moving.

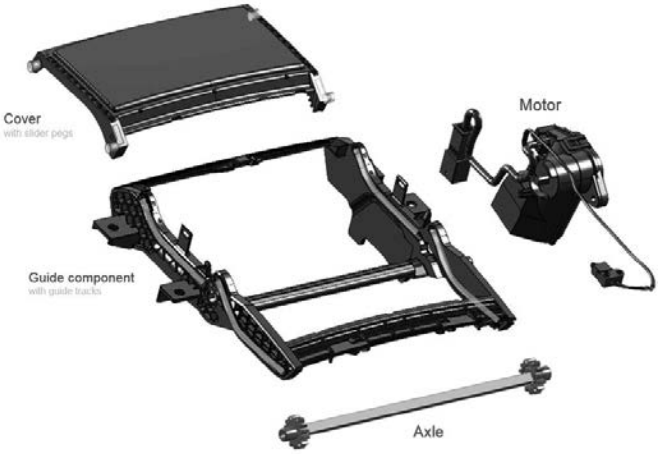

Fig. 6: Exploded view of the HUD

To ensure lack of problems in use, four different plastics are used in the cover, with each one perfectly matched to its task. The guide component, designed to be torsionally resistant over all temperature ranges, is the interface with the instrument panel and accommodates the movable cover. For these reasons, it is designed as a two-component (2K) part. For the first material component the selection fell on glass-fiber-reinforced polycarbonate / acrylonitrile-butadiene-styrene (PC/ABS). The highest requirements apply to the cover guide tracks as regards rigidity, dimensional stability even under climate influences, friction and wear resistance. For this reason, as the second material component polybutylene terephthalate (PBT) is used for the cover guide tracks. In addition to the requirements just mentioned, special requirements also apply to the movable cover. Since this component is in the visible area it must fit into its environment with visual harmony and with little reflectiveness when sunlight falls on it. It is therefore also designed as a two-component part. The main component is a

coated PC/ABS. The slider pegs which engage in the guide tracks in the guide component must be specially adjusted to requirements and have a low coefficient of friction and a high abrasion resistance. For this reason, polyoxymethylene (POM) was selected as the second material component for the cover.

3 Innovative lightweight construction in series production

3.1 Integrated passenger airbag

Lightweighting concepts suitable for high-volume production are used in all areas of the instrument panel of the new Tiguan.

The first major pillar of lightweighting development is the design of that part of the instrument panel environment concerned with the passenger airbag. Here the central element is the airbag deployment channel. Its tasks include a secure fastening of the airbag module and reliably guiding the airbag in the event of airbag deployment. The airbag deployment channel is thus the interface with the airbag aperture in the instrument panel. These tasks must be executable over the lifetime of the vehicle and under all extreme weather conditions.

In the evolutionary process from a multi-part metal deployment channel, to a separately welded-on plastic deployment channel in the new Tiguan, 650 g in weight has been eliminated since the last vehicle generation. Figure 7 illustrates the various stages of weight reduction coupled with simultaneous process simplification and reduction in the number of parts.

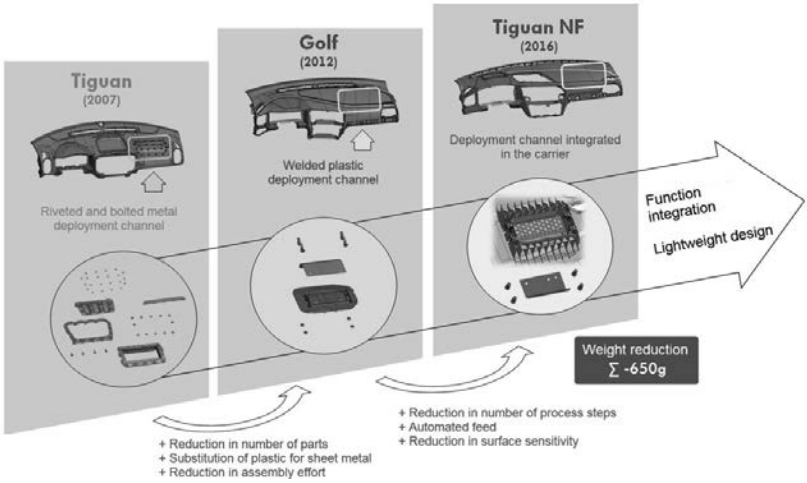

Fig. 7: Evolution of the airbag deployment channel

In the current stage of evolution, the formerly separate plastic deployment channel is integrated into the foam carrier to form a single component. Here a component with high crash requirements is fitted into the flat component. Due to the distribution of the plastic melt between these two areas, warp-free injection molding is the special challenge. This calls for a needs-oriented design of the functional elements of the deployment channel. Greatly stressed areas in airbag deployment are reinforced by a precisely designed ribbing package in such a way as is required by the various local stresses. With the aid of FEM analyses, sections of the now integrated deployment channel geometry could also be reduced with weight optimization. Development of the gating and cooling channel system was carried out in parallel with this load-oriented designing of the component. The component geometry of the integrated plastic deployment channel has thus been designed with due regard to loading and production requirements.

The foam carrier of the instrument panel is made of glass-fiber-reinforced polypropylene and is physically foamed with the aim of lightweighting. To do so, a quantity of nitrogen is input into the plastic melt during the injection-molding process. Alongside weight reduction, this method offers advantages since it is possible to dispense with the classic holding pressure. This gives the component a high dimensional stability and reduces the tendency to warp.

In addition to the lightweight effects we have mentioned, the integrated plastic deployment channel system results in a marked simplification or reduction in process steps as compared with the predecessor model and yields benefits in the competitive arena. The airbag module of the new Tiguan is fastened into the integrated deployment channel system with the aid of metal bushings inserted in the mold and directly overmolded. From a number of bolted, riveted and welded parts made of metal we now have a single component with its attachment elements directly integrated by being inserted and positioned in the injection mold.

3.2 Lightweight design of one-piece base bodies

Alongside the integration of the airbag deployment channel in the foam carrier of the instrument panel, the use of a one-piece base body is decisively responsible for the lightweighting effect. The previous series-production concept has a two-part structure with three additional air duct components which need to be welded just as the two structural components do. Here the air guides for the air vents are separated from the structure and take the form of separate air ducts made of polyethylene (PE) foam. The concept development of the old and new Tiguan models are compared in Figure 8.

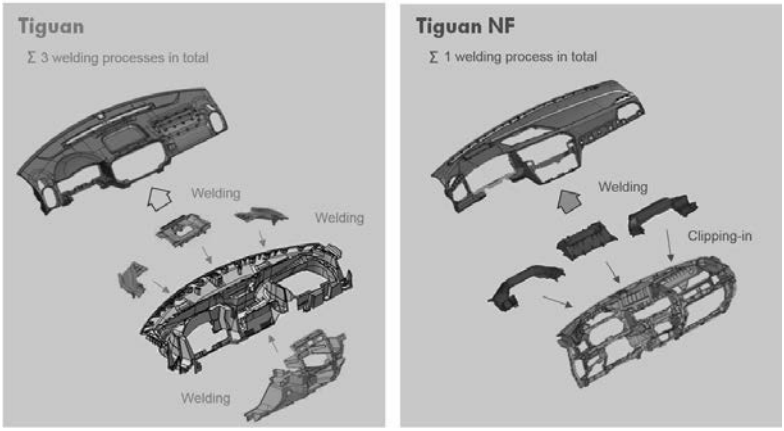

Fig. 8: Comparison of the base body concepts

One special challenge was the tooling design with the demolding vectors arising from very different functional requirements. These different requirements derive from requirements re-

lating to pedestrian protection, ease of assembly, windshield defrosting, accommodation of infotainment devices, and the mounting of further add-on parts, such as glove boxes. By using the most varied concepts for splits, all technical requirements were satisfied and implementation for large-scale production assured (Figure 9).

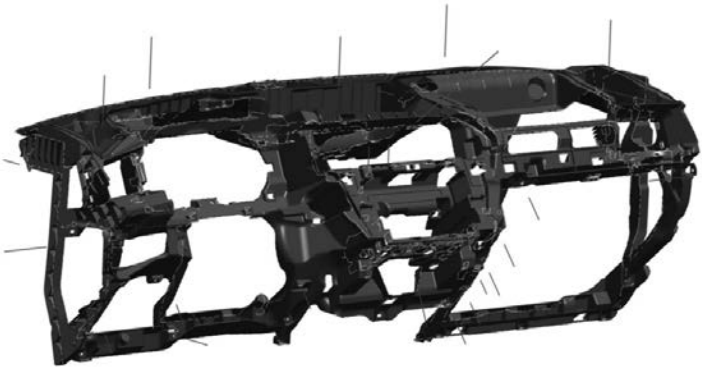

Fig. 9: Split orientations in the base body

The use of expanded foam ducts also had a positive effect on vehicle acoustics. In comparison with conventional injection-molded parts, the foam ducts showed considerable improvements in losses due to air leakage and in sound absorption. In addition, the required cross-sections can be increased by an optimized utilization of installation space in comparison with injection-molded parts, this being in the interest of customer benefits. The overall design of the base body including the foam air guides unifies innovative lightweighting with the simultaneous integration of additional functions.

3.3 Reduced-density spray skin

The third pillar of lightweight design of the new Tiguan instrument panel is the material and the production process of the skin as surface of the instrument panel.
The surface is formed by a three-layer composite of foam carrier, polyurethane foam and skin. This construction for an instrument panel soft to the touch is in the classic case often made from a polyvinyl chloride (PVC) slush skin or polyurethane (PU) spray skin as the top layer. Here the top skin layer is a single-layer film about 1.0 - 1.5 mm thick. The new Tiguan

has a PU spray skin as the instrument panel film. The wall thickness can be partially reduced by the spraying process in the production of the PU film and thus set selectively according to requirements. This results in weight being saved in comparison with a PVC skin, which for production reasons necessarily has a constant wall thickness and whose minimal thickness as defined by the relevant location must be applied to the entire component. With the spray skin, in contrast, the wall thickness can be increased locally at critical points or areas under special stress. This improves the inherent rigidity and contour accuracy of the skin which renders the use of additional measures such as inserts and wire frames superfluous. The result is a further reduction in weight. In the case of the new Tiguan, the PU spray skin has two layers. The top layer consists of an aliphatic polyurethane. This layer is characterized by having not only good weather resistance and resistance to UV radiation but also good tearing-open properties in the event of airbag deployment. Located out of sight beneath this layer is a foamed aromatic polyurethane layer. The job of this second PU layer is to support the top layer when it is under mechanical stress. At the same time the density has been reduced, thereby yielding another weight saving (cf. Figure 10).

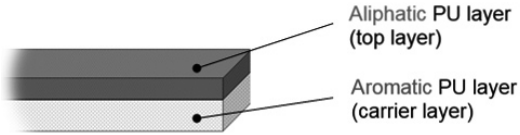

Fig. 10: Structure of the PU spray skin in the new Tiguan

4 Summary

The instrument panel of the new Tiguan opens up new pathways in the field of surface appeal and lightweight design. By using laser graining to reproduce a geometric technical surface structure it has been possible to put an innovation into practice in automotive large-scale production which offers new possibilities in freedom of design and in precision. The kinematics of the head-up display cover have made a harmonious surface possible for the instrument panel. The lightweighting measures implemented in the instrument panel of the new Tiguan have resulted in a weight saving of over 2 kg compared to the predecessor model. A major contribution is made here by the integration of the airbag deployment channel, concept modification of the carrier structure with air guides, and the selection of the surface skin.

3D simulation for lightweight construction in the plastics processing industry

Dipl.-Ing. **M. Kurz**, SimpaTec GmbH, Reutlingen

Abstract

The eyes of the automotive industry are very much focused on the year 2020.

The EU has committed itself to reduce greenhouse gas emissions by then by at least 20% compared to the year 1990. Since road traffic makes up a good quarter of all CO_2 emissions, this means a special responsibility lies in this area. Cars account for almost half of road traffic emissions.

This aspect provides the automotive industry with a significant challenge. On the one side it is to be countered by new, more efficient technologies, more efficient designs and lower weight.

In the context of weight reduction, the subject of plastics plays a major rôle in many places. This might be in replacing metal castings by short-glass-fiber-reinforced components but here so-called special processes are also increasingly playing an important part.

Two processes, RTM and physical foaming – in its most widespread form the so-called MuCell® process – have in particular made their mark in recent years.

Injection stands at the center of the RTM process. Since the most varied materials and the most diverse injection strategies are used, the problems are also of a multifarious nature. These problems, as was so often the usual way in the past, can be identified by trial and error and then the appropriate countermeasures taken. Today, however, the development engineer and plastics processor have a more reliable and more effective tool available in the form of 3D process simulation. With 3D simulation, aspects such as dry spots and race-tracking can be modeled even in advance.

In the case of reactive systems, simulation also delivers findings with regard to filling problems resulting from an excessively advanced reactivity. In addition, the warpage to be expected can also be calculated. Alongside fiber orientation and reactivity, thermal aspects are also taken into consideration here.

The challenges of foaming are very strongly influenced by the question of cell density distribution and cell size distribution. Even these aspects can be covered today via 3D simulation and thus identified at an early stage by the user and possibly manipulated.

However, a process-optimized product does not represent the completion of development. Local material properties, such as fiber orientation, porosity (during expansion), temperatures, pressures and many more besides can be input into the FEM simulation via the corresponding interfaces. This is used not only for a more precise design of the products but also counteracts the aspect of overdimensioning.

This paper gives an overview of current simulation possibilities and by means of examples even their limits in the topic areas mentioned are outlined.

1. Resin transfer molding (RTM

Alongside the classic methods of draping by hand and spraying, RTM also belongs to the LCM (liquid composite molding) group of processes.

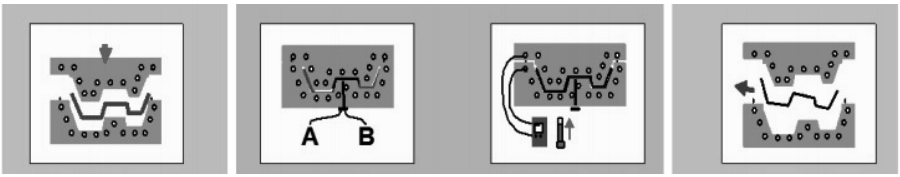

Fig. 1: Schematic representation of the RTM process

In addition to the classic RTM method there are also variants such as VARTM (vacuum-assisted RTM), in which resin infiltration is optimized with the help of vacuum technology, and CRTM (injection-compression RTM), in which the mold is slightly open during resin infiltration and a compression stroke follows.

What all these methods have in common is that dry mats are impregnated with a liquid matrix. In this way high-performance composite components can be produced.
The methods are finding their way into the automotive industry and the demand for simulation tools capable of designing for these new processes is also increasing.

With the full 3D capabilities of Moldex3D it is possible today to simulate the process variants used in practice and for this various control options are available:

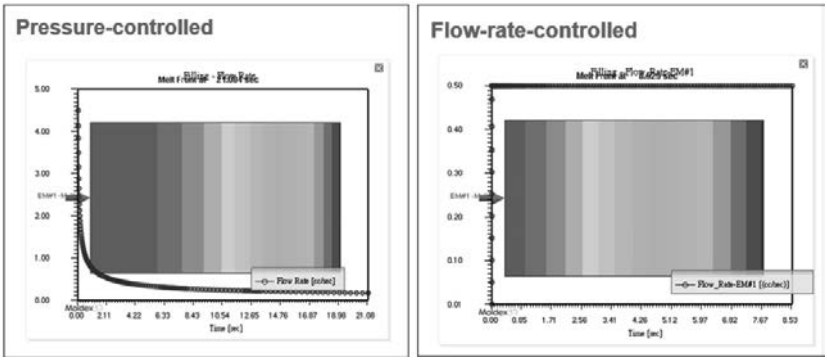

Fig. 2: Filling control variants

The necessary control modes are also available for simulating multi-inlet components (cascading or simultaneous):

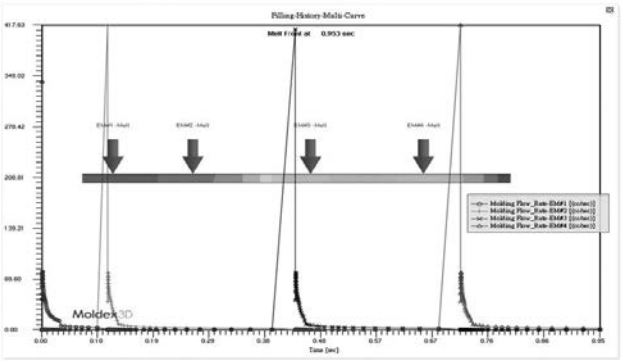

Fig. 3: Multi-inlet control

An optimum flow pattern for an RTM component is achieved not only by the right control of the injection points but the selective use of venting areas in the molds also has a great influence on the course of the flow front.

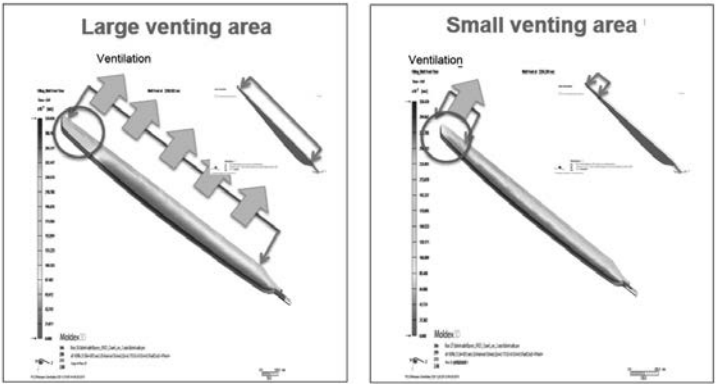

Fig. 4: Venting simulation

To achieve the desired properties of composite components, the fiber mats are aligned very specifically to the loading conditions in the workpiece. The permeabilities of these mats differ according to orientation and this in turn has a major influence on the filling process for the components.

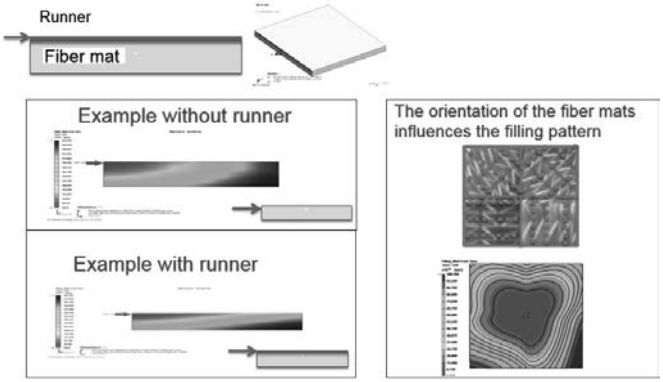

Fig. 5: Influence of fiber orientation

The simulation approaches available in Moldex3D can be used not only in the field of technical RTM components but also right up to large components in automotive bodies or shipbuilding.

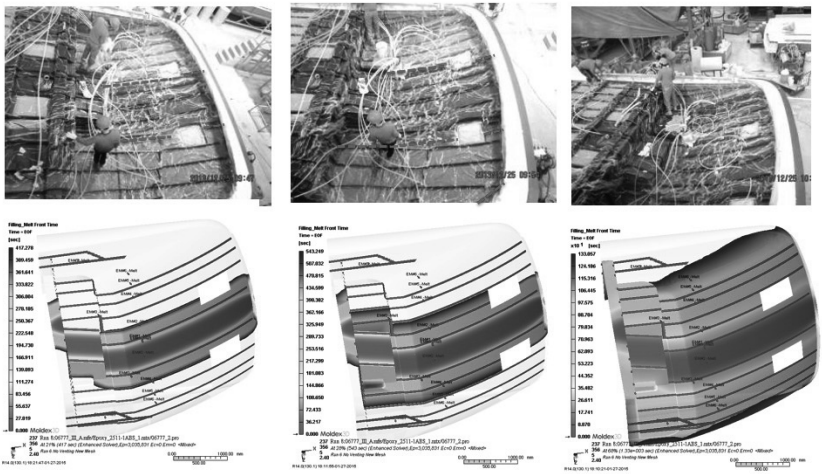

Fig. 6: Example of RTM application

2. Physical foaming

Due to functional elements and the rigidities required, injection-molded technical components often have marked differences in wall thickness. These areas of different thickness are very critical not only in the production process but also with regard to surface quality, not to mention the component weight.

There are various approaches to reducing sink marks, optimizing wall thicknesses, and making components lighter.

Well-established on the market are physical foaming applications (for example, the technologies of the Trexel company) in which a supercritical fluid in the melt is brought into a phase which subsequently in the cavity by expanding cells compensates for the pressure drop caused by volumetric shrinkage.

This creates typical structures in the components.

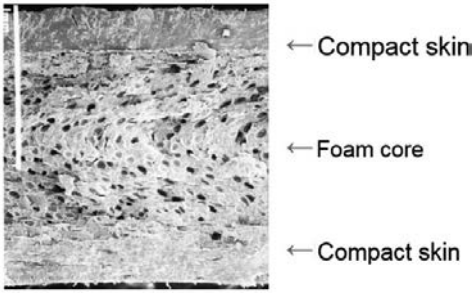

Fig. 7: MuCell® foam structure in the component

Moldex3D provides a full 3D simulation approach for designing components and tooling for this special process.
With the help of nucleation models, simulation results are obtained for cell density distribution in the components.
Cell growth models make it possible to predict the expected cell sizes in the various areas of the component.

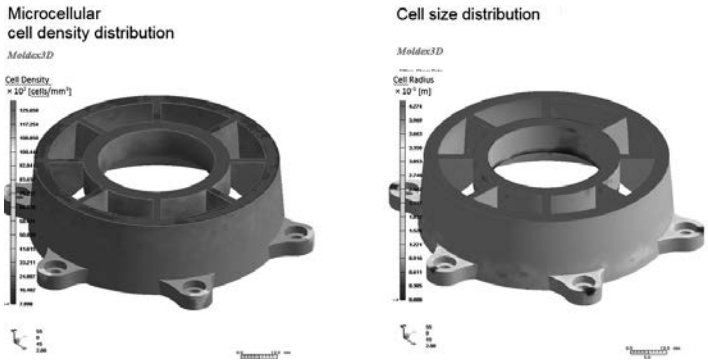

Fig. 8: Cell density distribution and cell size distribution

For further optimization of quality in MuCell® applications, a whole series of combined processes have been established which can also be mapped in Moldex3D.

In special applications it makes sense that despite the expansion in the cavity a classic holding pressure should be maintained via the injection unit for a specific period of time. This can also be simulated.

To reduce premature expansion at the flow front during filling, applications with gas back-pressure have been implemented in practice:

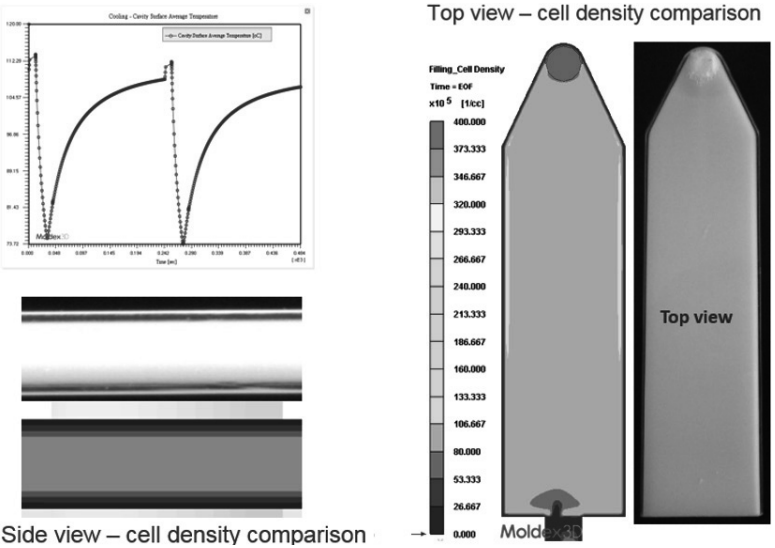

Fig. 9: Comparison of gas back-pressure in simulation and in practice

Another commonly used way of minimizing foaming during filling are applications with core-back strokes. Here a simultaneous expansion of the component at the parting surface is controlled via a short opening stroke in the mold.

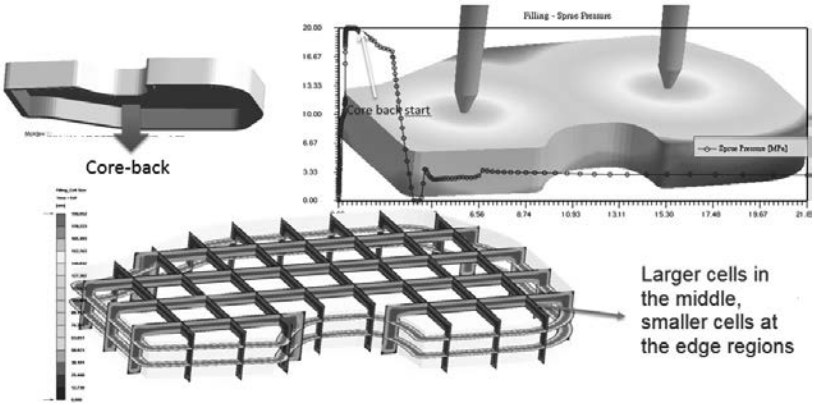

Fig. 10: Result following a core-back stroke

All these variations can then be subsequently further combined with the numerous possibilities of simulating variothermal processes available in Moldex3D.

3. Optimization of process, tooling and component

In addition to the use of latest manufacturing technologies, simulation methods also support classic optimization approaches on the side of constructive component design.

By a rigorous implementation of component design appropriate for plastics, an optimized tool design and process simulation running in parallel with design work, completely new roads can be taken in plastic components due to the possibilities of functional integration. Here it is not only component weight which can be saved but also entire components in the module can be substituted via holistic approaches – and this is reflected in considerably more efficient production processes.

Let us take as an example here a process of the EuWe Group International company in which their reworking of the Golf center console meant that one component and thus a complete production step could be eliminated.

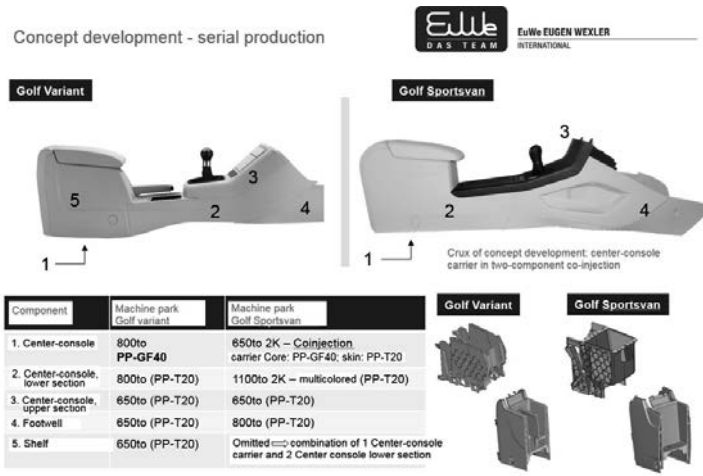

Fig. 11: Reworking of the center console

The substitution of a separate storage compartment has been made possible by producing a carrier (glass-fiber-reinforced polypropylene) in which the outer skin / visible side of the storage compartment (talc-reinforced polypropylene) in the case of the analog component can be created by co-injection with the same mold.

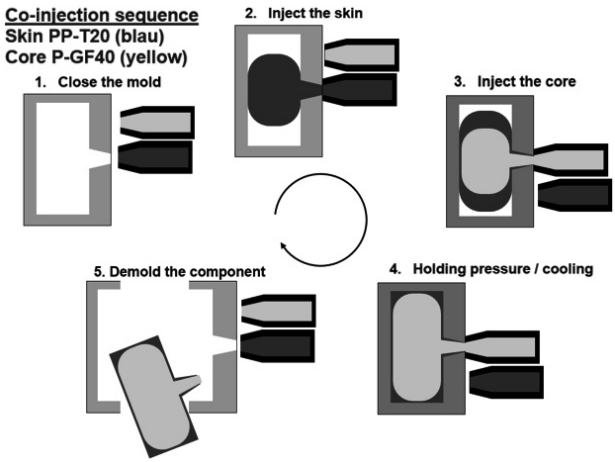

Fig. 12: Co-injection sequence

Simulation was used to carry out the complex identification of the optimum injection point by which the right thickness of the skin material is guaranteed at all parts relevant to visibility and simultaneously also the right wall thicknesses of the core components for mechanically stressed areas.

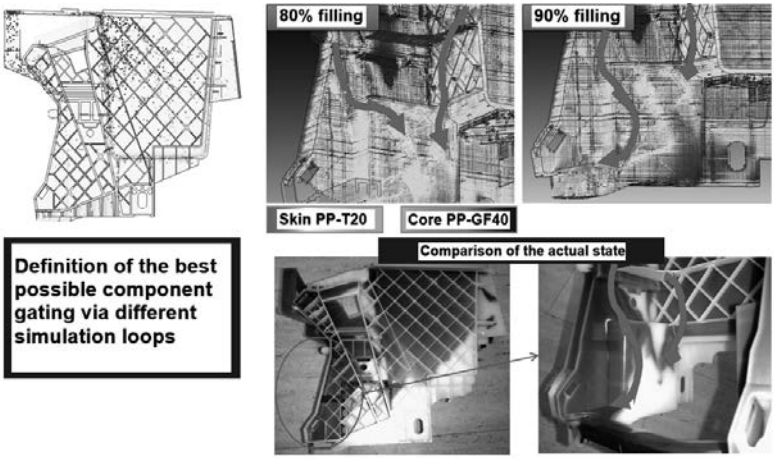

Fig. 13: Co-injection simulation

4. Interfaces with FEM simulation

In addition to the design methods and special procedures described, Moldex3D offers a whole series of further add-ons by which processes in addition to classic injection molding can be evaluated by simulation.

All these simulation capabilities offer a deep insight into what is happening within the component and even the mold. This results in a variety of production-specific product properties which previously were not or only very partially taken into consideration in classic FEA.

These include, for example, in a great measure information about orientations in fiber-reinforced components. Depending on the component geometry, the injection point and the kind of plastication, great differences may arise here which manifest themselves in markedly anisotropic component properties.

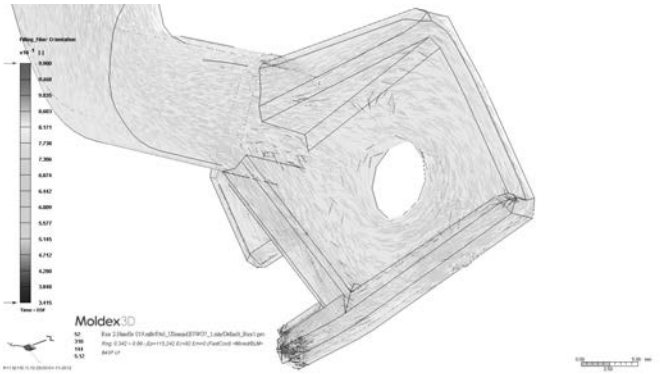

Fig. 14: Example of fiber orientation

To calculate these effects, a fiber model with tags was developed in Moldex3D which permitted a realistic simulation of the fiber orientation.

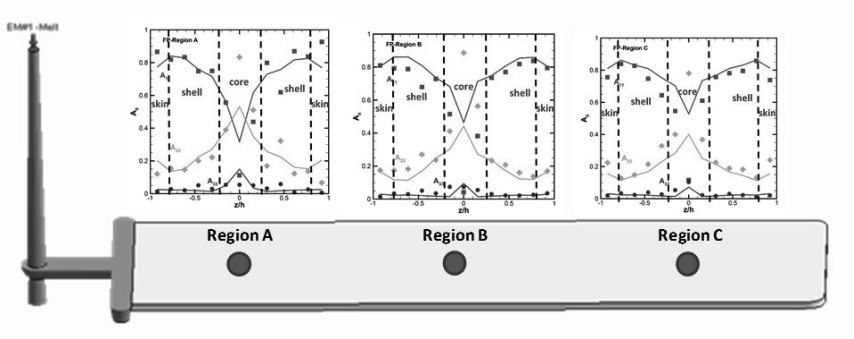

Fig. 15: Evaluation of the fiber model

The possibilities are not restricted solely to orientation but even fiber concentrations / fiber separations and fiber fracture can also be calculated – the last aspect not exclusively within the mold but also during plastication.

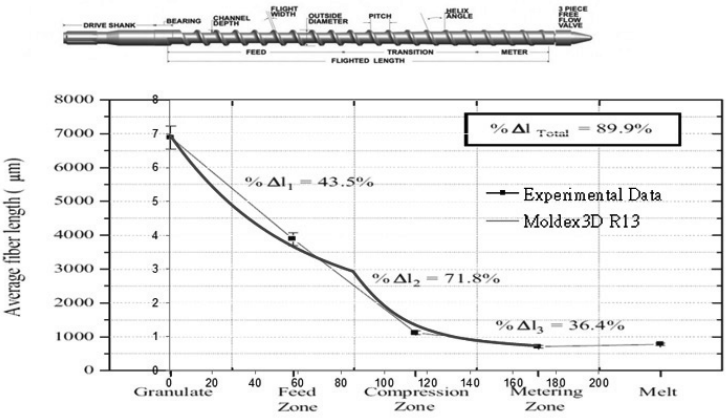

Fig. 16: Decrease in fiber length during plastication

All of this information, including temperatures and stresses can be transferred via FEA and micromechanics interfaces to standard tools (Ansys, Abaqus, Dyna, Pam, Marc, Radioss, and Nastran).

As regards special processes, it is even possible in Moldex3D to make information about the resulting porosity of foamed components available to structural FEA with the aid of Digimat.

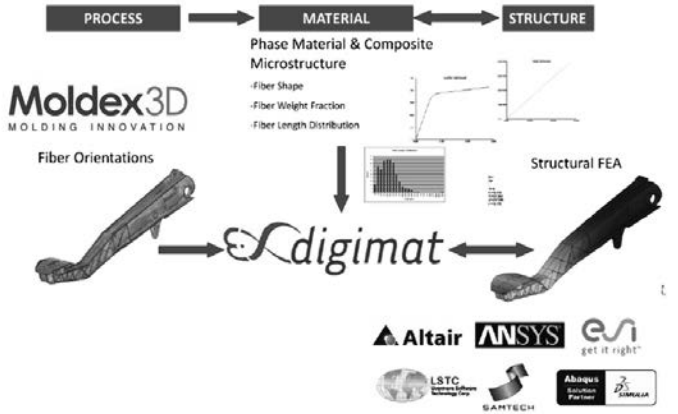

Fig. 17: Process simulation - material modeling - structural mechanics

Innovative PUR surfaces – self-healing and more

Dr.-Ing. **I. Kleba**, **J. Emig**,
Rühl Puromer GmbH, Friedrichsdorf

Abstract

With puroclear® a new generation of PUR coating materials has been developed for the vehicle interior and successfully introduced onto the market, such as in the fine-wood steering wheel of the new Mercedes S-Class. puroclear® distinguishes itself firstly by having adjustable self-healing properties which offer a considerable increase in suitability for everyday use. The creation of permanent scratches is significantly minimized. And who isn't annoyed at the sight of the first scratches? Secondly, puroclear® convinces by other benefits such as in particular in-mold release during processing and low processing temperatures, which also deliver economic advantages over conventional technologies. puroclear® is thus ideal for fine-wood components in the vehicle interior. Coating takes place by the RIM process, either by flooding a prefabricated carrier component or in the form of an integrated process with injection molding. For components in the piano-black look this last offers an interesting alternative to cost-intensive painting, both for purely decorative parts and even for complex trim panels in the center console area. However, even functional components, for example, with integrated switches and / or backlit elements, are possible as various studies have shown. Furthermore, developments with a medium- to long-term focus are underway whose aim is to make the benefits of puroclear® accessible even to exterior applications - up to and including bionic functional surfaces.

1. We as consumers - the rift between premium aspirations and disappointment

As consumers we really are a very special kind of species. On the one hand we allow ourselves to be easily seduced by glitz and glamor and when buying a car reach for cars with high-gloss equipment elements. On the other hand, we are actually at the same moment also fully aware that it is precisely surfaces of this type which are more likely to be vulnerable, for example, to being scratched in everyday service by rings, keys, and zippers or by our children playing. When we make our purchasing decision, we all too readily suppress such thoughts in favor of a more or less pronounced desire for luxury. Most of us then are all the more annoyed when we find the first scratches, which, in most cases, are inevitable.

Even when the pain eases the longer we have the car and as the number of scratches rises, we should not tire of pondering how we can at least alleviate this pain along the auto production value chain. Quite some time ago we at Rühl Puromer therefore asked ourselves the question in regard to the vehicle interior as to what we on the materials side could contribute. In this context, we came to the conclusion that as consumers we really would not care about a scratch appearing, provided it disappeared again of itself after a while. In our view the existing approach of making surfaces harder and harder is not conducive to success here. This is because polymeric materials have a finite hardness far below many other materials and in the case of shiny surfaces tend to be sensitive to scratching.

There is no question that even existing interior surfaces have reached a very respectable standard with regard to scratch resistance, and developments are certainly also continuing. From our point of view, the supreme discipline is however to give the corresponding components, such as trim, steering wheels, cover panels and so on, a high-gloss, hard-looking surface which is also retained up to a certain level of force applied from outside. If the external force impacts are too high – such as, for example, a zip catching against the steering wheel during exit from the vehicle or a key dropped in the center console - we allow a scratch to arise but ensure through an appropriate material structure that the scratch heals itself after a certain length of time. From our point of view, self-healing properties are therefore the magic word for future premium-segment high-gloss or even matt surfaces. This is effected by a new generation of coating materials on a polyurethane (PUR) basis with the name of puroclear®. It is mainly applied in the RIM process by flow-coating over a prefabricated carrier component (such as wood trim parts) or in an integrated injection-molding process the surface of a (film-laminated) thermoplastic substrate. Flow-coating composite parts for surface finishing is another option.

2. Starting point and working principle of self-healing

The point of departure for development was the knowledge obtained within the framework of a rather long-term, publicly funded development project called Nanoskin. The aim of this project was to give transparent plastic parts an antireflective coating using defined nanostructured surfaces. At the end of the project an instrument panel element with an antireflective surface was created as a demonstrator. During the course of development it emerged that not only are the high transparency and other optical properties of correspondingly designed PUR systems ideally suited for such applications but so too are their low-viscosity properties for shaping. The latter made it possible for the first time for the contours

of nano-structures to be precisely reproduced in a tool surface, this being essential for the anti-reflective effect.

Another item on the wish list was a structure which should last as long as possible in order that the anti-reflective effect should not be immediately lost again in daily use due to scratches, for example. As the partner responsible for materials in the development project, Rühl Puromer delivered on the material requirements by developing a highly transparent PUR system with self-healing properties. This exploited a characteristic of PUR chemistry that by selecting special raw materials a particular macromolecular structure can be created. On the one hand this consists of a three-dimensional network of the chemical compounds typical of polyurethanes as predominantly crosslinked polymers (Figure 1, top left). On the other hand, molecules are incorporated by special system components in the polymer chains, thus forming so-called hard segments within the polymer structure with a high percentage of strongly polar urethane groups. Chain length within these hard segments and also their number can be selected via the chemistry, and consequently the resultant properties as well. As a result of demixing processes (phase segregation) during the polymerization reaction in the mold, highly polar hard segments of this kind congregate in paracrystalline short-range order areas. Primary actors within these so-called hard-segment domains are the hydrogen bridge-type bonds between the neighboring urethane groups, considered to be the strongest interchenar binding forces. In light of this, hard-segment domains of this kind are also referred to as physical crosslink points.

Considered as a whole, phase segregation thus creates paracrystalline hard microphases which are covalently connected by soft segments to form a three-dimensional network. Here the amorphous and more or less flexible soft-segment matrix gives the polymer material its elastic deformability and its flexibility at low temperature. The polyurethane owes its hardness and strength to the chemical covalent bonds within the polymer structure in combination with the crystalline physical crosslink points.

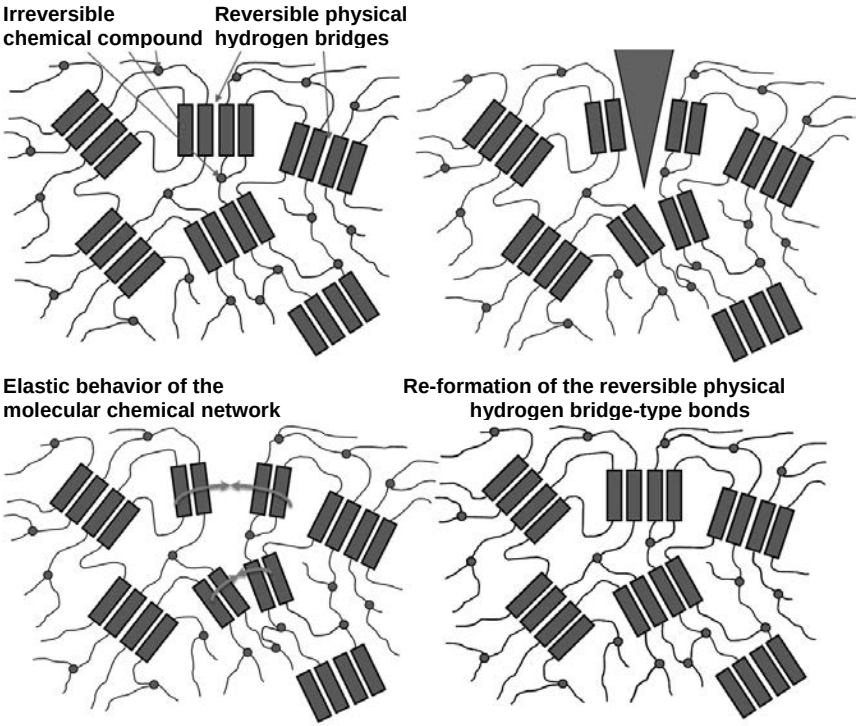

Fig. 1: Working principle of self-healing

As a result, further time-dependent physical effects occur in the region of the scratch. First of all, the stresses in the material or within the soft-segment matrix induced by the external force are stored in the displaced and/or deformed areas of material. These internal stresses are in the truest sense of the word the driving force behind the self-healing effect. Due to the frozen-in stresses the material surrounding a scratch starts moving back in the direction of its original position. In other words, the scratch gradually closes up again (Figure 1, bottom left), hand in hand with a fall in the internal stresses. This process can take a greater or lesser amount of time, depending on the material settings of the puroclear® formulation. Firstly, the self-healing thus exploits the *memory effect* typical of plastics. A second, central physical phenomenon then completes the self-healing of puroclear® systems. Once the macromolecules have moved close enough to each other as the scratch closes, they start to interact again with each other on an interchenar basis. The strong hydrogen bridge bonds can reform

and the hard segments of the individual macromolecules once again congregate to make crosslink points (Figure 1, bottom right). A three-dimensional network consisting of chemical and physical crosslink points reconstitutes itself. The scratch has repaired itself.

This explanation of the self-healing effect of puroclear® systems shows not only how physical phenomena can be deliberately provoked by means of a sophisticated chemistry and used to obtain a clear boost in day-to-day practicality. It also shows directly the limits of self-healing. If the external force is so great that even chemical crosslink points are destroyed, then they will no longer be able to regenerate themselves. Notwithstanding this, the self-healing effects described above will still continue to function and at least help to reduce the damage. However, a full reformation is no longer possible. More or less pronounced damage still remains. If the external force actually removes material this damage will not regenerate either. In such cases, however, it is no longer possible to speak of an incident of normal daily use. It thus almost verges on intentional damage.

3. puroclear® - in a class of its own

What sounds good in theory, of course, must prove itself in practice as well. In this regard, extensive tests conducted at various OEMs and suppliers of this new type of material class, which was thoroughly tested here, showed that puroclear® offers a significantly improved surface protection and thus a considerable increase in suitability for everyday use. This is also confirmed by its first instances of use in series production and by reports from the field.

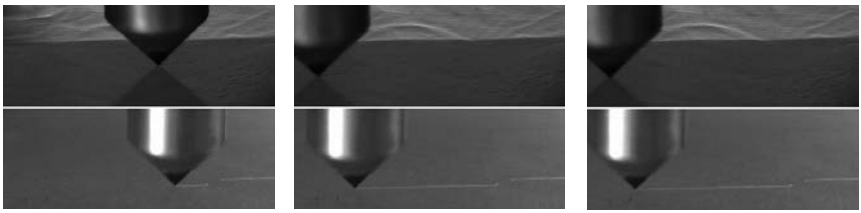

Fig. 2: Excerpts from a modified Erichsen test: puroclear® (above) and PC (below) (source: University of Heilbronn, Polymer Institute for Plastics Engineering)

Figure 2 shows an example of the reaction behavior of a puroclear® variant (top in each case) compared with a polycarbonate (bottom) in the context of a modified Erichsen test carried out in the Nanoskin research project at the University of Heilbronn at the Polymer Institute for Plastics Engineering. In this test in the case of puroclear® the scratch starts to close up again even while the test spike is still moving. By the time movement ceases the start

area is already no longer recognizable (Figure 2, center). At the end of the test the scratch has rapidly and completely closed up (Figure 2, right). In the case of the polycarbonate on the other hand the scratch is retained to its full extent and irreversibly so.
Based on the findings from the various development projects, puroclear® has developed into an entire product family. Today they can be classified in this way:

A) Hard puroclear® systems
    1. puroclear® standard without self-healing effect
    2. puroclear® with slow self-healing
       (about 1 to 5 days depending on the material setting)
    3. puroclear® with rapid self-healing
       (from a few minutes to hours, depending on the material setting)
B) Soft PU systems on a puroclear® basis
    1. puroclear® systems for dynamic loads (such as a switching function)
    2. (pigmented) puroskin® application with leather-like appeal / tactile qualities and a high UV stability (for example, light-colored surfaces in the interior)
    3. puroclear® systems for UV-stable applications with high elongation at break

The transition between the different product groups can be set fluidly, as it were, and flexibly. There is consequently no such thing as *the* puroclear®. The focus is rather on customizing the material individually to the customer's wishes. In many cases nuances of the tactile qualities decide a particular choice of one or the other system settings – in other words the selection criterion tends ultimately to be subjective.
Furthermore, puroclear® does not appear to be in any way restricted to transparent coatings as the 'clear' part of its name would seem to imply. Notwithstanding this, puroclear® systems, with their glass-like properties with regard to a high optical transparency and the least possible change in color value under standard lighting, are virtually predestined as the next generation, for example, for fine-wood trim components and fine-wood steering wheels. Even in their pigmented form they can still clearly unfurl their advantages, for example, as the highly demanded but also vulnerable piano-black surfaces. Entirely new possibilities are also created by puroclear® formulations with a set translucency.

4. Properties at a glance

The new self-healing effect also requires a rethinking of our testing and assessment activities within the context of OEM specifications. Self-healing is still not included in the correspond-

ing scratch-resistance tests. A number of OEDs are however already working on revising the test procedures accordingly. In the simplest case, the assessment period could be extended. Table 1 shows at the top the results from the Erichsen test, in which the sample was assessed both immediately after the test and also after 15 minutes and then a further 15 minutes. In the present example of a rapidly self-healing puroclear® setting, no permanent starting impression can be observed, as is the case with conventional PUR coatings, immediately after release of a load up to 10 N. When the load is increased to 15 N the starting impression has disappeared after a brief 15 minutes, while at 20 N, a load which polyester paints cannot tolerate, this takes as little as 30 minutes.

- Scratch resistance / self-healing effect (according to Erichsen, at RT)
  (depending on the specific puroclear® formulation)
  - 10 N OK (immediately)
  - 15 N OK (after about 15 minutes without starting impression)
  - 20 N OK (after about 30 minutes without starting impression)
- Hardness / haptics: 70 Shore A – 88 Shore D
  (from soft to hard) self-healing to 80 Shore D
- Solar simulation: OK (240 h - DIN 75220-D-IN1-T)
- Alternating climate test: OK (504 h: -30 – max. +90 °C, 0 – max. 80% rel. humidity)
- Chemical resistance: OK (crockmeter, sunscreen cream, etc.)
- VOC / FOG: < 70 / 125 ppm (requirement max. 100 / 250)

Table 1: puroclear® properties at a glance (test according to Daimler standards)

However, outstanding scratch resistance alone is yet not enough to qualify for use in the interior of a vehicle. Here additional criteria must be satisfied, in solar simulation and chemical resistance, in the alternating climate test and also in emissions testing, to give just a few examples. Table 1 shows a selection of corresponding properties, all of which in this case meet Daimler standards. Here the requirements to be met will vary according to the OEM and the application. In the case of a steering wheel, resistance to hand perspiration and to sunscreen certainly constitute a key aspect. Even these criteria specific to the steering wheel are satisfied by a special puroclear® formulation, thereby opening up the road to the first use in series production.

5. Possibilities of increasing efficiency with puroclear®

In addition to the self-healing properties which surely interest and delight us most as end users, for us as competitors in the plastics industry there are also other features which determine the use of a new material. Once again, there are also economic aspects which contribute to influencing this decision. And here too puroclear® has something to offer. Table 2 gives an overview of the benefits of puroclear® for processors. Costing should here include not only the price of the material as such but also downstream aspects relating to savings, as the following information shows.

- Self-releasing (target: off-tool parts production)
  - Reductions in reworking and the scrap rate
  - Saving on external release agent, release agent application and extraction and thus cycle time savings as well
- Lower processing temperatures of 60-80 °C
  - Savings on energy and investment
  - No yellowing, machine shutdown possible
  - Improved flow properties / lower pressure ⇨ less scrap
- Pumpable at room temperature
  - No preheating ⇨ lower investment
- Shorter curing, increase in productivity
- No skull-and-crossbones marking

Table 2: Benefits of puroclear® for processors at a glance

5.1 Self-release during processing

A necessary evil of PUR technology is certainly the use of external release agents during processing in order to secure reliable demolding of components. The use of external release agents

- incurs costs in the form of the external release agent
- requires a longer total cycle time
- makes it necessary to use a suitable extraction unit, and
- calls for greater maintenance and cleaning work for both the tool and the production environment.

To sum up, it costs time and money. The most varied efforts have been made for many years or even decades to avoid this drawback or at least to minimize it. Some developments, such

as coating the tool surface, failed because the coatings lacked sufficient durability in the daily routines of industrial production. There were also and still are attempts being made to work with sheets or most recently with sheet-like semi-finished products which serve as demolding aids. Solutions of this kind are here and there in service.

The use of internal release agents in the PU system has also made some progress in recent years. There are now a number of series applications where quasi-self-releasing, or at least easily separating PU systems are successfully used, such as, for example, in the manufacture or cargo floors and rear shelves which use puropreg® systems containing an internal release agent. The frequency of treatment with mold release agent when external release agents are used ranges from a few cycles (8-10) to a few production shifts, and in exceptional cases, even to several days of production. The success of an internal release agent solution is highly dependent on the PUR system used. Basically, the higher the density of the PUR material, the better the chances of an IT solution.

But, as is well known, the problem lies in the details. Accordingly, not only must self-release during production be taken into account but also the subsequent steps in further processing of the component. In many cases, the question of sufficient adhesion to other materials should be considered, such as for a carpet lamination in cargo floor production. And combining different materials to create hybrid solutions will certainly continue to increase in the future solely on account of cost pressures.

It is precisely when components are coated, either by painting or by flooding, that good adhesion to the substrate must be ensured, and this even with a material solutions involving an internal separating effect. With regard to the puroclear® systems this contrary question was resolved not only by using a very specific internal release agent but also by optimizing the PUR chemistry with respect to a good separation effect but avoiding any negative effect on the properties of the material. Using an internal release agent will not therefore on its own solve the problem.

What did emerge from this long-term development task actually surprised us a little. We have already run processes in which up to 1500 demolding operations were possible without a fresh application of release agent. This means that with performance of this kind it is entirely justified to speak of a self-releasing PUR system. However the 1500th demolding is not yet the end – in fact the series was concluded successfully. Upcoming tasks for series production will show how far forward this efficiency-boosting benefit of puroclear® IT system variants can still be pushed.

It is however certain that this ‘self-release’ feature brings with it considerable economic benefits to ourselves as competitors in the plastics industry. Looking at the hard facts:

1. Much much less external release agent is required
2. The full cycle is permanently reduced
3. Less investment due to reduced extraction costs
4. Less maintenance and cleaning outlay for tool and the production environment
5. Less secondary finishing due to reduction in the problem source, the release agent
6. Capability of implementing off-mold parts production, as is already being done today for selected parts.

To this we may add that the introduction of a self-releasing material solution of this kind is almost a fundamental condition for being able to efficiently combine flooding with a PUR surface even with injection molding of the carrier component as a single integrated process. The elimination of the disturbing step of release agent application, which the injection molder regards as dubious anyway and as a thorn in the side, permits an ever closer approach of the cycle times of the two process steps of injection-molding of the carrier component and flooding, which should then if possible be running simultaneously. An integrated process of this kind, called the ColorForm or clearmelt process depending on the machine manufacturer, now offers an interesting alternative to the classic painting process with its susceptibility to flaws, for example, for piano-black parts. The very low viscosity of puroclear® systems at a processing temperature of just 60-80 °C makes its contribution to permitting even very thin coatings. And let us once more remind outselves that the Nanoskin project was the point of departure for the developments. Were an external mold release agent to be used, every nano-structure would already have disappeared before even the first drop of coating material could flow into the mold. Self-release consequently makes even a major contribution to the precise reproduction of structured surfaces.

5.2 Shorter curing times and lower processing temperatures

Let us stay with the integrated process of injection molding and flooding. Figure 3 shows a demonstrator component manufactured in this way. In this particular case, curing times of just 40 seconds were possible for the puroclear®. This thus already comes close to the cooling times of the carrier component and cycle times of less than 60 seconds are possible by using mold insert technology. Admittedly, this component has a relatively simple structure, for example, with relatively little ribbing on the underside. However, the more complex the carrier component, the closer the cooling time comes to the curing time for surface coating, which is always relatively simply structured. During the course of mold proving for various

components, some applications were present in which the injection-molding process had a decisive influence on the cycle time.

Substrate:
Coating:
Injection time:
Curing time:
Cooling time:
Cycle time

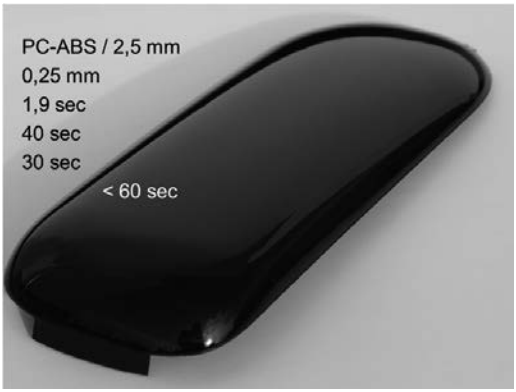

Fig. 3: High-quality piano-black look in injection molding by flooding with puroclear®

Certainly the thickness of the coating and the design of the carrier component also play an important part in the curing time. Reaction times of 90-100 seconds were thus achieved in fine-wood trim parts with a coating about 1 mm thick, which gives the final component or the real wood structure its great impression of depth. Here account should be taken also of the natural material wood as a direct substrate. Even though these times are greater than those in the above example, they still deliver a respectable saving of about 25% as compared with flooding by means of the flooding systems in common use.

The curing times to be realised with puroclear® thus make possible not only direct savings in existing technologies but also the implementation of new integrated and thus highly efficient methods, especially as an alternative to classic painting with its high scrap rates. Here it is not only the excellent self-releasing properties which are important but the relatively moderate processing temperatures of only 60-80 °C also make their contribution since, as regards mold temperature, they come close to the mold temperature in the injection molding of thermoplastics. In this respect the processes would couple together well.

The lower mold temperatures also provide a further benefit. In comparison with the temperatures of around 90-110 °C which are usual today in the production of real wood parts, these temperatures are considerably lower and this with shorter curing times as well. Not only is energy thus saved but it is also more pleasant for operators. In addition, high temperatures for longer periods result in the material yellowing. This circumstance means that the machine

has to be cleaned when production breaks or downtimes last longer than two or three days. This costs time and material. Lower temperatures and the chemical composition of puroclear® systems means that over long periods of time they do not yellow and production breaks of over one week are possible with a suitable machine setting (for example, intermittent cycle). This means that starting up again after plant shutdowns, such as at Christmas, is a comparatively simple matter.

5.3 Lower investment

The processing temperature plays a rôle even in machine investment. Outlay on machinery is thus lower when temperatures are below approx. 80 °C, because above this temperature special machine elements and components must be used. In addition, as the processing temperature rises so too does outlay on ensuring constant temperature control.

Savings in investment are in addition made possible by the fact that puroclear® system components (polyol and isocyanate) can be pumped at room temperature. This means that the preheating station previously required can be dispensed with. Furthermore, costs for extraction at the mold and also the equipment for application of mold release agent are also reduced on account of the self-releasing properties of the corresponding puroclear® systems.

6. Application examples and future potential

The steering wheel of the new Mercedes S-Class is the first mass-produced part in which the self-healing properties of the puroclear® systems, following extensive testing and inspections for this new class of materials, now had to prove themselves in practice. For some time now, another application has been in service: a fine-wood steering wheel with a puroclear® surface in the CLS series of models in the up-market C-Class. And other applications in this component segment will surely follow.

Fig. 4: Fine-wood steering wheel of the new Mercedes S-Class: self-healing in the supreme discipline (manufacturer: Quin)

In addition to use in the steering wheel, more series applications for fine-wood parts have been added very recently. At this stage it is the advantages of self-release which are primarily being exploited here. However, it is only a matter of time before puroclear® systems with a stronger additional focus on self-healing properties are used in this area as well. Here components are predestined for the center console area where a key might be dropped and cause damage.

But even beyond fine-wood applications inside the vehicle, there are several development projects and studies in progress in the field of components with the piano-black look, the high demand for which appears to be unbroken. An obvious use first appears to be for trim parts as a less expensive alternative to painting, and this is currently under intensive evaluation. However so far, as concept studies focussed rather on the medium term, complex panels for the center console with both high-gloss and matt areas and also numerous openings for control elements have also, for example, been produced.

High-gloss and matt finish in a single production step

Fig. 5: Complex control panel as a demonstrator (Skintec® Messrs. Kostal, image: Kostal)

Furthermore, the use of puroclear® for different functional components has been successfully tested. One example was with a somewhat softer formulation for fully flooded control panels with the corresponding tactile feedback. Other projects include components with backlit function displays and capacitive switches. Furthermore, the high contour accuracy in casting can be used to create not only a matt appearance but also other surface structures. In the long term developments will certainly be in the direction of functional structures, such as have already started with the Nanoskin project for anti-reflective coating of surfaces. We can therefore look forward to the next series applications.

7. Summary and outlook

With puroclear® a new generation of coating materials has been developed and successfully introduced onto the market which, due to its adjustable self-healing properties, offers not only a considerable increase in suitability for everyday use but even economic advantages over conventional technologies which are delivered by additional benefits such as self-release in particular. Here the innovatory potential of the puroclear® family was so extensive that in 2015 the jury of the SPE (Society of Plastics Engineers, Inc.) bestowed the ***SPE Innovation***

Award 2015 in the field of automotive interiors on Puromer Rühl GmbH and its partners. A crowning achievement here was equipping selected components with a bionic surface in the form of a sharkskin structure (Figure 6).

Fig. 6: Components with a sharkskin surface in the interior and exterior as a demonstrator at the SPE Award Ceremony 2015

Initially the focus was on the vehicle interior. But this was rapidly followed by the question as to whether there were possibilities of use for the exterior so that self-healing properties and/or self-release could be exploited there too. Here too there are several development projects in progress – one in collaboration with Audi AG which aims at exploiting specific properties of puroclear® as a paint substrate material on CFRP components and thus the K2013 exhibition project of KraussMaffei with Rühl Puromer, Henkel and other partners. Other developments are aimed at using the puroclear® surface directly as a visible part on the vehicle exterior. A series of requirements have already been satisfied here, such as passing with flying colors scratch resistance in the carwash test, chemical resistance to, for example, tree resin, and solar simulation with regard to gloss and color. Nevertheless intensive further development of the puroclear® systems is required so that here too all product specifications can be satisfied. This task we are tackling in order to make the advantages of puroclear® coating materials accessible also to the exterior in future – then perhaps even for bionic surfaces with a sharkskin structure for demonstrable improvement of exterior aerody-

namics. For this the last SPE awards gave a further innovation prize in this regard – this time to Messrs Frimo with Rühl Puromer as one of the partners.

Mono-polymer lift-gate solution cuts CO_2 emissions

G. Liraut, Renault sas, Guyancourt Cedex, France;
A. Tebib, Trinseo, Paris La Défense, France

Abstract

Trinseo (NYSE: TSE), a global materials company and manufacturer of plastic, latex and rubber, has developed a full thermoplastic lift-gate solution in a joint development project with Renault, the Paris-based automaker. This new solution has been commercialized and implemented in the series production of the 2015 Renault Espace. Renault is using the same material and design process for the front-end carrier of the Espace, which allows the car manufacturer to better rationalize material sourcing and leverage injection-molding technology in-house to produce lighter parts. The material selection and design methodologies from this project are not only limited to this vehicle model, but will be applied to the Renault Megane, the Talisman and other car models.

Through virtual process simulations—from testing the materials' specific requirements to analyzing their performance in the final part design—Trinseo contributed its expertise to solve various material challenges involved in designing a full thermoplastic structural part.

- This resulted in the first thermoplastic lift-gate solution for the Renault Clio in 2012. Both teams collaborated closely in the engineering phase to design the actual structural part of the lift-gate. Trinseo also applied its expertise in the material development implementation phase to select and test the materials required to fulfill the specific requirements for a lift-gate. To achieve this, extensive process simulation has been conducted at Trinseo's global Application Engineering & Design Centre (AEDC).
- The design and material development expertise of the Renault Clio was leveraged in developing the lift-gate for the new Renault Espace in 2015 which required a larger plastic part resulting in new technical challenges.

1 Introduction: building on long-term partnership and expertise

Vehicle weight reduction is one of the most important ways of improving fuel efficiency and reducing CO_2 emissions. Safer and environmentally sustainable vehicles are a priority for European authorities. This is why the automobile industry has been searching for an efficient alternative to steel components for a long time. To stay ahead of market demands and meet these sustainability priorities, Renault has been partnering with Trinseo for many years to explore how material development can contribute to the car manufacturer's strategic lightweight projects.

With the fourth generation of the Renault Clio, introduced in autumn 2012, the French car manufacturer was able to reach its ambitious target of reducing the weight of the lift-gate part by approx. 15%. Functional and design specifications and current recycling requirements tightened the project parameters further.

For the lift-gate of the Clio, the use of a lightweight polymer was proposed by Renault. The automobile manufacturer started working with Trinseo to initiate the engineering phase of this research and development effort. The following overview of the development project for this lift-gate solution illustrates the synergies that are possible when newly developed polypropylene materials are combined with improved part geometry and processing technologies.

2 Technical challenges encountered in both lift-gate projects

2.1 Creating a good fit with high durability

A complex car part like the lift-gate must meet high standards for visual appeal, have good dimensional tolerances and fit throughout the in-use temperature cycle and be able to invisibly accommodate many hidden elements such as hinges, lock mechanisms and electrical wiring. At the same time, expansion and durability (in particular of the structural support part of the lift-gate) are critical factors, since the lift-gate is subject to mechanical and climatic forces. Finally, the lift-gate must be able to fulfill its function while remaining stable and watertight.

Up until 2012, common metal / plastic combinations for lift-gate constructions included:

- Metal exterior and structural support, combined with a thermoplastic interior (TF-PP and ABS)

- Duroplast[1] exterior and structural support, combined with thermoplastic interior (TF-PP, ABS)
- Thermoplastic exterior (TF-PC/ABS, TF-PP) on steel-reinforced thermoplastic structural support (LFG-PP) with thermoplastic interior (TF-PP, ABS).

The fourth-generation Renault Clio, with its novel, almost entirely thermoplastic three-part lift-gate solution, marked a turning point when it was introduced in 2012. A 15% TF-PP was used for the interior, which is UV-stable and shows high scratch and impact resistance, as well as low gloss. Compared with other interior TF-PP materials, its low density (only 1.01 g/ccm) and good flow characteristics permitted thin walls and lower weight while still fulfilling all mechanical requirements.

The major challenges were:

- **Assembly and fit and finish**
- **Durability**

2.1.1 Assembly and fit and finish

This manufacturing challenge was definitely the most daunting aspect of creating the lift-gate which the project team had to solve. Two major aspects are to be considered:

- The assembly of the two different parts (the structural part and the inner skin) of the lift-gate. The two plastic parts had to be assembled together in such a way that they formed one final part. This is extremely challenging because both plastic parts have different shrinkage and warpage behavior which meant iterations in the part and tool design. The individual injection-molded parts needed to fit in a fixture in order permit a robust, durable laser weld between the two parts. This was addressed through selective rib placement. Ribbing created a part which deforms less after molding. Process simulation also permitted the use of ribs for adding strength and rigidity and to ensure that the final part had very low warpage. It was equally important that the connection between the glass window and the structural part fitted as well. Ultimately, the final part had to be acceptable for Renault's assembling process.

[1] Duroplast is a composite thermosetting plastic, a close relative of formica and bakelite. It is a resin plastic reinforced with fibers (either cotton or wool) making it a fiber-reinforced plastic similar to fiberglass [Wikipedia].

- The fit and finish of the lift-gate part with respect to the car's body in white (BIW): another key requirement is to have a good fit between the lift-gate and the BIW. In other words: when going through temperature cycles, the lift-gate must retain its dimensions to prevent water entering the interior of the car. Accordingly, significant effort was devoted to obtaining a good connection between the lift-gate and the BIW by means of additional mechanical simulations and experiments. Due to the stiffness of the glass, the window introduces additional rigidity and durability to the assembled part.

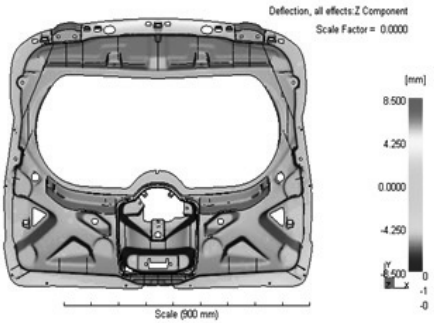

Fig. 1: Rib placement to create a part which deforms less

2.1.2 Durability

Another important manufacturing challenge was the durability of the final part. Durability has two aspects:

- The durability of the part needed to guarantee a perfect seal between the lift-gate and the body in white. Given that the part was going to be subjected to different temperature cycles, it had to be watertight under all temperature conditions. In addition, it was also important to create space and apply design solutions to ensure that expansion and shrinking of the part due to temperature was possible.
- Perceived durability of the lift-gate by the end consumer – haptics. Renault conducted several consumer tests amongst users to measure the perceived touch and feel of the plastic-lift gate. The part was perceived as more durable than the incumbent metal version.

2.2 Meeting performance and process needs

The development challenges of the Renault Espace project primarily centered on achieving the required dimensional stability of the lift-gate's assembly at different points of the production process, including the laser welding process as well as a temperature cycle that impacted the rubber seal's watertightness and visual perception of the gap between the lift-gate and BIW (body in white). The team also needed to design the lift-gate using plastics which would be suitable for laser welding. During the development process, the project partners therefore used process simulation to visualize and anticipate the behavior of the polymer materials. This method allowed the teams to not only optimize the large structural part's dimensional stability, but also meet the project's overall weight reduction goal.

3. Conceptual phase: the prototype and specific simulation technology used

When developing the Renault Clio lift-gate, Trinseo supported Renault in the engineering phase with process simulations to obtain the right design concept for developing a thermoplastic lift-gate. As mentioned previously, a lift-gate is a complex application for several reasons: it needs to fit perfectly onto the car and has numerous functions that must be accommodated. Additionally, it is subjected to many external influences. Exposure to high or low temperatures in a humid environment can cause deformation issues which must then be addressed to guarantee watertightness. To help improve impact resistance, expansion and durability of the structural part of the lift-gate, Trinseo's engineers introduced a long-glass-fiber-filled polypropylene resin (LGF-PP) to meet such requirements. By increasing the glass content of the molding material, the lift-gate is able to gain improved stiffness.

To select the right materials, extensive experience in producing thermoplastic solutions for automotive applications is required. The Application Development and Design Center of Trinseo supported Renault with their process simulation expertise.

The CAE tools of the AEDC group played an important role in the process optimization including improving the design of the hot runner system and the placement of the injection gates. These factors have a significant influence on optimizing the length distribution of the glass fibers in the final injection-molded part. The lower portion of the structural component needed special attention because of the gap dimensions. Here, it comes down to the finest details, so virtual prototyping was used to calculate the expected part warpage using LGF-PP models. Based on the findings from virtual prototyping, the strategic placement of additional

ribs in the design succeeded in reducing warping by 50%, thereby significantly improving dimensional stability.

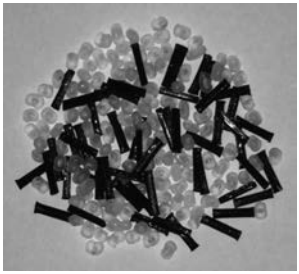

- Thickness definition
- Strategic rib placement
- Geometry concept
- Stiffness requirements / loading cases

Fig. 2: Material selection

- Hot runner definition for LGF
- Parametric optimization
- Plastification screw design definition
- Trinseo fiber distribution analysis

Fig. 3: Part design

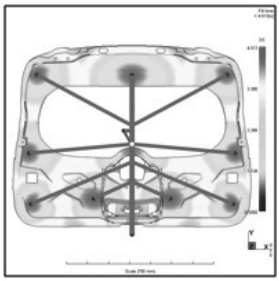

Fig. 4: Tool design and process optimization

3.1 Proven advantages of LGF-PP

LGF-PP provides a number of benefits. LGF-PP such as Trinseo's INSPIRE™ long-glass-fiber-filled polypropylene resin helps to meet the automotive component's stiffness and durability requirements while enabling significant lightweighting. As the automotive industry evolves, so do industry demands and requirements. In the past, resin manufacturers provided materials that satisfied the demands and requirements for the specific part. Today's industry is more focused on meeting the same requirements but at a minimal weight and cost. There is unanimous agreement in the industry that using LGF-PP is an interesting concept to examine. For instance, when producing a structural part such as the lift-gate using INSPIRE™ LGF-PP, a 15 to 20% weight reduction potential can be achieved, as opposed to producing it in steel. The glass content of the molding material determines the basic stiffness of the component, and increasing glass content will result in a higher part stiffness. The stiffness and the low density of the polymer not only enables lightweighting but also results in cost reduction.

In addition to the fact that it enables lightweighting, an added benefit is that fillers in a polymer such as LGF-PP also reduce the shrinkage of the material compound, making the part produced with these filled PP's fit more easily next to adjacent parts than an unfilled polymer would. This structural part fits into the car's metal structure (i.e. BIW) and therefore needs to have an excellent fit with acceptable gaps between parts. By adding the LGF to the polymer, engineers have a better control over the thermal expansion and can guarantee a tighter gap control.

3.2 Limitations tied to LGF-PP

A common challenge is the delicateness of the fibers: when LGF-reinforced PP is being processed, it is important to incorporate the longest possible fibers into the final part because that will result in the best mechanical properties. However, during the injection-molding process, most of the long fibers break during plastification and before injection of the material into the mold. Understanding this phenomenon is crucial to ensuring that sufficiently long fibers remain intact in the final molded part. Renault closely collaborated with Trinseo during the development of the lift-gate concept to resolve these types of manufacturing challenges.

3.3 Understanding fiber distribution and orientation

Consequently, understanding fiber distribution and their orientation in the final part is essential. Through extensive R&D, Trinseo has achieved a fundamental understanding of the effect of adding long glass fibers to polymer and how processing methods have an effect on the performance of the final part. By taking fiber orientations and length into account as calculated by process simulation, the quality of the mechanical simulations improves correspondingly. That is how Trinseo's R&D and Engineering departments developed virtual prototypes using optimized Computer-Aided Engineering (CAE) tools. Using the customer's part geometry (CAD) in simulations, Trinseo can predict the mechanical behavior of the part including calculated fiber orientations and length and can recommend further optimization of the part design with regard to, for instance, wall thickness.

As experienced firsthand by Renault, the molding process greatly affects fiber length. By analyzing the fiber length distribution using Trinseo's proprietary technique, it was possible to link this to the plastification screw of the injectionmolding machine more than to the mold and/or part design. By using a so-called 'soft' screw, the fiber length could be optimized on Renault's machine

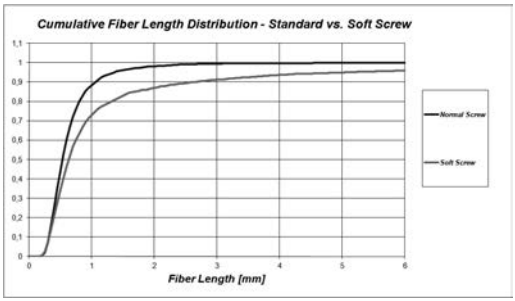

Fig. 5: Optimization of fiber length by using a 'soft' screw

4 Production phase: fine-tuning materials to Renault's production process

In 2002 Renault was already aware of the engineering capabilities of Trinseo from prior projects using LGF-PP, such as the structural development work that Trinseo performed on the front-end carrier (FEC) of the VW Golf. For that application, the functional design and production requirements presented similar complexities, with metal and thermoplastic to be combined into a single solution.

In the realization / production phase of the Renault Clio lift-gate, Trinseo offered both material development and processing support. In the selection of the materials, Trinseo was confronted with several challenges due to the complexity of the part. The selected materials were tested and fine-tuned to Renault's specific production process including injection molding, painting, bonding and welding. The final lift-gate design consisted of three parts:

- The inner skin is injection-molded using a talc-filled polypropylene compound from Trinseo and connects via laser welding to the structural part.
- The structural part is produced using a long-glass-fiber-filled polypropylene (LGF-PP) concentrate developed by Trinseo. This concentrate is diluted directly in the molding machine with the appropriate PP co-polymer resin.
- The outer skin was proposed to be made using Trinseo's INSPIRE™ At-Press talc masterbatch concept. The final material is made into plastic through blending of the three components, these being polypropylene impact co-polymer, specifically formulated 70% talc masterbatch and the required color concentrate, allowing for a tailored mechanical performance to meet the OEM-specific application requirements.

Fig. 6: The three-part construction that forms the Clio's lift-gate

Fig. 7: Full thermoplastic lift-gate solution of the Renault Clio

Building on the success of the Renault Clio lift-gate, the team started working on the Renault Espace's lift-gate. The desired performance attributes, dimensional stability, and weight savings were achieved through a combination of factors, starting with the selection of the optimal combination of Trinseo's long-glass-fiber-filled polypropylene (LGF-PP) and PP compounds. To best utilize the material properties and to meet all necessary performance requirements, while also minimizing its weight and cost, the lift-gate design was engineered with this thermoplastic material selection in mind. Following the Clio part- and tool-design concept, construction of the tool and part geometry was made similar in order to ensure the necessary molding productivity and part quality while optimizing warpage of this larger lift-gate.

Fig. 8: Trinseo's LGF-PP used to build a durable yet lightweight lift-gate for the Renault Espace

5 Specific material characteristics of Trinseo's LGF-PP

For both lift-gates a long-glass-fiber polypropylene (LGF-PP) material system was introduced for the structural part. By increasing the long-glass-fiber content the robustness and stiffness of the injection-molded parts could be increased. Renault also worked with the plastics producer to optimize the part construction, tool design, and injection-molding screw selection suitable for producing this LGF-PP lift-gate.

The LGF-PP solutions from Trinseo are designed for lightweight optimization and customer flexibility when developing structural car components. For the lift-gate of the new Renault Espace, Renault is using a 60% glass concentrate system, which is diluted with neat polypropylene to achieve the direct proportion of glass needed.

6 Process of using LGF-PP

Processing LGF-PP materials is challenging. For dilution systems, the dosing of a cylindrical LGF-PP glass concentrate (60%) and a spherical dilution PP material must be conducted in a consistent way in order to achieve stable glass contents of, for example, 40% glass in the final part. Basically, fluctuations in the dosing unit are directly translated into fluctuations in the produced parts. The differences in geometry and thus flow properties within the dosing unit between a cylindrical granule and a spherical one can lead to unwanted fluctuations in the resulting parts. In contrast, when dosing is measured through weight properties, it allows for a better control of the produced parts, with a stable glass content as well as a good total weight ratio.

Another potential issue can be the stability of the glass concentrates. The higher the glass content, the more critical the stability of the granules becomes. Due to the large number of plastic lift-gates Renault needed to produce, Renault asked for Trinseo to transport its LGF-PP material for silo storage in bulk. Being the first time Trinseo's LGF-PP concentrate had been delivered in bulk via trucks a close technical follow-up was required to ensure high product quality at any time from production in Trinseo's plant until processing at Renault. To achieve this, Trinseo tested the product quality after production, after bulk loading and unloading, at several stages within the conveying system at the Renault plant and right before use in the injection-molding machine.

In addition, conveying glass-filled material also usually creates dust due to friction. To overcome this, the right hardware set-up, together with a material that withstands even harsh conveying set-ups, were selected by Renault to ensure a clean and stable production process.

7 Results of the project: decreased weight for increased sustainability

Replacing metal with thermoplastics enabled Renault to achieve a 15% weight saving over its metal version and offered the company more design freedom with less upfront investments. In addition, because the base polymer of the lift-gate solution as a whole is the same for all components, the part can be easily recycled. All these factors taken together result in the benefit of this lighter weight assembly lowering the fuel consumption and CO_2 emissions of Renault cars and 'driving' towards a more sustainable future.

This approach also permits bonding of the structural and inner part using laser welding, which is novel considering the large size of the assembly. Regarding the handling and quality perception of the assembly, Renault's thermoplastic lift-gate solution is perceived by the user as outperforming its metal alternative when in use. This solution also provided improved NVH (noise, vibration, and harshness). In addition, Renault's manufacturing department was able to fully commercialize this solution by implementing a robust production process, which has resulted in a cluster-free LGF-PP part, while using the masterbatch approach for this high volume of parts.

The material selection and design methodologies from this project are not limited to only this particular vehicle model. Renault have confirmed that they will also apply this technology to the Renault Megane, the Renault Talisman and other planned car models.

Fig. 9: Renault Clio model and full thermoplastic, developmental lift-gate solution

Fig. 10: New Renault Espace 2015 model with full thermoplastic lift-gate

8 Summary and outlook: the road ahead for lightweight solutions

Through close collaboration over the past five years between the material supplier and the car manufacturer, an innovative lift-gate concept has been designed and produced, paving the way for commercialization in the Renault Espace 5 and other vehicles in the near future. Weight savings, styling freedom, recycling and function integration are the main objectives. With the full thermoplastic lift-gate solution, Renault not only contributes to weight reduction for optimal fuel efficiency but also responds to waste management recycling guidelines, promoting recyclability without disassembly of the application. Knowing that the lift-gate solution is made with the same base polymer, the part can be easily recycled and used in other future applications.

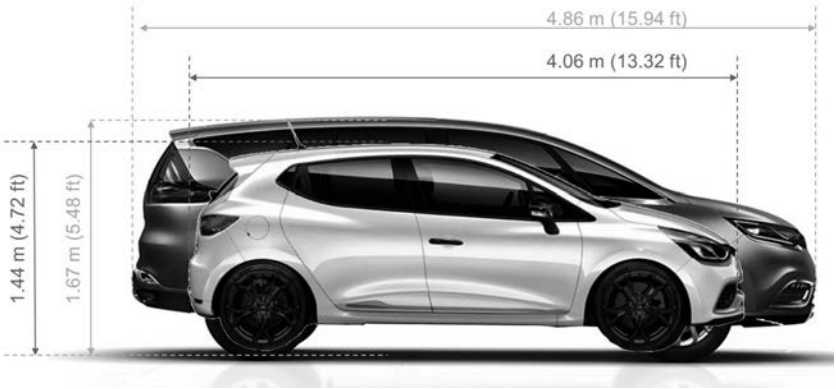

Fig. 11: From a small to a larger structural part with the Renault 2015 full thermoplastic lift-gate

***Key results of the project were the following*:**

- The all-thermoplastic lift-gate offers a **15% weight saving** over its metal equivalent
- Easier **recyclability**
- Bonding of the structural and inner part using **laser-welding for a large part thereby avoiding non-recyclable adhesives**
- **Excellent fit and finish allowing for small gaps between body panels**
- **Material selection and design methodology** can be leveraged **on future models and other parts** (front-end carrier)

Key benefits of LGF-PP for semi-structural applications are the following:

- Weight reduction of 15% or more
- Cost efficiencies - reduced material, production, application costs
- Dimensional stability - stiffness, low coefficient of thermal expansion
- Durability - impact, scratch and mar, long-term thermal aging strength
- Appearance - low gloss, UV stability
- High level of dimensional stability
- Processing flexibility - Trinseo At-Press technology
- Recycling by regrinding and re-processing

Class A Compression-Molded Carbon-Fiber Hood

Development and production of the Cadillac ATS-V and CTS-V Hood

Dr. **J. J. Laux**, Magna Management, Cham, Switzerland;
H. Moore, Polycon Industries, a Division of Magna Exteriors Corp., Guelph, ON, Canada;
J. Ingram, Magna Exteriors Corp., Concord, ON, Canada;
J. Kowalski, Magna Exteriors Corp., Troy, MI, USA

Abstract

The development and volume production of a Class A, Painted Carbon-Fiber Hood, presented challenges to both the Magna Exteriors development and the production teams. Global collaboration, geographical proximity to our customer and visible, shared objectives enabled completion in a relatively short time.

1. Introduction

Cadillac has been a leading luxury auto brand since 1902. In recent years, Cadillac has engineered a historic renaissance led by artful engineering and advanced technology. Since its inception in 2004, Cadillac's V-Series has driven remarkable power and performance capability into the brand's growing luxury car range. Building on the strengths of the award-winning ATS and CTS product lines, the V-Series adds impressive track capability to what was already the lightest and most agile-driving car in the luxury class. The result is a dual-purpose luxury performer – a car with true track capability right from the factory that is also a sophisticated luxury car on the road. Power-to-weight ratio is substantially improved with the selective and precise use of carbon fiber. A lighter hood is a major contributor to the ideally balanced weight ratio that a high-performance vehicle requires. Cadillac V-Series – where the racetrack meets the road. Inspired by top-of-the-line, race-ready vehicles, they are tailor-made to bring stunning performance to everyday driving. "Cadillac's V-Series is the best example of Cadillac's emerging product substance – and the purest expression of the passion at the core of the brand," said Johan de Nysschen, Cadillac President [1].

2. Functional design

Almost every exterior panel on the Cadillac V-Series is unique, from the fascias and fenders, to the hood, rear spoiler and rocker moldings – and every one was designed to support the car's capability. "All of the design elements have a purpose," said Andrew Smith, executive director, Cadillac Global Design. "They contribute to lift reduction, enhanced cooling, reduced mass or all of the above." [1]

The unique elements include:

- A lightweight carbon-fiber hood using heavy tow unidirectional carbon-fiber epoxy prepreg material
- An air-extracting vent that not only pulls hot air out of the engine compartment, but helps reduce lift, at speed, by channeling air pulled through the radiator out and over the top of car rather than allowing trapped air to exit under the car.

When Cadillac gave the go-ahead to Magna Exteriors, in January 2013, to manufacture a Class A, Painted Carbon-Fiber Hood for the 2016 ATS-V Coupe (Fig. 1), the 2016 ATS-V Sedan (Fig. 2) and the 2016 CTS-V Sedan (Fig. 3), they clearly specified basic requirements that included excellent surface quality, lightweight and high dimensional stability. This is reflected in the use of clearly defined materials and processes to yield a product that is significantly lighter than the previous product, while meeting all quality, performance and safety targets. The use of innovative technologies and lightweight materials had a significant influence on the performance of the vehicle.

Fig. 1: Cadillac 2016 ATS-V Coupe. Picture courtesy of General Motors (GM)

Fig. 2: Cadillac 2016 ATS-V Sedan. Picture courtesy of GM

Fig. 3: Cadillac 2016 CTS-V Sedan. Picture courtesy of GM

3. Enter Magna Exteriors

Starting in 2009, Magna Exteriors had embarked on a broad-based technology push for lightweight carbon-fiber-based composites. One of the new technologies to emerge from this advanced development effort was an out-of-autoclave Class A carbon-fiber epoxy composite that was produced by compression molding a unidirectional carbon-fiber epoxy prepreg, in a matched metal tool, at elevated temperature, with a cycle time that had never been previously achieved. At the same time, General Motors (GM), one of our largest customers, was looking for a Class A-capable, carbon-fiber composite for future car models. Based on the preliminary outcome of this development of compression-molded Class A parts, GM nominated Magna Exteriors for the hoods of the all-new Model Year 2016 Cadillac ATS-V and CTS-V.

4. Material selection and development

With regard to Materials of Construction, we chose a low-cost 50K industrial carbon fiber from Zoltek [2] for our Class A unidirectional carbon-fiber epoxy prepreg. This became the selection of choice due to a good balance between cost and performance. Our advanced studies had shown that a low areal weight, wide width format, unidirectional carbon-fiber prepreg gave us the best surface quality versus alternatives such as bond-stitched textiles or woven products.

As for a matrix system, together with our prepreg supplier Barrday Advanced Material Solutions, based in Cambridge, Ontario, Canada [3], we developed a fast-cure, high T_g (180°C) epoxy prepreg resin system that was fine-tuned to yield a prepreg with excellent fiber spreading and uniformity. To aid processing, the prepreg also had to have a sufficient level of tack that balanced the need for handling and cross-ply production, yet be capable of preforming and loading by automated transfer.

The next attribute that required attention was prepreg resin viscosity. At the time, most prepregs on the market were tailored for an autoclave process. Magna's compression molding process, in matched metal tooling, presented new challenges, namely melt characteristics, gel time and final cure cycle that took place over a time scale of minutes and not hours. Prepreg resin viscosity was modified to minimize bleed of the resin system during melt, gel and compression phases.

Finally, not only did the resin have to deliver a rapid cure, to allow high volume production from one mold, it also had to exhibit a very high level of ductility and fracture toughness, which was more important for the inner reinforcing panel. Furthermore, a high level of resin and color clarity was required for the exposed-weave inner panel variant.

The carbon-fiber composite development was supported by a number of material design and characterization loops. Typical material design loops included: 0 / 90 ply book development and optimized cross-ply design. These were then assessed using numerous material characterization methods such as tensile and compressive testing at room, hot and cold temperatures, G_{1c}/G_{2c} fracture toughness measurements and DMA.

5. Process development

Magna's out-of-autoclave process employs compression molding in matched metal tooling to ensure a high-quality part with molded surfaces on both sides of the carbon-fiber composite. Compression tool design for unidirectional carbon-fiber prepreg had to be developed for maintaining thin-wall stock, achieving required tolerances, and tool seal-off. To this end, a large database of best practices was generated from trials in 2D and 3D prototype molds. Magna invested in a modified tool that was cut to 50% scale, to allow for early phase development.

In moving towards our ultimate goal of producing 3D parts with an automated process, the development of an End of Arm Tool (EoAT) for achieving both pick-up and release of the prepreg was required. While part demolding uses standard high-temperature suction cups, material loading of the uncured prepreg blank in the compression tool required a far more sophisticated EoAT. The need for picking-up and preforming the 2D blank was addressed in the design of the EoAT. Creating an 80% preform became one of our many early development efforts.

At this point in the development, we faced a number of difficult design challenges, especially in the area of the Hood Scoop on the Class A outer panels. To solve these issues, Magna Exteriors developed engineering capability using Siemens Fibersim [4] for drapability analysis of carbon and glass laminate projects. Evaluation of forming capability and evaluation of trimmed blanks are estimated based on the desired 3D design geometry. This is then turned into flat patterns for use in cutting the 2D blanks. Additionally, the Fibersim outputs are used for our CAE predictive models. The ply tables are generated and mapped to the mesh model with full orientation data included. Magna Exteriors uses both LS-Dyna [5] and Abaqus [6] for laminate modeling. Dyna has been the primary package we have used for in-house generated design studies.

For the Cadillac V-Series hood projects, Magna Exteriors was sourced on a build-to-print basis. General Motors developed the design contours, and ply stacks were generated in global $[0/90/0]_s$ and global $[0/90]_s$ configurations. We applied Fibersim primarily to evaluate potential flat patterns, and then looked at the hot spots created based on various aggressive

contour regions. The manufacturing process is difficult to map, due to multiple plies being stacked, then formed under pressure at elevated temperature. The drapability analysis focuses on one ply at a time, and assumes various hold points that may or may not be consistent with the production process.

Without being able to change any of the existing build-to-print data, we were able to manage any of the cut-away lightening holes and detail items such as the Hood Scoop areas. We focused on manipulation of the cutout geometry to help influence the drapability of the 'areas of concern'. Fibersim was used to create the blanks, and these were subsequently optimized for scrap reduction. By identifying regions of concern, and looking at the effect of darts, slits and other features, the engineering group was able to help the manufacturing team to develop process improvements (Fig. 4).

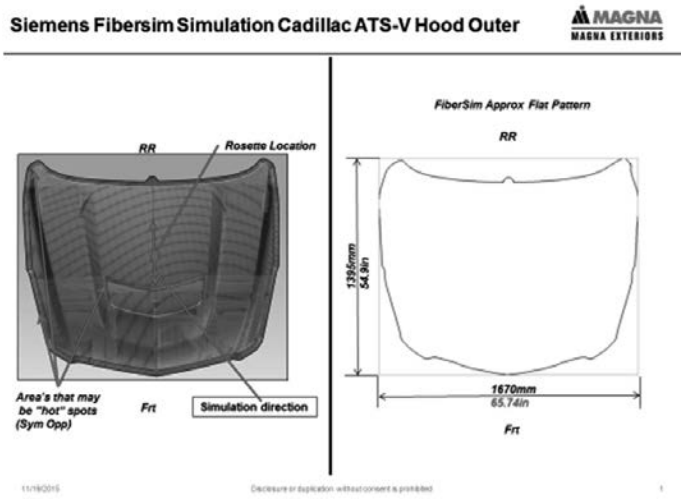

Fig. 4: Draping simulation example from the ATS-V Class A hood outer

An additional concern, through all these trials was the development of an external mold release. This presented a major challenge to both solvent and water-based external mold-release suppliers, as very few carbon-fiber-reinforced part molders use matched metal tooling and the number of parts produced per day was previously very low. Hence, external mold-release optimization for a high-volume environment that would provide multiple releases per tool, still needed to be developed.

After demolding the parts and cooling to room temperature, our next challenge was to develop a trimming process to deliver the final trimmed parts. After a dedicated development program that investigated attributes such as nesting, robotic versus 5 axis CNC milling, router bit type, design and coating optimization, together with trim-edge quality versus speed and CNC programming, we chose to go with a 5-axis CNC router process.

The last area of our process development efforts focused on developing a paint process based on a high-bake (121°C) paint system that required specific surface preparation, film build and temperature profile optimization.

6. Production

In our Polycon Industries production division [7] we operate a fully automated preforming and molding operation to produce the required Class A outer panels and structural inner panels for the Cadillac ATS-V and CTS-V (Fig. 5). Tools were sourced from Century Tool & Gage Co. [6]. Post molding, we employ a 5-axis CNC machine to create critical design features. The adhesive is a robotically applied 2K structural adhesive. The final assembly is achieved using an automated bond cell. The adhesive is fully cured as it moves through the paint shop. The hoods are body-color-matched, using a traditional North American high-temperature bake paint system utilizing a 1K / 2K (BC / CC) in 6 colors and fully assembled. Inner panel versions are produced in body color as well as exposed-weave carbon.

The outer Class A panels are produced with a 1.2 mm $[0/90/0]_s$ configuration, while the structural inner panels are produced with a 0.8 mm $[0/90]_s$ configuration. The exposed-weave inner on the CTS-V uses an additional layer of twill to produce the exposed-weave look. Due to the high exotherm associated with the processing of epoxy resin prepregs, special efforts were devoted to develop a very unique and efficient way to remove heat from the mold. Polycon chose high pressure, hot water over steam or oil as the heat transfer media.

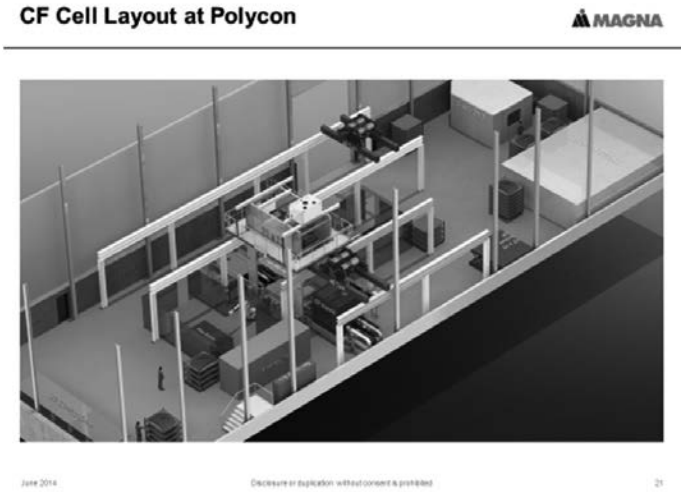

Fig. 5: Carbon-Fiber Class A Production Cell Layout at Polycon. [7]

7. Conclusion

Overall, Magna Exteriors reduced weight from the previous models by a 20% mass savings over an aluminum hood. This decrease in weight is directly correlated with a vehicle performance increase (e.g., Weight Reduction, Reduced Aero Load Deflection). A reduced effort in opening and closing these hoods was also noted. Furthermore, these carbon-fiber hoods meet Pedestrian Safety Standards (Ped Pro).

References

[1] Cadillac Pressroom. http://media.cadillac.com/media/us/en/cadillac/vehicles.html

[2] ZOLTEK Corporation. http://zoltek.com/

[3] Barrday Advanced Material Solutions. http://www.barrday.com/materials.html

[4] Fibersim. http://www.plm.automation.siemens.com/en_us/products/fibersim/

[5] LS-Dyna. http://www.lstc.com/products/ls-dyna

[6] Abaqus. http://www.3ds.com/products-services/simulia/products/abaqus/

[7] Polycon Industries a Division of Magna Exteriors Corp., Guelph, ON, Canada. http://www.magna.com/capabilities/exterior-systems/about-magna-exteriors/location

Perspectives in automotive polymer glazing

Polycarbonate makes use in side and rear windows possible

H. Schmidhuber,
Webasto Roof & Components SE, Stockdorf

Synopsis

Making mobility more and more sustainable is a continuously strengthening social demand which has gained a permanent place in the product specifications of car manufacturers and suppliers. In the roof area Webasto focuses here primarily on lightweight design. Against a background of increasingly strict limit values for CO_2 emissions and due to the increasing popularity of electric vehicles, weight-saving is becoming more and more important.

A rule of thumb is that a weight reduction of 100 kilograms results in a reduction in carbon dioxide emissions of 3.5 g/km for vehicles with petrol engines and 3.0 g/km for diesel vehicles. Gains are also made in agility and thus more driving pleasure. Bearing in mind that if weight were unchanged this additional agility would require higher performance (so-called performance compensation), the comparison actually indicates a reduction in carbon dioxide emissions of approximately 8.5 g/km.

Polycarbonate (PC) is a lightweight material which has been used in cars for some time. Currently plastics make up about 15% in the automobile, of which nearly one third is polycarbonates. These are however mainly applications relating to panels or the passenger compartment. So far only a few transparent polycarbonate parts have been installed in vehicles. This particular polymer is basically transparent like glass, but can be given any hue. Over the years the potential of this high-tech material has however somewhat slipped out of the frame for the industry. Polycarbonate still has its future ahead of it, especially as a material for glazing. It makes weight reductions of more than 40% possible in windows. Furthermore, it is absolutely fracture-resistant and can be given virtually any shape.

Webasto has gained experience in the development and production of polycarbonate components over more than a decade. Materials and processes are now ready for a significant expansion of the use of polycarbonate, not only in the roof area but also for the all-round glazing of cars.

Webasto - progress from tradition

Headquartered in Stockdorf near Munich, Webasto is one of the 100 largest automotive suppliers in the world and among the top 15 of this sector in Germany. The company has been family-owned since its foundation in 1901. As a supplier it operates in three business segments: roof systems, convertible roof systems and heating systems. In 2014 more than 10,000 employees at over 50 locations generated revenue of around 2.5 billion euros.

Innovation is literally a tradition at Webasto: founder Wilhelm Baier sr., who first made bicycle parts such as rims, mudguards and chain guards, made his entry into the automotive sector in the 1930s when the automobile was finally able to celebrate its conquest of the world. In 1932 Wilhelm Baier constructed the first folding roof for cars, which could be opened or closed with a few simple operations. Just three years later, he designed a so-called 'automobile fresh air heater' for water-cooled engines. It later became known under the name ‘Flüstertüte’ (that is, megaphone).

The heating systems division covers heating, cooling and ventilation systems for passenger cars, commercial vehicles, special purpose vehicles, rail vehicles, motorhomes and boats. In addition to fuel-powered car auxiliary heaters and parking heaters, electromobility is also an important pillar of Webasto's growth strategy. Here a highly efficient, electrically-powered heating system has been developed for hybrid and electric vehicles which heats the interior during the journey. Series production of the system started in 2015 at the Neubrandenburg plant.

Webasto has been an established supplier of convertible roof systems since 2000. Today it has the most comprehensive range of convertible top systems on the market. Technical standards are set by, for example, the innovatory electric drives for the roof systems, which are very quiet in operation and impress with their low weight. To reduce the total weight of the convertible roof systems, Webasto is currently using light-weight materials such as aluminum and magnesium.

In the field of roof systems, Webasto makes sunroofs, panorama roofs and solar panels. In addition to traditional materials, polycarbonate is also used here. In 2003 the company started work on setting up its own plastics competence center in Schierling near Regensburg. Innovative roof elements made of polycarbonate have been manufactured there since 2007, such as, for example, the transparent roof for the Smart. All in all a sum in the order of hundreds of millions of euros has been invested so far in Schierling. Production capacity runs to a good million components per year made of polycarbonate.

Thanks to a variety of innovative technologies Webasto knows how to set standards over and over again. For example, the solar roof developed by the company has been recognized by

the European Union as an eco-innovation. Currently, as of November 2015, it the most efficient eco-innovation on the market. Eco-innovations of this kind, recognized by the EU, grant the automobile manufacturer a credit in CO_2 emissions. Another, also outstanding innovation, is Webasto's development of a transparent polycarbonate roof system with infrared absorption, which effectively counteracts heating-up of the passenger compartment.

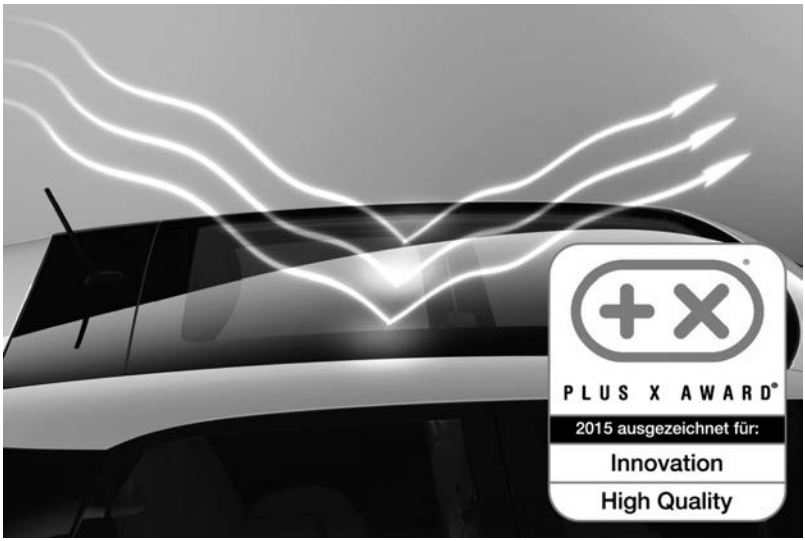

Fig. 1: Polycarbonate roof system with infrared absorption

Innovation history

Milestones in the development of plastics in automotive glazing

Weaknesses of glass – advantages of polymers

Up to the present day automobile windows have been made of glass. Its share in vehicles has been increasing continuously over the past 20 years. In 1985 this averaged approx. 3.5 m^2, and today is about 4.6 m^2 per car. The reasons for this are varied: one of the two fundamental aspects is the higher driving safety offered by improved all-round visibility. The second fundamental aspect is the ever-increasing desire of the customer for the greater feeling of well-being during his journey afforded by more light in the interior. The area of the windshields and rear windows in particular has increased and transparent panoramic roofs open up a completely new and almost unobstructed view upwards for the vehicle occupants.

But glass does have its weight. The current average 4.6 square meters of glass thus weighs 53.9 kg. Here half of this area is laminated safety glass (with a thickness of 5.5 mm) and the other half is single-pane toughened safety glass (with a thickness of 4.3 mm). The relevant glass thicknesses here are the mean values of the various types of glass actually used by automakers. In times in which automobile development is markedly affected by resource conservation and the reduction of fuel consumption and emissions, strategic lightweighting is one of the most important technological trends amongst automobile manufacturers and their system partners in the supply sector. Due to the elevated position of the glass windows in the vehicle, the center of gravity is a long way up. This has a lasting negative effect on, among other things, the driving characteristics of the car.

Certain transparent plastics are a possibility as alternative lightweight materials for the glazing. They are crystal clear, can be given virtually any color, are also impact resistant yet actually weigh less than the current material glass. If you were to replace the above-mentioned average glass area in the car of 4.6 m^2 with polycarbonate, the weight would fall from 53.9 to 30.6 kg - a saving of more than 40%.

However, with polymers such as polycarbonate it is not only weight reductions which can be achieved. They also have the great advantage over glass in that they as thermoplastics can be molded into virtually any shape. On the one hand, this gives both designers and engineers new freedoms and possibilities while on the other hand also bringing economic advantages. The high degree of functional integration makes it possible to reduce the number of parts normally required and thus cut process and production costs.

One aspect which has not yet been mentioned and which is currently of great importance in the automotive industry is safety. This is precisely where polycarbonate displays one of its greatest strengths: unlike glass, this material does not splinter. Polycarbonate is almost indestructible, which is why this material is already in use today in many areas related to safety. Police forces throughout the world have long been using shields made of polycarbonate. And it is precisely here that the material has made inroads into automobile construction: numerous police vehicles are already fitted with polycarbonate windows as an effective protection for occupants against the possibility of smashed glass.

Available applications to date in the overall market

In addition to Webasto's roof for the Smart and the applications already mentioned, a large number of other polycarbonate applications are currently in series production and many of these are also non-transparent. To take just the automobile, polycarbonate is found, for example, in fixed rear side windows, in the covers of headlamps and direction indicators, in spoilers, pillar trim, decorative trims and also various applications in the area of the dashboard and the steering column.

History of innovations in plastics in automotive glazing – milestones in development

As an innovative supplier, Webasto started in 2003 to investigate transparent polymers as an alternative to glazing with glass. In specific terms, a comparison was made of the properties of polycarbonate (PC) and of polymethyl methacrylate (PMMA, commonly known as plexiglas).
The two materials were investigated on the basis of four levels of decision-making:

1. Design (moldability)
2. Functional integration
3. Safety, and
4. Quality

Following extensive and thorough investigations, Webasto's decision at that time was to concentrate entirely on polycarbonate. If there were only very few or only trivial differences between the two materials as regards design (moldability) and functional integration, polycarbonate did offer considerable advantages as regards safety (impact strength, fracture resistance, thermal resistance) and quality.

Technical basics of polycarbonate

Polycarbonates are amorphous, thermoplastic polymers. Polycarbonates are still a relatively new group of materials. The first polycarbonate to achieve prominence was developed by Bayer in the 1950s under the name Makrolon®. Polycarbonates are crystal clear, impact-resistant and break-resistant. Their elongation at break is 120%; the comparable figure for single-pane toughened safety glass is less than 5%.
Its light transmittance is over 90%, almost as high as glass. Its density of 1.2 g/cm^3 is only about half of the density of the glass normally used in vehicles (about 2.5 g/cm^3). Webasto uses Makrolon® AG2677 from Covestro (formerly Bayer MaterialScience) which was specially developed for automotive glazing and roof modules.

At 0.65x10^{-4}/K (temperature range 23 °C to 55 °C) the thermal expansion coefficient of polycarbonate is significantly higher than that of single-pane toughened safety glass (0.09x10^{-4}/K in the temperature range 20 °C to 300 °C).

Layer structure

In the current Smart roof, for example, transparent polycarbonate panels have a thickness of 5.25 mm and are back-injected with a black component consisting of a polycarbonate / acrylonitrile-butadiene-styrene blend (PC/ABS). These two layers are coated top and bottom with both primer and hard coat. The primer layer serves as UV protection and has a thickness of 1.2 to 4.0 µm (permissible tolerance range in production). The hard-coat layer is 4.0 to 12.0 µm thick.

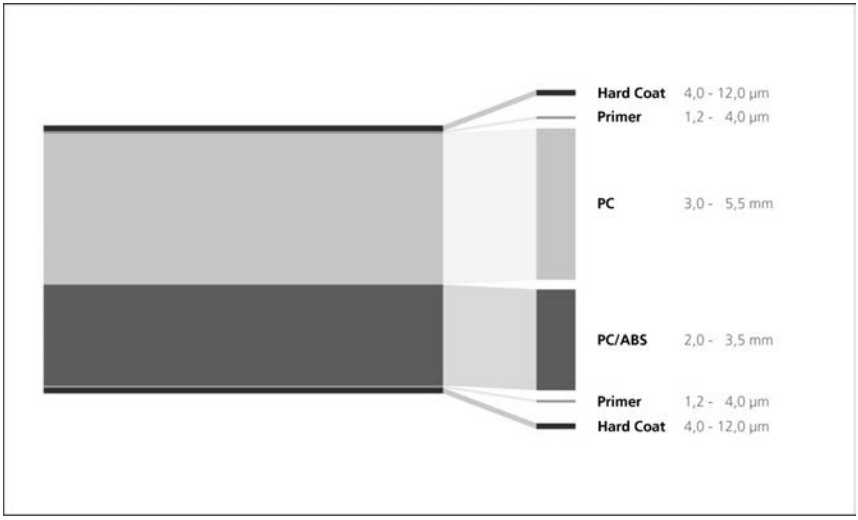

Fig. 2: Layer structure of a polycarbonate panel

Manufacturing process

Webasto combines Makrolon® AG2677 with the current generation of a coating system from Momentive. It consists of a primer (SHP 470 FT 2050) and the actual protective layer (AS 4700F). The polymer is thus given a glasslike surface structure which guarantees scratch-resistant Class A surfaces. This secures a high and durable quality in accordance with automotive standards.

Webasto controls with the greatest precision a variety of parameters in production to ensure the coating performs its protective function and in conjunction with the polycarbonate offers flawless transparency and surface quality. Together the primer and hard-coat layers have a thickness which corresponds to roughly one quarter to one eighth of the diameter of a human hair.

One special challenge is that a system of this kind does not allow secondary finishing. This means that the exact thickness and uniformity of the coating must be 100% secured by the process development and control. And this with areas of up to 1.3 m^2, such as the Smart roof.

In 2004 Webasto commenced work at the new plant in Schierling near Regensburg, Germany on developing a production process to meet these requirements. Series production began in 2007 with the first transparent Smart roof. Currently the second-generation transparent roof for the Smart is in production at Schierling. To date nearly 630,000 roofs for the Smart have been shipped. With continuously improved processes which run in clean rooms, not only transparent polycarbonate roofs but also various cover panels are also being produced at Schierling.

Webasto uses a special injection-compression molding process to produce large-area components. For components of this kind the disadvantage of classical injection molding, of which this process is a special variant, is that they are permeated by internal stresses. These stresses in their turn often lead to twisting of the component in the subsequent coating and stoving process. The visible consequences of this would be unacceptable cracks in the coating. Webasto's injection-compression molding process on the other hand provides largely stress-free components since the material is injected into a mold opened by just 2 to 5 mm and correspondingly lower injection pressures are required. The mold does not close until all of the melt is in the mold.

If it is a roof system being made, such as for the Smart, the purely glazing element is created in the first step. Next, items such as fasteners, spacers, guide rails, and positioning pins are injected onto the underside.

The part is then given 24 hours to relax following rapid cooling to room temperature. Here the residual stresses disappear which were still present following the temperature fluctuations and associated thermal shrinkage of the material.

Clean-room conditions are absolutely essential since any contamination in the coating processes larger than 5.0 µm in size would mean rejection for the roof. Finally, any particles still present on the components after injection-compression molding are removed before coating commences.

Coating is the most sensitive part of the entire process. Both primer and hard coat must be applied precisely and with the right thickness to all parts of the component. In the case of the

primer, which ensures the UV resistance of the polycarbonate element, the tolerance range lies between 1.2 and 4.0 µm. The second layer, the hard coat, looks after scratch resistance and its thickness may vary only between 4.0 and 12.0 µm.
Applying a self-developed and patented method, Webasto carries out the coating by flooding: robots let the primer flow out of hoses and onto the components. Flooding follows precisely defined tracks, firstly on the underside and then on the top. Here this precision depends on the sagging and drying properties of the primer – Webasto controls both via various parameters. Finally this coating is stoved.

Fig. 3: Coating a polycarbonate element by flooding

Finally, the same process is repeated with the hard coat. All in all this coating process takes less than 5 hours. In the final inspection which follows, another check is made to ensure that every component meets the high quality requirements of Webasto and its customers. Here each component is both measured automatically and also visually inspected by an employee since as yet there is no process-reliable method available for this.

Polycarbonate applications by Webasto on the market

Based on this comprehensive know-how Webasto can already offer its customers various polycarbonate solutions in the roof area. For example, U-shaped panels are being produced for various vehicle models for different manufacturers – these partially surround the sunroof or pop-up roof and are made in a single piece without joints. These panels are characterized by their low weight and enclose the sliding and panorama roofs at the front and sides. In this way a jointless transition to the roof of the vehicle is created and the entire roof surface receives its high-quality full-glass look. For the VW Beetle, Webasto developed for the first time a so-called O-panel which frames the roof on all four sides.

Fig. 4: VW Beetle with O-panel

For the third generation of the Smart Fortwo, Webasto supplies its second-generation panoramic roof made of polycarbonate. This roof system lets plenty of light into the interior and thus creates a comfortable, generous feeling of spaciousness for the occupants. Visually, it is a perfect extension of the windscreen. Starting with the launch of the second generation of roofs all transparent Smart roofs absorb solar energy and thus counteract heating up of the vehicle interior. This means that the air conditioner does not need to be used so frequently. This is achieved by the infrared absorber integrated into the polycarbonate.

Challenges and opportunities

A variety of challenges emerge from the material properties of polycarbonate and the current situation. However, this also creates opportunities. Let us examine these in the context of four relevant dimensions:

Dimension 1: Customer
Dimension 2: Technology
Dimension 3: Economics
Dimension 4: Legislation

Challenges and opportunities: the customer

There is no respite in the customer's desire for more daylight entering the interior through the roof. The polycarbonate sunroof which Webasto is currently developing will be a breakthrough in this endeavor and let more light into the vehicle interior. At the same time weight is perceptibly reduced.

Similarly, the requirement for greater safety is fulfilled thanks to the outstanding properties of polycarbonate panels. Even when a car overturns neither the polycarbonate roof nor the polycarbonate side windows will splinter: occupants are thus effectively protected.

Polycarbonate provides novel elements for the design language of the stylist, ones which are impossible in glass. For example, ribs or edges can be extended into the fixed rear side windows. Other instances of functional integration are also made possible, such as brake lights invisibly integrated into the rear window or spoiler.

The ever more stringent CO_2 limits are forcing automakers generally to place even greater emphasis on lightweight construction. In addition there are also certain special aspects.

Special fittings, such as heavy glass roofs, are not taken into account in the current mandatory test cycles to determine fuel consumption and CO_2 emissions. In other words, they do increase standard fuel consumption. In the WLTP procedure – Worldwide-harmonized Light-vehicle Test Procedure – which will apply in future, optional extras are also included. The pressure to save weight is thus increasing even for optional equipment.

The goal of making electric mobility attractive for as many motorists as possible also gives an even greater importance to lightweighting. The biggest hurdles here are the ranges of electric vehicles – in most cases very short – and the cost of batteries. Every kilogram of weight saved either extends the range or even means savings in batteries.

With polycarbonate going beyond the roof into the side and rear windows, automobile construction attains a new level of quality in saving weight. The use of polycarbonate in this area means a considerable increase in the weight advantage for the entire vehicle fleet.

Challenges and opportunities: technology

New possibilities are also emerging today in the technological field, especially as regards improvements in the quality of polycarbonate components. Basically, unprotected polycarbonate has little scratch resistance and is also sensitive to UV light and weathering. Scratches in components must be avoided because they inevitably affect perceived quality when viewed from above. In the case of glazing, the unobstructed view of the occupants would also be impaired. The aim is therefore to protect the polycarbonate elements against yellowing and gains in opacity.

All three challenges have been overcome by the materials and processes employed by Webasto. Coating with primer and hard coat affords reliable protection for the polycarbonate and guarantees a consistently high perceived quality which without compromise meets the high standards both of the automobile manufacturers and of Webasto.

The high degree of thermal expansion calls for further measures. If a polycarbonate roof one meter in length is heated from 20 to 90 °C, it will expand in length by 4.6 mm. In the case of fixed elements, Webasto uses suitable bonded joints and also special geometries to ensure that the strictest requirements in appearance and function are met despite this thermal expansion. In addition, Webasto is actively collaborating with Covestro on reducing thermal expansion even in the raw material by incorporating special additives. For movable polycarbonate elements such as sunroofs, thermal expansion is fully compensated for by special kinematics.

In comparison with glass, polycarbonate has a low inherent stability which can become a challenge for large, movable polycarbonate elements. The modulus of elasticity of the polymer is 2400 MPa. For single-pane toughened safety glass the value is 70 000 MPa. In the sunroof development project which is currently in progress Webasto is setting the requirements even higher: since a one-to-one substitution of polycarbonate for glass would not be economically worthwhile, the polycarbonate sunroof now being created would dispense with a sheet metal frame and foam cladding, as is otherwise usual with glass. By application of special processes Webasto has succeeded in compensating without loss of quality not only for the lower inherent stability of the polycarbonate but also for the omission of these reinforcements (sheet metal frame and foam cladding).

Challenges and opportunities: economics

The manufacturing process described above makes clear the great effort required in the production of polycarbonate components. To this we may also add the very high cost of the extremely complex and large molds. With respect to the individual component, polycarbonate would not therefore be competitive in costs with glass.

However, if we expand our field of view and take additional relevant factors into account in the costing, the picture changes considerably. Now if the aspect of 'weight reduction' is added to the reckoning and the fact that a polycarbonate component is about 40% lighter than a comparable component made of glass is taken into account, this offsets a significant part of the additional costs. As a rough guide value in the automotive industry, one kilogram of weight saved corresponds to 5 euros in additional costs.

Increasingly stricter CO_2 limits are making weight-savings increasingly important. Lightweighting in roofs and windows is even more valuable than in other elements because the weight saved lies relatively high up in the vehicle and thus the center of gravity is perceptibly lowered.

In addition, structures made of polycarbonate permit, as already mentioned, a comprehensive integration of functions, which thus reduces costs elsewhere. If until now it has been, for example, fastening elements integrated directly by injection-compression molding into the components, solutions which go much further than this will become available in the future. These include, for instance, the integration of a third stop lamp in a polycarbonate rear window or spoiler. In this way polycarbonate systems can become even more cost-competitive with regard to glass.

A further reduction of process costs through further simplifications is entirely possible. New coating systems thus promise a major advance. Curing could take place 'cold' and thus much more efficiently. A further simplification can be expected from one-pack coatings which do not require a separate primer. The wealth of experience which Webasto and its partners have now accumulated also makes cost-reducing optimizations possible in the tooling area.

Challenges and opportunities: the legislation

Changes are on the way even in our fourth dimension, that of the legal framework.

Currently the use of polycarbonate in vehicle glazing is restricted to individual areas by the standards UN ECE R43 (Europe) and ANSI Z26.1 - 1996 (USA) and also by the usually much stricter requirements of the automobile manufacturers. Plastic panels, for example, are generally permitted in the roof. In the case of the rear and side windows, however, requirements diverge. Although plastic windows are generally permitted in this part of the vehicle depending on the region or country, in certain areas, however, approval is only granted after an individual inspection.

The most stringent specifications apply to the windscreen and front side windows. Since these have the greatest importance for the driver's vision, they must meet the highest requirements. Until now these two standards basically do not permit windscreens or the front side windows to be made of plastic. But ECE R43 changed in this regard in the autumn of 2015: since October it is permissible to use plastic as a material for windscreens provided certain tests are passed. It is probable that from mid-2016 the European standard will also allow front side windows to be made of plastic.

With this autumn's change in the ECE with regard to windscreens, new test procedures have also been introduced and thus a major weakness of the previous system removed. Until now both European and the US standards required the so-called Taber abrasion test which was developed in the 1970s for evaluating glass panels. Here the material sample is rotated while abrasive wheels press down on the sample from above with a defined force. The measure of the quality of the material is the turbidity (haze) found after a defined number of revolutions.

In the case of the glazing relevant to the driver's vision – that is, the windscreen and front side windows – after 1000 cycles haze must not exceed 2%. In the case of the other windows, values below 10% after 500 cycles are permissible, and this requirement can already be satisfied by the current polycarbonate windows.

However, the current test procedures only inadequately reproduce the real stresses to which car windows are exposed. Furthermore, the results achieved with polycarbonate windows are not sufficiently reproducible in these tests.

At the instigation of the Plastic Glazing Informal Group new test procedures for windscreens are now included in the revised UN ECE R43. The Taber abrasion test does however continue to form part of the standard. Now, however, three other tests may be applied as alternatives: according to the sand trickling test, turbidity must be less than 5% while according to the carwash test (Amtec Kistler test) and the wiper test it must be less than 2%. However the

previous test can only be replaced by all three of these tests. As regards the front side windows, the ECE regulations are due for revision in mid-2016.

These new methods provide the first reliable information about how the windows actually behave in real service. Particularly in the case of coating manufacturers, the new situation could even give a boost to the search for further improvements. Since it is now permitted for the large windscreens to be basically made of polycarbonate, this opens up a major economic potential for the coating manufacturers. In testing carried out by Webasto, specimen panels made of polycarbonate and coated with AS 4700F passed the three new tests. However a further improvement is demanded by the automobile manufacturers. For such requirements Webasto and its partners are continually working on further development of the polycarbonate systems.

Webasto Polycarbonate 360

The developments we have described have a great potential for Webasto. On the one hand the aforementioned trends now give the advantages of polycarbonate glazing a much higher importance than was previously the case. In a certain respect polycarbonate used to offer solutions for problems which at that time had not yet become acute. This is now changing. The need to exploit the advantages of the material will continue to grow.

On the other hand, Webasto will then be able to supply the right products to satisfy these requirements. After much more than a decade of development work and years of production experience, the company now masters both materials and processes and is working with its partners on the continuous development of both.

The current roadmap at Webasto for polycarbonate currently includes the following development steps:

1. Open roofs
2. Fixed side windows (rear)
3. Rear windows with integrated functions such as tail lights, window heaters
4. Movable side windows (front and back)
5. Windscreen

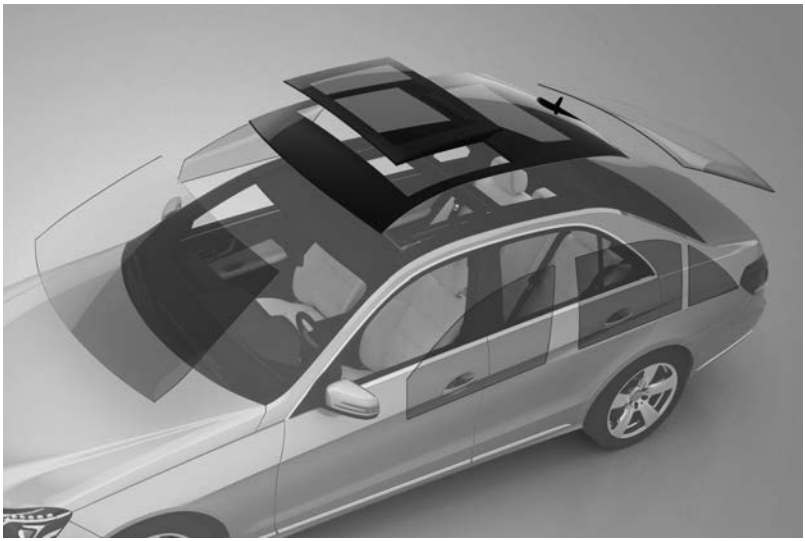

Fig. 5: Webasto PC 360 - polycarbonate applications around the car

This approach Webasto has brought together under the name 'Webasto Polycarbonate 360'. Webasto is amenable to pushing development further in collaboration with an OEM; we are ready to replace all glass areas with polycarbonate.

Carbon core: the use of CFRP in the body structure of the BMW 7 Series

Dipl.-Ing. (FH) **M. Derks**, BMW AG, Munich

Abstract

This contribution describes the Carbon Core CFRP composite concept in the body structure of the new BMW 7 Series in the context of lightweight components in the vehicle. The construction methods and manufacturing concepts worked out here for composite structural components in high volume production are described. By intensive process chain collaboration in the design, materials and technology fields and also in the supplier network it was possible to integrate the material concepts presented into conventional body construction.

1. Derivation of the lightweight concept for the BMW 7 Series from the expectations of our customers

In the automotive luxury class customers have always been particularly partial to elegance of line with exclusive materials, a high level of driving comfort and an appealing ambience in the interior. Innovations such as driver assistance systems, infotainment, and new control elements will in future be increasingly important selection criteria in the purchasing decision. The buyer perceives the attributes of driving comfort, dynamics and efficiency via an agile but yet comfortable overall vehicle concept with a low center of gravity and good axle load distribution. The complete fulfillment of all legal and safety requirements applicable in the various markets naturally goes without saying for BMW AG.

Despite many new innovations, enhanced comfort features and the fulfillment of additional statutory requirements, the new BMW Series 7 has a lower center of gravity than its predecessor, an axle load distribution of precisely 50:50, and with a 4.5 l fuel consumption is currently the 'CO_2 champion' of its class. A major contributor to this is the fact that a clear weight reduction over its predecessor has been achieved by means of a cross-vehicle lightweight package.

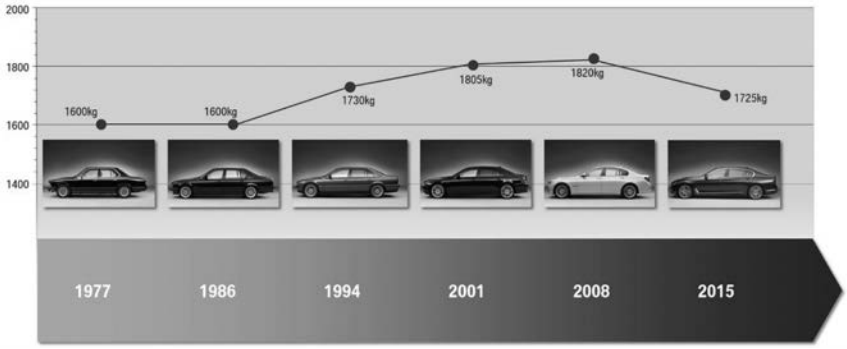

Fig. 1: Weight-savings in the current BMW 740i compared with predecessor models [2]

A central element is the body structure referred to as Carbon Core. Due to the mixed construction approach using CFRP, super high-strength steels and aluminum, the intelligent body concept achieves an increase in both the strength and rigidity of the passenger cell coupled with a markedly reduced vehicle weight.

The lightweight concept also includes a selective use of aluminum in the body and chassis as well as a consistent optimization of details. In addition to the doors, the luggage compartment lid is also for the first time made of aluminum. Rigorous optimization in the lightweight design as regards wheel suspension, brakes and wheels has enabled a reduction of up to 15% in comparison to predecessor models in the unsprung masses so critical to the chassis design and has raised suspension comfort to a new level [2].To this we may add weight-optimized joining technologies and also a close-to-source thermal and acoustic shielding for the engine which has allowed a reduction not only in its overall scope but also in the weight of the insulating materials required. The innovative insulating concept simultaneously ensures another improvement in acoustic comfort.

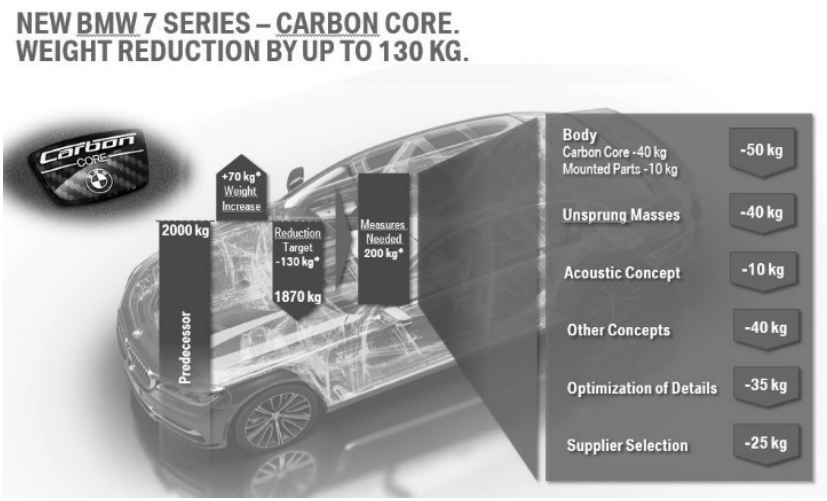

Fig. 2: Breakdown of lightweighting measures in the current BMW 750Li xdrive [2]

2. The mixed construction concept in the body of the BMW 7 Series

BMW is using for the first time in conventional body construction the materials steel, aluminum and CFRP in combination for high-volume production. Four different CFRP and three aluminum technologies were employed to refine the material concept. The result is that the total weight of the body is only 331 kg since these measures enabled a weight reduction of 40 kg [2]. In total, eleven aluminum components and sixteen CFRP components are used in each body. The use of secondary aluminum and the production of carbon fiber using 100% renewable energies has a markedly positive effect on the sustainability balance sheet.

Fig. 3: The Carbon Core body

In addition to the classic functional design of the body for fiber composite materials, from the point of view of the process, material integration represents a considerable challenge in the series development of a mixed construction of this kind.

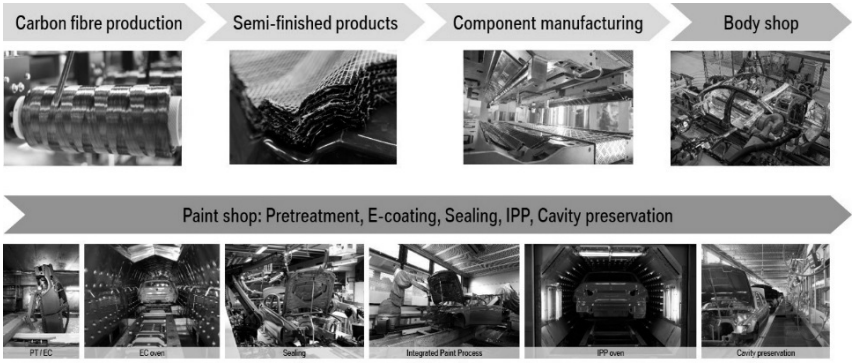

Fig. 4: Process chain for hot-curing adhesives in the Carbon Core production concept [4]

Adequate joining techniques which can compensate for the differences in the linear expansion of materials as they pass through the paint shop ovens are just as important as an ap-

propriate corrosion protection concept. For this reason CFRP primarily lends itself to use in the dry zones of the body where galvanic separation of the materials is in principle ensured solely by the structural adhesives used. While a tightly-clinched rivet concept is applied when joining aluminum and steel, a floating rivet concept is used for the CFRP / metal composite. The reason for this is that the connecting elements must secure the strength of the joint in the curing process during passage through the cathodic painting ovens when materials expand differently. Riveting basically secures the handling strength of the joint until the body has passed through all cleaning baths and has cured in the cathodic dip painting process.

3. Carbon Core: CFRP materials, manufacturing processes and applications

For two decades now BMW AG has been optimizing its processes and construction methods for automotive lightweighting with a view to using composites as efficiently as possible. Figure 5 shows the essential basic geometries, all of which are used in the body design of the 7 Series. Each type of construction has its justification in the sense of a holistic fulfillment of goals in implementing overall vehicle objectives in terms of function, costs and efficiency.

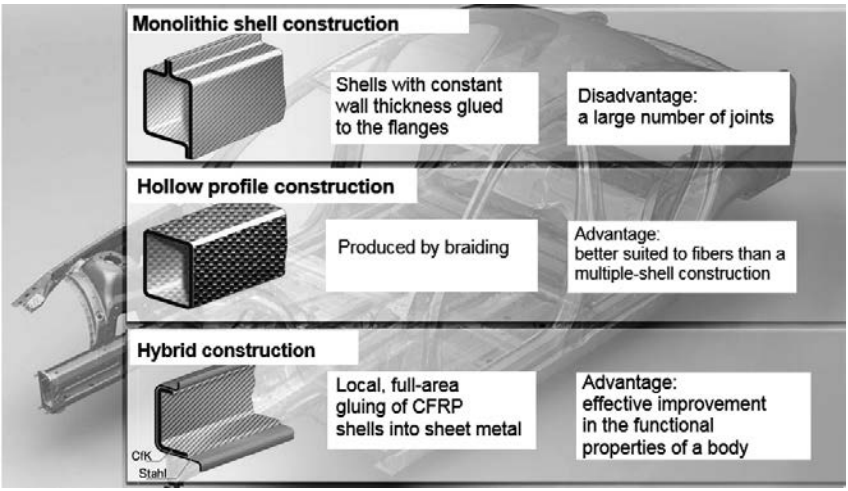

Fig. 5: Basic construction types for composites in automobile manufacturing [3]

The sixteen components are produced using four different technologies. These will be presented in what follows. Figure 6 shows in detail which components are used with which type of construction or technology.

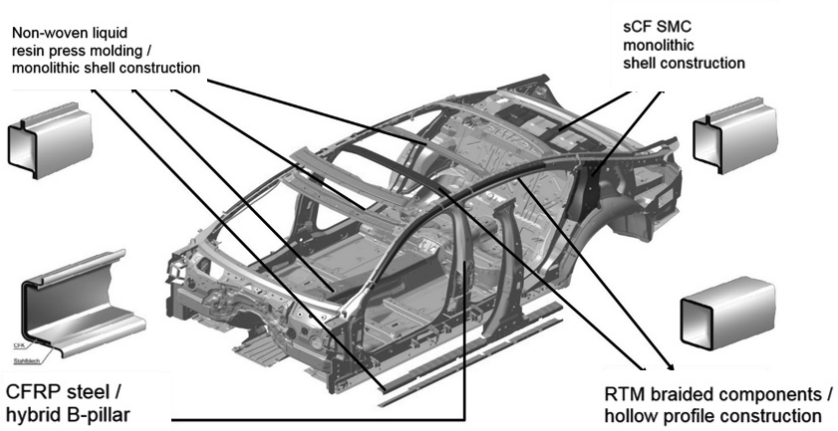

Fig. 6: Technologies, materials and construction methods

A large number of flat and monolithic components are used in the body construction. In fact it was actually for BMW i vehicles that the liquid resin press molding process was developed for these components. In this regard a new production line has been set up in the Dingolfing plant for the new 7 Series. It covers about 19,000 m², has five presses, and in the production concept for the 7 Series the material systems have been optimized with regard to faster cycle times and the downstream milling process. Figure 7 shows an overview of this new production facility, starting from the handling concept for the non-wovens and finishing with the trimming of the components.

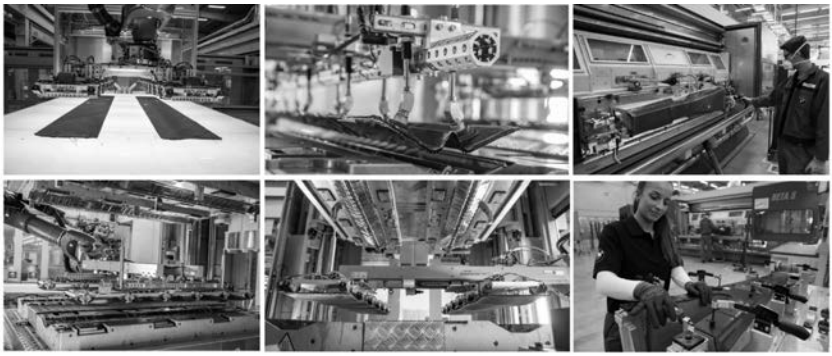

Fig. 7: Production of liquid resin press moldings at the Dingolfing plant [1]

A considerable improvement in the materials utilization ratio for CFRP was also achieved thanks to the optimized processes. In parallel with this, the recycling concepts from the BMW i projects have been developed further on a continuous basis in order to allow the use of textile cuttings in structural components. Here material development and the industrialization team focused on the SMC press molding process which was able to handle the quantities required for high-volume production. Figure 8 shows the process sequence. Reusable materials coming from the textile processes are prepared here to open up the fibers so as to create optimal saturation and orientation as a semi-finished product for the pressing process.

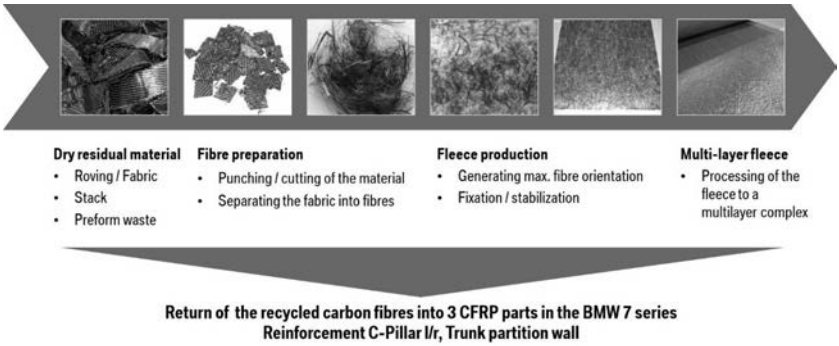

Fig. 8: CF-SMC recycling concept for structural components [1]

The hollow profile construction of the reinforcement of the roof frame and of the B pillar roof arch delivers high rigidity and strength to the body at minimal weight. The challenge in manufacturing feasibility was to reproduce in the RTM process the very long geometries and also flow paths with variable cross-sections. For a production of 500 parts per day, industrialization of the braiding and injection processes was considerably accelerated by, among other things, the use of thermoplastic cores and in addition a process was developed whereby the cores were removed from the RTM part and then recycled. Figure 9 shows the component in combination with the roof frame.

Fig. 9: RTM braided component, roof frame reinforcement

The steel/CFRP hybrid material in the B-pillar makes a significant contribution to passive safety and to lightweighting. In automobile manufacturing the outer part of the B pillar is often made from hot-formed steel. Here a piece of sheet metal consisting of several sections, steel

grades and thicknesses is so shaped by thermal application that a component with wall thicknesses of 1.3 - 2.2 mm is created. By back compression molding with a CFRP prepreg optimized especially for these production processes, the steel walls are in part given additional thickness with CFRP and thus selectively optimized. This effective reinforcement of the component resulted in a saving of 2.8 kg on each side of the body since it was possible to make a considerable reduction in the thickness of the steel walls.

Fig. 10: Steel / CFRP hybrid B-pillar

4. Summary and outlook

The very first use of CFRP as a lightweight material in conventional body construction is, in the context of a high-volume project, a milestone in body development.
Here the synergies resulting from the carbon-intensive designs of the i vehicles have been exploited to make these lightweighting technologies much more flexible and efficient for CFRP utilization in BMW's production network. In the context of the mixed construction con-

cept we have presented, there are wide-ranging opportunities for our external partners in the development of materials and technologies. In future there will be a need, for example, for the simulation and design of improved joint concepts for composite material systems in conventional bodywork. Tooling concepts and production processes suitable for high-volume series require resin systems optimized with regard to cost, cycle times and function, and also faster textile production processes. Other great advances have been made in CFRP recycling. These allow secondary materials to be used in a wide variety of applications and processes in the automotive sector. In the light of collaboration with the external partner network in research and process and material development, prospects are very promising for future applications in body structures.

[1] M. Ahlers, Klaus Sammer, New BMW 7 series – Carbon Core, EuroCarBody October 2015 Bad Nauheim

[2] F. Schek, Wie Leichtbau die Herausforderung in der Luxusklasse meistert – Am Beispiel des neuen BMW 7ers, ATZ Conference Lightweighting, October 2015 Stuttgart

[3] M. Derks, F. Birzle, H. Pfitzer, CFK bei der BMW AG – Heute/Zukunft, VDI-K conference Mannheim, March 2007.

[4] J. Sczepanski, BMW 7 Series – Carbon Core. Challenge to the Paint Shop, Bad Nauheim November 2015

Injection-Molded Carbon-Fiber Grille Opening Reinforcement

Development and production of the 2016 Ford Mustang Shelby GT350 GOR

Dr. **J. J. Laux**, Magna Management, Cham, Switzerland;
L. Vanin, Plastcoat, a Division of Magna Exteriors Corp., Brampton, ON, Canada;
S. Grgac, Magna Exteriors, Concord, ON, Canada;
G. Schalte, Magna Exteriors, Troy, MI, USA

Abstract

First to market, this injection-molded carbon-fiber composite grille opening reinforcement (GOR) for the 2016 Ford Shelby GT350 Mustang utilizes Magna's patented resistive implant welding (RIW) technology. The 20% carbon-fiber PA 6.6 resin offers a weight reduction of 25-30% over current glass-fiber-composite metal hybrid bolsters. The advanced joining technologies utilize electrical currents in the joint line. This unique bonding technology allows for a closed box section to increase the stiffness and structure of the product.

1. Introduction

One of the most iconic performance Mustang nameplates of all time is returning, Ford confirmed recently with the unveiling of the all-new Shelby GT350 Mustang. The Shelby GT350 Mustang is the latest in an all-new line of Mustang fastback and convertible models, including the specially designed 50th Anniversary Edition Mustang. More than 9.2 million Mustangs have been sold since the car's 1964 debut [1].

The original Shelby GT350 introduced in 1965 established Mustang's performance credentials. The all-new 2016 Shelby GT350 Mustang, in which Ford shed weight by using a lot of carbon fiber, is a world-class performance vehicle, designed to tackle the planet's most challenging roads – an all-day track car that's also street legal [2].

The new GT350 builds on Carroll Shelby's original idea – transforming a great everyday car into a dominant road racer – by taking advantage of a dramatically improved sixth-generation Mustang to create a truly special driving experience. Driving enthusiasts behind the wheel of a Shelby GT350 can expect to be treated to the most balanced, nimble and exhilarating production Mustang yet.

Ford engineers took an innovative approach with the GT350. Rather than develop individual systems to perform well independently, every component and shape is optimized to work in concert; balance is the key. While paying rigorous attention to detail, the team pushed the envelope with cutting-edge materials and technologies.

“When we started working on this car, we wanted to build the best possible Mustang for the places we most love to drive – challenging back roads with a variety of corners and elevation changes – and the track at weekends,” said Raj Nair, Ford group vice president, Global Product Development. “Every change we made to this car was driven by the functional requirements of a powerful, responsive powerplant – nimble, precise handling and massive stopping power [1].”

2. Balanced dynamics

The new Mustang platform is the strongest in the history of the brand, with torsional stiffness increased 28% over the previous model. That stiff structure ensures the suspension geometry remains consistent, even under hard driving on back roads and tracks. Front stiffness is further improved on the GT350 with a cutting-edge injection-molded carbon-fiber composite grille opening and optional lightweight tower-to-tower brace. The front track has been increased while spring rates and bushings have been recalibrated all around, with ride height reduced compared to Mustang GT [1].

3. Obsession with detail

“Everything we changed on the GT350 is purely functional-driven design, with the goal of improving the overall performance of the car,” said Chris Svensson, Ford design director, The Americas. “We optimized the aero shape of the car, and then fine-tuned what was left to increase downforce and cooling airflow.” All bodywork from the windshield forward is unique to this high-performance model and up to 50 mm lower than the Mustang GT [1].

“We took the best Ford Mustang yet and massaged every aspect of the car that affects the performance driving experience,” said Jamal Haredi, chief engineer, Ford Global Performance Vehicles. “We tested endlessly on the most challenging roads and tracks in the world, and we believe serious drivers will love the Shelby GT350 Mustang.” [1].

4. Description of the component

Grille opening reinforcements are used to structurally tie the upper rails (shotguns) to the lower frame rails, provide the general shape of the front end, absorb energy during a frontal impact, provide a rigid mount for crash sensor, and facilitate attachment schemes for com-

ponents such as headlights, hood latch, and front fascia assembly. The GOR increases the overall body stiffness at the front of the vehicle and can be easily unbolted to remove the engine if necessary.

5. Drivers for innovation

When Ford chose Magna Exteriors in early 2013 to manufacture a lightweight carbon-fiber GOR for the 2016 Shelby GT350 Mustang (Fig. 1), they clearly specified the basic requirements that had to be met.

These requirements included:

- Significant reduction in weight due to CAFE standards, higher performance and lower total cost of ownership
- Equivalent stiffness, NVH modal targets and dimensional stability
- Deliver impact pulse to sensor
- Need for a package-efficient design to fit reduced space due to 10 mm lowered hood surface that required an all-new design
- Meet under-hood appearance requirements
- Minimize tooling investment.

This is reflected in the use of clearly defined materials and processes to yield a product that is significantly lighter than the previous product, while meeting all quality, performance and safety targets. The use of innovative technologies and lightweight materials had a significant influence on the performance of the vehicle.

Fig. 1: The all-new 2016 Shelby GT350 Mustang

6. Design methodology

Packaging a new, lightweight GOR in a predetermined packaging space, meeting or exceeding the vehicle performance requirements, and maintaining the same mounting locations and features, required an extensive amount of CAE and CAD work using the latest proprietary techniques. After evaluating a number of preliminary design variations, Magna settled on a 'First to Market' two-piece box section, all-plastic GOR design.

Due to fit and function in areas around the shotgun and a 10 mm lowering of the hood to improve aerodynamics, the size of boxed sections was limited in certain areas. This required additional ribbing and higher local thickness in the part. In addition, crash pulse signal management was very important in the development of the new design. The system needs to offer energy transfer to crash sensors in crash events. The stiffness of the structure is able to meet this requirement. Once the crash pulse signal and air bag deployment is understood better, additional weight savings can be achieved.

For the GOR, Magna designed a multi-cavity tool, in which both the upper and lower structures were molded simultaneously. This large-family mold was designed with multiple hot-runner drops to reduce the required clamp tonnage and to improve processing. With this injection-mold tooling design, we were able to capture all design features that were previously in metal. Overall, we were able to realize up to 75% reduction in capital investment due to

the elimination of metal stamping tools and reduced injection-mold complexity in comparison with the previous GOR design. Furthermore, we did not need to rework the tool to achieve the required part dimensions.

7. Manufacturing process

A 20% carbon-fiber-reinforced PA 6.6 resin was chosen as the substrate material to mold the two components of the Shelby GT350 Mustang GOR assembly. This material provides high strength properties at a low material density resulting in lightweight but very strong components. Warpage simulation, coupled with material characterization, was used to predict molded-part warpage. Due to our historically low confidence in warpage simulation, we were driven to build the tool to nominal position. After final processing in the molding operation, the top shotgun mounts exhibited warpage, outboard, of approximately 2 – 3 mm. Final tuning to nominal position, the result of extensive studies on how best to stabilize parts after demolding while still warm, was successful. Warpage study versus actual part exhibited correlation to within 85% accuracy.

To combine the two components into an enclosure assembly, Resistive Implant Welding (RIW) was chosen as the ideal welding process. The welded enclosure forms part of the structure used for stiffness and rigidity necessary to meet hood-latch slam tests. Enclosed geometries are an efficient means of optimizing material usage to minimize part weight and costs.

In designing the part with ability to create closed profiles with the RIW process, Magna Exteriors and BASF used the latest methods of topology optimization to fit the limited and predetermined packaging space based on multiple vehicle load cases. Once the rough CAD shape was determined, Magna Exteriors created a design that was feasible to manufacture. An initial manifold and runner system was designed and a mold-filling simulation was carried out. BASF implemented their proprietary ULTRASIM software to map the fiber orientation of the carbon-fiber composite [3]. This required a large amount of material characterization as an input to generate the map. This map of the fiber orientation through the thickness and over the entire part is used to create a variable material card. The material card is used to complete final simulation to show effects of injection molding on physical part performance.

As already described, the RIW process is a new patented process from Magna which is a key enabler of this success [4] [5]. Destructive testing shows strong cohesive bonding for coupons welded using the RIW process. Conventional methods used to RIW-weld two components together were only partially effective for welding carbon-fiber-filled materials. Issues with stray current leakage across the part were observed during initial weld trials. Alternative

implant materials and processing parameters were developed specifically for carbon-filled resins to ensure a proper weld along the entire part length.
Resistive Implant Welding is a welding process that makes use of placing a consumable wire mesh material between two composite substrates (Fig. 2).

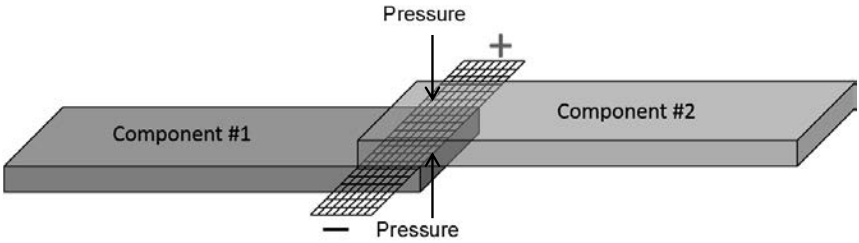

Fig. 2: Resistive Implant Welding (RIW)

A current is applied to opposite ends of the wire mesh while contact pressures are applied above and below the weld joint interface. In a short period of time, the wire mesh heats up due to resistance heating, melting both mating surfaces of components #1 and #2. The pressure applied to the outside surfaces of the joint interface force the molten material of the two components to flow through the wire mesh and mix with molten resin from the opposing surface. After sufficient heat and pressure are applied to ensure resin flow through the mesh, the current is removed from the circuit to allow the molten resin to solidify at the joint interface while still under pressure. The parts are then removed from the welding cell (Fig. 3) following a short cooling cycle. The technological advancements developed for the Resistive Implant Welding are patented [4].

Fig.3: The GT350 GOR Welding Cell

Resistive Implant Welding is a unique process which allows very discrete and controlled heating of mating surfaces. Sufficiently high pressures applied to the joint interface ensure homogenous mixing of both parent materials through the joint interface. Sections through a RIW joint show no joint interface distinction, implying that the joint strength is as strong as parent substrate. A section through an RIW joint is shown in Fig. 4. The three dark circular objects are sections through 0.23 mm diameter wire used in the mesh material at the joint interface. The smaller white lines and dots illustrate the fiber distribution throughout the resin substrate.

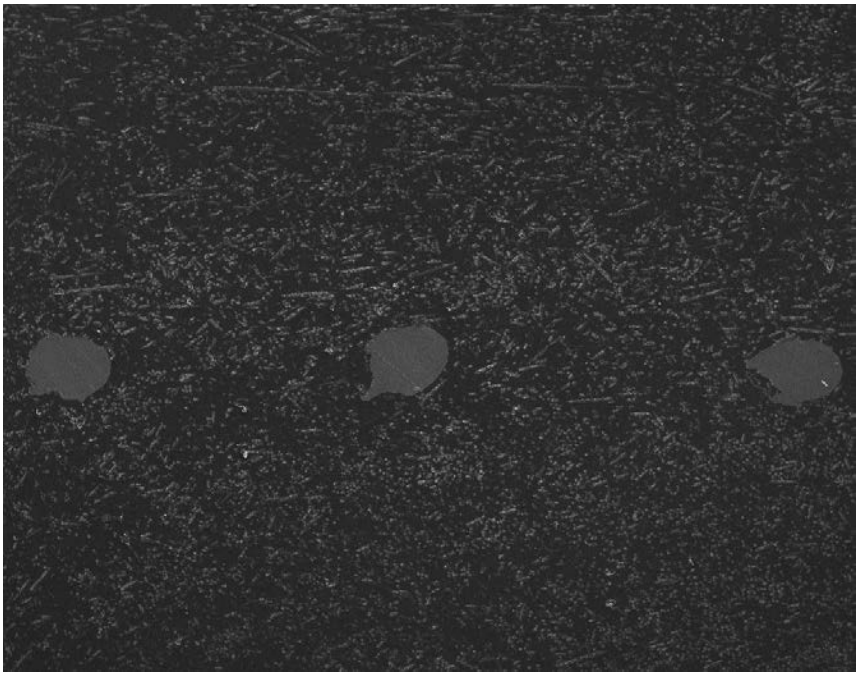

Fig. 4: A section through an RIW joint

Parts such as the GT350 GOR are located relative to one another and held in dimension during the welding process ensuring finished parts are very dimensionally repeatable. Welding fixtures with compliance mechanisms have been developed to accommodate for part warpage ensuring mating surface conform to one another and to nominal dimension. It has been found that enclosed structures welded using RIW are more dimensionally stable and require less adjustment than any other manufacturing process used to generate structure. This includes other common technologies in production today such as Plastic Metal Hybrid.

To speed up the RIW process, an automated mesh dispenser was developed (Fig. 5). The robotic mesh dispenser heat-stakes the wire mesh onto a molded component precisely where the joint interface is designed into the part. This development speeds up the entire welding process so it can be operated in the same cycle time as the injection-molding machine. A complete welding cell situated alongside an injection-molding machine can weld parts as they are removed from the machine. This reduces overhead costs and improves quality because it does not require an offline manufacturing cell which would need extra part

transportation, WIP storage, and additional handling. A patent was granted outlining the technological advancements for automated mesh dispensing [5].

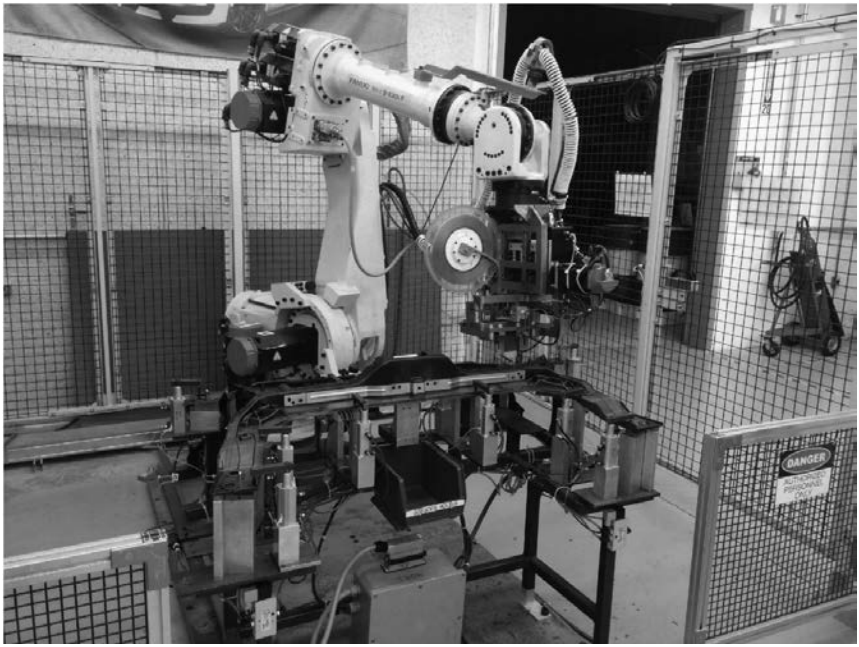

Fig. 5: The Shelby GT350 Mustang GOR Mesh Dispensing Cell

Another key development for the GT350 GOR was establishing methods to accommodate the complex weld geometry. Wire mesh has a maximum bend angle of 45° before the mesh openings become too small to allow molten material to pass through. In order to accommodate the 80° bend angle requirements of the part, a new method of stacking wire mesh at intersection points was developed to allow the desired angle to be incorporated into the part design. This proved to be very effective in the GT350 GOR where a total of 6 different weld circuits were employed to meet complex design requirements (Fig. 6).

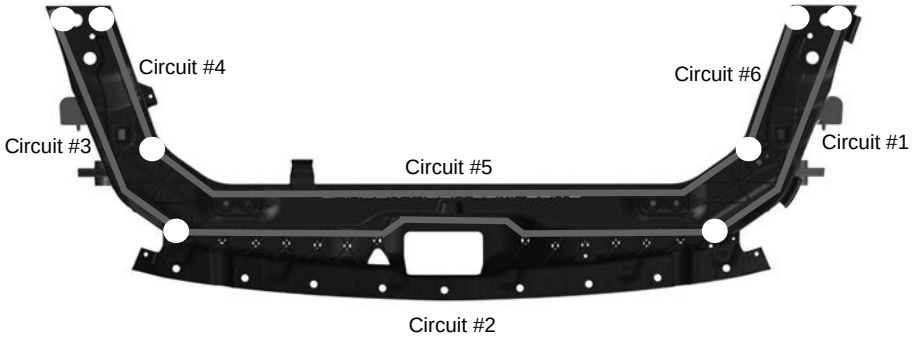

Fig. 6. The 6 different weld circuits required to weld the GT350 GOR.

8. Conclusion

The two-piece box section design and the properties of the carbon-fiber PA 6.6 resin eliminated the need for five steel stampings, while achieving a 24% mass reduction, and improved aesthetics, leading to the elimination of the beauty cover and associated part and assembly costs. The combination of the RIW process and structural application of this resin has not been implemented in a serial production previously. Hence, this is the first component to empoly a two-piece design that is joined using the RIW process and this resin. The previous design utilized five different metal stampings with the injection-molding process commonly referred to as Plastic Metal Hybrid. The secondary RIW joining process required additional fixtures to apply pressure to the two parts during the welding process. The RIW implant was modified to accommodate the carbon-fiber reinforcement in the resin. Carbon-fiber material anisotropic data were developed for higher accuracy in the full-vehicle predictive structural simulations. Direct weight savings of 1.2 kg (24%) versus the previous design, and a total of 2 kg system weight reduction with the elimination of the beauty cover, which provides a more technical appearance as an added benefit, was achieved.

This new GOR for the 2016 Shelby Mustang GT350 has an overall system weight of 3.6 kg versus the previous version of 4.8 kg for direct part-to-part baseline system comparison. Elimination of multiple stamping tools and a simpler injection tool reduced tool capital investment cost up to 75%. Additional efficiencies in the part could be achieved, if more package space were available in the initial design. The current part is designed around an existing vehicle architecture. The key enablers for the weight savings are the Magna patent-

ed RIW process [4] [5], Ultramid A3WC4, a 20% carbon-fiber PA 6.6 resin from BASF [6], and a two-piece box section design.

This solution is transferrable to vehicle platforms with a removable front-end structure (such as a GOR or a Front-End Module) which are currently using all-metal, metal overmolded with plastic, or plastic with bolt-on reinforcements. The RIW process grants the ability to economically create closed profiles using the injection-molding process. Other plastic manufacturing process such as extrusion, and blow molding are limited in shape, detail, dimensional stability and overall part size. This coupled with an ultralight carbon-fiber composite material opens the door to lightweighting many conventional structures such as liftgate modules, cross-members, door modules, front-end carriers, tailgates, step bumpers, running boards, etc. The technology creates the ability to create additional content in these systems.

In addition to meeting stiffness and modal performance of the prior design with stamped inserts, this part offers better aesthetics, resulting in elimination of the beauty cover. All design features which were captured from the previous design were captured in the all-carbon-fiber composite design as well as other additional features, such as the retaining feature for the hood prop rod. An all-composite structure offers better acoustic performance as well, like composite engine mounts, the composite offers an order of magnitude higher coefficient of damping than steel which would translate to less noise for the engine compartment.

The RIW welding process provides an economical and quick method to structurally bond two large injection-molded parts. The RIW process allows two plastic components which are in contact with one another and a conductive implant at the intended weld seam to be joined by passing an electric current via resistance heating. The material properties of the PA 6.6 20% carbon-fiber resin allows the GOR to achieve a weight saving while meeting functional requirements. As a result of the RIW process, designers and engineers can develop a closed-box section in the very limited and predetermined design space. The closed box section was critical in meeting the system engineering requirements. Total cost of ownership for the system results in cost savings for low production volume vehicles, and has the potential to mitigate or lower most of the carbon-fiber cost in the vehicles with higher production volumes. If elimination of the beauty cover is applied to the total system cost, there are additional capital cost savings. Since the new part is mostly made of composite thermoplastic material, it can be reground and recycled.

References

[1] The Ford Motor Company Mediacenter. https://media.ford.com/content/fordmedia/fna/us/en/products/cars/mustang/shelby-gt350-mustang.pdf

[2] The Ford Motor Company Mediacenter. https://media.ford.com/content/fordmedia/fna/us/en/products/cars/mustang/shelby-gt350-mustang.html

[3] BASF ULTRASIM. http://performance-materials.basf.us/ultrasim

[4] US-P 8,361,583 B2

[5] US-P 8,323,444 B2

[6] BASF Ultramid. http://product-finder.basf.com/group/corporate/product-finder/en/brand/ULTRAMID

Determination of thermal damages undergone by plastic parts in stochastic environments: application to air ducts

L. Gervat, **M. Lacuve**, **J.M. Fiard**, **G. Gauge**, **F. Bekaert**,
Renault Technocentre, Guyancourt, France

Abstract

Two important levers to reduce CO_2 emissions are weight reduction and more efficient powertrains. More efficient powertrains means smaller, lighter and hotter engines. High-temperature-resistant plastics are therefore a useful tool to achieve these objectives. However plastics have two limitations: they are expensive and sometimes, despite their ever-higher resistance, they fail to meet the requirements set by classical design methods to replace metal in high temperature environments, i.e. ageing at the maximum temperature seen by parts during their expected lifetime.

This paper describes a more accurate way of estimating the real damage suffered by plastic parts in environments with stochastic exposures, typical of the under-bonnet environment.

As an example of applications, we show how the method allows a secure use of polyamide in a turbo outlet duct.

Plastics: a chance and a challenge

The automotive industry has always been very proactive in embarking on new technologies. This trend has always been highly valued by customers. Until recently improved comfort and safety features were simply added to the previous model, resulting in an ever-increasing weight, compensated by ever-increasingly powerful engines. Growing environmental concerns have changed this situation. Cars must also reduce their CO_2 emissions, hence every effort must be made to reduce weight and to improve the efficiency of powertrains. This means hotter engines because of downsizing, twin-turbo, EGR, stop & start, and so on.

Plastic and composites are helpful in reducing weight, but, unlike metals, plastics are very sensitive to heat: engineers must learn how to use them efficiently in these new challenging environments.

Heat and polymers

Most of the properties of plastics are very dependent upon temperature: modulus, tensile strength, impact strength, CLTE, shrinkage, melting, etc. These changes can be character-

ized and predicted thanks to well-known transitions such as the glass transition or the ductile/brittle transition. But polymers also age. They age physically by reorganizing their amorphous phase and sometimes their crystalline phases. But they also age thermally – in fact, they degrade.

In many – but not all – cases, the degradation consists in a thermo-oxidation which leads ultimately to a dramatic change in molecular weight. These degradations affect – and may be characterized by – many criteria such as visual, mechanical properties, smell, warpage, chemical composition, etc.

In our industry, it is usual to characterize the aging of polymers by their so-called half-life, which is the time at a given temperature after which the polymer loses half of a property. The most common property used to determine the half-life of polymers is tensile strength or unnotched Charpy. Unnotched Charpy is more sensitive to surface degradation, hence can detect degradations at an earlier stage than tensile strength, but on the other hand, it is often less representative of characteristics that may lead to part failure, and is also more likely to undergo larger standard deviations. In this paper, the half-time, or $t_{50\%}(T)$, will refer to the time of continuous exposure after which dumbbells lose 50% of their tensile strength, as measured by ISO 527-2/1A/5.

The effect of thermal degradation on mechanical properties

The degradation starts by a chemical reaction that ultimately often leads to either chain scission or crosslinking. It usually does not significantly impair the macroscopic mechanical properties of the plastic until the molecular weight reaches a critical value, Mc, below which mechanical properties degrade rapidly (**Fig.** 1):

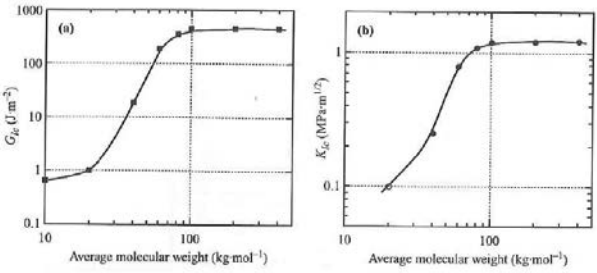

Fig. 1: Effect of the molecular weight on the value of (a) GIC and (b) KIC for PMMA [1]

Depending on the polymer, the threshold usually ranges from 5 to 10 times the molecular weight between entanglements, Me [2] [3]. For polyamide 66, Me was estimated by Wu at 2 kg/mol [4], whereas Mc was estimated between 15 to 20 kg/mol for Mn, *i.e.* 30 to 40 kg/mol for Mw [5].

Thermal degradation mechanisms and kinetic

In the case of polyamide, degradation mechanisms are well documented and start with the loss of a hydrogen in alpha of the nitrogen as illustrated in **Fig.** 2 [6] [7]:

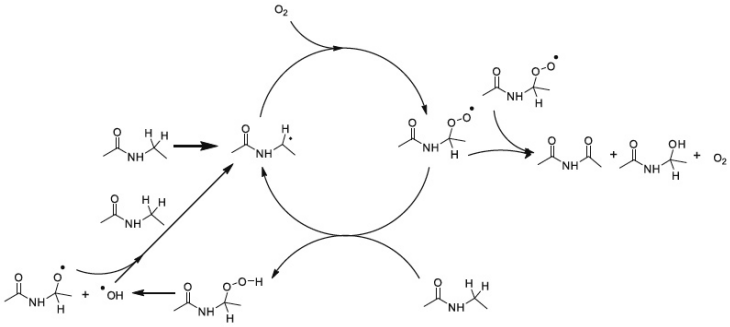

Fig. 2: Polyamide theromoxidation mechanism

From a microscopic point of view, the kinetic of each elementary reaction A → B follows the well-known Arrhenius law: $d[A]/dt = - d[B]/dt = - k [A]^n$, with $k = k_0 e^{-\frac{E_a}{RT}}$

k_0 being a constant, R the ideal gas constant, T the absolute temperature and E_a the activation energy, *i.e.* the energy barrier that separates the initial and the final products (Fig. 3):

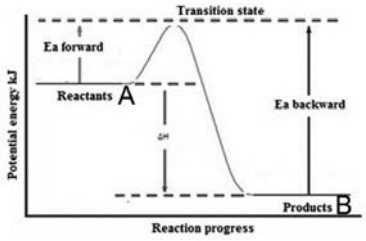

Fig. 3: Schematic representation of the activation energy Ea

Macroscopically, despite the fact that observed phenomena are usually consequences of multiple microscopic causes, it is often possible to follow and predict their evolution with a similar equation. In particular their half-life $t_{50\%}$ which often follows the following equation:

$$t_{50\%} = k e^{\frac{E_a}{R.T}}$$

E_a being the apparent activation energy.

The 'law' is not universal. In particular, the apparent activation energy depends strongly on the characteristics followed [8]. Fig. 4 shows for instance the Arrhenius evolution of several characteristics during the aging of a polyamide 6: each one has a different apparent activation energy!

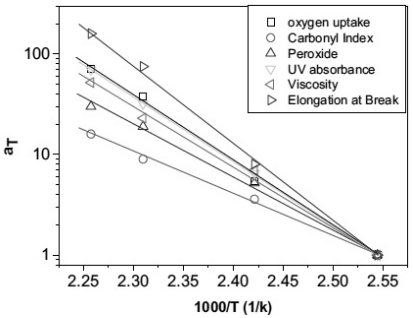

Fig. 4: Evolution of Arrhenius laws as a function of temperature for different methods for a PA6 [7]

However, for many polyamides, if we stick to one characteristic - the tensile strength for instance in our case - the apparent Arrhenius law taken from $t_{1/2}(T)$ is usually well respected (cf. for instance Fig. 5):

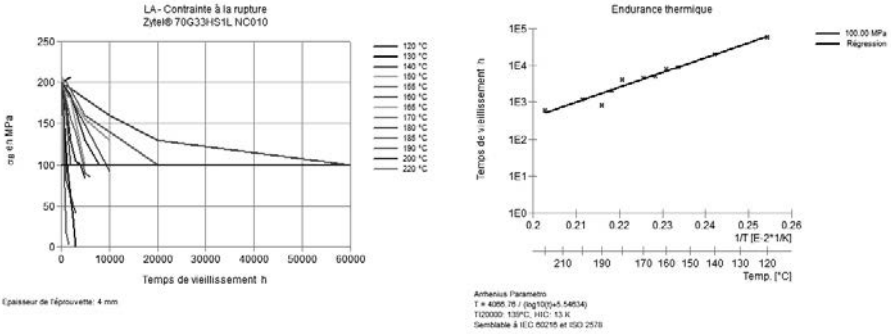

Fig. 5: Arrhenius law drawn from tensile strength data of a PA66-GF30 from CAMPUS® [9]

For many chemical reactions involving covalent bonds, the activation energy is close to 80 kJ/mol. At ~100°C, this value complies with the well-known rule of thumb: +10°C ≅ x 2 t, t being the exposition time (but x 1.5 @ 200°C). For polyamides, all the grades in our study have an apparent activation energy between 55 and 115 kJ/mol.

How to predict thermal degradation in a random environment?

Once the kinetics of degradation of a plastic under exposure to a continuous high temperature is known, how do we take the information into account in order to design under-hood parts subjected to a stochastic thermal environment? Mechanical engineers just need to be sure that the characteristics of the plastic will still be good enough to ensure the part functions up to its required service life.

As it happens, every engineering plastic brochure cites a continuous temperature up to which it is supposedly safe to use the product. For automotive engineers, the continuous temperatures correspond to the maximum temperature at which a part may be maintained for a long and continuous period. But what precisely does it mean for chemists? We have questioned our major raw material suppliers about the definition they use. Table 1 summarizes their answers:

Table 1: Definitions of the maximum continuous temperature according to seven major raw material suppliers to the automotive industry

Supplier	Max continuous T° definition
A	Flex. strength: 50%, 1000h
B	Tensile strength, 50%, 3000h
C	Elastic modulus, tensile strength, tensile elongation, 50%, 2000h
D	Tensile strength, 50%, 20 000h
E	« it depends on the part the material is used for »
F	Tensile strength, 50%, 2000h
G	Tensile strength, 50%, 1000h
H	Tensile strength, 75%, 1000h

The conclusion is that there were as many different answers as chemists questioned. It is therefore necessary to ask for actual data by a known and agreed criterion in order to be able to compare materials on a fair and comparable basis.

From our end, we decided to choose the same criterion as chemist 'B': a polymer is suitable for a continuous temperature T_c, if $t_{50\%}(T_c) \geq 3000h$. Actually, it is very easy to reconcile these data with the traditional way parts designers estimate the thermal requirement of parts *i.e.* an exposure to T_c during an estimated total time of service τ_e (usually 2000 or 3000 hours). This is very straightforward, but is it an optimized way of characterizing the thermal degradation of a polymer? In many cases it leads to a highly over-engineered part, but, in some cases, as we shall see later, it may also paradoxically lead to some risk-taking.

Let $\dot{d}(T)$ be the rate of degradation of the polymer at a temperature T, defined as the ratio of the consumed degradation time to $t_{50\%}$:

$$\dot{d}(T) = 1/t_{50\%}$$

If we let $\tau(T)$ denote the total duration for which the plastic is exposed at any temperature T.The elementary degradation undergone by the polymer at T is thus:

$$d(T) = \frac{\tau(T)}{t_{50\%}(T)}$$

If the part is continuously exposed to a unique temperature T during a total period τ, then the total damage would be:

$$D(T,\tau) = \frac{\tau}{t_{50\%}(T)}$$

When a part is designed to function properly up until the tensile strength of the plastic is halved, then the polymer should be chosen so that $D(T_c, \tau_e) = 1$

Let us now calculate the real damage suffered by the plastic at the end of its lifetime.
With the same notation, the actual damage suffered by the plastic is:

$$D = \int_0^{\tau_e} \frac{dt}{t_{50\%}(T(t))} \cong \sum_T \left(\frac{\tau(T)}{t_{50\%}(T)}\right)$$

Each elementary damage $d(T)$ is easily obtained from half-life times given by apparent Arrhenius plots as shown in Fig. 5.
As an example, Fig. 6 illustrates the calculation for a polyamide 66. Here, for instance, at 170°C, $t_{50\%}$ is 10 000 hours, so if the total time of exposure at this temperature is τ(170), that is 1 000h, then the elementary damage is: d(170) = $\frac{\tau(T)}{t_{50\%}(T)}$ = $\frac{1\,000}{10\,000}$ = 0,1

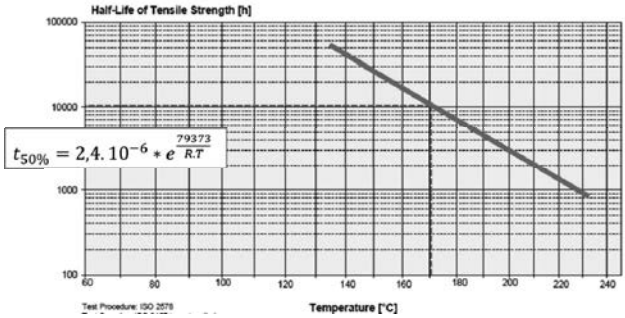

Fig. 6: Example of a half-life calculation at 170°C for a PPA: $t_{50\%}$(170) = 10 000h

Once the elementary damages is known for each class of temperature, the total damage at the end of the life of the part can be estimated by adding together the elementary damage of each temperature segment.

Of course, there are numerous ways of driving a car. Each car will experience a different temperature profile. For some parts, the most severe temperature profile will correspond to a car mostly driven at a high speed on a (German) motorway, whereas other parts will suffer more in a car often stuck in traffic jams of a hot and busy city, and yet others in a car driven by a caravan owner in a mountainous region. To take all these possible situations into account, Renault simulate a large number of the temperature profiles experienced by parts in various situations. The results are called the t-T curves, which give, for each temperature T, the duration $\tau(T)$ during which the part is exposed to this temperature. For instance, Fig. 7 gives the temperature distributions for different profiles of frequent motorway drivers.

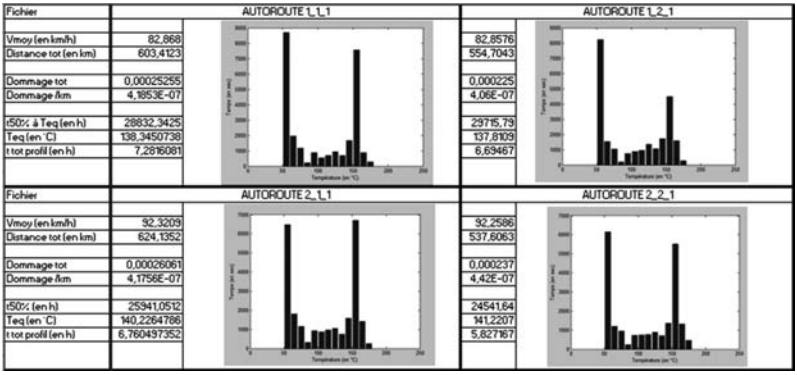

Fig. 7: Temperature distribution for 4 different driving profiles on a motorway

Each profile leads to damage. After calculating the damage for the various other environments, a damage distribution diagram is drawn, from which the percentage of drivers who may reach a given level of damage is estimated (Fig. 8).

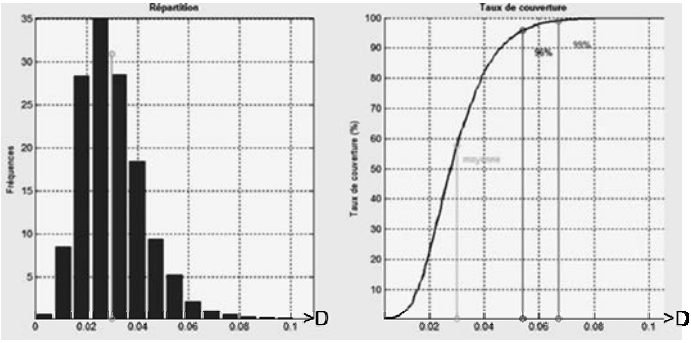

Fig. 8: Damage for various combination of profiles

Here again, when a part is designed to properly function until the tensile strength of the plastic is halved, then the polymer should be chosen so that D = 1 for 100% of the profiles. If D < 1, the part has been over-engineered, whereas if D > 1, the part may fail before its expected life duration. In the example given in Fig. 8, the 1% harshest drivers will use only 6.7% of the thermal lifetime of the plastic, *i.e.* 1/15 of the total time the part could have stayed in operation.

On the other hand, the damage calculated with the traditional approach at T_c during τ_a would give:

$$D(T_c, \tau_a) = \frac{\tau_c}{t_{50\%}(T_c)} = 2.1$$

This plastic would therefore not have been accepted for this part, whereas the more refined analysis has shown it is in fact over-engineered 15-fold.

Experimental

To test the theory, we retrieved two turbo air ducts in glass-reinforced PA66 and PPA: 196 thousands of kilometers for the PA66 and 65 thousands of kilometers for the PPA. We asked Pr. Lemaire and his team at CNEP to analyse them, and to compare them to a virgin material but also to the same material aged in a controlled way (in an oven at set temperatures).

The methodology used was described in a paper presented by PSA a few years ago to SFIP [10]. The analysis is based upon quantitative measurement by infra-red spectroscopy (IRTF-

PAS and µ-IRTF) of the carboxylic acid concentration across the thickness of aged samples, as shown in Fig. 9 and Fig. 10.

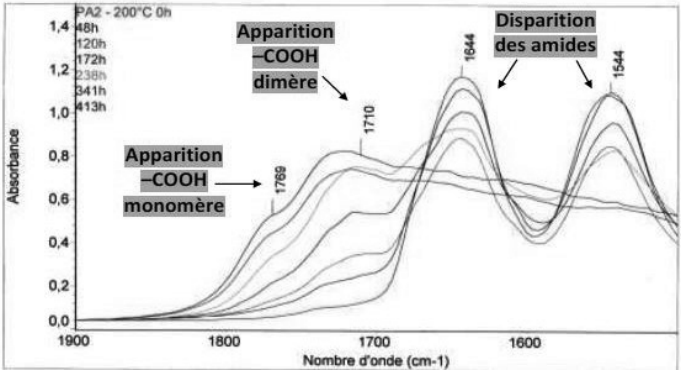

Fig. 9: Evolution of characteristic bands during PA66 ageing [10]

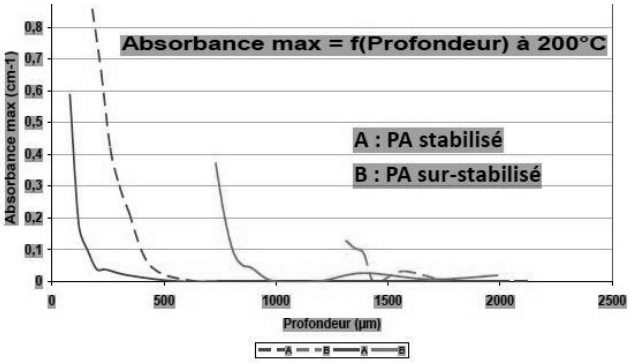

Fig. 10: Carboxylic acid absorbance across the thickness of different types of polyamide samples aged at 200°C

The study is not yet finalized, but the first infra-red profiles are already available. Fig. 11 shows the complete µ-IRTF spectra obtained by transmission through ten 40µm microtomic slices sampled through the thickness of the aged (196,000 km) air duct made of PA66-GF20: As expected, the meaningful evolution is concentrated in the 1500-1800 cm^{-1} region, as detailed in Fig. 11: The increased concentration of carboxylic acid is significant but limited to the first 40µm of the duct (cf. bands at 1710 cm^{-1} (dimer) and at 1771 cm^{-1} (monomer) – the band at 1730 cm^{-1} being attributed to esters of possibly burnt oil).

Fig. 13 shows the measurements taken on the 65,000 km PPA duct. The oxidation signature of the 1710 cm-1 carboxylic acid band is already detectable on the surface, but is almost undetectable in the 40µm thick first microtomed layer. Pr. Lemaire estimates that the IRTF-PAS used in these measurements may analyse the first 10 to 15µm of the surface. So it is estimated that the extent of oxidation was limited to this thickness.

Preliminary results on the PPA, suggest that this thickness of oxidation is obtained approximately at 1/50 of τ_e, so a rough estimation of the degradation factor D would be around 2%, in perfect accordance with our prediction above.

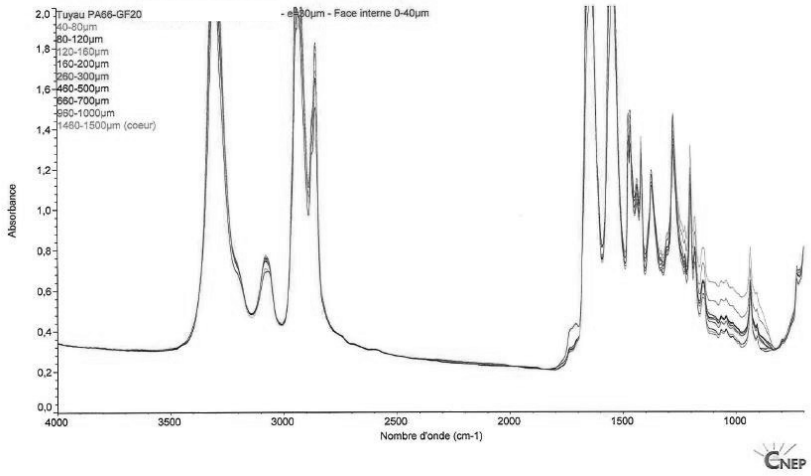

Fig. 11: µ-IRTF across the thickness of a 196,000 km PA66-GF20 turbo air duct

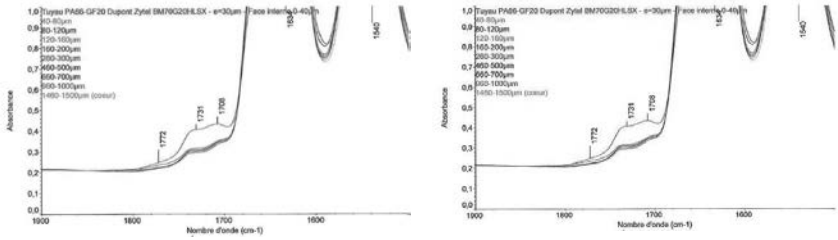

Fig. 12: IRTF-PAS and µ-IRTF of respectively the internal surface and the first 40µ of the aged PA66 air duct (196,000 km)

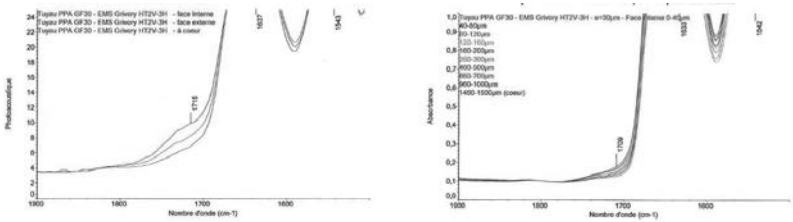

Fig. 13: IRTF-PAS and µ-IRTF of respectively the internal surface and the first 40µ of the aged PPA air duct (65,000 km)

Discussion

Depending upon the polymer and the temperature range to which it is exposed, the predominant degradation mechanism may come from a unique chemical reaction within the entire temperature range considered, but it may also vary depending upon the temperature. Pr. Celina has for instance calculated that the thermal degradation of polypropylene follows two very different Arrhenius processes with a crossover temperature (temperature at which the two processes equally contribute) of 83°C [10]. In such cases, a sound lifetime prediction requires a slightly more complicated mathematical treatment.

Polyamides may also have two or three different Arrhenius processes along the usual range of temperatures observed under the bonnet for plastic parts, and curvature may occur at high and low temperatures (Fig. 14). A similar approach would therefore be beneficial. However, it would be more difficult to apply and the extra gain would not be so significant. Indeed, at low temperature, the actual kinetic is often higher than extrapolated from the Arrhenius line of the middle temperature range, but the amount of degradation undergone is negligible. At high temperatures, the extrapolation also sometimes deviates from reality, and it leads to an

overestimation of the damage, resulting in an extra safety margin. However, this margin is negligible compared to the 30-fold over-engineering found when comparing the Arrhenius to the traditional T_c-based approach.

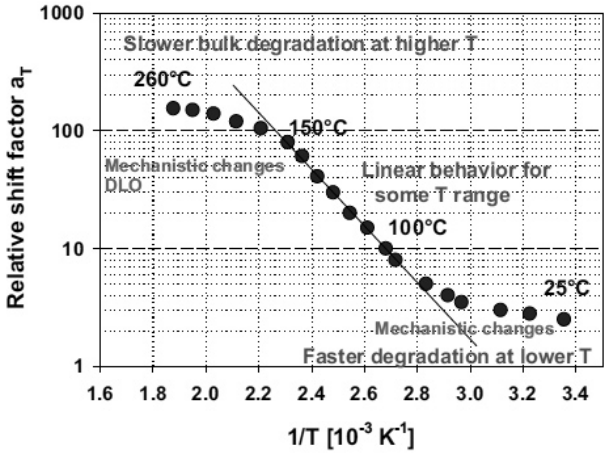

Fig. 14: Kinetic of polyamide degradation as a function of reciprocal temperature [8]

Among polyamides that may exhibit several Arrhenius processes are the ones stabilized with a recently introduced so-called 'shield technology'. This technology is based on the idea of forming a crust on the surface that can act as a barrier against oxygen. To achieve it, chemists add various additives which aim at triggering the formation of enough radicals at a given temperature to favor crosslinking over chain scission (cf. Figure 2). This technology was gradually introduced during the last decade by several major polyamide suppliers. It works very well for pass in the traditional heat-aging test at very high continuous temperatures. However, at slightly lower temperatures, or under cyclic conditions more representative of real life, the additives might adversely create radicals that would increase the rate of degradation. A later publication will show that even with such singular products, the Arrhenius approach can be used to detect and prevent possible early degradation at lower temperatures.

Conclusion

Traditional material testing based on a continuous exposure to a single high temperature may be misleading if applied in random environments such as under-hood parts.

It has been demonstrated that an Arrhenius approach is a safe alternative which allows a more precise selection of polymers according to the real thermal needs of parts.

References

[1] L. Monnerie, F. Lauprêtre and J.-L. Halary, Polymer Materials, Wiley, 2011.

[2] H.Kausch, Matériaux polymères. Propriétés mécaniques et physiques. Principes de mis en oeuvre, Laussane : Presses Polytechniques et Universitaires Romandes, 2001 .

[3] B. Fayolle, *Polymer,* vol. 45, p. 4323–4330, 2004.

[4] S. Wu, *Journal of Polymer Science : Part B: Polymer Physics, 27, 723,* 1989.

[5] C. El-Marzy, Thesis : "Durabilité de produits innovants de robinetterie en polyamide 6,6"» 2013.

[6] P. Cerruti, «Thermal-oxidative degradation of polyamide 6,6 containing metal salts» 2010.

[7] P. G. W. Dong, «Influence of temperature on thermo-oxidative degradation of polyamide 6 films» 2010.

[8] M. Celina, «Review of polymer oxidation and its relationship with materials performance and lifetime prediction» 2013.

[9] «CAMPUS(r),» [on-line]. Available: http://www.campusplastics.com/campus/en/datasheet/Zytel%C2%AE+70G33HS1L+NC010/DuPont/52/05ca06e9#page26336.

[10] M. Celina, «Accelerated aging and life time prediction: Review of non-Arrhenius behaviour due to two competing processes» 2005.

Simulation of plastics in crash conditions at Volkswagen

Requirements relating to safety-relevant plastic components

Dipl.-Ing. (FH) **E. Glas**, Dr.-Ing. **L. Greve**,
Dipl.-Ing. **O. Steiln**, **J. Čopík** (M.Sc.),
Dipl.-Phys. **R. Flögel**, Volkswagen AG, Wolfsburg

Abstract

Simulations have in recent years become a central development tool for almost all the requirements relating to the vehicle but especially for the development of passive safety properties. Unfortunately the mechanical behavior of plastic parts under dynamic loading is in some cases not yet adequately reproduced in simulation. This makes the computational design of safety-relevant components more difficult; too many tests are still required to validate the simulation models. There are three main reasons for this. Firstly, the material models used to date are inadequate. Secondly, the variation in material properties during the production process is still not taken sufficiently into account. Thirdly, even today there are still no adequate tolerances for mechanical parameters of the plastic parts and the raw materials.
Volkswagen is therefore working on a program whose goal is to solve these problems for crash-relevant plastic components. To achieve this objective, the automotive and plastics industries need to work together shoulder to shoulder.

1. The problem

Deformation and fracture behavior are still inadequately mapped in simulation for plastic components in crash loading cases. This is however necessary for the design of, for example, the greenhouse for compliance with FMVSS 201. Fig. 2 shows a section through the model of head impactor upon impact with the headliner and the deformation element behind it. The main stress distribution in the PP deformation element in the simulation is shown on the left-hand side of Figure 2, while the photograph on the right shows the fractures in the deformation element after the test.

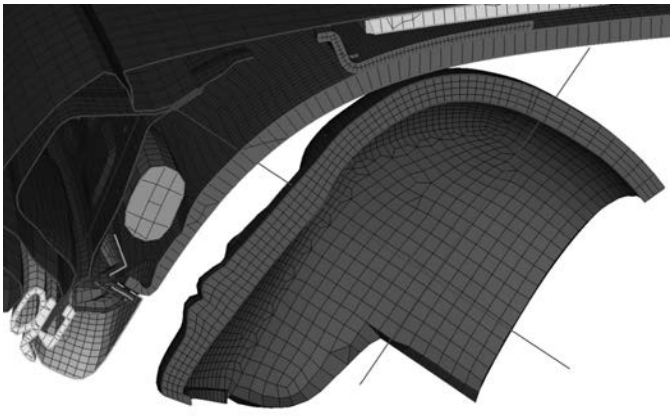

Fig. 1: Head impact FE simulation

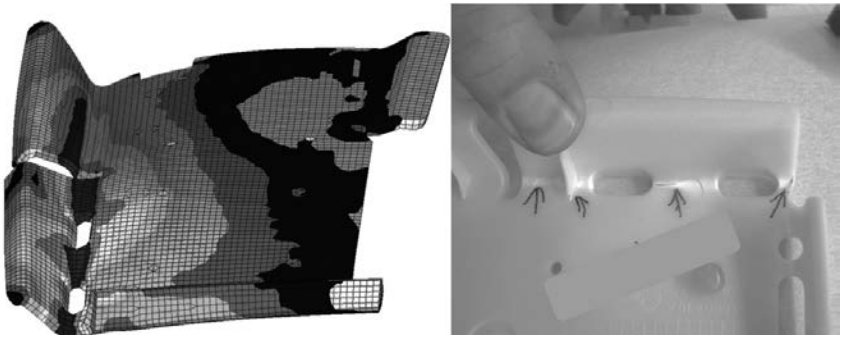

Fig. 2: Deformation element on head impact, left: in the FE model, right: after the test

With the material models currently used, the fracture behavior of the ribs and thus too the impactor delay relevant to evaluation are often not sufficiently precise. For this reason a large number of tests are required to adjust the simulation models. Similar problems arise in other crash disciplines, such as, for example, in pedestrian protection in the impact with the leg impactor or in door panel models in side-on collisions.

The different fracture behavior in test and in simulation is essentially due to the underlying material model used for the plastic not being suitable for loads of this kind. Material scatter and production-related influences are further uncertainties which make it difficult to design safety-relevant components for the crash scenario.

Analysis of the situation reveals three main problem areas and thus fields of action:

1. Material	2. Component	3. Requirements
• Assumption of incompressibility analogous to metals is often inadequate for plastics • No comprehensive characterization of materials: characteristic values determined only via tensile or bending tests • Tension-compression flow asymmetry ignored • Failure as a function of the load state reproduced inadequately	• Discretization • Production influences: - Weld lines - Fiber orientation	• Inadequate description of the mechanical properties of materials and components in delivery specifications • Tolerances of the material properties not adequately defined • No uniform test specifications

2. Material characterization and modeling

Discrepancies between test and simulation are attributable not only to discretization but also to the underlying material model for the plastic. The previously used standard material model (MAT 103 in Pam-Crash) was designed for steel. Here the stress-strain characteristic is determined in standardized tensile or bending tests at different strain rates. As a flow condition the validity of the yield stress hypothesis of *von Mises* is presumed, which in simple terms assumes that flow arises from the variables of the stress deviator irrespective of the hydrostatic stress state. In combination with the assumption of an associated flow which results in a plastically incompressible deformation behavior, a model of this kind is a great oversimplification for typical non-reinforced thermoplastics. For the talc-filled thermoplastic (PP/PE-TD16) tested in Fig. 2 there is a marked asymmetry of flow behavior under tensile and compressive stress. The pronounced volume dilation observed calls for a compressible plasticity model with a pressure-dependent flow rule. An isotropy of the mechanical properties resulting from the injection process is equally visible.

A first material model for implementing these properties was developed in 2011 for the modular material model (MMM) of Volkswagen Group Research and continuously expanded. A summary of the plasticity model taking into account tension-compression flow asymmetry, volume dilation and anisotropic flow behavior is given in [1]. The model has been expanded to take into account the marked plastic strain rate stabilization and the damage (softening) induced by volume dilation.

The model parameters were calibrated on the basis of a comprehensive material characterization of talc-filled polypropylene / polyethylene (PP/PE-TD16). An extract from the test results (solid curves) is shown in Figure 3. The other curves represent the simulation results using the standard model (dotted lines) and the newly developed isotropic model in MMM (dashed lines). With the new model all tests can be simulated with very close agreement. In many tests the standard model does show, however, significantly larger discrepancies with regard to the test curves.

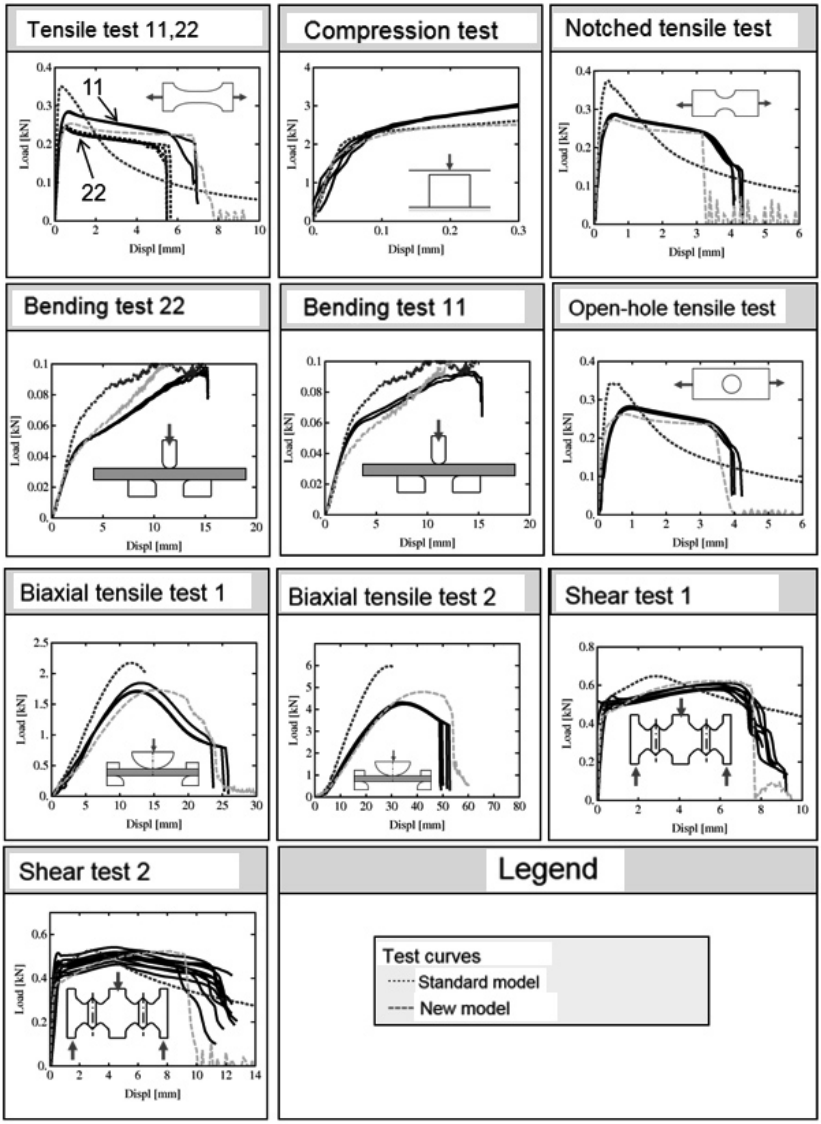

Fig. 3: Extract from the test program

The discrepancies observed when using the incompressible standard model are also shown in Fig. 3. In the test only a moderate necking of the test specimen cross-section due to volume dilation was observed. Unlike the newly developed model in MMM, the incompressible standard model, which was calibrated to close agreement under a pure bending load, cannot reproduce this deformation mechanism.

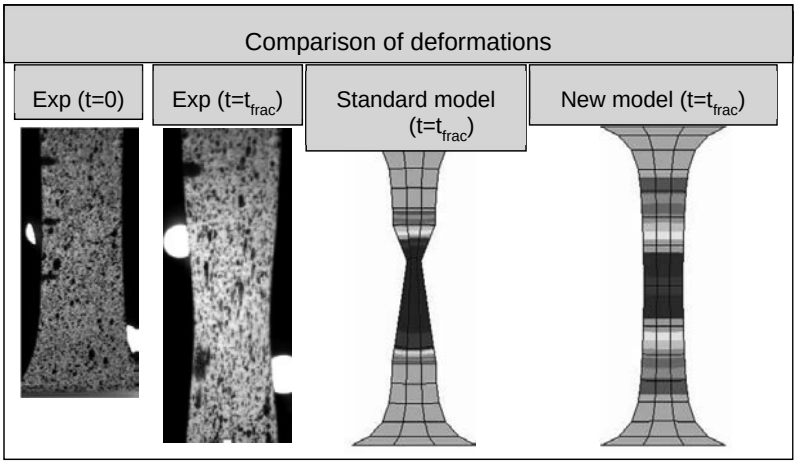

Fig. 3: Comparison of necking of test specimens in the uniaxial tensile test at the time of failure

3. Inclusion of production-related influences in the component model

The properties of plastic parts are determined by the properties of the raw material, by processing and, depending on the material, also by ageing. It is important to take processing into account if an accurate forecast of the fracture behavior of plastic components under crash loading is to be made. In many cases the assumption of homogeneous material parameters throughout the component model does not reflect the real heterogeneous distribution of strength properties in plastic components.

Plastics produced by injection molding are heterogeneous and anisotropic since the microstructure forms with local differences in the component during the processes of injection and cooling (see, for example, [3]). The distribution of the properties in the component is here influenced by pressure, temperature, geometry and gating. The scattered strengths and elongations at break associated with this are measurable using tensile specimens taken from different parts of the component. Elongation at break is considerably lower in particular

where flow fronts meet during injection (see, for example, [5]). For this reason, component failure in crashes often starts from the weld lines.

Due to the fiber orientation, anisotropy is even more marked in short-fiber-reinforced plastics than in unreinforced plastics. Both across and along the fiber orientation these composite materials exhibit considerable differences in material behavior (see Fig. 4). Due to local variance in flow rates and directions during the injection process, the fiber orientation and thus the strength properties in the component are also heterogeneous.

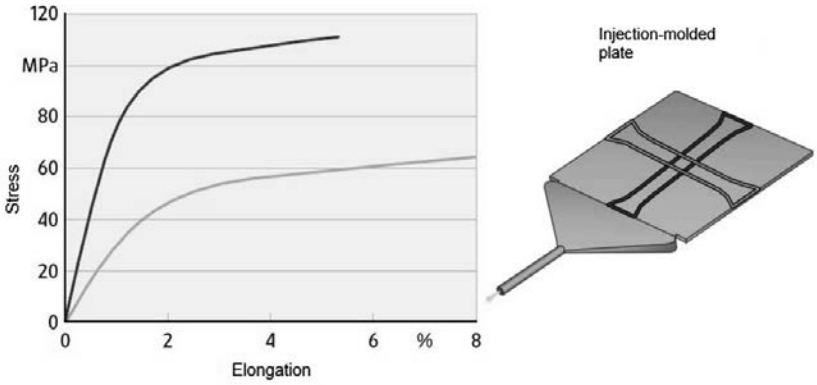

Fig. 4: Stress-elongation behavior as a function of fiber direction [4]

Using injection-molding simulations it is possible to localize weld lines and fiber orientations in the component. Existing interfaces to the FE solvers for structural analysis permit local assignment of different material properties in the component model. Material properties can therefore be overlaid on the FE mesh as a function of the fiber orientation.

Bends, joints, sudden thickness changes and voids create notches in the component which under loading lead to high tensile stresses. Cracks thus frequently start from the notch roots. The element edge lengths of the FE model are downwardly limited in order to obtain acceptable computing times for the crash simulation. This limitation means that sharp-edged radius forms are represented too coarsely to allow a precise calculation of the notch stresses actually occurring. They are underestimated. The consequence of this is that cracks cannot be reliably forecast in the crash model.

Current research activities aimed at improving failure prognosis include the analysis of alternative 3D discretization possibilities with increased mesh fineness as well as the identification of possibilities for model regularization with a given mesh fineness in current vehicle crash models.

4. Testing the material model using the example of a deformation element for head impact

To test the new material model, drop tower tests were carried out in which a spherical impactor strikes a deformation element (see Fig. 5). The acceleration values are measured in the impactor. The diagram shows the mean acceleration curve from the tests (solid line) together with the simulation curves which were calculated using the MMM with different mesh fineness. The dotted line is based on a discretization with a mean edge length of 1 mm while a mean edge length of 0.5 mm is associated with the dashed line.

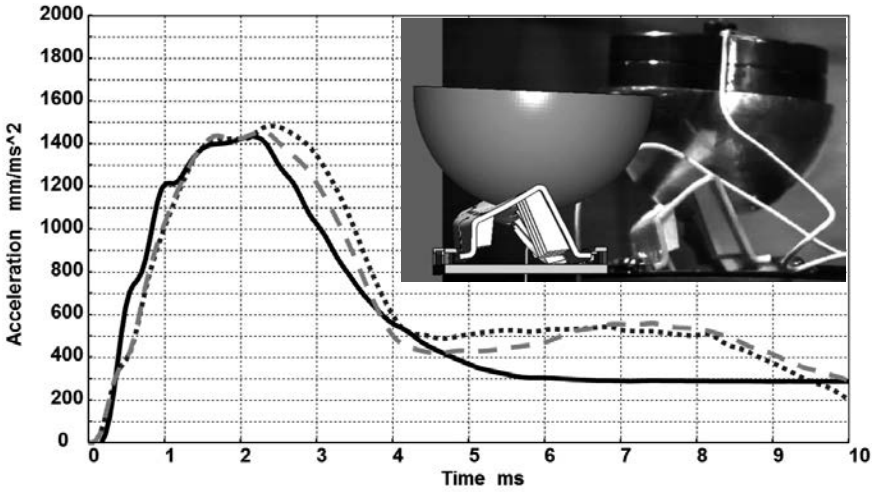

Fig. 5: Comparison between mean acceleration curves, test (solid line) and simulation with different mean element edge lengths (dotted: 1 mm, dashed: 0.5 mm)

Both in the acceleration curves as well as in the corresponding fracture patterns (see Fig. 6) the simulations are in good agreement with the test. Fracture failure at the rib root is in particular only reproducible by the new MMM. Rib failure starts on the acceleration curves after

passage through the maximum. Here the MMM curve fits the test curve better than the standard model. The finer discretization (dashed line) brings an additional improvement.

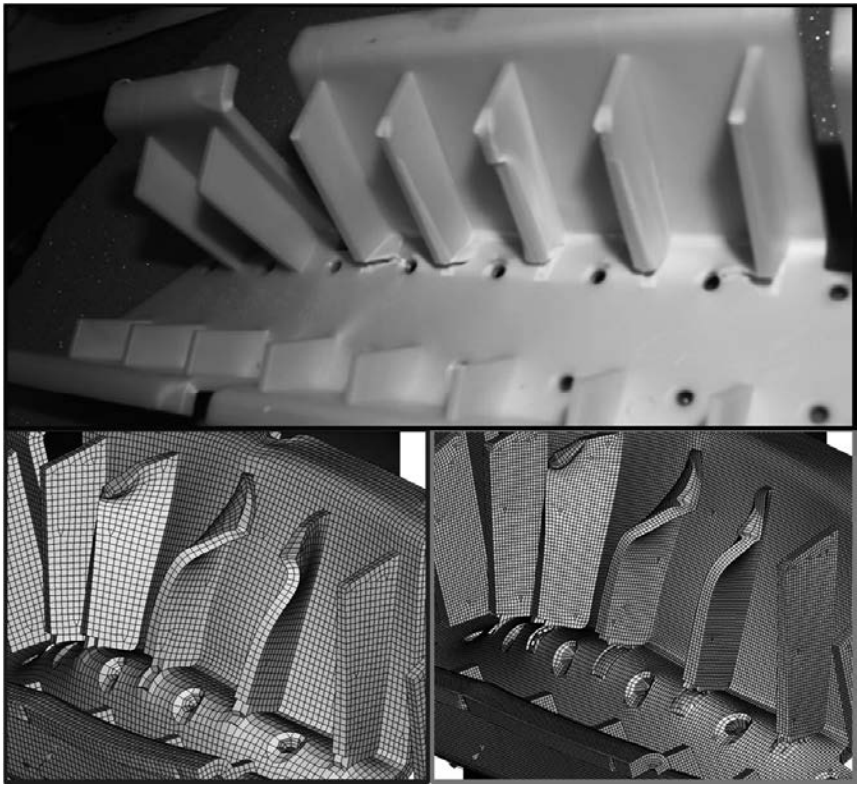

Fig. 6: Comparison of the fracture patterns between test and simulation with different mean element edge lengths (bottom left: 1 mm, bottom right: 0.5 mm)

From the comparison of acceleration curves between test and simulation it is however also clear that from about 5 ms recovery is not yet represented with enough accuracy. There are already a number of partial approaches to improving rheological models which take thermo-mechanical, visco-elastic and visco-plastic properties into account. Implementing the mechanisms relevant to crash simulation in a material model framework which is usable in industry is the subject of current research work.

5. Requirements applicable to plastic components

The mechanical requirements which Volkswagen places on plastic components are poorly defined today with regard to the crash design. Technical delivery specifications only lay down minimum values for a few parameters. These figures are based on simple static tensile tests. This means that a precise computational design of the components is not possible.

As stated in Chapter 2, a more comprehensive characterization of the plastic is needed for the crash calculation (see Figure 3). This means that the corresponding test specifications for crash-relevant components must be standardized. A good starting point could be the test conditions defined at VW for the MMM.

For the aforementioned reasons, the plan is for sensible limits for characteristic values relevant to design to be defined in the technical delivery specifications. This requirement should apply in particular to components which are designed for the crash situation.

6. Agreement of the automotive industry to new standards

Since different manufacturers frequently use the same plastics, each automaker basically has the same requirements for material data for dynamically stressed components. To successfully tackle the major job of characterizing the large number of plastics used it would certainly make sense for all parties to work together on this issue.

It would be helpful if tolerances for mechanical characteristics were jointly specified and test configurations uniformly defined for characterization of the materials. In this way it would also be possible for the plastics industry to supply standardized data along with each material. Constantly changing test configurations for different users could thus be avoided. The economic advantage would be significant for all parties involved.

References

[1] Greve, L., Fehrenbach, C.: Mechanical testing and macro-mechanical finite element simulation of the deformation, fracture, and short circuit initiation of cylindrical lithium ion battery cells, Journal of Power Sources, Volume 214, 15 September 2012, pp. 377-385, ISSN 0378-7753, http://dx.doi.org/10.1016/j.jpowsour.2012.04.055.

[2] Koukal, A.: Crash- und Bruchverhalten von Kunststoffen im Fußgängerschutz von Fahrzeugen. Dissertation TU Munich 2014

[3] Hellwege, K.-H., Knappe, W: Die Festigkeit thermoplastischer Kunststoffe in Abhängigkeit von den Verarbeitungsbedingungen. Research reports of the State of North Rhine-Westphalia, Cologne and Oblagen: Westdeutscher Verlag 1960

[4] Glaser, S.: Integrated simulation of crash-loaded fiber-reinforced thermo-plastic parts. EuroPam Prague 2008

[5] Kolling, S., Seelig, T., Sun, D.-Z.: Verbesserung der Crashsimulation von Kunststoffbauteilen durch Einbinden von Morphologiedaten aus der Spritzgießsimulation. Forschungsgesellschaft Kunststoffe e.V. Report 2011

Development of a crash simulation method for long-fiber-reinforced thermoplastic (LFT) components based on fiber orientation from mold-filling simulation

L. Schulenberg, **J. Lienhard,**
Fraunhofer Institute for the Mechanics of Materials IWM, Freiburg;
Dr. **D. Niedziela, I. Shklyar, Dr. K. Steiner**,
Fraunhofer Institute for Industrial Mathematics ITWM, Kaiserslautern;
Dr.-Ing. **B. Lauterbach,** Adam Opel AG, Rüsselsheim

Abstract

The development of a method for the crash simulation of components made of long-fiber-reinforced thermoplastics (LFT) can be divided into three parts. First of all, a process simulation is developed which can locally correctly predict fiber-orientation distributions and fiber-volume concentrations. For this purpose a consistent model of the dynamic equations has been developed for the filling simulation, fiber-concentration change and fiber orientation of long-fiber-reinforced thermoplastics which reproduces the coupled interactions in the rheological model given by analysis. One implementation of the model is on the CoRheoS simulation platform and is validated on the basis of extensive experiments. Next, an injection-molded LFT material from the Sabic company is characterized by experiment on both the micro and the macro levels. Various methods are applied to analyze the microstructure. Fiber-orientation distributions and fiber concentrations are however determined primarily with the aid of computer tomography (CT). Mechanical characterization is carried out in macroscopic tests with different stress states and strain rates. Here local differences within a sheet were investigated more precisely on the one hand, and on the other the removal positions of the specimens were selected such that the results were on average representative of the properties of the injection-molded sheets. Special sample shapes suitable in particular for dynamic testing were used for the entire characterization. In the case of the shearing tension sample, its shape was a new material-specific development. Following parametrization the basic mechanical properties are included in a material model. A material model is presented which can be applied efficiently in crash simulations due to its combination of an analytical micro-mechanical approach to the approximation of anisotropic elastic stiffnesses and a

phenomenological description to reproduce plastic and visco-elastic properties. Effects such as damage and failure are also taken into account with the aid of an isotropic approach. It was implemented in the finite element code LS-DYNA. The parameters of the newly developed material model were calibrated by inverse simulation with the help of the macroscopic characterization tests. The method developed is validated by simulation of the entire process chain from injection-molding simulation, transfer of fiber-orientation distributions and fiber-volume content to the FEM model (mapping) and finally to the crash simulation using a series component as currently installed by the car manufacturer Daimler AG. The result is compared with experimental test data. In addition, the crash test is simulated with an isotropic material model and the results compared.

1. Introduction

Due to their high strength coupled with low weight, long-fiber-reinforced thermoplastics (LFT) have a great potential as lightweight materials, especially in automotive engineering. The large number of possible combinations of fiber and matrix materials gives a broad spectrum of material properties which is expanded even further by the variability of fiber volume content and fiber length. Special challenges emerge here in the development of crash-relevant components made of LFT, such as bumpers, front-end or door modules, which must meet demanding requirements as regards their crash safety. With LFT, the relevant characteristics, such as strength and elongation at break, depend very greatly on the local fiber orientation [1]. In the case of a load perpendicular to the fiber orientation, the effect of fiber reinforcement actually almost disappears entirely. The problem is that the distribution of fiber orientation depends not only on the production process but also on the component geometry and can only be determined experimentally by great effort. The analysis of microsections or investigations of computer tomograms involve a great deal of expense and for this reason are only feasible for individual locations and not the complete component. There is thus a great need to develop a computational method which allows a reliable, predictive evaluation of LFT components under dynamic loading.

Simulation of injection-molding processes

Modeling the fiber orientation is based on the Folgar Tucker equations which have also been used successfully for years for short-fiber-reinforced plastics. All commercial products on the market are based on this approach. However, there are additional effects, such as fiber-fluid (feedback to viscosity), fiber-fiber and fiber-wall interactions, which are dominant with long

fibers but which can mostly be ignored with short fibers. Preliminary work at the ITWM was able to show that these effects can be modeled by the addition of suitable potential terms [2]. However, all these interactions lead to local segregations or dilutions – in other words, to a local change in fiber concentration – which have a considerably more decisive effect on the resulting structural-mechanical properties and on the crash behavior than do minor deviations in fiber orientation. There are modeling attempts for separations of suspensions and these are all essentially based on the so-called Phillips model [3]. However, these models deal with round particles and not long fibers.

Material modeling of long-fiber-reinforced thermoplastics

Taking fiber-orientation distribution from mold-filling simulation into account in calculations of LFT components using commercial FEM codes has so far not been possible due to the lack of a validated material model which covers not only anisotropic but also non-linear properties with the same computational effort as typical elasto-plastic material models. The problem is the need for micromechanical approaches which send CPU processing times soaring. In the material model which has been developed here these micromechanical approaches are only used for predicting the effective elastic stiffness tensor. One benchmark with these so-called analytical homogenization methods for a long-fiber-reinforced plastic has recently been published in [4] , taking SMC (sheet molding compound) as an example. The material model developed here applies the analytical homogenization method according to Mori and Tanaka [5] while using the fiber-orientation distribution from process simulation according to Advani and Tucker [6] and has emerged as the best approximative method. For this reason it is used for determining anisotropic stiffnesses. This homogenization only needs to be solved once, at the beginning of calculations. Non-linear material properties such as viscoelasticity and plasticity are formulated anisotropically with a phenomenological material model.

Crash-relevant experimental studies

Quasi-static and dynamic tests were carried out on the LFT material under different stress multiaxialities in order to determine parameters in the material model for describing non-linear material behavior such as plasticity, damage and failure. Particular emphasis was placed on a detailed characterization of strain rate dependence. A number of experimental studies regarding thermoplastic matrix materials may be found in the literature. In [7], for example, an increase in the modulus of elasticity and in strength was observed as the strain

rate increased. It is known of thermoplastic homopolymers that as the strain rate increases, ductile deformation behavior changes into brittle deformation behavior [7]. This deformation behavior is attributable among other things to the influence of isothermal conditions when strain rates are static as compared with adiabatic conditions at higher strain rates. As is known from [8], as a result of the injection-molding process, core layers and outer layers are created which have a considerable influence on mechanical behavior. Experimental studies of LFT which focus on the strain rate [9], [10], [11], [12] unanimously report slight increases in moduli and marked rises in strengths occurring at higher strain rates. In [10] and [12], higher elongations at break have been measured as the strain rate increases. From these results it emerges that the capacity for energy absorption increases the faster the material is loaded. These results are contrary to the results of [7]. Creating a crash-relevant anisotropic material model for an LFT material therefore calls for extensive experimental studies to enable the simulation also to include the fiber-orientation distribution, fiber concentration, multiaxiality and the strain rate, and to describe them correctly.

2. Modeling rheology and fiber orientation

Modeling the fiber orientation is based on the Folgar Tucker equations which have also been used successfully for years for short-fiber-reinforced plastics. However, additional effects, such as fiber-fluid (feedback to viscosity), fiber-fiber and fiber-wall interactions, are dominant with long fibers which can mostly be ignored with short fibers. Preliminary work at the ITWM was able to show that these effects can be modeled by the addition of suitable potential terms [2]. The model equations for the injection-molding simulation of long-fiber-reinforced polymers are thus:

$$\begin{aligned} \nabla \cdot v &= 0 \\ \rho(\partial_t v + \nabla \cdot (vv)) &= -\nabla p + \nabla \cdot \sigma + \rho g \\ \rho c_p(\partial_t T + \nabla \cdot (vT)) &= \nabla \cdot (k \nabla T) + \sigma : \kappa \end{aligned} \qquad (1)$$

Here v is velocity, T temperature, p pressure, σ stress, κ the deformation tensor, g gravitational acceleration, and c_p, ρ, η, k the material properties of the polymer. The correct form of the stress as a function of the other variables will be discussed in detail below.

For the filling simulation, a VoF approach is used as well for describing the filling front. The fiber-orientation dynamic is based on the Folgar-Tucker equation, which has also been used successfully for years for short-fiber-reinforced plastics:

$$\frac{D}{Dt}A^{(2)} = M \cdot A^{(2)} + A^{(2)} \cdot M - 2A^{(4)} : M - 6C_i\dot{\gamma}(A^{(2)} - \frac{1}{3}Id)$$

$$M = \frac{\lambda+1}{2}\nabla v + \frac{\lambda-1}{2}(\nabla v)^T; \qquad \lambda = \frac{(l/d)^2-1}{(l/d)^2+1} \tag{4}$$

The Folgar-Tucker equation is solved for the fiber-orientation tensor $A^{(2)}$. γ is the scalar shear rate and C_i is the diffusion coefficient. Fiber properties are input into the model via the length l and the thickness d of the fibers.

Overall, with a suitable closure relation this yields a closed system for the 4th order orientation tensor $A^{(4)}$. In what follows the customary orthotropic closure approximation is used for determining the coefficients [13]. Another iteration loop along with improvement of the model was required in order to correct the influences of the fiber bundles and the associated effective change in the ratio of fiber length to fiber diameter, the aspect ratio a. To do so, the so-called variable lambda model according to [14] was implemented.

Fiber-fiber interaction and also fiber-wall interactions are taken into account by means of a so-called Maier-Saupe term which effectively intensifies an existing fiber-orientation direction. This is because due to fiber-fiber contact in the case of long fibers, fiber orientations are intensified in one main direction or along the wall [2]. This local approach to wall interaction has not been pursued further since it usually requires a very fine computational grid in order to reproduce the resulting effects correctly numerically.

However, all these interactions lead to local separations or dilutions – in other words, to a local change in fiber concentration – which have a considerably more decisive effect on the resulting structural-mechanical properties and on the crash behavior than do minor deviations in fiber orientation.

First of all, a literature search was conducted and the Phillips model [3] customary for particle concentrations was generalized to cover fiber suspensions by replacing the necessary parameters with effective equivalent quantities (radius, surface). The transport equation for the fiber concentration ϕ is:

$$\partial_t \phi + v\nabla \cdot \phi = -\nabla \cdot (\phi J(\phi, A^{(2)})) \tag{5}$$

Here the drift velocity J, which leads to a separation or fiber concentration, is defined as follows:

$$J(\phi, A^{(2)}) = K_{coll}\sigma_{ell.}\nabla(\phi\dot{\gamma}) + K_{vis}\sigma_{ell.}(\phi\dot{\gamma})\nabla \ln \eta_{eff} \tag{6}$$

The quantities K_{coll}, K_{visc} are diffusion constants due to fiber collisions or due to viscosity gradients and are of the order of magnitude of unity. The collision cross-section σ_{ell} is to be generalized especially for the fibers since the original Phillipp model is only concerned with spherical particles. In this regard an extended search of the literature was carried out which also covered related research fields such as the dynamics of polymer chains [15], [16]. Building on this related work, a model was developed for the fiber-concentration and fiber-orientation dynamics which would be adequate for application to LFT injection molding. The following expressions emerged here for the two unknown terms:

$$\sigma_{ell.} = \pi d^2 \left(1 + (\frac{l}{d} - 1)A : A\right)$$

$$\nabla \ln \eta_{eff} = \frac{d \ln \eta_{eff}}{d\phi} \nabla \phi = \frac{d \ln \Gamma(\phi)}{d\phi} \nabla \phi \qquad (5)$$

The whole model can be briefly summarized as follows:

- The Navier-Stokes equations are solved for velocity and pressure. In addition, thermal effects are also taken into account via the temperature equation and temperature-dependent material parameters. For the filling simulation, a VoF approach is used as well for describing the filling front.
- The fiber-orientation dynamic is based on the Folgar-Tucker equations, which have also been successfully used for short-fiber-reinforced plastics for years. Fiber-fiber interaction is covered by a so-called Maier-Saupe term, which effectively intensifies an existing fiber orientation.
- Local fiber-concentration differences are described by a particle concentration in accordance with the standard Phillips model. Here, for the generalization to cover fiber suspensions, the necessary parameters were replaced by effective equivalent quantities (radius, surface).

Coupling these three equations via the rheological law is essential to the entire description – in other words, the stress-strain relationship as a function of the fiber concentration ϕ and the fiber orientation A.

$$\sigma = \eta_{eff} \kappa = \eta_s(T, \dot{\gamma})[\kappa + \Gamma(\phi)\kappa + \Gamma(\phi)\beta(a)(A^{(4)}\kappa - \frac{1}{3} A^{(2)} : \kappa Id)] \qquad (6)$$

$$\Gamma(\phi) = \frac{2\phi}{1-\phi} = \frac{1+\phi}{1-\phi} - 1; \quad \beta(a) = \frac{a^2 + 6.5 - 6\ln(2a)}{2\ln(2a) - 3}; \quad a = \frac{l}{d}$$

Here the connection can be calculated explicitly by then only dealing with the ratio of fiber length to fiber thickness. The previously usual factor $N_p = \Gamma(\phi)\beta(a)$ separates into a purely concentration-dependent factor $\Gamma(\phi)$ and a geometric factor for long fibers $\beta(a)$ .By inputting the fiber characteristics (fiber length and fiber thickness) and also the fiber concentration (here this always means the volume concentration) explicit values of N_p are obtained which previously had to be determined by parameter identification.

A finite volume method for structured networks has been developed for the fully coupled model described above for the filling simulation calculation of long-fiber-reinforced polymers with full coupling of the fiber-concentration and fiber-orientation dynamics and this method implemented in CoRheoS, the ITWM's own software framework.

3. Development of a material model taking fiber-orientation distribution and fiber-volume concentration into account

The material model has been implemented as a user material routine in the commercial FEM program LS-DYNA/Explicit. The basic equations of the implemented model are presented.

Approximation of the anisotropic stiffness tensor takes place in a two-step homogenization. First of all, following [5], the effective transversally isotropic stiffness tensor $\mathbb{C}^*$ is calculated:

$$\mathbb{C}^* = \left[c^i\mathbb{C}^i{:}\,\mathbb{A} + (1-c^i)\mathbb{C}^m\right]{:}\left[c^i\mathbb{A} + (1-c^i)\mathbb{I}\right]^{-1} \qquad (7)$$

Here c^i designates the fiber volume content, $\mathbb{C}^i$ the isotropic stiffness tensor of the fiber material (glass), $\mathbb{C}^m$ the isotropic stiffness tensor of the matrix material (PP), $\mathbb{I}$ the unit tensor of the fourth order and $\mathbb{A}$ the strain localization tensor. The last includes the fiber geometry information – that is, the aspect ratio (AV: fiber length to fiber diameter). $\mathbb{C}^*$ is thus the estimate of the effective stiffness of the composite for a unidirectional fiber orientation. The fiber-orientation distribution is taken into account in the second step. Using Advani and Tucker's approach, the transversally isotropic stiffness tensor is averaged in the various spatial directions with the aid of the fiber-orientation tensor A_{ij} from the mold-filling simulation. In this regard, see [6].

A phenomenological approach was selected for the plasticity. For a unidirectional fiber-orientation distribution, the material is transversally isotropic. In this case, the flow criterion according to Hill can be used, which can, according to [17], be described as follows:

$$\begin{aligned}(G+2F)tr(\boldsymbol{\sigma}^2) + 2(M-G-2F)\ tr(\boldsymbol{\sigma}^2\cdot\boldsymbol{B}) \\ + (5G+F-2M)\ tr^2(\boldsymbol{\sigma}\cdot\boldsymbol{B}) - \sigma_y\big(\varepsilon_p\big) = \Phi(\boldsymbol{B})\end{aligned} \qquad (8)$$

Here $\boldsymbol{\sigma}$ is the Cauchy stress tensor and $\sigma_y(\varepsilon_p)$ the comparative stress as a function of the plastic strain ε_p at which flow occurs. The parameters F, G, and M control the start of flow in the different directions of the anisotropy. The orientation tensor $\boldsymbol{B} = \boldsymbol{e} \otimes \boldsymbol{e}$ is defined by the dyadic product of a unit vector $\mathbf{e}$ and itself. The eigenvectors $\mathbf{e}_i^*$ of the fiber-orientation tensor A_{ij} arise from the main fiber orientations. In this way, equation (8) introduces three independent flow criteria $\phi(\mathbf{B}_i)$, which are differentiated by the orientations of the anisotropy ($\mathbf{B}_i = \mathbf{e}_i^* \otimes \mathbf{e}_i^*$ where $i = 1,2,3$). The result of this is three stress tensors $\boldsymbol{\sigma}(\mathbf{B}_i)$, which are calculated from the numerical solution of $\boldsymbol{\phi}(\mathbf{B}_i) \leq 0$ where $i = 1,2,3$. The effective stress tensor $\bar{\boldsymbol{\sigma}}$ is then calculated from the weighted mean value, whereby the eigenvalues a_i (eigenvalues of A_{ij}) are used as weightings:

$$\bar{\boldsymbol{\sigma}} = a_1\boldsymbol{\sigma}(\boldsymbol{B}_1) + a_2\boldsymbol{\sigma}(\boldsymbol{B}_2) + a_3\boldsymbol{\sigma}(\boldsymbol{B}_3) \qquad (\phi)$$

The notation $\boldsymbol{\sigma}(\mathbf{B}_i)$ symbolizes the dependence of the stress tensor in question to the orientation $\mathbf{B}_i$.

Thanks to Maxwell elements connected in parallel it was possible to take viscous effects into consideration. By way of illustration, taking the example of the one-dimensional case, the continuum mechanical material model is presented in Fig. 1 as a rheological circuit.

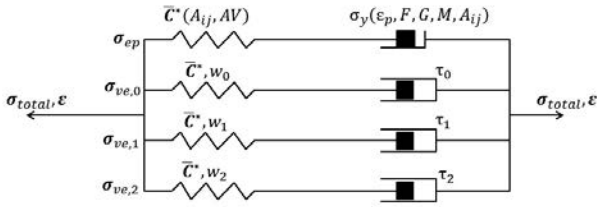

Fig. 1: A one-dimensional representation of the visco-elasto-plastic material model.

The first of the four parallel-connected elements symbolizes with its spring and friction elements the anisotropic elasto-plastic material model already described. The other three parallel-connected Maxwell elements consisting of spring and damper reproduce the viscous effects of the material. $\boldsymbol{\sigma}_{ve,i}$ is the stiffness tensor of the i-th Maxwell element, τ_i are the relaxation times of the linear damper elements and $\bar{\mathbf{C}}^*$ is the anisotropic stiffness tensor already determined. When the anisotropy in the viscosity is taken into account, a so-called convenience approach is used as a simplification. Here the anisotropic stiffness tensor with the help of a scalar parameter w_i scales the anisotropic stiffnesses equally in all directions of the ani-

sotropy. The relaxation times affect the material behavior analogously. The visco-elasto-plastic stress tensor $\boldsymbol{\sigma}_{\text{total}}$ is calculated by adding together the individual stress tensors:

$$\boldsymbol{\sigma}_{total} = \boldsymbol{\sigma}_{ep} + \boldsymbol{\sigma}_{ve,0} + \boldsymbol{\sigma}_{ve,1} + \boldsymbol{\sigma}_{ve,2} \quad (10)$$

Interactions between the different load states and their effects on damage are not fully understood for LFT. For this reason, six independent damage variables d_α where $\alpha = 1, \ldots, 6$ are introduced in the description of damage behavior. They describe independently of each other the damage development associated with the individual stress components. The stress tensor is expressed here as a six-dimensional vector. Murakami's book provides a detailed description of tensorial expressions for damage [18]. The 'damage effect tensor' $\mathbb{M}$ which he introduces there has been adapted and in the present case of application is described as follows:

$$\mathbb{M} = \begin{bmatrix} 1-d_1 & 0 & 0 & 0 & 0 & 0 \\ 0 & 1-d_2 & 0 & 0 & 0 & 0 \\ 0 & 0 & 1-d_3 & 0 & 0 & 0 \\ 0 & 0 & 0 & 1-d_4 & 0 & 0 \\ 0 & 0 & 0 & 0 & 1-d_5 & 0 \\ 0 & 0 & 0 & 0 & 0 & 1-d_6 \end{bmatrix} \quad (11)$$

In the undamaged case all damage variables are $\mathrm{d}_\alpha = 0$. Failure occurs as soon as a variable reaches the value 1. The undamaged stresses σ_α are reduced by the term $(1 - \mathrm{d}_\alpha)$ and the damaged stress state calculated as follows:

$$\sigma_\alpha^{\mathrm{dam}} = (1 - \mathrm{d}_\alpha)\,\sigma_\alpha \qquad \text{where} \qquad \mathrm{d}_\alpha = \left(\frac{\|\varepsilon_{\alpha,\max}\|}{\varepsilon_f}\right)^g \quad (12)$$

Damage development depends on the absolute value of the historical maximum of the corresponding strain component $\|\varepsilon_{\alpha,\max}\|$. The material parameter ε_f for the failure strain and the exponent g for describing damage development are used in calculating the damage variables d_α. In the described case, one and the same failure strain ε_f is used. The failure strain differs depending on the type of load and can thus be formulated as a function of the stress multiaxiality σ_{triax} as the function $\varepsilon_f(\sigma_{\text{triax}})$.

4. Experimental characterization of materials

Injection-molded test sheets made of LFT with 30 wt.-% glass-fiber content (STAMAX 30YK270 from the SABIC company) were used for material characterization. Both macroscopic mechanical tests and micro-structural computed tomography scans (CT) were carried

out. Fig. 2 shows the removal plan in the example of flat tensile test pieces. In order to investigate macroscopic material behavior in different stress states, different test piece geometries for tensile, notched tensile, shearing tensile, puncture, waisted puncture and compression test pieces were cut out of the test sheets (). A detailed description may be found in [19]. In what follows we shall deal with the most important results of testing.

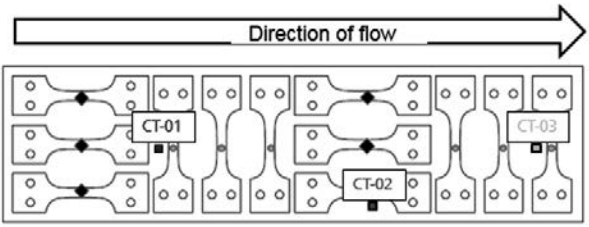

Fig. 2: Test piece sheet of injection-molded LFT (300mm x 80mm x 2.8mm) with removal plan for flat tensile test pieces at 0° and 90° to the direction of flow and also for computed tomography test pieces CT-01 to CT-03.

Table 1: Types of test pieces for material characterization (not to scale9

					
Tensile test piece	Notched tensile test piece	Shear tensile test piece	Puncture test piece	Waisted puncture test piece	Compression test piece

So as not to neglect the influence of the sampling position, test pieces were sampled from all over the sheet (see example of the tensile test piece in Fig. 2). Although this increased the scatter of the results, it was also possible to investigate even local properties arising from the production process. Global and local strains were determined from videos of the tests using the gray-scale correlation method (DIC, digital image correlation) and ARAMIS software. Investigations into strain-type dependency were carried out for the various multiaxialities at several nominal strain rates. In each case force-displacement curves or technical stress-

strain curves were obtained from global measured lengths on the test pieces and characteristic values determined for the individual tests. In addition to the measurement of global quantities, local strains and temperature increases were determined with the help of microlenses and a high-speed infrared camera. Forces were measured with a 30kN piezo-force measurement cell and a patented, low-vibration IMW measurement cell. Fig. 3 shows the averaged technical stress-strain curves for the 0°, 45° and 90° tensile tests. Each curve represents a test series with a single strain rate and at least three tests.

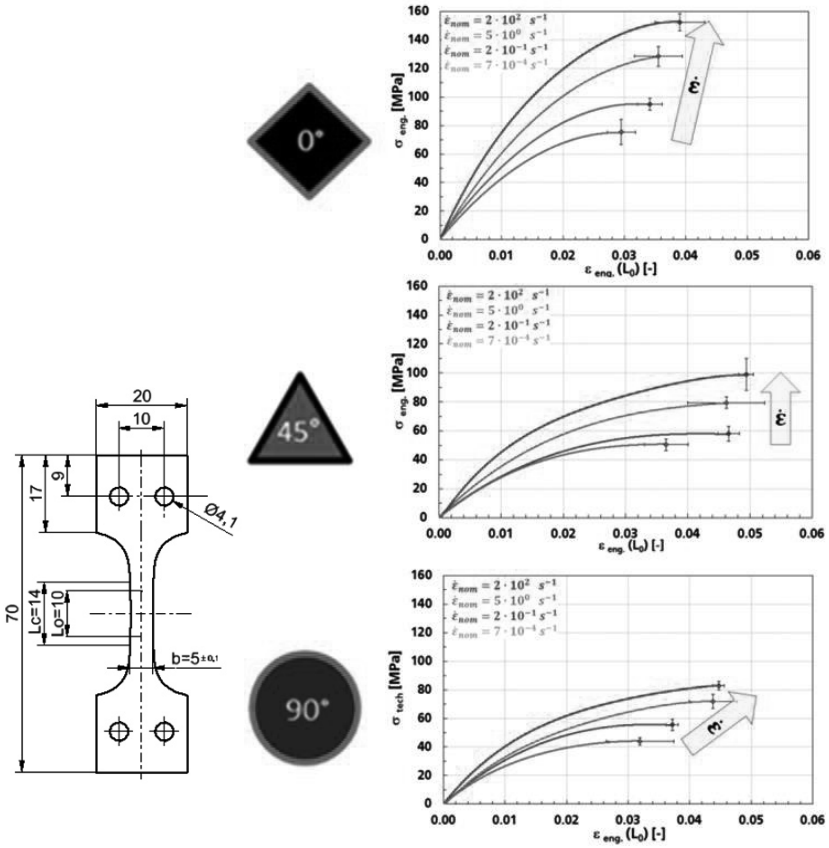

Fig. 3: Tensile tests at 0°, 45° and 90° to the direction of flow at four strain rates (right) and the corresponding tensile test piece geometry (left).

The test pieces in a series were taken from different positions on the STAMAX sheets in order to avoid neglecting the scatter of results due to the influence of the production process. At the end of each curve the standard deviations of the fracture stresses and fracture strains in a test series are plotted in the graphs as error bars. A marked influence of the strain rate can be seen. As the strain rate increases, the fracture stresses increase on average by 100% and the initial gradients by 60%. Furthermore, as the strain rate increases a tendency for fracture strains to increase may also be seen. With the aid of a Gaussian fit function, Figure 4 plots stiffnesses against orientation.

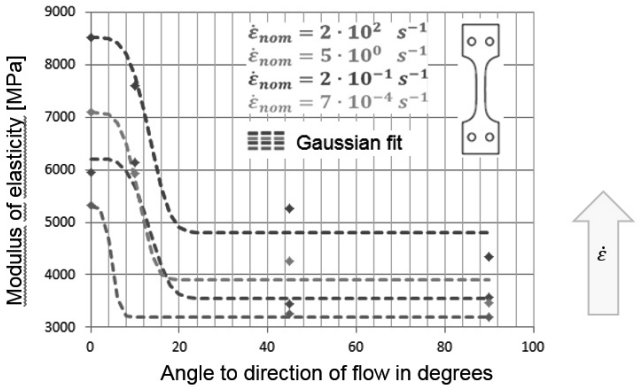

Fig. 4: Moduli of elasticity from tensile tests as a function of orientation to the direction of flow. The diagram shows mean values for all test piece positions of an orientation and an adjusted fit function, the probability density function according to Gauss.

In order to characterize a multiaxial stress state of the LFT material as a function of strain rate, puncture tests were carried out at four test speeds.

Out-of-plane deformation in the puncture tests required two high-speed video cameras in each case to analyze the local strains with 3D-ARAMIS. The test speeds correspond to the speeds in the tensile tests but the highest speed was reduced by a factor of two to 1400 mm s^{-1} in order to reduce the influence of dynamic effects on piezo-force measurement. The force-displacement curves after the load maximum even cover post-fracture behavior, something of great importance to energy absorption in crash-relevant components.

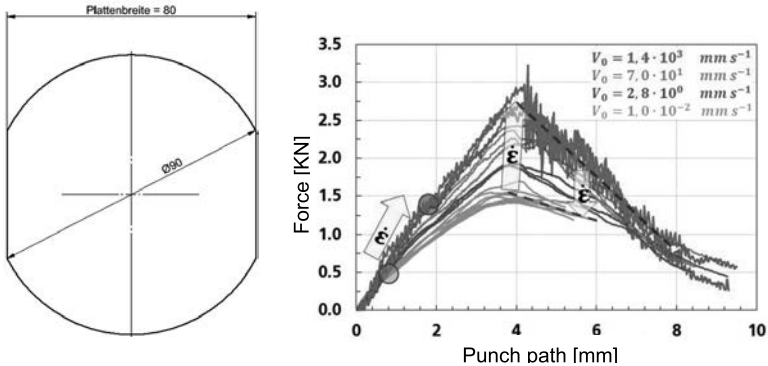

Fig. 4: Test piece geometry in puncture testing (left). Force-displacement curves for four test speeds (right). Clearly recognizable is the dependence of damage initiation (indicated by circles) on strain rate, the maximum force and post-fracture behavior.

5. Simulation results of material characterization

5.1 Mold-filling simulation of the test piece sheets

The filling simulations for the *Sabic* sheets were carried out with the STAMAX 30YK270E material data, in other words, for a fiber weight content of 30 wt.-%. The mean fiber length was 1.04 mm and the mean fiber diameter 19 µm, which gave an aspect ratio of approximately 53. The injection time was 2 seconds, the polymer was heated to 230 °C for injection, and the mold temperature maintained at 50 °C.

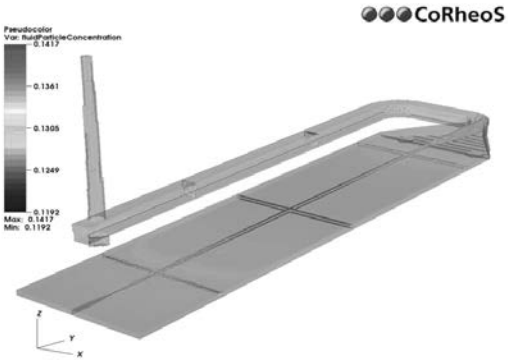

Fig. 5: Fiber-concentration distribution in selected cross-sections of the sheet flow.

Fig. 5 shows the concentration distribution with the following behavior:

- The concentration distribution over the sheet thickness shows a slightly lower concentration at the edge.
- The concentration increases in the direction of filling flow of the sheet.

To calculate the fiber orientation and fiber concentration of the Sabic sheet, the geometry of the sheet, including the feed system, was constructed and a comprehensive simulation study carried out to determine the model parameters. Here the open diffusion parameters were varied systematically and compared with the orientation and concentration measurements taken at the locations of the µCT test pieces. The result of the parameter and validation study is a parametrization of those model parameters still free which falls within the range of the physically feasible limits of these parameters and results in the following values:

$$K_{coll} = 0.175,\ K_{visc} = 0.175,\ k = 0.5,\ C_i = 0.0025, W = 7 \qquad (3)$$

Comparison with the µCT analyses in particular showed that all of the effects which occur, such as local fiber-concentration differences in the thickness direction and the fiber-orientation patterns over the thickness, are reproduced by the model.

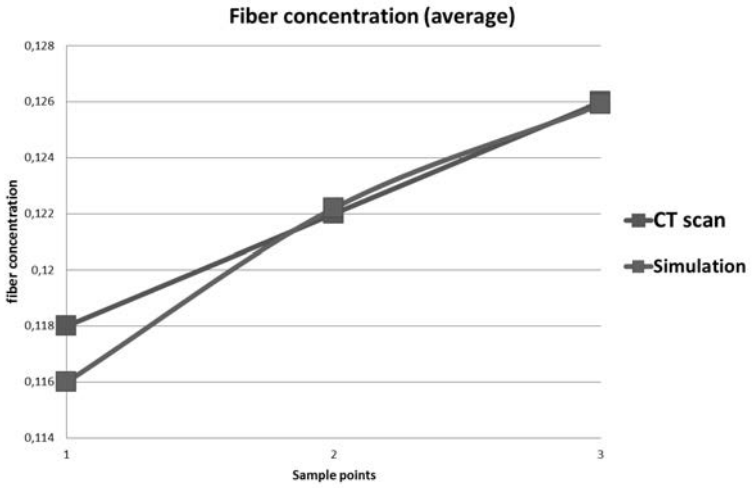

Fig. 6: Comparison of fiber concentrations at the three sampling points with the values obtained from the µCT scans.

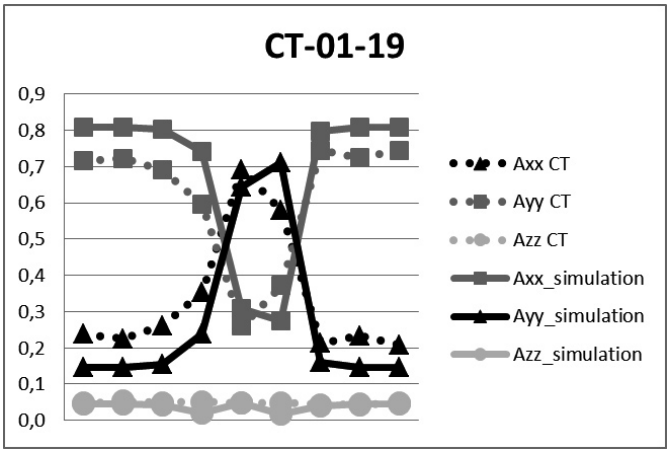

Fig. 7: Fiber orientation plotted against sheet thickness at sampling point CT-01-19. Comparison of simulated and measured fiber orientations on the three coordinate axes.

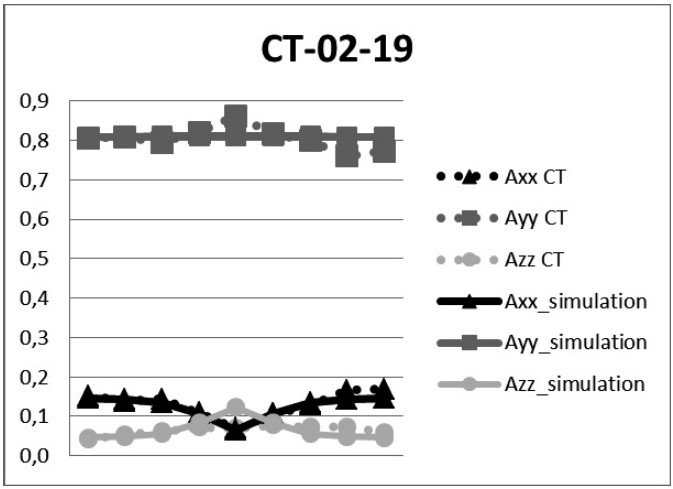

Fig. 8: Fiber orientation plotted against sheet thickness at sampling point CT-02-19. Comparison of simulated and measured fiber orientations on the three coordinate axes.

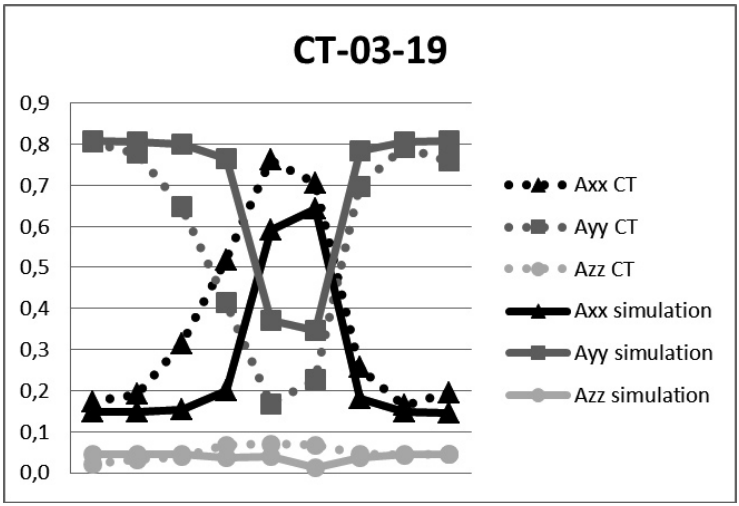

Fig. 9: Fiber orientation plotted against sheet thickness at sampling point CT-03-19. Comparison of simulated and measured fiber orientations on the three coordinate axes.

Local fiber orientations over the sheet thickness also show good agreement both qualitatively (crossing of orientations in samples CT-01 and CT-03) and quantitatively (absolute values at the edge and at the sample center) since even the image-analytical evaluations of µCT scans are to be regarded as having resolution error.

5.2 FEM simulation of sample tests from mechanical characterization of material

The mechanical material characterization tests for tensile, notched tensile, puncture, waisted puncture, compression and shear tensile test pieces were post-simulated in LS-DYNA. Taking into consideration the fiber-orientation distribution from the mold-filling simulation, the parameters of the anisotropic visco-elastic-plastic material model developed were adjusted by inverse simulation of the tensile tests. The locational dependencies of the flat tensile tests could be reproduced well by mapping the fiber-volume concentration and fiber-orientation distribution (Fig. 10).

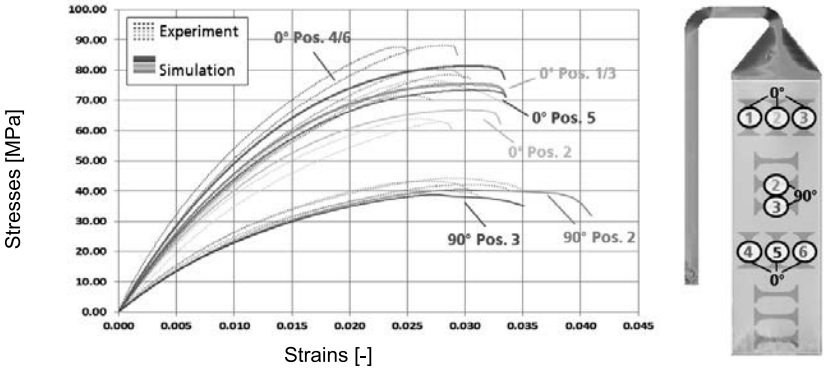

Fig. 10: Comparison between experiment and simulation with the UMAT of the quasi-static tensile tests. Different fiber orientations and fiber-volume concentrations produce different stress-strain curves for the different positions.

In addition, an isotropic elasto-plastic material model (LS-DYNA: MAT_024) was calibrated which averages the orientation-dependent characteristic material values over the orientation. The simulation results of the user material model (UMAT) are compared. As can be seen from Fig. 11 and leaving anisotropy aside, even the strain-rate dependencies with varying initial gradients are better reproduced by the visco-elastic formulation of the UMAT than by MAT_024.

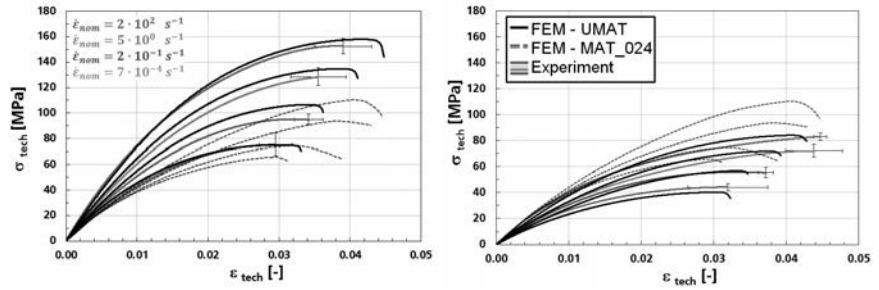

Fig. 11: Comparison between simulations with the UMAT (anisotropic), MAT_024 (isotropic) and the experiments in strain-rate-dependent tensile tests at 0° (left) and 90° (right) to the direction of flow.

The parameters of the damage model were calibrated with the aid of sample tests of different stress multiaxialities. Fig. 12 shows the failure curve over the stress multiaxiality of the UMAT. Here the critical element (failure onset) from the simulation was primarily considered and the moment of crack initiation in the experiment compared with that in the simulation. The GISSMO failure model (Generalized Incremental Stress-State-dependent damage MOdel) was adapted for the isotropic material model (MAT_024). Here the failure criterion is the effective plastic strain as a function of stress multiaxiality.

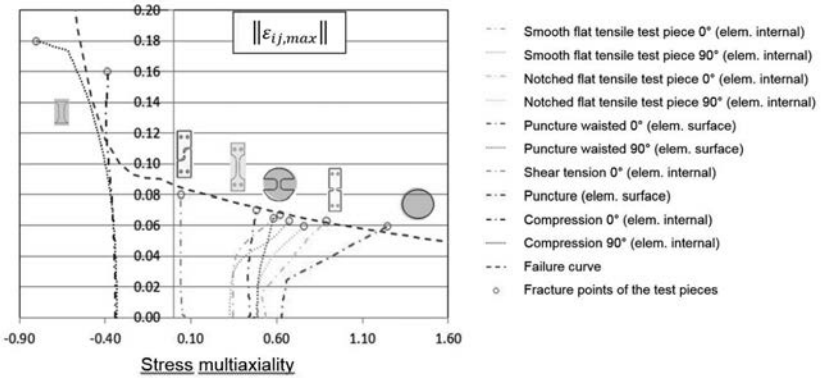

Fig. 12: Failure strains as a function of stress multiaxiality (modified approach according to Johnson-Cook) for the anisotropic USER material model (UMAT) which has been developed.

The puncture test shows an early onset of damage and a slow development of the damage up to failure with an early crack initiation in the center and an outward, slowly progressing crack propagation of three or four cracks. To initiate an early failure, the failure strains (Fig. 12) are lower with biaxial loading. Since only a very fine FEM mesh would be in a position to reproduce this crack propagation, the simulation and experimental curves do not match exactly. The differences between the material cards (MAT_024 and UMAT) are minor. The simulations show the same crack initiations.

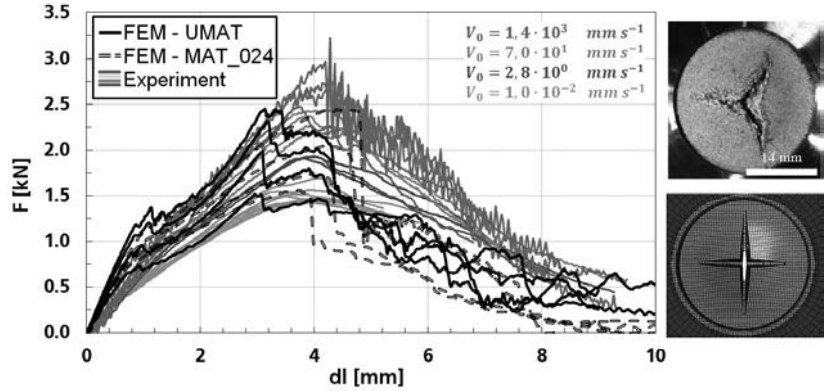

Fig. 13: Left: Comparison of the force-displacement curves for UMAT and MAT_024 simulations and also the experimental puncture tests. Right: Comparison of fracture images of simulation (bottom) and experiment (top).

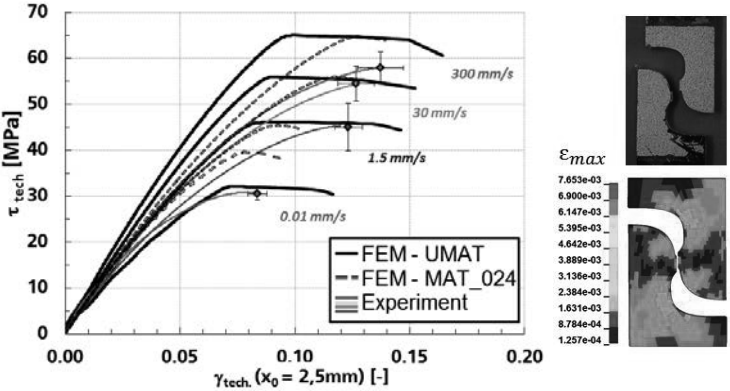

Fig. 14: Comparison between the UMAT and MAT_024 simulations and the experimental shear tensile tests with error bars. The contour plot (right) shows the principal strains in simulation at failure in the quasi-static test.

The experimental results of shear tensile tests and the results of the simulation are shown in Fig. 14. Mapping of the dynamic failure strains turned out very well. In the shear tensile tests no change in the initial gradient with the strain rate was observed. The visco-elastic modeling

of the UMAT thus overestimates the dynamic shear stiffnesses in contrast to the elasto-plastic modeling of MAT_024.

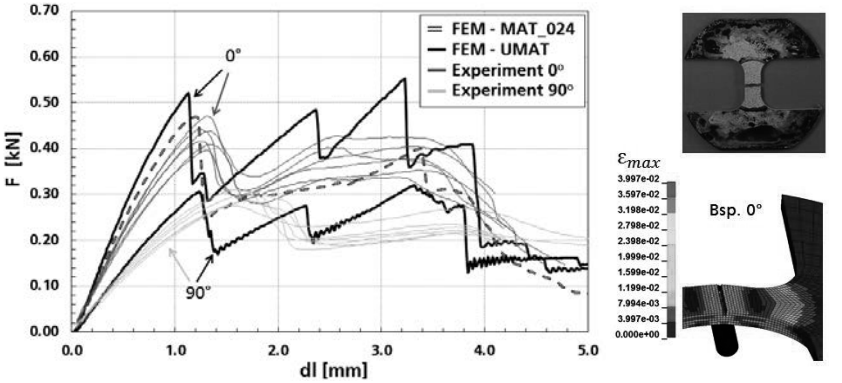

Fig. 15: Comparison between the simulations of the user routine (UMAT) at 0° and 90° to the direction of flow, the isotropic material model (MAT_024) and the experiments of the quasi-static waisted puncture tests. The contour plot (right) shows the principal strains in simulation with the UMAT in the 0° test.

For a first validation the waisted puncture test is post-simulated. The simulation results (Fig. 15) when using the anisotropic material model (UMAT) reproduce anisotropy well despite a slightly brittle failure. When the isotropic material model is used, it becomes clear here that the mean stiffness selected from the tensile tests was too stiff an approximation and ultimately in the waisted puncture test resemble the force-displacement curves of the tests at 0° to the direction of flow.

6. Method validation in the component test

To validate the method, an airbag housing manufactured by Autoliv B.V. & Co. KG was tested under crash-like loading in a drop-weight tester. The test machine used for this series of tests is a model 8100SA drop-weight impact tester manufactured by DYNATUP. Fig. 16 shows the CAD model of the construction developed for the clamping device showing the airbag housing clamped in place. Due to its simplicity of design and high variability it was this variant solution which was selected.

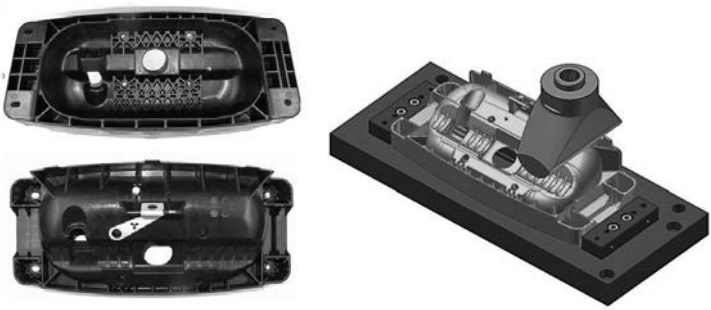

Fig. 16: Airbag housing showing exterior (top left) and interior (bottom left) as well as the construction developed for the clamping device for component testing, showing the clamped component and the drop-weight tower punch.

6.1 Mold-filling simulation on the component level

In the filling simulation of the demonstrator component, that is, the airbag housing, the same material data specifications were used as for the Sabic test sheets, since the same material was involved. Accordingly, no changes or adjustments were made to previously determined model parameters. The filling time for the airbag housing is 3.6 s, the material is melted at 250 °C and the mold temperature maintained at 40 °C.

Fig. 17: A_{xx} component of the fiber-orientation tensor following filling of the airbag housing.

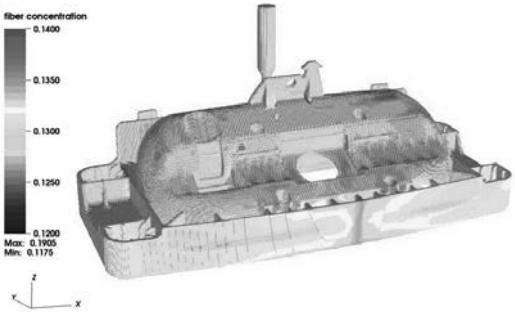

Fig. 18: Fiber-concentration distribution following filling of the airbag housing.

Two samples were taken from the real injection molding at predefined critical locations and µCT tomograms prepared and analyzed. Position F is close to the impact point in the drop-weight tower test, while position G is at a complex point on the ribbing. In exactly the same way as with the test sheets the fiber orientation was evaluated here too via the component thickness. The following diagrams show comparisons of the local fiber orientations for the two samples, F and G.

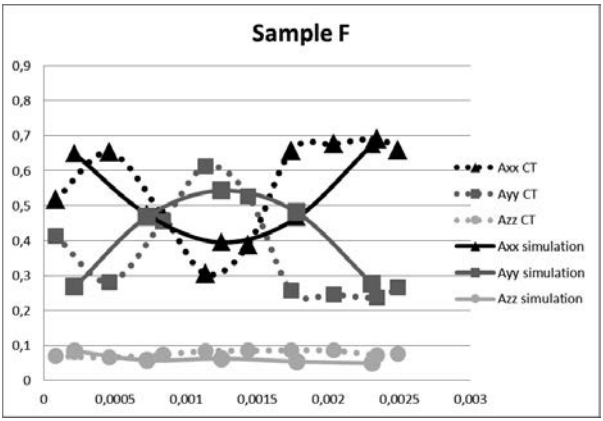

Fig. 19: Comparison of the fiber-orientation components of µCT scans and calculations in the airbag housing at sampling point F.

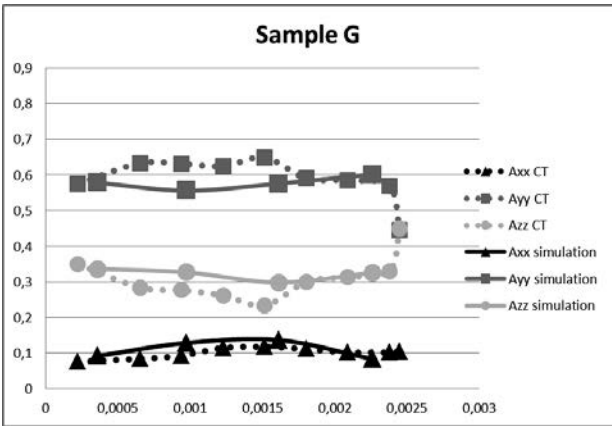

Fig. 20: Comparison of the fiber-orientation components of µCT scans and calculations in the airbag housing at sampling point G.

6.2 Data mapping

For the structure-mechanical calculations at the IWM the fiber-orientation and fiber-concentration data were mapped onto the computational meshes for the crash calculation. *FOmapper* , the C++ program developed by the ITWM, takes the local fiber-volume content and the local fiber orientation calculated with the CoRheoS process simulation program and maps them onto the finite-element mesh (LS-DYNA) being used for structural analysis (with a locally variable anisotropic material model). The process simulation mesh (CoRheoS) is a structured mesh consisting of rectangular hexahedra (brick elements). The structural analysis mesh (LS-DYNA) is an edge-adapted unstructured mesh which can consist of shell elements or 3D continuum elements. The case to be considered is one in which the domain which defines the structural analysis mesh is a subset of the domain which is described by the process simulation mesh. Should however nodes of the structural analysis network lie outside the domain of process simulation, an extrapolation procedure is applied to assign reasonable values to these nodes.

6.3 Crash simulation

FEM models with three different discretizations were prepared for the crash simulation of the airbag housing (Fig. 15). Here it is expected that a very fine and precise discretization with

tetrahedral elements will be able to cover local heterogeneities best and thus deliver the best simulation result.

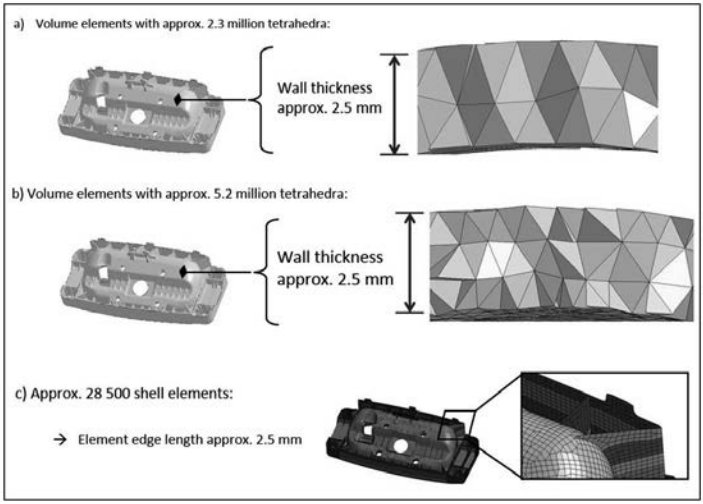

Fig. 21: Discretization of the FEM models of the component. Under-integrated linear tetrahedral volume elements (a and b). Fully integrated linear shell elements with 7x4 integration points (c).

A coarser second tetrahedral mesh simplifies not only the geometry but there is also less local information available from the injection-molding simulation. Thus, for example, the fiber-orientation distribution is averaged over thickness to just two elements. A shell model, as used most frequently in crash simulations, is also simulated using two material models. Even though the fiber-orientation distribution has very good resolution with 7 Gauss points on the thickness axis and 4 on the shell plane, the geometry is still shown only in a very simplified form.

The material model which has been developed (UMAT) and which takes into account differences in stiffnesses and strengths due to the fiber-orientation distribution shows in the simulation better agreement in crash energy absorption that does the isotropic material model (MAT_024) (Fig. 22). One exception is that force is slightly overestimated in crack initiation. The initial gradient in the simulated force-displacement signal is also slightly steeper in the user material model than in the experiments.

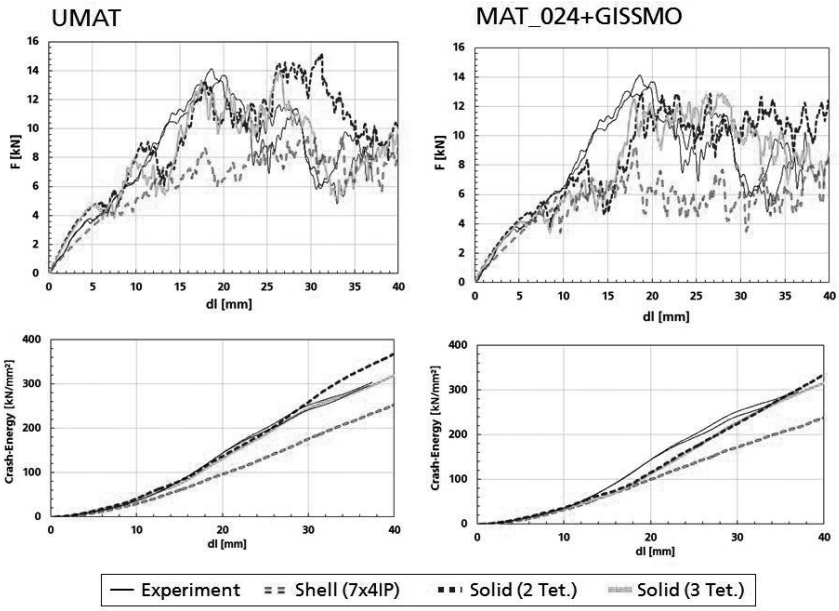

Fig. 22: Top: Force-displacement curves from the simulations of the three FEM models with the anisotropic material model which was developed and inclusion of the fiber-orientation distribution (left) and the isotropic material model (right) compared with the experimental tests. Bottom: Integral of the force-displacement curves for comparison of crash-energy absorption.

All simulation results basically show acceptable agreement with the experiments. The relatively good results of the isotropic material model are attributable to adjustment in the upper strength range of the orientation-dependent scatter and have already been discussed in the example of the waisted puncture test. The problem in this isotropic adjustment is overestimating component strength at those places in the component where the fibers are at 90° to the load and no longer contribute to the strength – in other words, only the matrix material describes the material properties. Even if the simulations of component tests using the isotropic material model show comparatively good agreement with the experiments, it remains an open question whether other loading cases do not deliver a markedly worse result and whether force in the simulation with the calibrated isotropic material model is not overesti-

mated. Crash-energy absorption would thus also be overestimated. Such a result would be unacceptable for component design.

7. Summary

In this project success was achieved in making the necessary extensions to the model for an injection-molding simulation of LFT. To reproduce the principle effects in LFT injection molding, a consistent formulation of the coupled filling simulation with the fiber-orientation dynamic and the concentration distribution was implemented. For this system it was possible in addition to determine analytically the essential model parameter, namely the rheology – in other words, the generalized viscosity law which alongside the usual temperature and shear-rate dependence also depends on the fiber-orientation tensor and the fiber concentration. The implementation of the model in prototype form in CoRheoS was validated with the aid of, among other things, local tomography scans. The complexity of the fully coupled system and the associated effort in calculation could if necessary be investigated in future work by means of a suitable decoupling of filling simulation, fiber concentration and fiber orientation. A mapping procedure has been developed and implemented for the consistent and robust mapping of the extended result data (local fiber concentration and fiber-orientation tensor) onto different FE grids for subsequent crash simulations. A material model has been developed and implemented in the LS-DYNA FE code which takes into consideration local fiber-orientation distributions and fiber-volume concentrations. The material characterization tests carried out with different loading types and with different crash-relevant strain rates have been successfully post-simulated with this user material model. All test piece simulations were better reproduced with the material model developed than with an isotropic material model. In simulations of the component in a crash, there were only minor differences between the isotropic material model and the developed user material model and this is due to an unsuitable averaging of the anisotropic characteristic values. The isotropic material model significantly overestimates strengths in the case of a load at 90° to the fiber orientation. In this project only a partial understanding of the complex damage behavior of the material was possible. Here the modeling was based on extensive experimental studies which focused primarily on the crash behavior of the material. In addition to the strain-rate-dependent characteristic values which were determined, these investigations, primarily due to the use of high-speed infrared measurement, yielded clear indications of different damage behavior with changes in multiaxiality and strain rate. Further investigations into damage behavior under crash-like loading are required into order to adapt the damage parameters of the material

model adequately and thus to allow satisfactory forecasting of multiaxial stress states and complex geometries.

9. Acknowledgments and note on funding

IGF Project 17334 N of the Research Association for Automotive Technology (FAT) has been sponsored by the Federal Ministry of Economics and Technology via the AiF under the program to promote joint industrial research and development (IGF) on the basis of a resolution of the German Bundestag. We should like to express our thanks for this support.

Thanks are also due for the support in kind and in services and also interesting discussions with and stimuli from the committee accompanying the project, consisting of the following companies:

Adam Opel AG	Dr. Ing h.c. F. Porsche AG	Robert Bosch GmbH
Altair Engineering GmbH	Dynamore GmbH	Roof Systems Germany GmbH
AUDI AG	Faurecia	SABIC
Autodesk	Ford-Werke GmbH	SIGMA Engineering GmbH
Autoliv B.V. & Co. KG	GNS mbh	SimpaTec GmbH
Behr GmbH & Co. KG	Johnson Controls GmbH	TRW Automotive GmbH
Celanese Engineered Materials	Key Safety Systems Deutschland GmbH	Volkswagen AG
Daimler AG	MAGMA Gießereitechnologie GmbH	Zegla-plast
		4a Engineering GmbH

10. References

[1] NEITZEL, M.: Handbuch Verbundwerkstoffe, 2004 — ISBN 3446220410

[2] LATZ; STRAUTINS; NIEDZIELA: Journal of Non-Newtonian Fluid Mechanics 165 (2010), No.13-14, pp. 764-781.

[3] PHILLIPS, A.: Physics of Fluids A 4 (1), 1992

[4] BUCK, F.; BRYLKA, B.; MÜLLER, V.; MÜLLER, T.; WEIDENMANN, K.; HRYMAK, A. N.; HENNING, F.; BÖHLKE, T.: Two-scale structural mechanical modeling of long fiber reinforced thermoplastics. In: Composites Science and Technology Vol. 117 (2015), pp. 159–167

[5] MORI, T.; TANAKA, K.: Average stress in matrix and average elastic energy of materials with misfitting inclusions. In: Acta Metallurgica Vol. 21 (1973), No. 5, pp. 571–574

[6] ADVANI, S. G.; TUCKER, C. L.: The use of tensors to describe and predict fiber orientation in short fiber composites. In: Journal of Rheology Vol. 31 (1987), No. 8, pp. 751–784

[7] DASARI, A.; MISRA, R.: On the strain rate sensitivity of high density polyethylene and polypropylenes. In: Materials Science and Engineering A Vol. 358 (2003), pp. 356–371

[8] MORTAZAVIAN, S.; FATEMI, A.: Effects of fiber orientation and anisotropy on tensile strength and elastic modulus of short fiber reinforced polymer composites. In: Composites Part B Eng. Vol. 72 (2015), pp. 116–129

[9] ALCOCK, B.; CABRERA, N. O.; BARKOULA, N. M.; REYNOLDS, C. T.; GOVAERT, L. E.; PEIJS, T.: The effect of temperature and strain rate on the mechanical properties of highly oriented polypropylene tapes and all-polypropylene composites. In: Composites Science and Technology Vol. 67 (2007), pp. 2061–2070 — ISBN 0266-3538

[10] FITOUSSI, J.; MERAGHNI, F.; JENDLI, Z.; HUG, G.; BAPTISTE, D.: Experimental methodology for high strain-rates tensile behavior analysis of polymer matrix composites. In: Composites Science and Technology Vol. 65 (2005), pp. 2174–2188 — ISBN 0266-3538

[11] FRITSCH, J.: Charakterisierung und Modellierung eines glasfaserverstärkter Thermoplaste unter dynamischen Lasten: Fraunhofer Verlag, 2012 — ISBN 978-3-8396-0333-8

[12] KANDER, R.G.; SIEGMANN, A.: The effect of strain rate on damage mechanisms in a glass/polypropylene composite. In: Journal of Composite Materials Vol. 26 (1992), No. 10, pp. 1455–1473

[13] CINTRA, J.S.; TUCKER, C.L.: Orthotropic closure approximations for flow-induced fiber orientation. Journal of Rheology, Vol. 39 (6) pp. 1095-1122, 1995

[14] SMITH, D.E.; MONTGOMERY-SMITH, S.; Jack, D.: Modeling orientational diffusion in short fiber composite processing simulations, in Proceedings of 2009 NSF CMMI Research and Innovation Conference, Honolulu, HI

[15] MA; GRAHAM: Physics of Fluids 17 (2005)

[16] KROCHAK; OLSEN, MARTINEZ: J. Fluid. Mech. Vol. 653 (2010)

[17] ARAVAS, N.: Finite elastoplastic transformations of transversely isotropic metals. In: International Journal of Solids and Structures Vol. 29 (1992), pp. 2137–2157

[18] MURAKAMI, S.: Continuum Damage Mechanics. Heidelberg, London, New York: Springer, 2012 — ISBN 9781118097298

[19] SUN, D.-Z.; SCHULENBERG, L.; LIENHARD, J.; HUBERT, F.; STEINER, K.; NIEDZIELA, D.; Shklyar, I.: Entwicklung einer Methode zur Crashsimulation von Langfaserverstärkten Thermoplast (LFT) Bauteilen auf Basis der Faserorientierung aus der Formfüllsimulation. IGF-Vorhaben 17334 N Forschungsvereinigung Automobiltechnik e.V. (FAT), (2015)

New development of SCR-tank systems: materials, functions, processes

Dipl.-Ing. **T. Rösch**, Veritas AG, Gelnhausen;
Dipl.-Ing. **U. Remmele**, Daimler AG, Sindelfingen

Abstract

On the way to reducing the emissions of internal combustion engines, and diesel engines in particular, injection-molded plastic tanks for the urea solution are being used more and more. This paper examines current legislation, the requirements profile of the tank and material selection, as well as presenting the general manufacturing process.

In addition, constructive solutions for the SCR-tank systems and the testing and validation carried out are discussed.

1. Functional principle of the SCR system

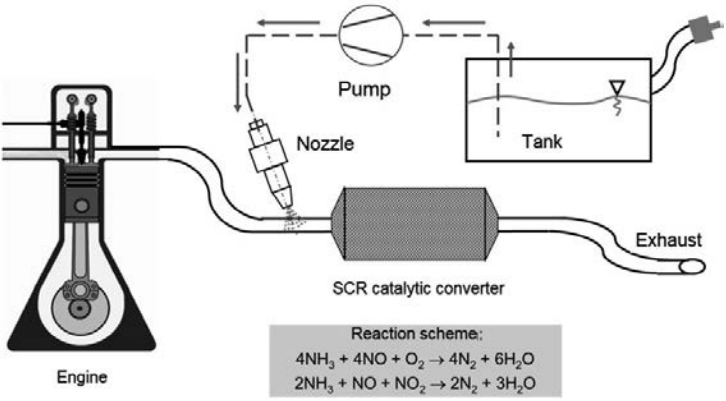

Fig. 1: Functional principle of SCR technology

2. Requirements

Diesel engine exhaust gas limits	EURO 4 as of 01.01.2006...	EURO 5 as of 01.01.2011...	EURO 6 as of 01.01.2015...
Carbon monoxide (CO)	0,5 g/km	0,5/0,45 g/km*	0,5 g/km
Hydrocarbons and nitrogen oxides (HC and NO_x)	0,3 g/km	0,23 g/km	0,17 g/km
Nitrogen oxides (NO_x)	0,25 g/km	0,18 g/km	0,08 g/km
Soot particles (PM)	0,025 g/km	0,005 g/km	0,005 g/km

Quelle: Daimler

Fig. 2: Legal requirements applicable to emissions

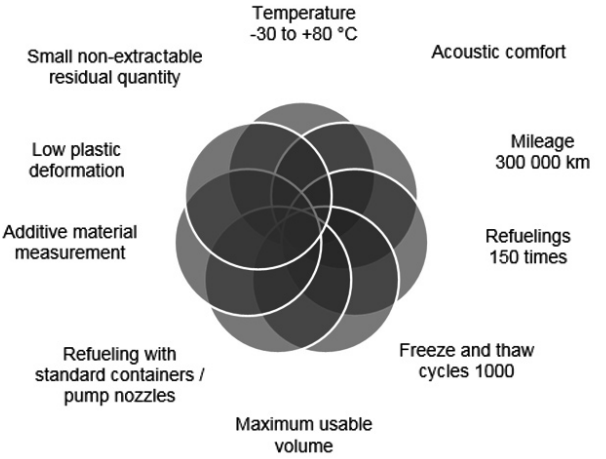

Quelle: Daimler

Fig. 3: Requirements profile for the SCR tank

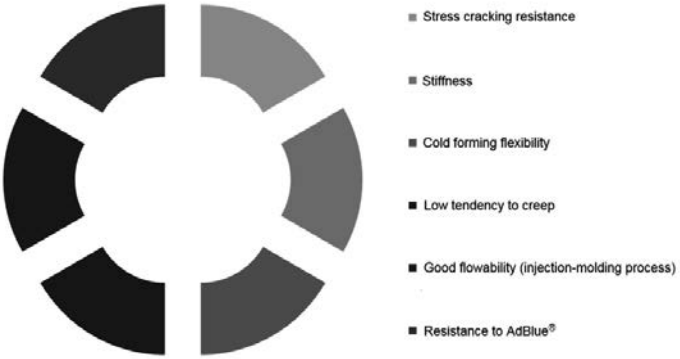

Quelle: Daimler

Fig. 4: Requirements profile for the polymers in the SCR system

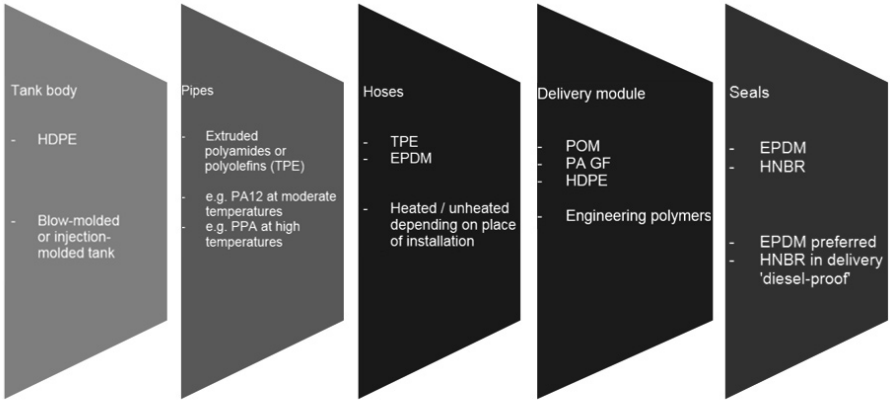

Quelle: Daimler

Fig. 5: Polymers used

3. Constructive design

- Precise compliance with the wall thickness in accordance with design specifications
- Efficient use of material by selectively stiffening measures
- Max. volume due to optimum use of the possible installation space
- Integration of construction elements and additional functions
- Simple installation of components into the open shells
- Reduction in process steps
- Weight and cost savings

Fig. 6: Advantages of injection-molding technology

4. Manufacturing process

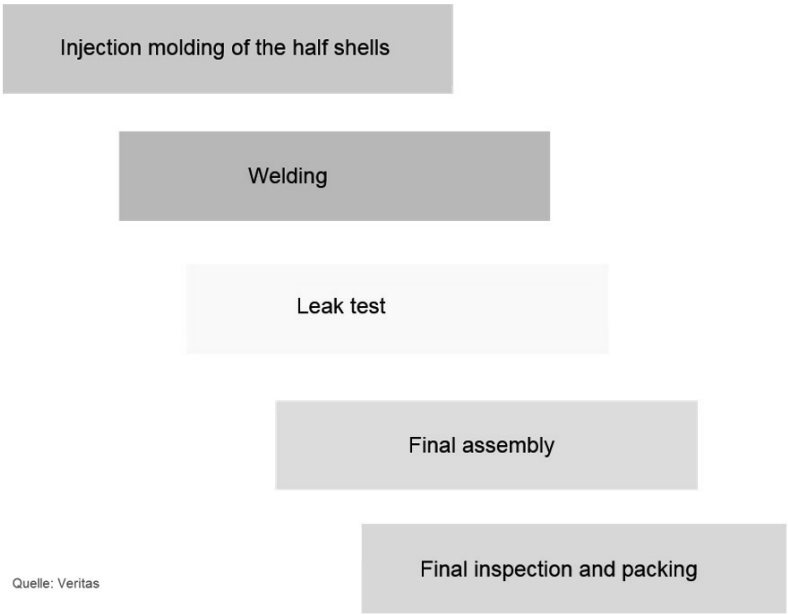

Fig. 7: Process steps in tank production

Quelle: Veritas

Fig. 8: Injection-molded tank system

5. Testing and validation

- Validation of processes
    - Microtome sections of the weld seam
    - Computer tomography of the weld seam
    - Tensile testing of the weld
    - Leak tests in the helium test rig

- Functional tests
    - Refueling tests
    - Burst pressure and robustness testing
    - Sloshing tests

6. Summary

Due to increasing emission requirements the demand for SCR systems will increase sharply over the next few years.

The choice of material requires a well-balanced consideration of:

- functional requirements of the product
- chemical resistance and compatibilities
- good and safe processability in the desired series-production process.

Injection-molding technology offers significant advantages in rational production and enables the integration of additional functions for a more valuable product.
The introduction of new manufacturing technologies also requires the development or expansion of testing and validation methods.
High-performing system suppliers minimize the interfaces in a vehicle project and make optimally balanced systems possible as regards functions.
A joint development between vehicle manufacturers and system suppliers is useful in the introduction of new products and technologies.

First plastic oil-pan module in the 911 Carrera: lightweight design and system integration

Dipl.-Ing. (FH) **J. Soares**,
Polytec Group, Lohne;
Dipl.-Ing. **A. Misala**,
Dr. Ing. h.c. F. Porsche AG, Weissach

Abstract

In terms of performance and efficiency, targets were set high in the development of the new six-cylinder Boxer engines of the Porsche 911 Carrera. In close collaboration between Porsche and Polytec Plastics an intelligent oil-pan module made of plastic has been developed which fully meets the specific requirements of the new generation of engines.

1. Introduction

Plastic oil pans open up diverse possibilities for integrating functional elements which were previously only possible at a significantly higher cost. Compared to versions made of aluminum, weight can be reduced significantly. Furthermore, economic potential can be boosted by the introduction of more efficient production processes. Plastic is the first choice here.

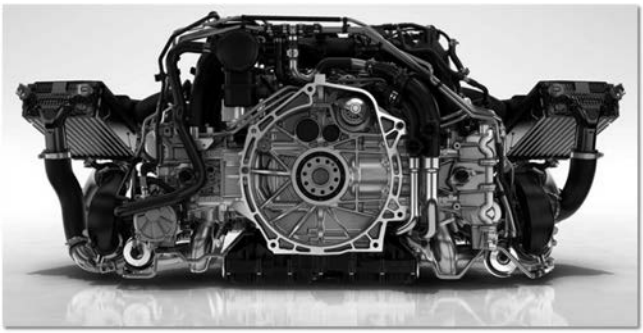

Fig. 1: The new 3.0-liter turbocharged engine of the Porsche 911 Carrera

2. Porsche 911 Carrera - oil pan

The oil pan module for Porsche's new six-cylinder Boxer engine basically consists of an upper and a lower section made of polyamide 6 with 30% glass fiber.

The particular design of the engine makes a two-part design necessary. The horizontal, opposed cylinders of this engine design requires a relatively flat oil pan with pronounced lateral protrusions arranged transversely, thereby holding the largest possible quantity of oil.

Fig. 2: Exploded view of the oil pan module, consisting of an oil-pan upper section, including the media lines carrier and the oil pan lower section.

A so-called media lines carrier is connected to the oil pan upper section by means of self-tapping screws. Various functions are implemented by the hot-gas welding together of the two halves of the media lines carrier. These include the oil return lines (1) for the two turbochargers to which special requirements apply as regards leakproofness.

The oil pump also draws the oil from the cylinder heads. Since air is drawn in as well as the oil, before the oil is fed into the oil circuit it must be largely defoamed. Here recourse is had to the principle of centrifugal separation (2). For this purpose two cylindrical oil-air separators ((2) in Figure 3 and Figure 4 detail) are realized in the assembly of the oil-pan upper section and the media lines carrier, and the mixture is input into them.

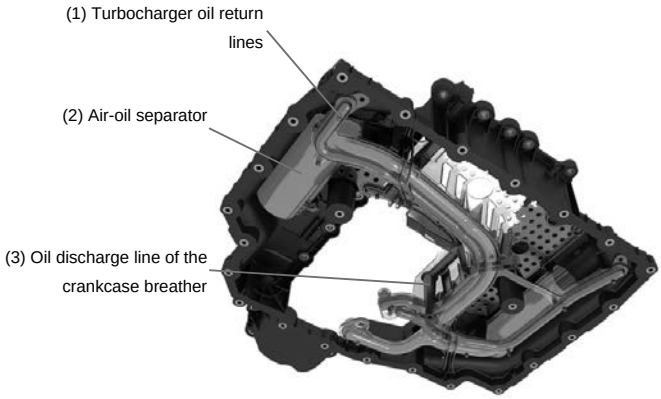

Fig. 3: Oil-pan upper section showing the three main functions of the integrated media lines carrier.

As the third oil line element, the oil return line duct from the crankcase breather has been integrated into the media lines carrier ((3) in Figure 3).
The basic geometry of the media lines carrier takes the form of a perforated plane which functions as an oil baffle (oil deflector).

Fig. 4: Centrifugal separation in the media lines carrier to separate the air-oil mixture

To ensure that oil is continuously sucked in from the center of the oil pan under all states of driving dynamics, the oil-pan lower section is equipped with a cruciform arrangement of baffles.

2.2 System integration compared with the aluminum version

By system integration we here mean the grouping together of subsystems into a higher-level overall system. This integration is made possible by the following features of the oil pan module:

- The use of a single material.
- The use of manufacturing processes with a greater degree of freedom in shaping (hot-gas welding).
- A design or arrangement of the functional elements appropriate to the manufacturing process.
- Simplification of the interfaces with regard to a favorable final assembly of the oil pan.

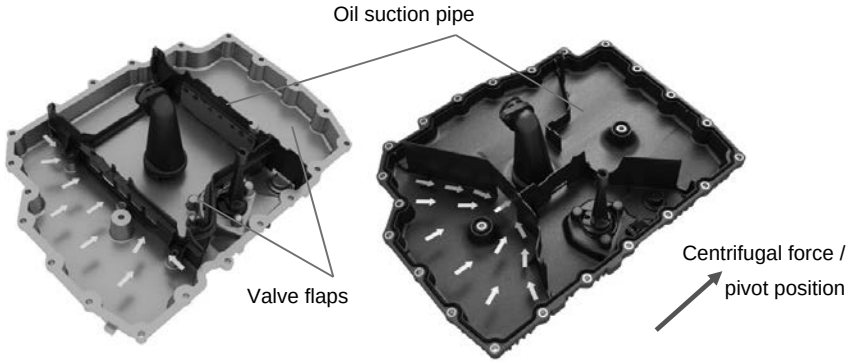

Fig. 5: Illustration of the partition box function of the aluminum pan (left) and the plastic pan (right)

While the plastic partition box took the form of an additional fitted component in the aluminum oil pan, it can now be fully integrated into the oil-pan lower section. This eliminates the gasket previously fitted between the partition box and the oil pan and also the valve flaps, thus yielding a cost-effective and robust system. Integrating the partition box into the oil-pan lower section results in greater design freedom. This meant that the required functionality could be realized with considerably less complexity in the construction (Figure 5).

By bringing together, as described above, the oil deflector, the air-oil separator and the turbocharger return lines, the media lines carrier is reproduced, as it were, in the plastic oil pan.

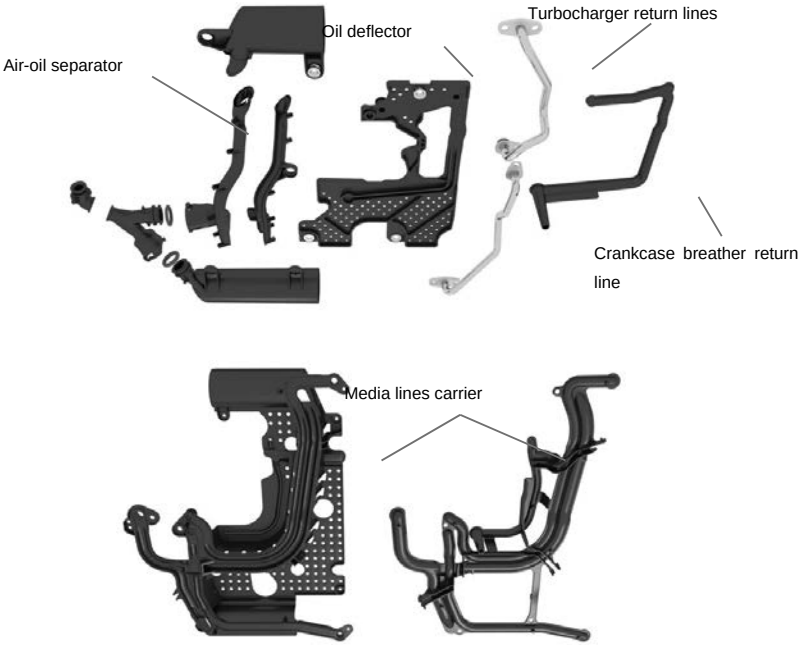

Fig. 6: Illustration of the components required to reproduce the functional elements integrated in the media lines carrier (top: aluminum oil pan, bottom: plastic oil pan)

In the aluminum version, integration of the oil return lines from the crankcase was already in progress in the oil deflector. Here the air-oil separator was made of six different plastic parts. The turbocharger return lines were separate steel pipes with the corresponding connectors at each end. By arranging the connection geometry at the oil pump and oil-pan upper section in a way appropriate for assembly and by optimizing the course of the oil lines, it was possible to ensure that this system integration would fit in with the constraints of production and still meet all functional requirements.

2.3 Comparison of weight breakdowns

At the beginning of the project, agreement was reached on objectives that the weight of the new oil pan should be reduced by at least two kg with respect to its predecessor. The two outer shells of the oil pan have the greatest potential here. By using plastic, the weight of the lower section could be reduced by 1.3 kg and of the upper section by 1.8 kg.

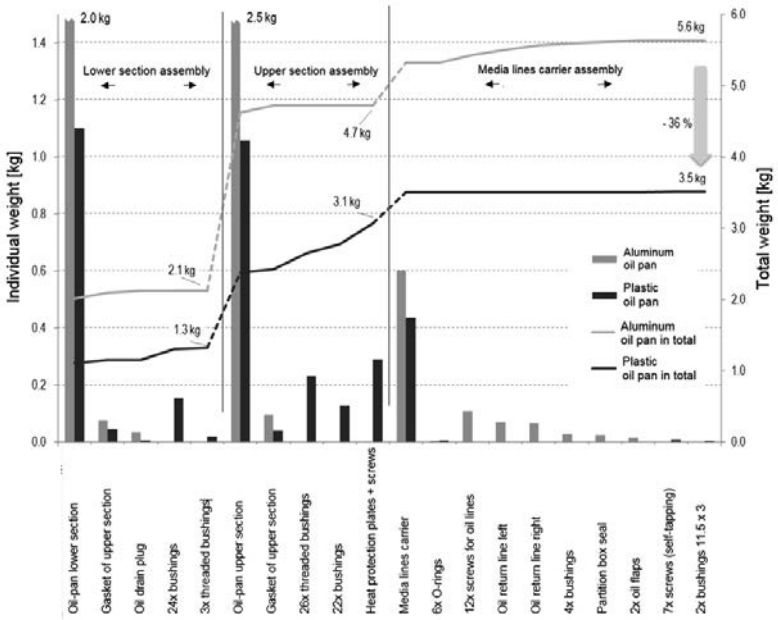

Fig. 7: Individual weights of the various function elements and totals

Not only was a straightforward weight reduction achieved by using PA6 GF30 but the wall thickness of the components was also optimized. In the case of the plastic oil pan this amounts to 2.5 mm. Despite the increase in weight due to reinforcement ribs to improve acoustic and mechanical properties the overall result was an additional weight reduction of 0.22 kg in the upper section and 0.4 kg in the lower section.

Conventional steel screws are used to connect the oil pan to the crankcase and between the upper and lower sections. This means that on the oil-pan upper section 22 bushings must be used on the crankcase flange side and 26 threaded bushings on the underside in order to ensure that the components are solidly screwed together. Together with the left-hand and

right-hand heat shields, this results in a weight increase of about 0.65 kg in order to secure a function comparable to the aluminum oil pan.

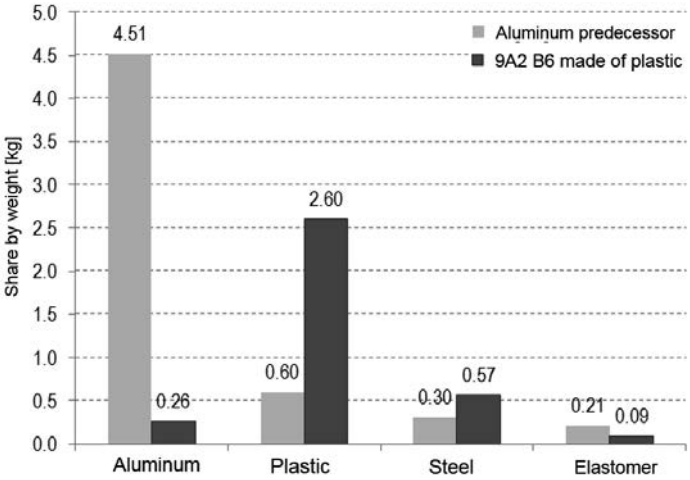

Fig. 8: Comparison of the weights of the different materials

If the volume of the bushings and threaded inserts is deducted from the aluminum upper section this does reduce the weight of the upper section from 2.38 kg to 1.06 kg (aluminum only or plastic only). Here too it appears that on the whole a massive saving of weight is effected despite the necessary use of function-securing elements.

A further element is functional integration. In the media lines carrier not only was the material of the turbocharger return lines changed but the number of screws reduced and different screw types used. While previously twelve screws were needed to fasten all components, now only seven are used, and for the most part considerably lighter, self-tapping screws.

The bottom line is that the weight target was fully achieved for the whole oil pan.

3. Special aspects of production

Comparison of the plastic injection-molding process and the aluminum pressure die-casting process from the economic point of view must take four main factors into account: the price of the raw material, tooling costs and the return on them, processing costs, and last but not least secondary finishing costs.

The advantages of plastic injection-molding production are well-known. It is worth mentioning that aluminum pressure die-casting tools have a shorter service life than plastic injection-molding tools. Tooling costs are thus generally cheaper for aluminum components and are thus at first sight probably the better option at lower production quantities. This view does not however go far enough since better functional integration is possible with plastic injection-molding and no mechanical secondary finishing is required. It is also worth mentioning that the energy costs for aluminum components are considerably higher than for production by injection molding. For example, with aluminum the process necessarily involves overflow and press residues, so that the amount of recycled material to be melted down again can, depending on the product, be as much as 70% [1] – an unthinkable figure in plastic injection-molding production.

The decision to use plastic must however be taken in the concept phase if the full capabilities of production in plastic are to be secured. Functional elements must be installed on a rational basis here, taking economic and ecological aspects in particular into account.

Functional elements can be integrated – in other words, molded onto the main body – or manufactured on a modular basis as a separate component with a defined interface with the main body. The complexity of a functional element can be cited as one major factor in the decision whether to integrate or not. With growing complexity, greater development outlay is required and there is an increased possibility of errors in production. The fact that the function element can be replaced during servicing or during the production process also plays an important rôle.

Taking these aspects into account, the oil pan of the Porsche Boxer engine is divided into three modules. The upper and lower sections form the outer shell of the oil pan. This division is primarily required for reasons relating to demolding. Massive undercuts means that a one-piece design is not possible, even with the help of splits. The two components are therefore connected together by a conventional flange seal using an I-profile gasket and the appropriate screws. For reasons relating to servicing and assembly, welding the two parts together permanently is not a reasonable solution. Furthermore, the connection of the oil pan to the crankcase is considerably smaller than the oil pan itself. For this reason a one-piece solution would mean the inclusion of numerous access paths for screwing onto the crankcase flange from below. Functional integration of the other components would not then be possible.

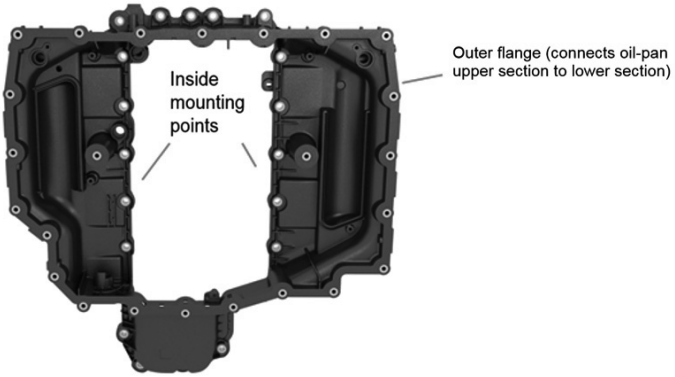

Fig. 9: View of the oil-pan upper section from below.

The oil lines in the media lines carrier are arranged in such a way that the carrier can be produced as a two-part, two-shell item (see Figure 6). The media lines carrier is then connected to the oil-pan upper section by means of self-tapping screws, with O-rings used as seals where the oil lines interface with the upper section. The structure is thus modular or replaceable.

Should the welding of the media lines carrier fail to be leakproof, the ensuing scrap costs are lower. The carrier is then removed and the oil-pan upper section with the 48 molded-in bushings reused.

Fig. 10: Left: Rotary indexing table for the bushings; center and right: placement and removal handling units on the nozzle and ejector sides respectively.

All of the oil-pan bushings are inserted in the mold and encapsulated in the injection-molding process. For this purpose a placement and removal unit which can rotate by 360° was

prepared. By means of a rotary indexing table, this takes up all bushings on the nozzle and ejector sides (Figure 10). Two robots are used to load the three holding units on the rotary indexing table. The completed component can be removed via a 90° rotation of the handling device.

Fig. 11: Semi-automatic installation of the gasket

To make it faster for the worker to fit the gasket, it is first prepositioned on a flat plate which has a groove in the mirror image of the gasket groove. The special shape of the gasket with its wing profile allows it to be easily inserted in the groove in the plate. The component is then set down on it and the gaskets pressed evenly from below into the groove in the component. The time advantage over the classic installation method, in which the gasket is fitted directly, arises from the use of the flat surface. The gasket is set down on the surface without careful positioning and can then simply drop into the groove after being slightly repositioned. The classic method does not use a flat surface and the worker must keep pressing the gasket from below in order to get it into the gasket groove. This takes time.

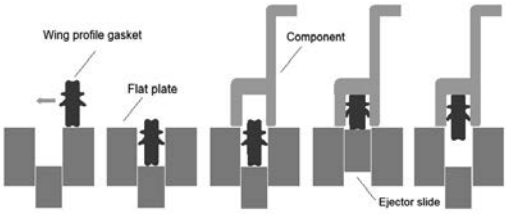

Fig. 12: From left to right, operations in the semi-automatic installation of the gasket

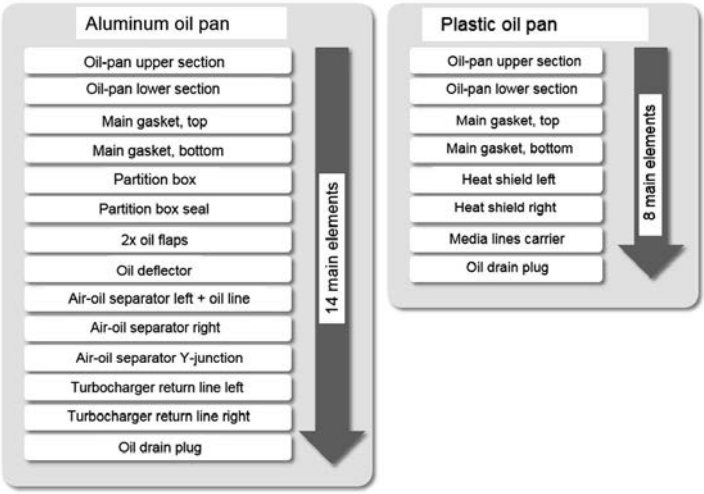

Fig. 13: Number of main elements of the oil pan to be produced at the suppliers

The simplification of the production process is also evidenced by the number of components now required. All in all the number of main elements to be manufactured on the supplier side has been reduced from fourteen to eight (Figure 13). Even more striking is the difference in the installation work required at the engine. While eight assembly steps were previously required for the aluminum oil pan, now it is only two (Figure 14).

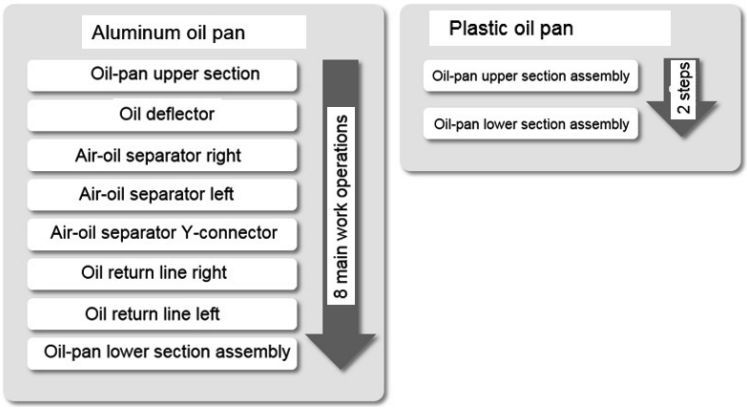

Fig. 14: Number of most important work operations in final installation at the engine.

4. Simulation and validation

To ensure the functionality of the oil pan, comprehensive simulations of the various loading states were carried out as early as the concept phase (Figure 15). In contrast to other plastic components in the engine compartment there were here some loading cases requiring special attention. One example is the loading arising from setting the engine down on a workshop floor. The floor contact area had to be selectively reinforced taking the eccentric center of gravity into account.

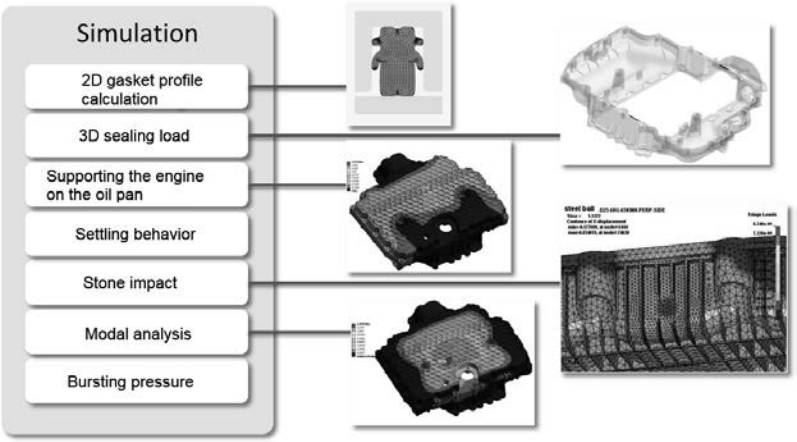

Fig. 15: Overview of calculation for the design of the component function

In designing the gasket between the upper and lower sections of the oil pan one special aspect had to be taken into consideration: unlike the conventional gasket, here both components are made of polyamide. This results in a considerably more yielding structure, especially under an elevated environmental temperature or oil temperature. The sealing system has been adjusted here so that the sealing load curve runs as flat as possible.

The honeycomb rib structure on the underside is an essential feature of the oil pan. The simulation indicates that external forces and inertial forces are distributed very evenly over the structure thanks to this ribbed geometry. In comparison with a random arrangement of the ribs there is a slight increase in sound radiation but when all existing loading cases are taken into account the advantages of the honeycomb structure outweigh this (see Figure 16). No acoustic abnormalities have been measured at the engine.

Property	Result of honeycomb structure	Result of irregular ribbing	Change [%]
	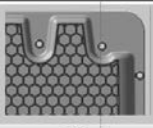		
Total deformation burst pressure [mm]	9,4	9,5	+1
Comparative stress burst pressure [MPa]	31,6	47,6	+50
Total deformation 1st EF [mm]	2,0	2,0	0
Comparative stress 1st EF [MPa]	8,2	17,9	+118
Total level outside at 115 dB inside [dB]	65,2	63,7	-2,5

Fig. 16: Direct comparison of the honeycomb and random structures

In addition to the simulation-based design, a number of validation tests were carried out to check the function [Figure 18]. Compared with cylinder head covers which encapsulate the engine in a similar way, oil pans, due to their special position, must have a high resistance to stone impact. The surface was blasted vertically with defined cast steel pellets from a stone impact simulator. Our investigations have shown that even at a bombardment energy corresponding to 140 km/h only superficial damage was caused. No leaks resulted in the oil pan.

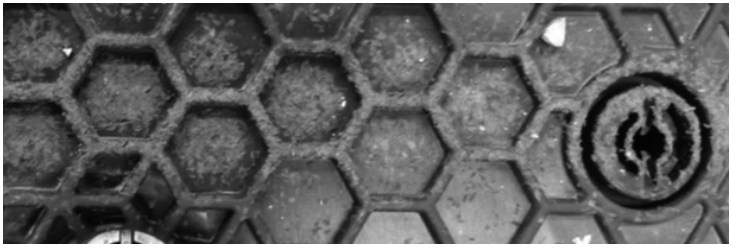

Fig. 17: Test image from stone impact testing at a firing velocity of 140 km/h

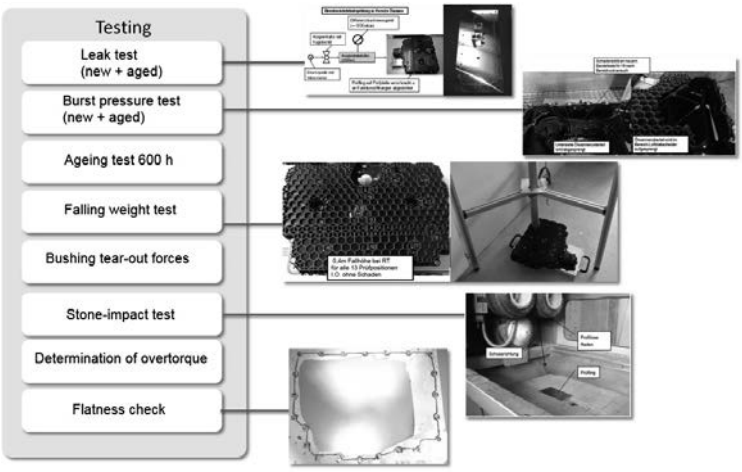

Fig. 18: Brief overview of the most important tests for evaluating oil-pan function.

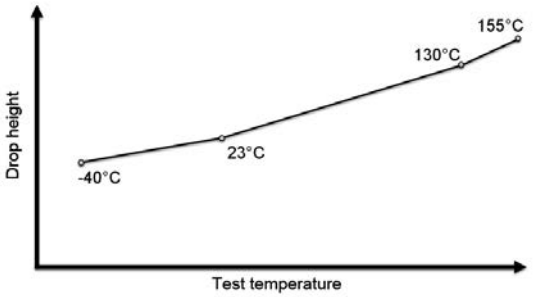

Fig. 19: Fracture drop height plotted against component temperature

Another quality characteristic is the falling weight test. Here a test piece is allowed to fall from an increasing height onto various positions on the oil pan. The test is performed at different ambient temperatures. As expected, the impact resistance of the polyamide material varies very markedly with temperature. In this regard aluminum has undeniably good properties but dents relatively quickly. Irreversible deformations are created which could, for example, negatively affect oil suction at the oil suction pipe to the oil pump. Although polyamide is softer in comparison it does nevertheless also have good recovery capabilities. The target value defined for this test was reached.

The long-term behavior of the polyamide used also plays an important rôle. Here long-term chemical-exposure tests were carried out for over 3000 hours below 150 °C. Results demonstrated that product properties remained very stable and that PA6 exhibited no disadvantages as compared with the PA66 mostly used for historical reasons.

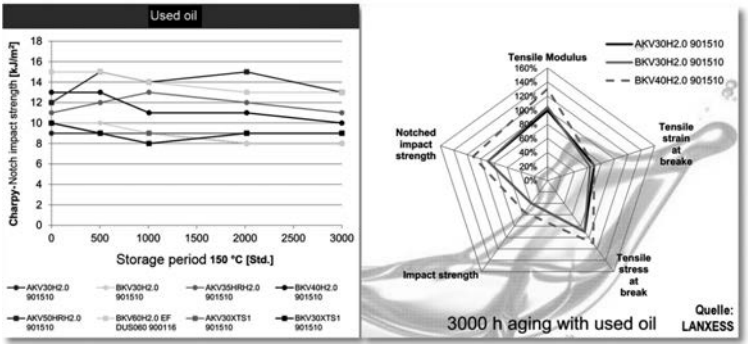

Fig. 20: Properties of different types of polyamide produced by Lanxess.

5. Outlook

The substitution of polymer materials for metals continues in passenger car oil pans. The general performance of this group of materials makes it eminently suitable for these components. It is expected that it will be possible to integrate more functions in the future. Particular attention should be given here to oil cooling and oil filtering. These functional elements have media-carrying aspects which can in principle be integrated in the oil pan. The connection location and the route of the lines could be reproduced in the oil pan. By using hydrolysis-stabilized polyamides it would then also be possible to integrate lines carrying cooling water.

[1] Energie- und ressourceneffiziente Produktion von Aluminiumdruckguss (2013) ; Springer Berlin Heidelberg ; pp.1-18 ; ISBN 978-3-642-39853-7

Plastic oil pan design for an optimized gasoline engine

Project management of novelty by failure mode analysis

J. M. Fiard, J. M. Cardona, Renault, Guyancourt, France;
P. Gauquie Mécaplast, Lens, France

Abstract

Following its strategy of accessible mobility for all, Renault has developed a new A-segment SUV with a new 3-cylinder gasoline engine dedicated to promising emerging markets like India. Renault engineering has focused on lightening the structure to secure benefits in both fuel consumption and production costs and thus obtaining an optimized gasoline engine. In this context an innovative polyamide oil pan has been developed. We focus in this paper on the challenges of using polymer material and liquid sealing with regard to the reliability of such structural parts under the hood. We describe the development process that has been applied with the original equipment manufacturer Mecaplast. The methodology is based on a failure mode analysis process such as breakage (brutal, fatigue, creep) and leakage. We explain the complementarity of the tests and the numerical simulations for the validation plan.

1. Introduction

Fig. 1: The Renault Kwid and its powertrain

This paper deals with the plastic oil pan of the new Renault Kwid launched onto the Indian market on September 2015 (cf. Fig. 1). One of the main user selling points (USP) of this product is its very competitive price. The main lever to reduce price is to reduce weight and

this contributes also to reducing fuel consumption and CO_2 emission. All the engineering departments at Renault and the OEM have worked continuously on reducing the mass of powertrain and vehicle, achieving a real breakthrough in terms of performance / mass ratio. To illustrate this point, we show in Fig. 2 a benchmark for cylinder blocks in aluminum alloy. The y axis is the total weight of the engine basis while the x axis corresponds to a performance index taking into account engine power, engine torque and NVH performance. One can see that the new engine is the leader amongst three-cylinder engines.

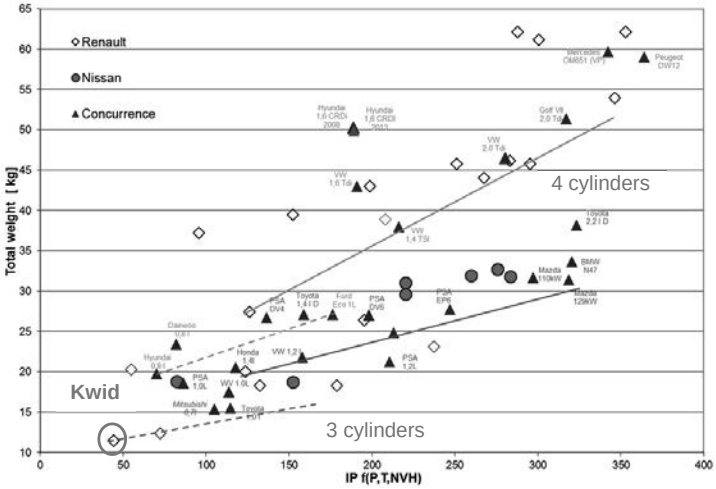

Fig. 2: Benchmark of cylinder block in aluminium alloy

Associated with an open-deck cylinder block without a skirt, the PA6-GF oil pan enable a saving of around one kilogram. Besides this choice, new gains were found by adopting a form-in-place gasket (FIPG) and a spin-on oil filter.

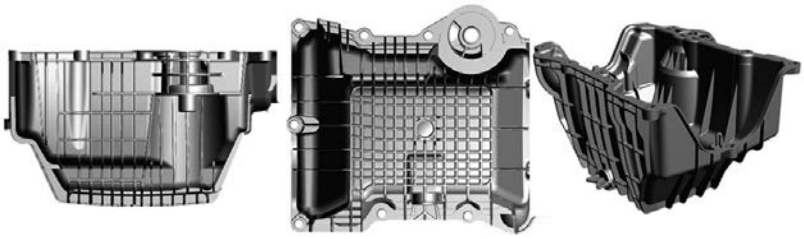

Fig. 3: Kwid oil pan

2. Design review by failure mode process

Besides the standard process of engine development, a process devoted to innovating parts called design review by failure mode (DRBFM) has been applied involving the core competencies leaders. If the DRBFM process fails to prove reliability, the back-up solution is adopted.

To start the process, one identifies the level of novelty of the part (scale from 1 to 5). For instance, the 3D sealing was new for Renault but not for Nissan when the FIPG with aluminum substrate and the thermoplastic oil pan were new for the both companies and were therefore considered more critical. The project and core competencies leaders thus focus on the failure mode analysis as illustrated for the oil pan in Fig. 4.

	Novelty		Failure Modes		Solicitations
	Specificity	Cotation			
FIPG	3D Sealing	3	Leakage	Leakage by lack of product	Product x Process Assembly
	Sealing between aluminium and plastic parts	4		Leakage by silicon extrusion	Product x Process Assembly
				Leakage by adhesive break	Aluminium part / Plastic part / Silicon compatibility
				Leakage by dynamic break	Thermal solicitations
					Engine excitation
Plastic oil pan	Plastic material	4	Breakage	Creep breakage	Assembly
				Static breakage	Thermal solicitations
					Oil pressure
				Fatigue breakage	Engine excitation
				Accidental break	Laying on the floor
					Shocks

Fig. 4: Oil pan failure mode analysis

For each failure mode, we associate physical criteria which can be measured or calculated for each pair (failure mode, solicitation). The criteria for leakage and breakage are presented in Fig. 5 and Fig. 10 respectively where we also indicate when used tests and/or numerical simulations. We explain below the action plan required to check that those criteria have been satisfied.

3. Leakage issues

We count four situations which could lead to leakage (cf. failure mode column Fig. 5).

The first one is due to the lack of product applied during processing in the plant. The second leakage risk is silicone extrusion due to distortion of the thermoplastic oil pan and the excessively large gaps after assembly. We must also make sure that the bolt tension is enough to keep parts in contact and prevent any relative motion between parts which would lead to an uncontrolled low-cycle fatigue failure of the gasket. Compatibility between the

aluminum parts (cylinder block and timing cover), the plastic oil pan and the FIPG was a main issue which required dedicated experiments. Finally, we had to prove that no failure could occur due to in-service stresses.

Failure Modes		Solicitations	Criteria	Test	Sim.
Leakage	Leakage by lack of product	Product x Process Assembly	Chamfer continuity		X
			Silicon thickness in chamfer	X	
	Leakage by silicon extrusion	Product x Process Assembly	Distortion after moulding	X	X
			Gap after assembly	X	X
			Tension need to correct part deformation		X
	Leakage by adhesive break	Aluminium part / Plastic part / Silicone compatibility	Cohesive	X	
			Roughness	X	
			Mechanical resistance	X	
			Oil compatibility	X	
			Ageing	X	
	Leakage by dynamic break	Thermal solicitations	Max admissible FIPG displacement	X	X
		Assembly & Thermal Ageing	Max admissible FIPG displacement	X	
		Engine excitation	Max admissible FIPG displacement		X

Fig. 5: Criteria for leakage

Lack of product

Silicone bead deposition depends mainly on a good chamfer continuity and a minimal silicone thickness.

Silicone extrusion

The non-cured FIPG should not be blown out by the air control pressure test in the plant (+50 mbar rel.). A specific experiment and a design of experiments has been done to establish the maximal gap criterion allowed between parts (cf. Fig. 6).

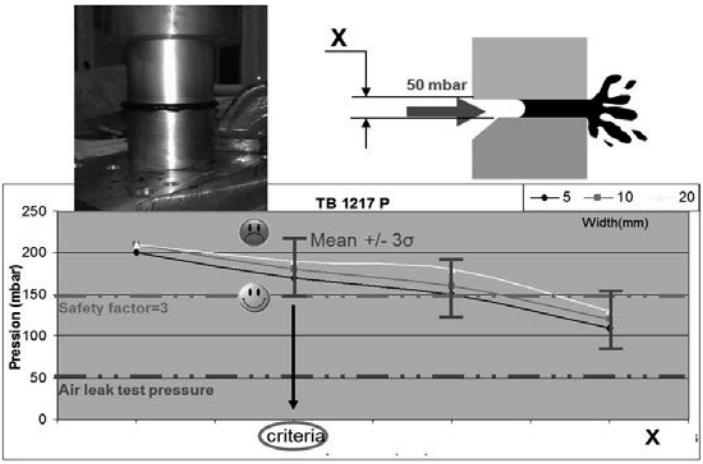

Fig. 6: Gap criterion

The clearance between oil pan and aluminum parts has been measured after many cycles and maintenance in hot conditions (145°) and cold conditions(-30°)**.**

Adhesive break

The way that silicone rubber could break – adhesive or cohesive breakage (cf. Fig. 7) – depends on the compatibility between the aluminum alloy, the thermoplastic resin and the silicone resin. Our aim is to be sure to eliminate adhesive breakage in order to profit from the elongation potential of silicone. We had no information at the beginning of the project regarding this compatibility. For this reason a design of experiments was conducted with 12 resins (four suppliers) with several viscosities. The tests were carried out with two PA6-GF and two PA66-GF thermoplastic resins and three surface treatments. The results show that five silicone resins have good bonding characteristics with plastic. Notice that the silicone resin must not be too much viscous if void creation during processing is to be avoided. Concerning the plastic parts, a minimum surface roughness is recommended in order to avoid plasma surface treatment (considered as a highly efficient back-up solution).

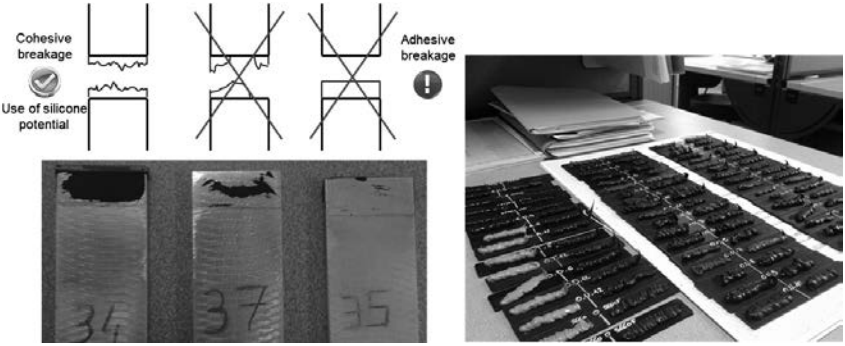

Fig. 7: Cohesive vs adhesive silicone breakage

Dynamic breakage

The elongation at break of FIPG, oils compatibility and the aging effect have also been studied. Indeed, an experiment was carried out at Renault to characterize shearing elongation (cf. Fig. 8). We thus obtain a physical criterion for the part's relative motion in terms of maximum admissible deformation for FIPG (<300%) and in terms of maximum displacement for parts (under the hypothesis of silicone thickness).

By the way, those experiments revealed that most of the resins have a good chemical resistance to oil and we observed the increase in elongation at break during the oil thermal-aging tests.

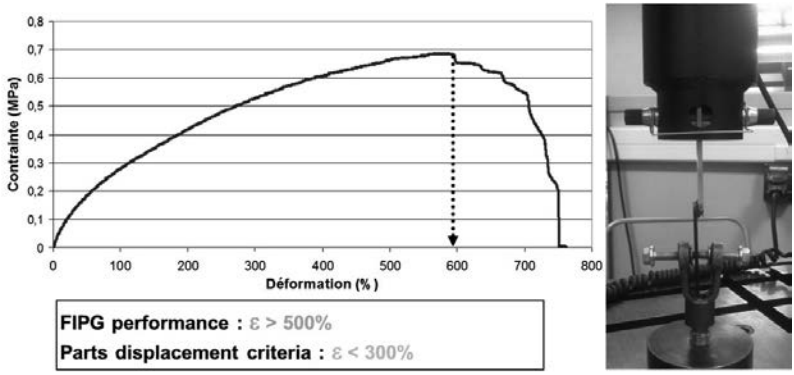

Fig. 8: Shearing elongation

Concerning engine excitation vibrations, Nissan provided fatigue test results (see the rig test in Fig. 9) with which a maximum relative displacement allowed between parts can be established.

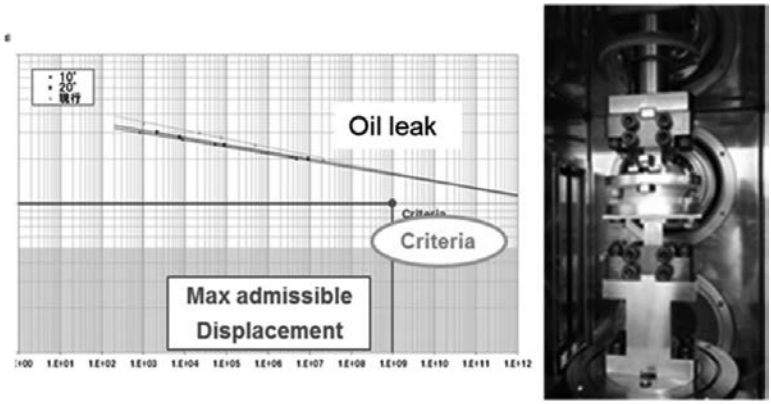

Fig 9: Fatigue results on FIPG

Numerical simulations (thermal expansion analysis) and measures (under hot and cold conditions) have been carried out to verify that deformation of FIPG is below criterion. Vibratory displacements have been simulated via a force response analysis and fully comply with fatigue criteria.

4. Breakage issues

Failure Mode		Solicitations	Criteria		Test	Sim.
Breakage	Creep	Assembly	Max creep fracture (@ equiv .temp.)			X
	Static	Thermal solicitations	Max stress fracture (@ peak temp.)			X
		Oil pressure				X
	Fatigue	Engine excitation	Max fatigue admissible stress			X
			First mode frequency > H1,5 +10%			X
	Accidental	Laying on the floor	Max admissible stress			X
		Shock	Stones impact by vehicles crossing (@130km/h) No cracks	Ribs must to resist to stone impact	X	X
				Skin must to resist to stone impact	X	X
			Crossing sidewalk	Ribs/skin	X	

Fig. 10: Criteria for breakage

We count four breakage situations which have been detailed in this section; the creep, static, fatigue and shock failure modes. But first it is crucial to have an accurate idea of the distortion after molding and of the local properties (Young's modulus as the first one) of the fiber-filled polymer after molding. This is done by rheological simulations as depicted in Fig. 11. Rheology simulations are also essential to identifying weaknesses at the internal merging flow front.

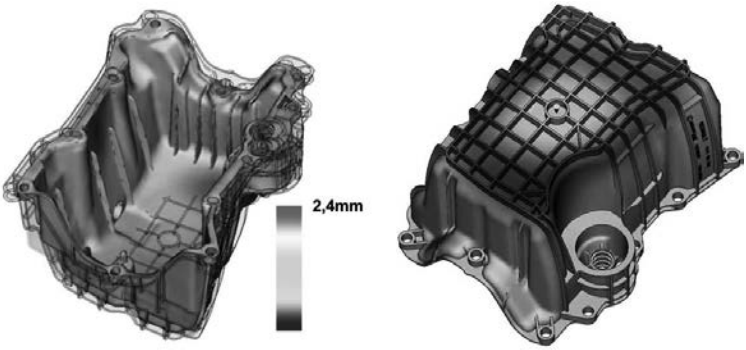

Fig. 11: Rheology simulation

Creep, static and fatigue breakage

Numerical simulations have been carried out to evaluate stresses and the displacement response to various loads: the tightening process on a distorted part, oil pressure, thermal load and engine vibration (Fig. 12). Our criteria are admissible stress for the oil pan and admissible displacement for the silicon rubber (see the gap criterion above). For such failure modes, numerical simulation is good enough nowadays for estimating the stresses in the structure. So we can take advantage of it to sort the designs and identify the better ones.

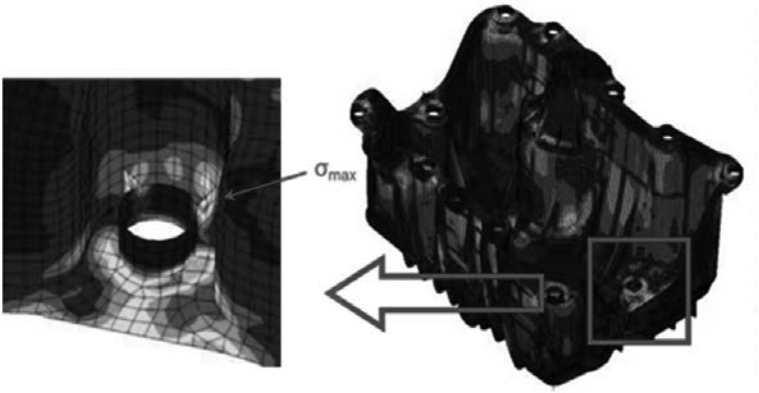

Fig. 12: Engine vibration stresses

However, it is quite impossible, except in particular cases, to compare calculation results directly with specimen experimental data (as ultimate tensile stress or fatigue limit) and it is necessary to take into account a safety factor (SF).

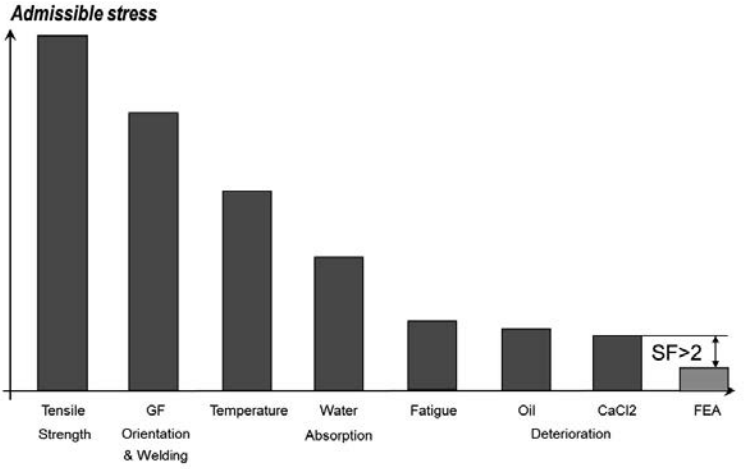

Fig. 13: Assessment of strength for fatigue failure mode

The first reason is because the thermoplastic parts have material properties which are non-uniform and anisotropic due to the variation in fiber density and fiber orientation. Secondly, the various deterioration mechanisms under the hood (thermal aging, oil aging, salt aging,

absorption and so on) as well as strength on welds are not properly modeled today and can be very scattered. So within the framework of the Renault-Nissan alliance, we apply a stress-strength reliability approach illustrated by a so-called 'bar graph' diagram (see Fig. 13). In this diagram we compare the strength of the part (deduced from specimen experiments) which falls as a function of the deterioration factors, to the stress applied, that is, the computed stress.

Accidental breakage

We have considered three types of accidental breakage due to shocks: bottoming out, stone impact and crossing sidewalks. For each case we differentiate between ribs and skin in order to assess the resistance of these parts. Bottoming out has been simulated and results have been compared to an admissible stress as done for creep, static and fatigue failure modes. For crossing sidewalks, vehicle tests have allowed the risk to be eliminated.

For the stone impact, rig tests with several impactors (cf. Fig. 14) have been carried out to determine properly the resistance in terms of the energy absorbed by ribs and skin.

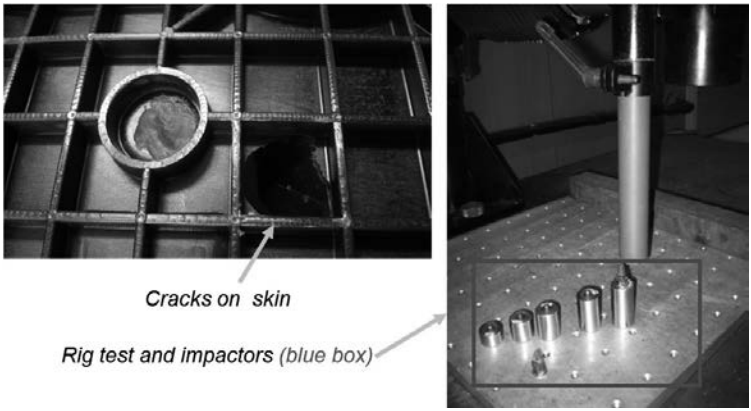

Fig.14: Stone impact crack and test rig

Once the admissible energy was determined for the ribs and for the skin, we were able to predict situations where failures could occur when cars collide.

Fig. 15 shows how the risk of breakage of the skin (because breakage of ribs calls for too much energy to be a problem) was eliminated during the project by a proper design.

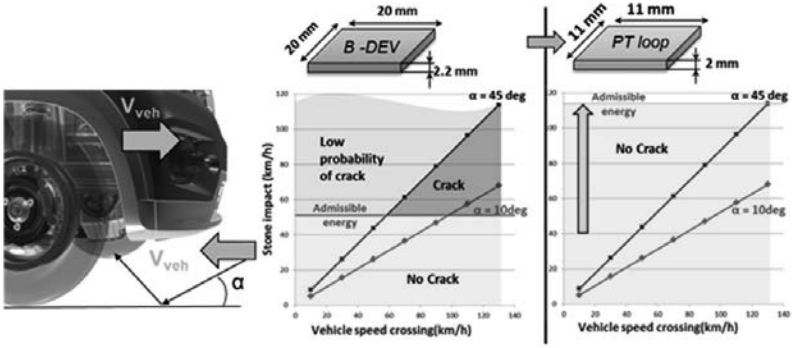

Fig. 15: Design to overcome stone impacts failures

In Fig. 15 the risk domain is bounded by a horizontal line which corresponds to the admissible energy for a given design and an oblique line corresponding to a maximum rebound angle. When reducing the space between ribs, the size of stone which could damage the skin is reduced, permitting a higher stone velocity for a given admissible energy.

5. Conclusion

The thermoplastic oil pan of the Kwid engine in combination with a 3D FIPG sealing is ultimately one of a kind. The main challenges were to retain the admissible geometrical dispersion in spite of the large size of the part and to demonstrate reliability in the case of stone impact.

The DRBFM process permitted an efficient management of risk relative to innovatory parts, focusing on the main risks and calling for demonstration of reliability. Notice that the oil pan and the FIPG have successfully passed all bench tests without calling into question the list of failure modes. Numerical simulation is a big help today in keeping to time schedules but suffers from a lack of modeling for the constitutive laws and for damage (cf. [1]). This situation implies applying asafety factor which cuts into the potential of polymer. Ultimately this project shows that expansion of plastic parts under the hood is possible but this will mean dealing with more failure modes due to the sensitivity of polymer to temperature and to contact with various fluids.

Acknowledgements

We are indebted to V. Bossavie and J.-M. Salondy who conducted the experiments at Renault for sealing and breakage issues respectively. The authors gratefully acknowledge the support provided by C. Le Coeur and G. Morin with their clear-sighted analysis.

[1] Fiard, J-M: Méthodologie de dimensionnement fiabiliste des pièces plastiques du GMP: SIA Congrès, Montigny, 2015

Thermally conductive plastics: a mineral solution

Thermal management in thermoplastics and thermosets

Dipl.-Ing. **T. Hilgers**, Quarzwerke GmbH, Frechen

Abstract

For many years additives based on mineral resources have played an important rôle as fillers in the plastics sector. Special fillers give thermoplastics and thermosets better properties as regards mechanical strength, thermal properties and dielectric properties. Recently however these traditional requirements have been joined by new ones. In particular the use of electrical components with a high energy density (processors, light-emitting diodes, electric motors, and so on) depends on an efficient dissipation of the heat produced while simultaneously maintaining the electrical insulationing function of the plastic materials used.

Although plastics have a very low thermal conductivity this can be increased significantly by the incorporation of additives with a high inherent thermal conductivity.

The various materials which can be used for conducting heat in thermoplastics and thermosets are surveyed. The focus here is placed on thermal conductivity, mechanical properties, and the commercial feasibility of heat-conductive plastics.

Important subject areas covered here will be the mechanisms of convection and thermal radiation necessary for heat transfer and also influencing factors such as, for example, filler content, particle size distribution and processability. A comparison is also made of the potential for weight reduction, the costs and the carbon-footprint calculation for manufacturing a heat sink made of aluminum and a heat sink made of plastic (polyamide 6-compound).

1. Introduction

Metals in the widest range of variants and implementations are well known for use in heat dissipation. Aluminum heat sinks and metal housings are in common use in the field of passive and active cooling in electronics. In either case, production is inevitably expensive. The more complex the geometry required, the harder it becomes to deliver it. A straightforward high-volume production of complex components as is familiar with thermoplastic and thermoset processing rules these materials out. All metals also have good electrical conductivity. However, there are applications where this electrical conductivity is undesirable. This means that appropriate insulation measures must be taken.

2. Heat transfer mechanisms

Materials in direct contact with a hotspot must carry the heat away from the component as rapidly and effectively as possible by means of conduction (heat transfer from one body to another).

Heat transfer by conduction is described by Fourier's law.

$Q = \lambda A \Delta T / d$

Q = rate of heat flow (W)

A = area (m^2)

λ = thermal conductivity (W/mK)

ΔT = temperature difference between the materials (K)

d = thickness of the material (m)

Table 1 gives an overview of the thermal conductivities and electrical resistances of various materials at room temperature.

Table 1: Thermal conductivity and electrical resistance of various materials

Material	Thermal conductivity [W/mK]	Electrical resistance [Ohm*m]
Copper	401	1.68×10^{-8}
Aluminum	205	2.82×10^{-8}
Iron	80	1.0×10^{-7}
Boron nitride (hexagonal)	30 ⊥; (600 ∥)	10^{13}
Aluminum oxide	30	10^{12}
SILATHERM	14	10^{13}
Magnesium oxide	30	10^{20}
Glass	1.05	10^{13}
Polymer	0.2 - 0.4	10^{11}
Air	0.024	3.3×10^{16}
Water	0.609	1.8×10^{5}

= electrically conductive

= electrically insulating

The first direct contact with a hot spot typically consists of a printed circuit board.

The heat must be transported away from the relatively small and compact circuit board with a small surface area via a heat sink or a housing with a large surface area and so to the destination location. [5]

This heat transfer is known as convection. Convection describes the transfer of heat from a solid body to a fluid medium (gas or water).

The heat transfer by convection is described by Newton's law:

$$Q = \alpha \, A \, \Delta T$$

Q = rate of heat flow (W)

A = area (m^2)

α = convective heat transfer coefficient ($W/(m^2K)$)

ΔT = temperature difference (K)

Figure 1 [2] shows heat transfer through a multi-layer wall.

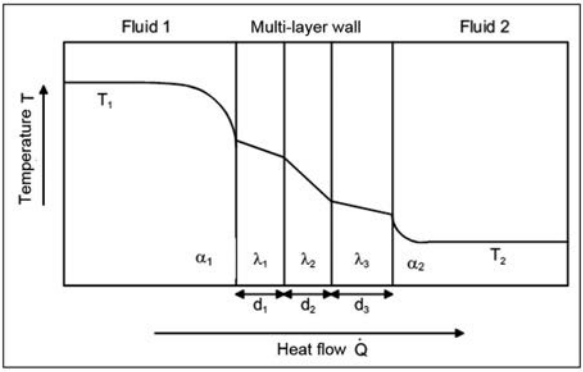

Fig. 1: Heat transfer through a multi-layer wall

With heat transfer a distinction is drawn between free and forced convection. Free convection is found with immobile media and forced convection with mobile media.

Air as a medium is the most common destination for the heat.

The heat transfer coefficients for free and forced convection are as follows:

Free air convection	5-25 $W/(m^2K)$
Forced air convection	10-200 $W/(m^2K)$
Free water convection	20-100 $W/(m^2K)$
Forced water convection	50-10 000 $W/(m^2K)$

It can be seen from Figure 2 [1] that above a thermal conductivity of approx. 1.5-2 W/(mK) of a heat sink the decisive step in reducing the contact temperature is convection.

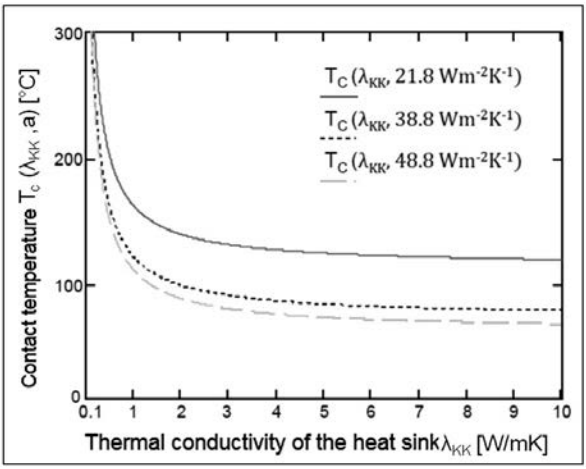

Fig. 2: Contact temperature as a function of the thermal conductivity of a heat sink for different heat transfer coefficients

Using thermally conductive plastics rather than metal gives full design freedom and can thus increase heat transfer by, for example, increasing the surface area of the component.

3. Increasing thermal conductivity in thermoplastics

Different properties of the additives play a part in increasing thermal conductivity in plastics. Figure 3 [3] which follows shows the various factors influencing thermal conductivity.

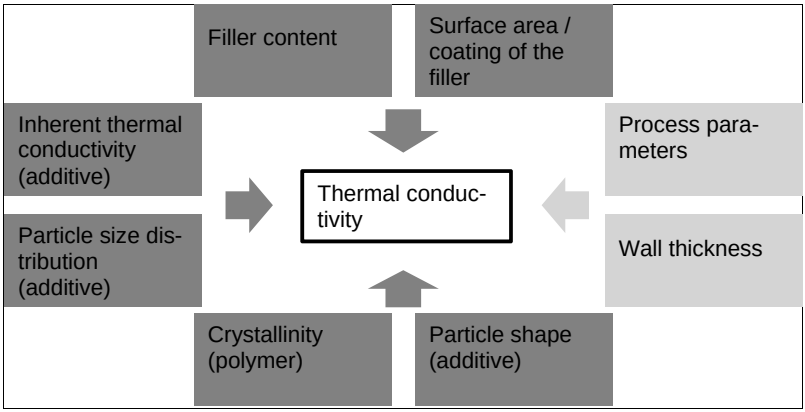

Fig. 3: Factors influencing thermal conductivity

In order to compare different heat-conductive additives, 65 m% of the additives were compounded in a polyamide 6 matrix. In the case of hexagonal boron nitride the concentration had to be reduced to 55 m% since the excessive embrittlement of the material meant that strand pelletization was no longer possible.
The products SILATHERM® 1360-400 AST and SILATHERM® 1360-010 AST only differ in their particle size. SILATHERM® 1360-400 AST has a D50 of 5 µm and SILATHERM 1360-010 AST a D50 of 23 µm.

In the case of the thermoplastic compounds, the various additives were compounded into the polyamide 6 via an extruder (Leistritz, ZSE 27 MAXX). Moldings were made from the compounds by injection molding (Demag, Ergotech 100/420-310):

Multi-purpose test piece (ISO 3167 Type A)
Sheet 80 mm * 80 mm * 2 mm

The test pieces needed for measuring thermally were machined from the sheets. The thermal properties of injection-molded parts differ depending on whether they are measured in the direction of flow or across it. To take this fact into account, measurements were taken as follows: to measure across the direction of extrusion (Z axis) disks with a diameter of 2.7 mm were cut out from a central position on the sheets. For determining the thermal conductivity in the direction of injection (X axis) six bars, each measuring 12.7 mm in length and 2 mm in width, were milled out in each case and then, after being rotated by 90°, clamped in a test piece holder. [4]

A NETZSCH LFA 447 NanoFlash (ASTME-1461, DIN 30905 and DIN EN 821) was used for determining the thermal conductivity of the filled polymer compounds. Tensile properties were determined following DIN EN ISO 527, impact strength according to DIN EN ISO 179 and HDT A as per DIN EN ISO 75. [4]
Table 2 shows results for the various additives in polyamide 6.

Table 2: Thermal conductivity and mechanical properties of filled PA compounds

Product in polyamide 6	Thermal conductivity		Tensile properties		Charpy impact strength	HDT A	Price	Mohs hardness / abrasivity
	X	Z	σ_M	Modulus of elasticity				
	W/mK	W/mK	MPa	MPa	kJ/m²	°C	€/kg	
65 m% SILATHERM® 1360-400 AST	1.3	1.2	93.7	10 000	42.2	142.5	2.9	5
65 m% SILATHERM® 1360-010 AST	1.5	0.9	92.2	11 100	37.8	150.5	2.55	5
65 m% aluminum oxide	1.5	0.9	88.8	9640	39.1	119.8	2	9
55 m% boron nitride	5.3	1.0	68.1	11 800	10.4	161.9	80	2
65 m% magnesium oxide	1.4	1.2	84.7	8910	31.6	120.0	5	6

Figure 3 [3] shows a relative comparison of property changes in PA compounds resulting from the various thermally conductive additives.

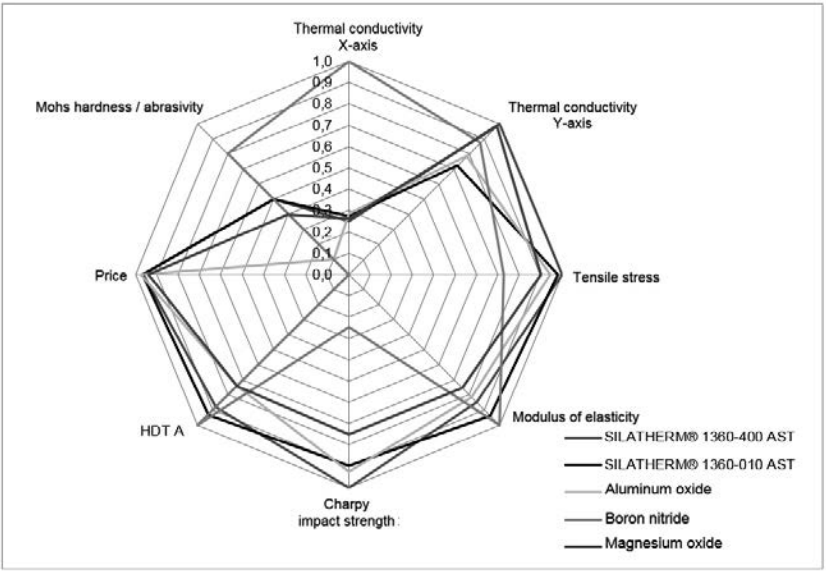

Fig. 3: Relative values of PA compounds with different additives

These values show clearly that the highest thermal conductivity can reached with boron nitride but the material costs are also the highest. However, it is not only the results for thermal conductivity and price which should be considered but also the changes in mechanical and thermal properties. The SILATHERM® range of products here shows a very well-balanced properties profile with very good mechanical properties and thermal conductivities up to 1.5 W/mK at filler contents of 65 m%.

When the filler content is raised to 75 m% thermal conductivity values of 2.3 W/mK can be achieved with the product SILATHERM® 1360-010 AST.

This indicates that thermal conductivity depends very greatly on the filler content of the polymer. Here the rule of thumb of 'the more, the better' applies.

In contrast, an increase in the filler content has a negative effect on impact strength.

Table 3 shows the relationship between thermal conductivity and mechanical properties and the filler content in the product SILATHERM® 1360-400 AST.

Table 3: Comparison of thermal conductivities and mechanical properties for different filler contents

Product in polyamide 6	Thermal conductivity		Tensile properties		Charpy impact strength	HDT A
	X	Z	σ_M	Modulus of elasticity		
	W/mK	W/mK	MPa	MPa	kJ/m²	°C
65 m% SILATHERM® 1360-400 AST	1.3	1.2	93.7	10 000	42.2	142.5
70 m% SILATHERM® 1360-400 AST	1.6	0.9	94.2	11 300	37.0	143.7
75 m% SILATHERM® 1360-400 AST	2.0	1.3	95.5	15 500	19.7	164.4

Should a thermal conductivity of 2 W/mK not suffice for the various applications, a secondary filler such as boron nitride can be added to the SILATHERM®. The following diagram 1 [4] shows the changes in mechanical properties, thermal conductivity and material price when boron nitride is added.

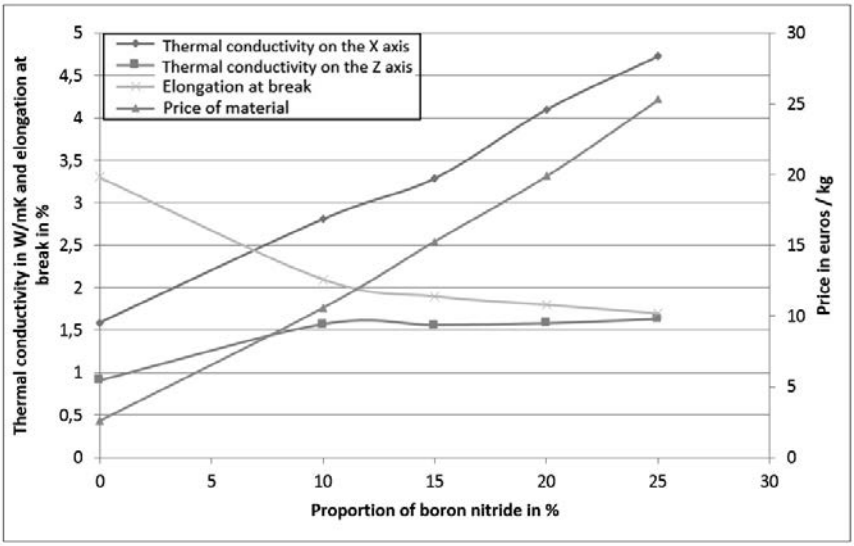

Diagram 1: Change in thermal conductivity and mechanical properties resulting from the addition of a secondary additive

4. Increasing thermal conductivity in thermosets

In addition to the experiments with thermoplastics, investigations were also carried out with thermosets, involving different additives, different particle sizes, different particle shapes, different coating systems and different filler contents.

The following resin system was used here:

Resin: ARALDITE CY 184

Hardener: ARADUR HY 1235 BD

Accelerator: ACCELERATOR DY 062

The resin system was first mixed with different fillers at 60 °C in the vacuum mixer. Curing was carried out for 2 hours at 100 °C and post-curing for 16 hours at 140 °C.

Once again NETZSCH LFA 447 NanoFlash (ASTME-1461, DIN 30905 and DIN EN 821) was used for measuring the thermal conductivity.

Just like the tests with the thermoplastics it emerged very quickly that increasing the filler content resulted in a sharp rise in thermal conductivity as well. For this reason our experiments focused not only on the increase in thermal conductivity but also on the resin system retaining good process capability / flowability. Table 4 shows the first results from different

additives (different minerals with different particle shapes) and different coating systems. Further attempts to increase thermal conductivity and improve mechanical properties by, for example, an optimized particle size distribution are currently being tested and will continue to be the focus of work in our product development department.
The SST coating system has been specifically developed for increasing the filler content in epoxy resin systems. All of the systems listed in the table still show good flowability. At the time of going to press it had not been possible to examine viscosity. These are included in the presentation.

Table 4: Results from different additives in epoxy resin systems

Product in epoxy resin	Filler content	Thermal conductivity	Tensile properties		Charpy impact strength	Price
	Vol.%	W/mK	σ_M	Modulus of elasticity		
			MPa	MPa	kJ/m²	€/kg
SILATHERM® 1360-007 EST	50.20	1.40	118	15 500	6.84	2.6
SILATHERM® 1360-007 SST	58.58	1.91	107	19 010	5.46	2.6
SILATHERM Plus® 1432-012 SST	72.01	3.76	53	39 255	1.77	10
Aluminum oxide	49.18	1.54	137	20 080	10.16	2

In addition to mechanical properties and thermal conductivities, dielectric properties play a major rôle in epoxy resin systems. For this reason the loss factor (tan δ) and permittivity (ε_r) were measured before and after immersion in water in accordance with IEC 60250. The test pieces were immersed for 100 days at 50 °C. Before their immersion in water all test pieces showed good values with a tan δ below 0.05 and a permittivity ε_r below 6.

Following immersion in water, the loss factor of the test pieces increased to more than 0.2 and permittivity to over 15. On the basis of these results, use of the SILATHERM® product series and aluminum oxide in outdoor applications is not recommended.

4. Carbon footprint

In addition to the thermal and mechanical properties and the thermal conductivity, a CO_2 assessment was made. This CO_2 balance was then compared with that of aluminum metal since aluminum is currently the most widely used material in the field of thermal management.

Table 5 shows the results for the carbon footprint.

Table 5: Values for the GWP of different materials

Material	GWP [CO_2eq]	References
Finely ground mineral powders	0.12 to CO_2 / to product	Life Cycle Inventory (LCI) from Industrial Minerals Association (IMA-Europe) Feb 2013
Aluminum metal	11 to 16 to CO_2 / to product*	Global Life Cycle Inventory Data for the Primary Aluminum Industry (2013) Life Cycle Impact Assessment (LCIA) results for the worldwide aluminum industry
Polyamid 6	6.7 to CO_2 / to product	Eco-profiles and Environmental Product Declarations of the European Plastics Manufacturers, Polyamide 6 (PA6), PlasticsEurope, February 2014

* Value greatly dependent on region

Taking a compound with 65% SILATHERM® and 35% polyamid 6, the GWP for this compound is approx. 2.4 to CO_2 / to product (i.e. compound) and thus better in climate protection by a factor of 4 to 6 than a comparable aluminum solution with 11 to 16 CO_2 / to product (with respect to weight). In the case of the injection-molding process, it is also possible to optimize geometry, such as, for example, giving a heat sink a thinner base plate. In this case, due to a possible weight reduction the factor would fall by 30% to 5 to 8.

5. References

[1] Christoph Heinle; Simulationsgestützte Entwicklung von Bauteilen aus wärmeleitenden Kunststoffen; Thesis Engineering School of the University of Erlangen-Nürnberg, 2012

[2] Simon Amesöder; Wärmeleitende Kunststoffe für das Spritzgießen; Thesis Engineering School of the University of Erlangen-Nürnberg, 2010

[3] HPF The Mineral Engineers; SILATHERM® - Mineralische Füllstoffe für wärmeleitfähige Compounds; Seminar: Wärmeleitende Kunststoffe – wie soll das gehen?, Kunststoff Institut Lüdenscheid, 22.05.2014

[4] HPF The Mineral Engineers; SILATHERM® for zur Verbesserung der Wärmeleitfähigkeit; Technical Information 8206 (04/2014)

[5] Dr. Jörg Ulrich Zilles; Adding heat management capabilities to thermoplastics and thermosets; LPS 2014 LED Professional Symposium, Sept 30th – Oct 2nd 2014, Bregenz, Austria, Conference Proceedings

Efficient approach to developing fiber composites

Dr.-Ing. **T. Müller**, BMW Group Munich

Abstract

Fast and efficient processes in material development contribute to finding the best solution for the customer. This means that the latest material technologies and findings are used in in vehicle development without delay and also make thrifty use of resources. The time window for integrating innovations must be kept as open for as long as possible. This makes it necessary to establish pragmatic and industry-oriented approaches in the development of fiber composite materials. Characteristic here is lower material consumption and lower outlay coupled with a faster acquisition of knowledge due to the use of non-refined raw materials.

Examples of this are the fiber-direct RTM process for basic characterization and the 2D crushing of new fiber-matrix systems. In the first case, the potential for lightweight construction and design is identified at an early stage and taken into account in the form of characteristic material values and a corresponding design in vehicle development. In the second case, components in impact zones can be designed on the basis of coupon tests of innovative materials.

1. Introduction: development of material systems

A successful product depends on the development of an optimal solution in terms of the criteria of properties, cost, weight and quality (see Figure 1). With electric mobility, the goal of lightweight design has moved closer into focus in automotive engineering. The weight savings achieved, for example in the body, are needed to compensate for the extra weight of the high-voltage batteries for the electric motor. Furthermore, weight optimizations are of great importance to sustainability and energy consumption, as well as dynamic driving characteristics [1]. Variant solutions must be investigated in the development of this optimal solution. Accordingly, in applying material lightweighting, for example, different material systems must be investigated to see how they meet requirements.

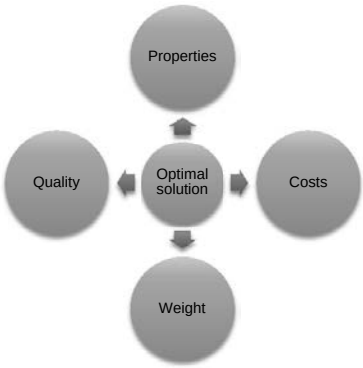

Fig. 1: Selection of the optimum material system according to PCWQ (properties, cost, weight, quality).

With increasingly challenging goals, such as maximum lightweighting at minimal cost, the proportion of mixed constructions rises. An increasing number of variant tests and assessments are needed to make possible the best development of the material systems with regard to property profile and utilization. It must be possible to do so with fast and efficient processes in materials development. This means that the latest findings must be quickly implementable in vehicle development while also conserving resources.

The approach described here of implementing this efficiently is based on an economic selection of materials and an early hardware-software reconciliation. As visualized in the development and validation pyramid, this means maximizing the findings gained from the relatively inexpensive and quickly performed hardware tests on the coupon level (see Figure 2).

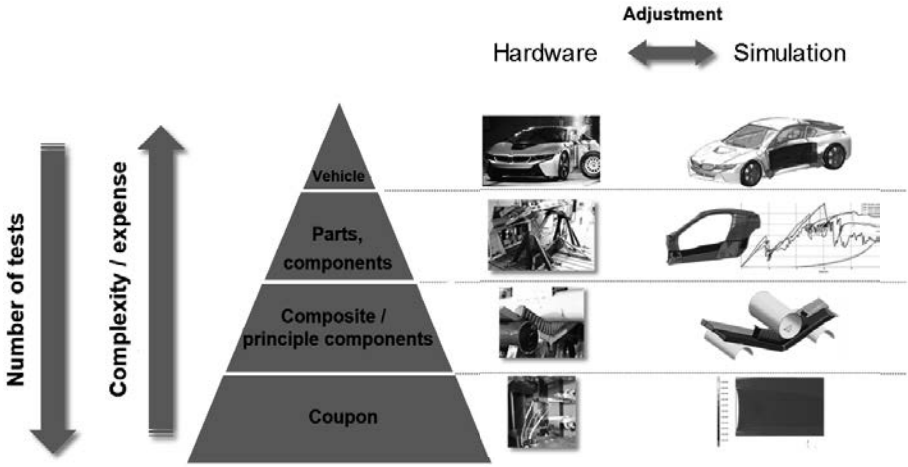

Fig. 2: Development / validation pyramid ([1] to [3])

With increasing complexity the number of hardware tests falls, and this is also reflected in the number of variants in the material systems under investigation. The complexity and cost of a test set-up increases as you go up the pyramid. If a restriction is made on the lowest level of the number of variants this will affect the subsequent levels. At best, expensive hardware tests on the 'Composite / principle components' and 'Parts, components' levels can be saved. This approach aims at increasingly performing inexpensive tests on the lowest level which already make it possible to obtain information about functions in the vehicle and thus enable variant limitation at an early stage.

2. Use of unrefined raw materials

Using unrefined raw materials in making coupons from continuous-fiber-reinforced plastics by fiber-direct RTM opens up new potential in the efficient development of fiber composites. The top part of Figure 3 shows the previous procedure in the hardware testing of new fiber-matrix systems for RTM (resin transfer molding) components. In investigating different fiber variants, for example, the quantities of fibers needed are first produced and then used in making textile semi-finished products. This is followed by stacking and cutting the textile semi-finished products to size. Finally, the stack passes through the preforming and punching processes. At the end, the first laminate sheets are fabricated by the RTM process. The coupons for material testing are taken from these laminate sheets.

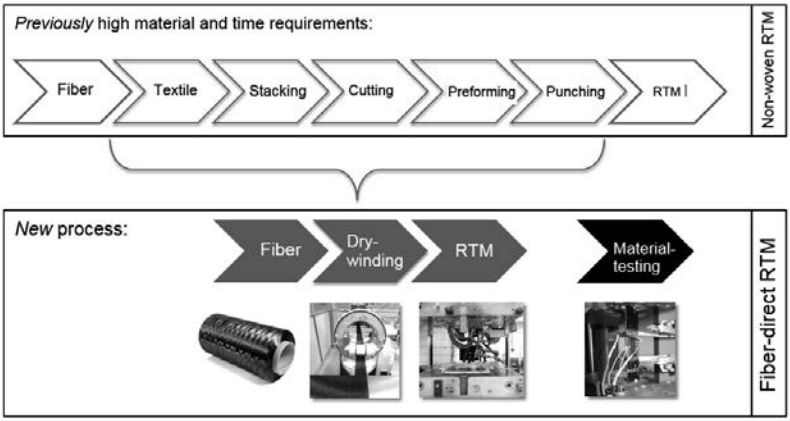

Fig. 3: The 'previous' and 'new' process chains for making laminates for material testing

The new process shortens the process chain between fiber and laminate production in the RTM process (see lower part of Figure 3). This means that textiles are no longer made from the fibers but rather left unrefined and wound onto a metal carrier. The wrapped sheet is inserted directly into an RTM mold. The laminate sheets thus produced are then available for material testing.

This new process chain significantly reduces the quantity of fibers used. Now only one fiber spool is needed instead of the minimum of fifteen previously required to produce non-wovens on the laboratory scale . Furthermore, the fiber spool only needs to hold about 30% of the amount of fiber used in making non-wovens, and this is a consequence of reducing complexity in the winding process. The material costs for a laminate sheet are reduced to 30% as a result of material savings and the omission of process steps (see Figure 4). At the same time the number of working days is halved. This means that twice the number of test material variants can be produced during the same period of time, at 60% of the cost of the original quantity.

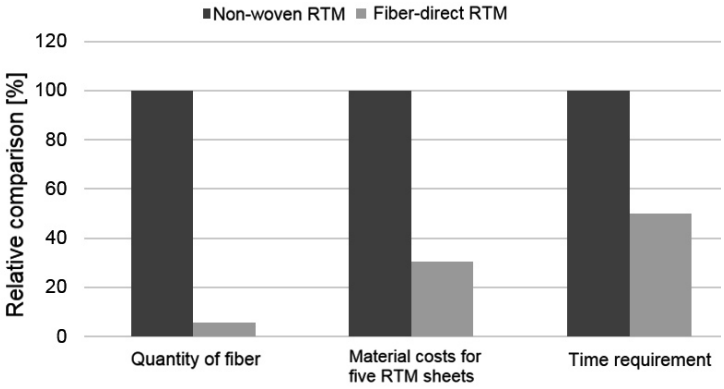

Fig. 4: Comparison of cost and effort for non-woven RTM and fiber-direct RTM (resin transfer molding) based on five RTM sheets.

3. Use of 2D crushing

With sudden planar loading, energy in the case of metals such as aluminum is converted by ductile deformation (see Figure 5, left). In contrast, with an even loading, energy in the case of CFRP laminate structures is absorbed by crushing, that is, breaking and reduction of the laminate to small pieces (see Figure 5, right). A comparison of the specific energy absorption values reveals a theoretical lightweighting potential of 50% for CFRP structures as against aluminum structures.

Moreover, a residual block results after ductile deformation of the aluminum structure (see Figure 6). If it is ensured that the broken CFRP elements can escape, energy absorption by crushing the CFRP does not in this case leave a residual block. This can, for example, be exploited to reduce space requirements in the vehicle front-end by using CFRP profiles instead of metal structures in the longitudinal axis of the vehicle. The resulting benefits can be used in geometric integration for increased freedom of construction and design.

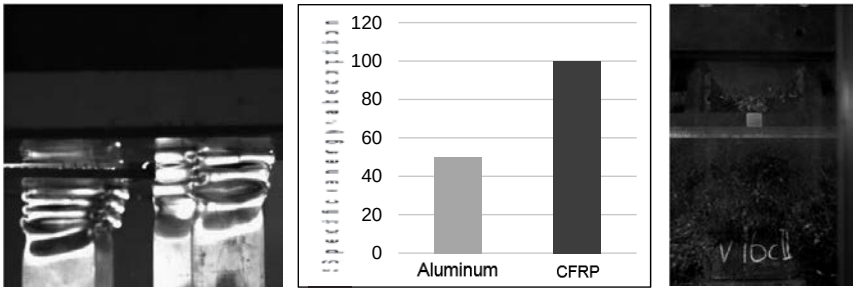

Aluminum: energy absorption by ductile deformation

CFRP: energy absorption by crushing

Fig. 5: Comparison of the energy absorption of aluminum and CFRP under planar impact loading ([4], [5]).

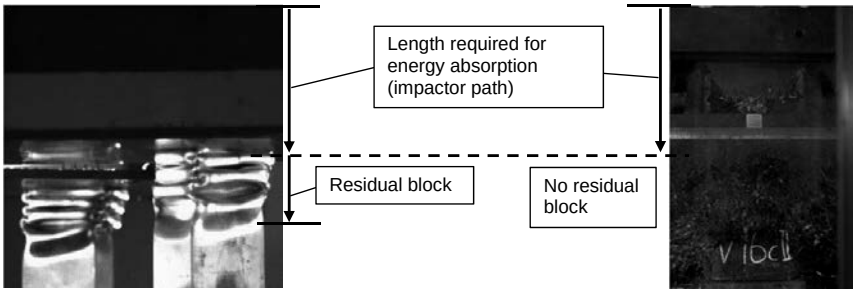

Aluminum: energy absorption by ductile deformation
→Formation of a residual block

CFRP: energy absorption by crushing
→ No residual block

Fig. 6: Deformation of the aluminum profile with residual block formation, and crushing of the CFRP profile ([4], [5]).

Crushing tests based on two-dimensional (2D) test coupons ([6], [7]) have been introduced at BMW to make possible an early assessment and validation of the examples and potentials described above. This means that no elaborate three-dimensional (3D) profile tests are now required for the first assessment of the crushing properties of fiber composite materials. Consequently the exchange and mutual adjustments between hardware and simulation on the new development path now take place one level further down the development / validation pyramid (see Figure 7). With the 2D crushing tests and the hardware-simulation adjustments it is now already possible to draw conclusions at the coupon level about crushing behavior (for example, in a vehicle crash) and define a first limit on the number of

variants. This means that subsequent and expensive crushing tests of profiles are in part avoided.

Standardized laminate and test structures were tested by 2D crushing in order to obtain information about the crushing behavior of 3D geometrical elements such as edge radii and wall thickness changes and their influence on the CFRP structure in crashes ([6], [7]). For example, pins were additionally screwed into the 2D crushing test apparatus to obtain the same delamination and crushing behavior in 2D test pieces as in the radii of 3D shapes. The pins are arranged such that they, like the radius of a profile, can prevent premature delamination in the crushing zone. The level of information obtained from 2D crushing tests is sufficient to allow the creation of FEM simulation models of 3D structures from the results of these tests. The first variant assessments and structure optimizations with regard to crushing can be made with these simulation models before the first 3D hardware tests are carried out.

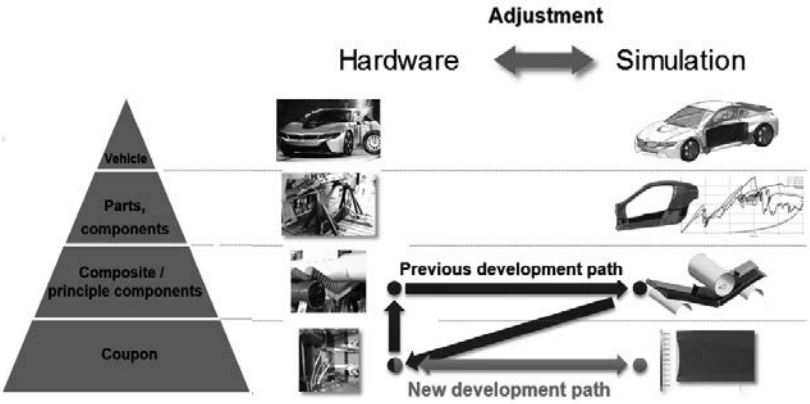

Fig. 7: Development / validation pyramid ([1] to [3])

4. Future challenges

Composite design and the associated use of the most varied material systems will make a substantial contribution to attaining future development goals [8]. Developing and validating optimum solution spaces always means a high number of variants need to be evaluated at the start. Issues such as fatigue in joints, corrosion protection as well as different thermal properties of materials are also to be examined intensively in the case of multi-material designs. Additional testing and investigation methods are therefore needed for an efficient

and cost-effective assessment of material variants. Even in the early stages of development these methods must allow dependable evaluations to be made regarding the subsequent complex service spectrum of vehicles. Efficient validation programs, based on interdisciplinary requirements management for fiber-composite structures with integrated electrical function carriers, have thus not yet been consistently worked out as an automotive standard. Possible examples here are CFRP roofs with sensor networks or integrated heating [9].

References

[1] F. Dirschmid, T. Wolff and T. Weiss: The BMW i8. In: EuroCarBody, Bad Nauheim, 2014.

[2] J. Kempf, R. Landmann, T. Müller: CFRP adhesive technology in the BMW i8. In: VDI Plastics in Automotive Engineering, Mannheim, 2015.

[3] European Aviation Safety Agency - EASA: Certification Specification for Large Aeroplanes CS-25. 2003.

[4] S. Engel, C. Boegle, J. Majamaeki, D.H.-J.A. Lukaszewicz, F. Moeller: Experimental investigation of composite structures during dynamic impact. 15th European Conference on Composite Materials, Venice, 2012.

[5] S. Engel, C. Boegle, D. Lukaszewicz: Crushing of composite structures and parameter identification for model development. 19th International Conference on Composite Materials.

[6] G. Barnes, S. Nixon, M. Schrank (2008): Composite crush simulation – emerging technologies and methodologies. URL: http://www.simulia.com/download/scc-papers/Automotive/composite-crush-simulation-emerging-technologies-2008-F.pdf (as at 03.12.2015)

[7] T. Francis, J. Hobbs, D. O. Adams, R. Roberts, G. Barnes: Predicting crashworthiness of composite laminates using ply decomposition. Aerospace Structural Impact Dynamics International Conference 2012.

[8] M. Ahlers, Klaus Sammer: New BMW 7 series – Carbon Core, In: EuroCarBody, Bad Nauheim, 2015.

[9] DE 102007040011 A1.

The innovative hybrid fleece molding (HFM) concept as a sustainable alternative in direct comparison with the door panel for the Volvo XC90

Dipl.-Ing. (FH) **F. Schumann**, Dipl.-Ing. **R. Ankele**,
IAC Group GmbH, Ebersberg;
M.Eng. **F. Jürgens**, Prof. Dr.-Ing. **H-J. Endres**,
IfBB, Hochschule Hannover

Abstract

This paper will examine the door panel of the XC90 in two manufacturing and material variants in terms of its technical and ecological characteristics. Special attention is placed on the newly developed hybrid fleece molding technology, which innovatively combines the two manufacturing processes of compression molding and injection molding, thereby creating sustainable, lightweight and rigid beam components for the automotive interior. In addition to consideration of the technical aspects, a first ecological assessment is made of the production and utilization phases with regard to conventional injection molding and the hybrid fleece molding technology.

1. Introduction

Modern automobile construction is more than ever deeply affected by a variety of often conflicting technical and economic requirements. Increasing customer requirements, stricter laws and political constraints call for automakers to supply lightweight, fuel-efficient and safe vehicles. Thrifty use of energy resources and the statutory reduction of CO_2 emissions consequent upon the problems associated with climate change have a considerable influence on the requirements applicable to future generations of vehicles. Here the weight of the vehicle is a significant control variable in influencing fuel consumption. [1]

The automotive interior too expects a contribution to the lightweight construction which is needed. Only by purposeful further development and the use of modern materials and processing technologies is it possible for current designs and additional comfort functions to be implemented with weight-neutrality. Not only standard materials with innovative properties but also composite materials, composite designs and hybrid construction methods will create new options for the car of tomorrow. [2]

2. Hybrid fleece molding as an alternative manufacturing technology

One practical example of a process in which several hundred grams per assembly is saved with comparatively manageable 'rethinking' is hybrid fleece molding (HFM) which we shall look at here. This is one of the IAC group's technologies and is based not only on customized material solutions but also on innovative processes and tool details. With this innovation, very light and yet rigid beam components can be fabricated, which are then in a further process step upgraded with a visible surface. Depending on the decor in question, this results in some very different areas of application: HFM is, for example, available for the trim parts of pillars, doors and trunks, but also for seat backs and even as instrument panel carriers. In Figure Fig. 1, the conventional injection molding process is compared with the innovative HFM process, which is described below.

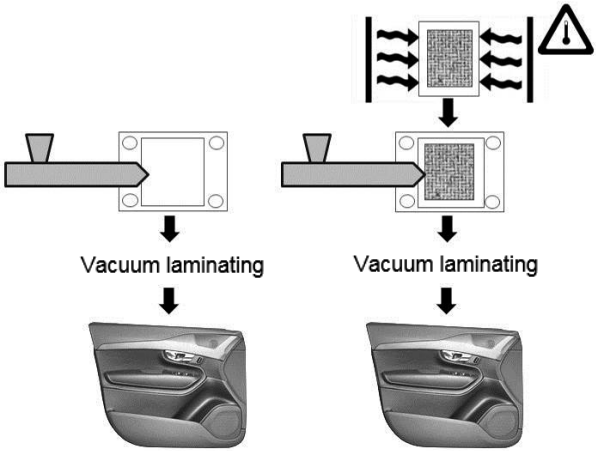

Fig. 1: Injection molding and hybrid fleece molding

Basically an HFM door panel consists of a thermoplastically bonded natural-fiber carrier component which during compression molding is simultaneously back-injected with plastic such that all structures required on the back of the component are created. This includes not only rib structures but also fastening points and weld zones. The possibilities of additional functional and component integration are also expanded by the geometric freedom afforded by the forming process of injection molding in comparison with conventional compressed natural-fiber panels, which have been in common use for decades in the automotive interior.

In a door trim panel, for example, these possibilities may include not only crash elements but also hooks or (cable) clips.
Beneficial to the customer are weight savings of up to 50% in comparison with conventional injection-molded panels as well as the minimization of additional components and joining processes for attachment to the panel, and in very general terms the use of renewable raw materials.
The IAC group has been developing this technology for several years now and can already look back on several advanced prototypes (see Fig. 2).

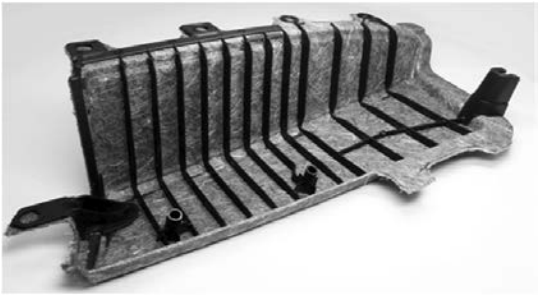

Fig. 2: Rear view of a door panel arm-rest as a hybrid fleece molding prototype

These include the arm rest for a Skoda, the B-pillar of a Daimler and now the driver's door panel for the current Volvo XC90. These examples are in each case in series production as acrylonitrile butadiene styrene (ABS) injection-molded components. In addition, further HFM projects are currently undergoing trials in the USA.

3. Hybrid fleece molding in practice

We will now look at how an HFM panel is manufactured. The 'hybrid fleece' semi-finished product is typically a pre-cut, needled mixed-fiber non-woven with a weight per unit area ranging from 1000 g/m² (or even less) to 1600 g/m². The natural fibers used include primarily flax, kenaf, hemp, or jute. Fiber selection and the mat structure depend on the component design and the degree of shaping involved.

The mat is first thoroughly heated in a panel heating system and this is advantageously carried out simultaneously with a first compression operation. This precompresses the mat. The process parameters and process control in this step influence not only the mechanical prop-

erties of the subsequent finished part but also ensure that odor problems are prevented or keep the thermal load on the natural fibers to a minimum.

The mat, now hot and floppy, is then transferred into a compression mold (or to needle grippers) and immediately compressed to the desired final thickness (1.5 mm, for example). It is irrelevant whether this is a vertical compression mold in an injection-molding machine or a mold in a horizontal press additionally fitted with a suitable injection-molding unit.
Whatever the case, the compression mold has the technical equipment to implement and control the simultaneous injection-molding process. In the present example of the door panel, a hot-runner system with seven gates and needle valve nozzles is used. Various plastics have already proved satisfactory, including high-flow polypropylene (PP) grades with 30% glass-fiber (GF) content. Since in the case of HFM the actual cavity is filled solely via the ribbing structure, the viscosity of the melt is a critical variable and the filling simulation is indispensable as an aid in component design. The mold temperatures are optimized here to give a compromise between the cooling time (for the mat) and the filling capability (of the ribs). In addition, as the mold closes, the outer shape of the component is trimmed. The projecting edge of the mat is cut away here but is left in the mold until the molding is removed.

4. Environmental accounting as a tool for the ecological assessment

Using lightweighting technologies properly from the sustainability and ecological points of view must always be preceded by a full life cycle assessment. The energy savings in the utilization phase due to lightweighting could possibly be cancelled out by a particularly energy-intensive manufacturing phase. [3]
The life cycle assessment (LCA) is an engineering instrument which compiles and assesses input and output flows (both the material and energy flows which go together into the process and which emerge from the process) and also the potential environmental impacts of a product system during the course of its entire life cycle or a section of its life cycle. [4] According to the international standards EN ISO 14040 and EN ISO 14044 the life cycle assessment is divided into four sections (see Fig. 3).
The scope of the assessment and the system boundaries emerging from it are defined in the first step, as is the so-called functional unit (reference quantity). In the second step, a physical balance sheet is prepared which covers all relevant material and energy flows (input and output).

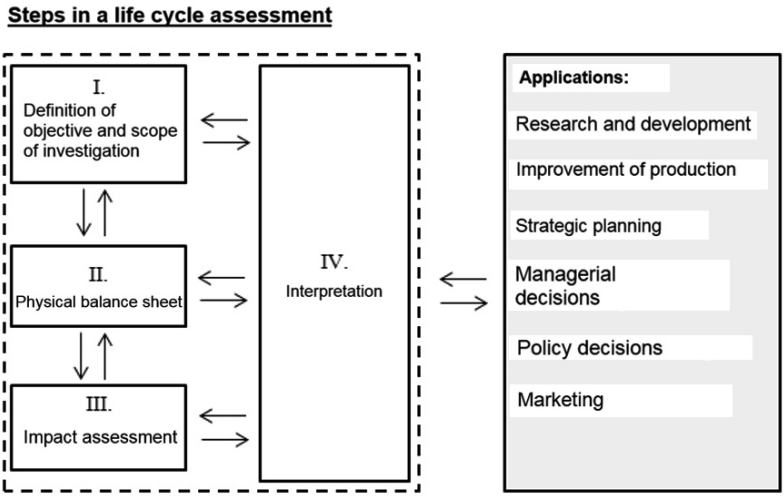

Fig. 3: Steps in a life cycle assessment [4]

This forms the basis for the impact assessment, which is carried out as the third step. Here the physical balance sheet results are assigned to different impact categories (such as greenhouse potential, acidification potential or eutrophication). Finally, in the fourth and final step of an LCA, the assessment results are analyzed and evaluated, as also conclusions are drawn and recommendations made. LCAs can be used for identifying possibilities for improving the environmentally related properties of products in different phases of their life cycle, for decision-making in industry, government or non-governmental organizations, and also for marketing purposes. [4]

An important further component of the life cycle assessment according to ISO 14040/44 is also an external critical review carried out by experts which verifies compliance with the specifications in the standards. In the case of research and development projects, an alternative is offered by early ecological assessments with overview LCAs or streamlined LCAs. Here an ecological examination based on the standards is carried out but not to the full scope of the standards. Firstly, there is no critical external review; secondly, generic records from databases are used in some cases for the assessment. Due to the absence of an external expert evaluation (not ISO-compliant) it is not to be communicated externally for marketing purposes and the like. This variant does however offer an opportunity of making an initial ecological assessment as early as when research and development projects are in

progress and also of revealing hot spots in the life cycle. Furthermore, these assessments provide a good basis for future ISO-compliant LCAs.

5. Overview LCA of conventional door panels and HFM door panels

The results of the overview LCA (first ecological assessment according to ISO 14040/44) are presented below. Within the context of preparing the LCA, both the conventional door panel and the new HFM door panel are analyzed over the production and utilization phases (see Fig. 4). Possible maintenance measures carried out during the utilization phase are not included in the assessment. Since the door carrier in question is permanently fitted with a number of additional components and there are as yet no recycling strategies for a complex component of this kind, the assessment does not include the end of-life phase.

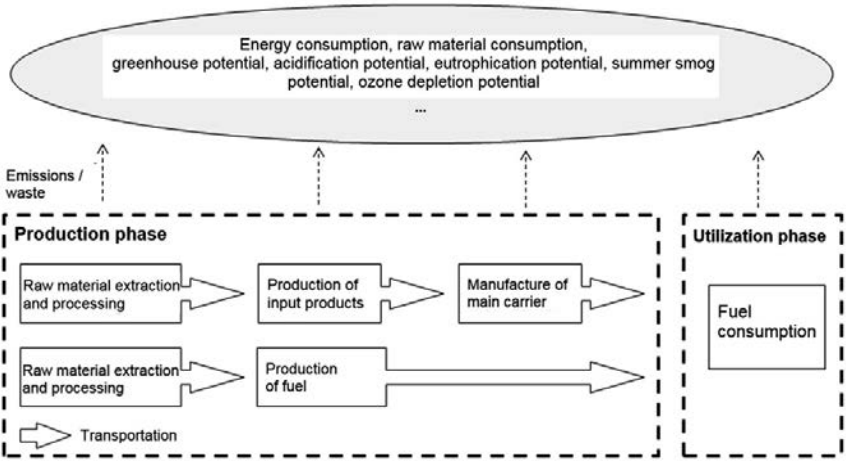

Fig. 4: Schematic representation of the life cycle phases taken into consideration (modified after [5])

As part of the overview LCA, the impact categories of abiotic depletion potential, acidification potential, eutrophication potential, greenhouse potential, ozone depletion potential and summer smog potential were considered. The LCA analysis and impact assessment is carried out with the GaBi LCA software and the impact assessment method CML 2001 (April 2013 version).

Production phase

There are significant differences in the production methods used for the various door panels. The now long-established method of injection molding is used in manufacturing the conventional door panel. For the new door panel, on the other hand, the innovative HFM process in combination with hot press molding is used. Even the raw material bases differ in the various door panels. If ABS only is used in the conventional door panel, in the new development a fleece made from flax and polypropylene fibers is used, as well as PP-GF30 for back-injection (see Fig. 5).

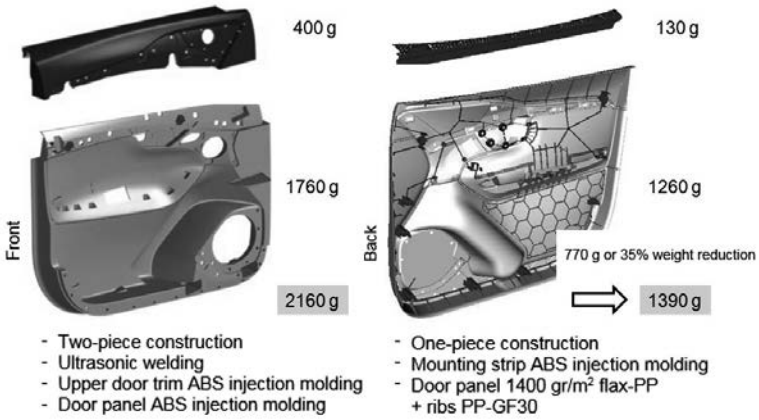

Fig. 5: The conventional concept of the Volvo XC90 door panel in comparison with the hybrid fleece molding prototype

In order to be able to guarantee the most accurate ecological assessment possible, the inputs and outputs of each manufacturing method were measured by the IAC Group in collaboration with the IfBB.

In addition to these primary data, secondary data were also used. The secondary data are data from databases of the GaBi LCA software. Examples of these are data sets for ABS and for transportation processes. Table 1 provides another overview of the base raw materials, production methods and data basis.

Table 1: General information about the different door panels

	Conventional door panel	HFM door panel
Basic raw material	- ABS	- Flax and PP fleece - PP + 30% GF
Production method	- Injection molding	- Hybrid fleece molding
Data basis	- Primary and secondary data	- Primary and secondary data

A preliminary assessment of ecological impacts in the production phase is given in Fig. 6 for different impact categories.

The basis for comparison of the various door panels is the conventional version which is assumed to be 100%.

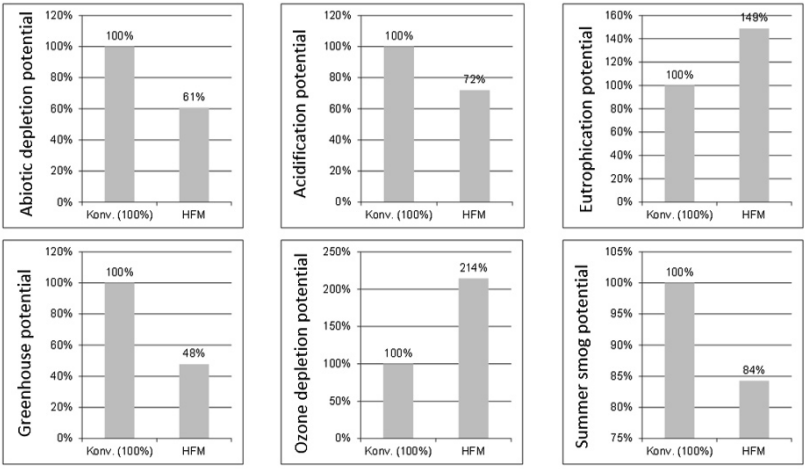

Fig. 6: Environmental impact of the production of conventional door panels (conv.) and of HFM door panels (HFM).

In the impact categories of eutrophication potential and ozone depletion potential, the HFM component sometimes has greater disadvantages than the conventional component. In this it is primarily flax fiber and polypropylene fiber production in direct comparison with ABS which is decisive. In particular, the additional emissions are due to the cultivation of the flax and the associated agricultural operations such as fertilization and rotting. In the remaining impact

categories the innovative HFM door panel had ecological advantages over the conventional version. In the case of greenhouse potential in particular, the HFM door panel emerges much better with a minimization of emissions of about 52%.

Utilization phase

The door panel has no direct ecological impacts in the utilization phase. In the automotive sector these impacts consist exclusively of fuel consumption and the production of gasoline. However, ecological impacts, such as carbon dioxide emissions, can nevertheless be reduced by weight savings and the resultant lower fuel consumption.

Substitution of the new door panel also means that in this example there is no need for the upper door trim as a component, which in turn means a weight reduction (in this regard compare also Fig. 5). However this further saving has not yet been included in the assessment.

In Fig. 7, the influence of distance travelled (from 0 to 250,000 km) on the greenhouse potential is shown as an example. Once again the impact of production of the conventional door panel is taken as the basis at 100%. Accordingly, the HFM door panel starts with a figure of 48%.

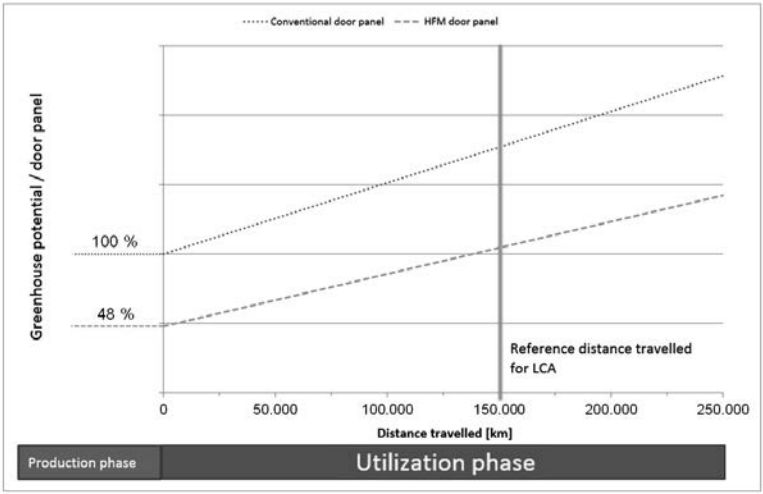

Fig. 7: Influence of distance travelled on the greenhouse potential of the conventional door panel and the HFM door panel.

Since the HFM door panel weighs less than the conventional door panel, this also means an advantage in the greenhouse potential per kilometer traveled. The situation is similar with all

other impact categories under consideration since the sole setscrew in the utilization phase is weight and thus fuel consumption. For the present assessment a distance of 150,000 km covered is assumed and related to the technical data of the Volvo XC90, taking into account the CO_2 emissions. At 150,000 km, there is a saving during the utilization phase of 27% for the HFM door panel compared with the conventional version with respect to the greenhouse potential.

Life cycle (excluding end-of-life)

The following total values for the different impact categories emerge accordingly from the ecological impacts in the production and utilization phases (see Fig. 8). Here the impacts of the conventional door panel are in each case assumed to be 100% and the HRM door panel compared with this.

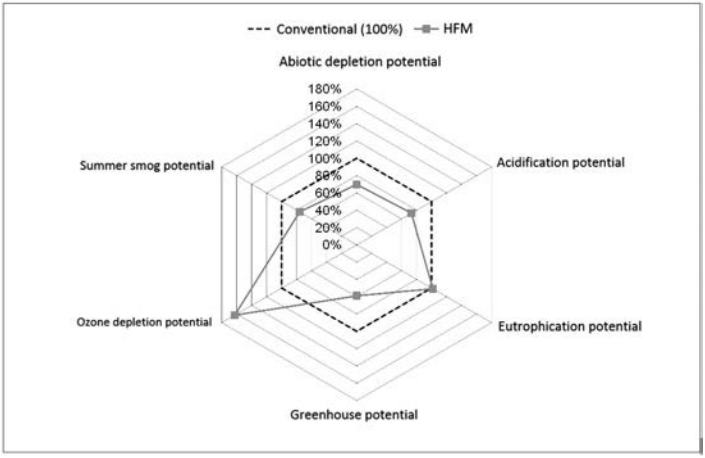

Fig. 8: Ecological impacts throughout the life cycle (production and utilization phases) for conventional door panels (conv.) and the HRM door panel (HFM)

Taking both the production and the utilization phases into account, the HFM door panel has the advantage over the conventional door panel, apart from the impact category of ozone depletion potential. In the important impact category of greenhouse potential, savings of approximately 41% are achieved (this stems from the different absolute values in the production and utilization phases which contribute to the potential for savings.

6. Outlook

This hybrid fleece molding concept offers a significant lightweighting potential for large-area carrier parts in the automotive interior. With an appropriate implementation of this innovative technology, on the basis of the prototype presented here, an estimated weight saving of up to 2.5 kg is estimated for the four doors of a SUV.

The present overview LCA also constitutes a first step in the ecological assessment of this method. Looking at the life cycle, the lower weight basically comes out very advantageously as compared with conventional injection-molded door panels. This is made possible and is supported by the use of natural fibers. However the flax fibers used here do in particular vary in their effects in the impact categories in the production phase. In a subsequent step the collected data are to be validated by preparing an ISO-compliant LCA and other types of fiber will be taken into consideration.

7. References

[1] Vollrath, K.: Leichtbau- Offensive beim Automobilbau. Blech-Rohre-Profile (2001) 2 pp. 57- 58

[2] Krenkel, W.: Verbundwerkstoffe: 17. Symposium Verbundwerkstoffe und Werkstoffverbunde. Darmstadt: Betz-Druck-Gmbh 2009

[3] Landesagentur für Elektromobilität und Brennstoffzellentechnologie Baden Württemberg (e-mobil BW GmbH) & Fraunhofer Institut für Produktionstechnik und Automatisierung (IPA): Leichtbau in Mobilität und Fertigung. Stuttgart: Fraunhofer Informationszentrum IRB 2012.

[4] Deutsches Institut für Normung – DIN: Environmental management - Life cycle assessment - Principles and framework (ISO 14040: 2006) and Requirements and guidelines (ISO 14044:2006). Berlin: Beuth- Verlag 2006.

[5] Chair of Building Physics at the University of Stuttgart, Department of Life Cycle Engineering: life cycle assessments and life cycle engineering 2015 http://www.lbp-gabi.de/46-0-Oekobilanz-und-Ganzheitliche-Bilanzierung.html (accessed: 24.11.2015)

Thermoplastic crash-absorbing elements made from PC/PBT (Makroblend®) as part of the side-protection concept of the BMW i3

Dipl.-Ing. (FH) **E. Meurer**, Covestro Deutschland AG, Leverkusen;
Dipl.-Ing (FH) **M. Hanigk**, BMW AG Munich

Abstract

Layout and implementation of an energy-absorbing element in order to manage the loads affecting the load-bearing structures during a side impact.

Reducing the amount of energy affecting the body structure, limiting the intrusion and keeping the retardation to a constant level in order to protect the high-voltage components was the main focus of the crash-management concept planned for the i3. This set of requirements demands ductile products with nearly constant mechanical properties over a wide temperature range. Driven by the limited available space a defined collapsing mode with adequate energy absorption of the absorbing system was needed to guarantee the safety of the vehicle at given parameters of loads and operating temperature.

To identify a suitable absorbing structure a number of comparison tests were conducted. The collective comparison of test results enabled optimization of property data for the finite element simulation used to define the layout of the final part. The prototype tests were conducted at BMW's laboratories whereas the simulations were carried out at Covestro. Based on the definition of the component behavior, the performance of the entire vehicle was configured by crash simulations.

An additional challenge was provided by the part design and the consequences for the injection-molding operation.

The good and close collaboration between BMW and Covestro (formerly Bayer Material Science AG) supported by Eckerle, the prototype maker and molder, guaranteed a smooth course for the project.

Driving motivation

The global ecological and economic changes of our society mean that new answers are being sought for personal mobility especially in urban areas. Electro-mobility could be the essential step for offering sustainable solutions in the future.

The new BMW i3 was planned from the very beginning as the first significant sustainable e-car for urban areas, tailor-made for emission-free propulsion and intelligent mobility in city areas and in daily commuting.
The typical BMW pleasurable driving experience at zero emissions, sufficient interior space despite the compact design, optimized for city use with the goal of meeting high safety standards were some of the requirements for the car.
The layout of the BMW i3 was therefore based on the Life-Drive Architecture with a combination of a drive module (rolling chassis made from aluminum carrying the drivetrain including the high-voltage battery) and the Life module with the body structure made of carbon fiber (CFK) (see Figure 1).

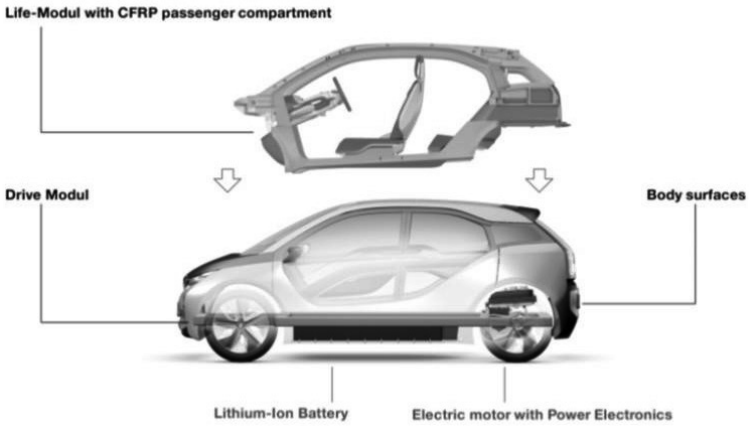

Fig. 1: Modular concept of the Life-Drive split

The use of the Life body made from carbon-fiber laminate offers a significant amount of weight reduction (approx. 250-350 kg compared with a similar electrically powered converted car), with positive effects on the driving range and the handling of the car. In addition an optimal usage of interior space and good crash performance could be realized.

Demands on the structure

The revolutionary layout of the Life-Drive architecture made from aluminum and carbon-fiber laminate required a harmonized crash-management concept. All frontal and rear crash loads were planned to be managed by the aluminum structure of the Drive module. All loads applied during the side crash should be managed by the Life module, with the main focus being

to ensure a safe space for all passengers and in addition to limit the load level applied to the high-voltage battery area.

The high-voltage battery was identified as the most critical section, leading to the following questions: How much of the installation space could be used as deformation zones? Which cross-section could participate in load distribution? and finally, considering high-voltage safety aspects, where were the areas where no deformation was allowed? (see Figure 2)

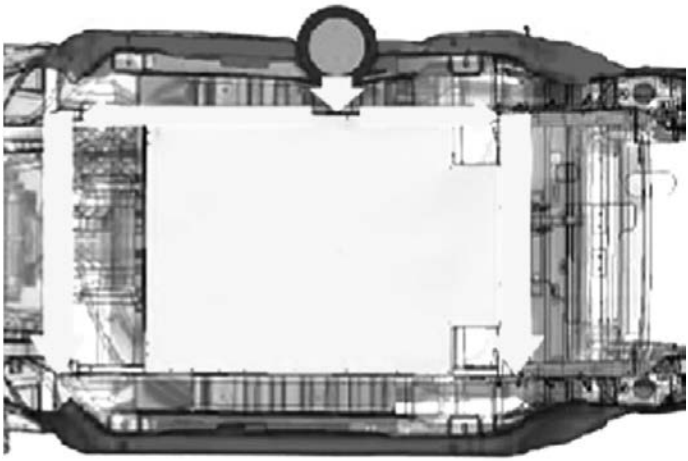

Fig 2: Load flow (arrows) around the high-voltage battery

The FMVSS214 oblique pole and the IIHS side barrier tests are mandatory for all side-impact requirements. They primarily affect the Life module and thus have to be managed primarily by the CF laminate system.

During the side-pole impact the body structure needs to absorb most of the energy before the pole reaches the area of the high-voltage battery. Due to the packaging and the driving-range requirements applicable to the high-voltage battery system only a limited deformation space less than 300 mm is available.

The carbon-fiber side frame has great strength, and its failure limits the energy absorption during deformation. The exterior side-frame structure absorbs the first part of the applied loads. The crash honeycomb and its rear-side structure is responsible for absorbing and transferring most of the intrusion energy. The inner portion of the side frame acts as a sup-

port bar for the crash honeycombs and leads the remaining forces into the body structure of the Life module.

The crash honeycomb shown in Figure 3 makes the main contribution to crash management. Its particular requirements and development will be examined in what follows.

<<

Fig. 3: Thermoplastic crash honeycomb and its location

Approaches to a solution

The required level of energy for the absorption structure is described by the full car performance and the known resistance moment of the high-voltage battery structure. The absorption level was clearly defined on the basis of the impact velocity, weight of the car and the available deformation space. Due to these facts it was obvious that this level of energy absorption could only be managed by a deformation process. In addition a preferably constant load level along the deformation travel was desirable. Metal-based solutions such as zinc foam or aluminium honeycombs, were not satisfactory due to the high initiation level and low compression volume. Even the PU-based foam systems could not meet the required performance level. A comparison of ductile energy absorption related to material performance is shown in Figure 4.The search therefore focused on a combined material and structural solution offering defined stiffness (initiation level) combined with long and high deformation mode.

As an optimal approach, a honeycomb-based structure was developed. The best constant energy absorption mode was achieved when folding the structure in a buckling process until the honeycomb had completely folded and blocked. The self-stabilization of the linked honeycomb structure during buckling is an additional benefit supporting the folding mode of the honeycombs.

Not only the design and material choice for the Life module was new ground for all partners, even the set of requirements related to the structure and the added components was new.

Even during the early stage of development the need for a close and focused collaboration between all participants was indicated. Even if the generic material data were well-known, the effects of specific design and component positioning on specific material characteristics were unknown and had to be explored and aligned step by step by the development partners.

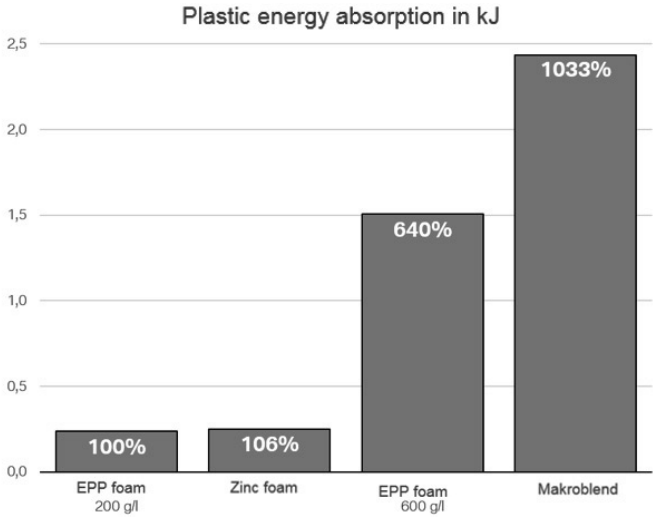

Fig 4: Energy absorption of different materials

The mode of interaction of the three development partners enabled each to contribute his specific know-how to generate an optimal result.

Material selection

Based on the previous overall material evaluation, material selection was narrowed down to two material groups. On one side, three phase-blended amorphous products, and on the other side amorphous products including a semi-crystalline phase. Keeping the requirements in mind, polycarbonate-based blends in particular were the material of first choice. The polycarbonate is responsible for constant properties along a wide temperature range and the other blend partners, such as ABS or PBT, are responsible for improved ductility especially at low temperatures. Due to good experiences with similar sets of requirements and an analysis of mechanical properties, three products made it to the shortlist.

A high-impact-modified PC/ABS Bayblend® T65 (which is an amorphous product from Covestro), a PC/PBT already used in a similar applications, and finally a Makroblend® KU2 7912/4 (another PC/PBT blend from Covestro), which is also still used for bumper applications today.

Based on testing done on prototypes the specific material profiles of the different materials were compared and evaluated with regard to their performance. The straight amorphous product exhibited not only high ductility but also excellent heat resistance up to 100 °C (see Figure 5) with nearly constant mechanical behavior and was therefore favored initially.

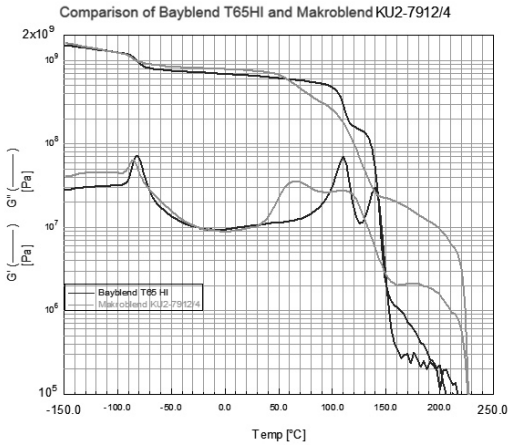

Fig 5: Shear modulus of Baybend® T65HI and Makroblend® KU2 7912/4 in comparison

During deformation tests of prototype honeycombs, especially after an alternating climate test and with low test temperatures, the Makroblend® KU2-7912/4 performed with a more homogenous deformation showing the preferred folding pattern.

Even though the straight amorphous Bayblend® offered higher heat resistance values the Makroblend offered better overall performance - this being the driving factor for material selection.

Calibration of prototype behavior with part simulation in order to generate material cards

The validation and calibration of the material properties based on a comparable structure was the essential step in the implementation of the project.

Based on the generic material data in combination with trials conducted at BMW laboratories a further development of material cards was carried out at Covestro Deutschland AG. The first prototype crash trials offered a good insight into the potential of the selected products and allowed first conclusions to be drawn regarding the deformation behavior of the absorber (see Figure 6), an important limiting factor due to the installation space available.

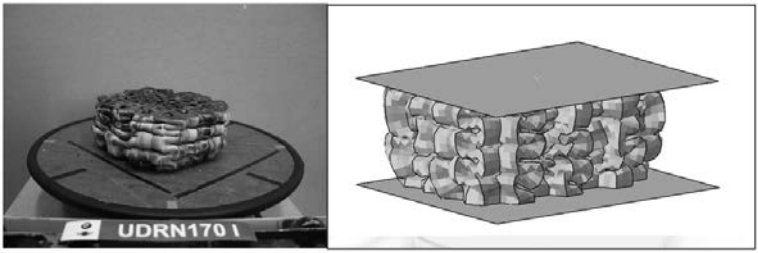

Fig. 6: Prototype and FE model compared in order to determine deformation behavior.

The measured force-displacement diagrams were compared with the results of simulation. Special effects relating to the honeycomb structure, the deformation process of each honeycomb and the inner stiffening of the honeycombs themselves were compared with the aid of high-speed recordings and FE simulations (Figure 7).

The effects of model translation in order to adequately align the real folding process with tested results was a major challenge followed by the generation of a suitable model in order to calculate the behavior of the full body structure. First analyses based on a simplified model with large elements resulted in unrealistic force peaks during the first deformation stage.

The above-mentioned results forced an adjustment of the stress conditions and strain values gathered during the test to avoid unrealistic failure results of the analyzed geometry.

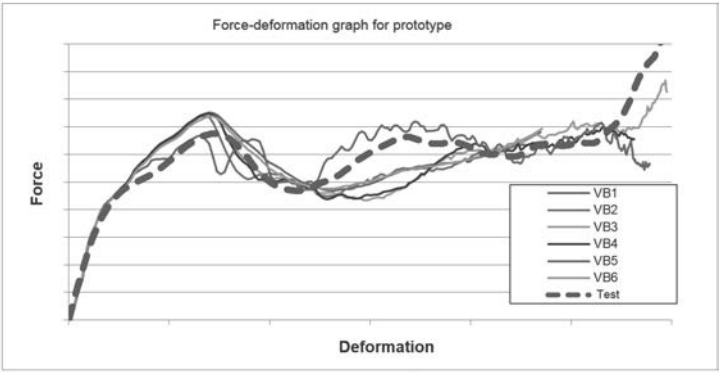

Fig 7: Identification of parameters influencing force-displacement behavior

The compilation of an extensive database to characterize part behavior was a key factor in the absorber layout. Inputting a wide variety of component trials and comprehensive image interpretation generated the necessary knowledge for the validation process.

After testing, the prototypes were sliced to enable comparison of folding patterns, a necessary condition of transferring the effects of selected discretization of the finite-element model.

Behavior at different temperatures was an additional driving factor for the component. Both at low temperatures (-30 °C) and high temperatures (+85 °C) comparable performance was to be delivered in order to offer adequate safety for the passengers across the complete service range. The material cards needed to be validated over the entire temperature range in order to ensure an acceptable prognostic quality regarding the failure behavior of the honeycomb structure.

Despite accurate preparation, surprises are common. During the validation test at -30 °C the prototype part was properly split by the falling weight. This effect occurred for the first time after the addition of trigger sections (see Figure 8). This specific failure mode did not show up during part simulation. The only hint of unpredicted performance was related to the high strain rates visible in the outer layers of the geometry, predicting a material failure at high speed deformation in combination with low temperatures.

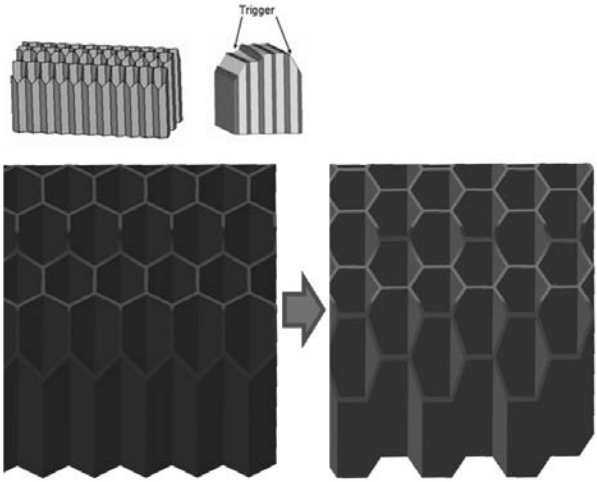

Fig. 8: The trigger mode and rotation of honeycomb layout

By turning the honeycomb structure by about 30°C (see Figure 8), thereby creating a roof-shaped design of the primary loading zone, the deformation process could be homogenized in the critical zone of the part. This design change resulted in reduced stress peaks and suppression of crack propagation in the outer zone of the part.

To represent a comparable deformation process by simulation, a dense finite-element mesh was indicated as not suitable for simulating the full body structure. The preparation of an analogous model precisely reproducing the deformation process on one side and acting as a base model for the full body analyses, but without causing a huge increase in the overall computing time, was done simultaneously. Thus the same mesh quality was used for component validation as was also required for validating the full body structure. Quality of prognosis and the invested calculation time for the crash simulation were the drivers for this approach.

Component simulation and transfer into full the body structure

In the course of the collaboration between BMW and the material supplier Covestro, crucial know-how on the performance of the crash absorber was gathered in basic testing and in FEM simulation of the prototypes. The previously determined material properties were then used for the simulation of the final component (Figure 9) and validated.

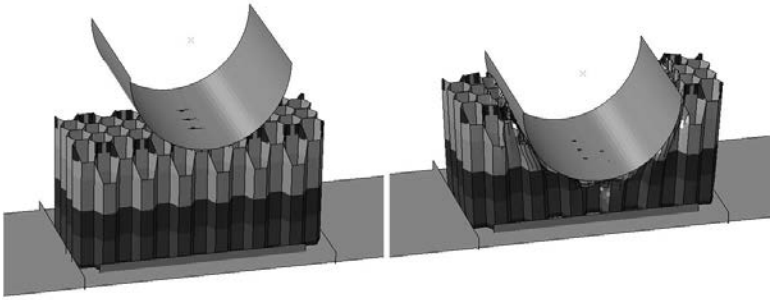

Fig. 9: Segment of the final component – before deformation and at maximum energy absorption

During subsequent integration into the full car body it was necessary to customize the geometry to fit into the available installation space. In addition a shaping of the trigger zones was defined. The triggering was indicated in order to guarantee an adjusted load leveling of each single component, which was also validated by component testing.
All insights obtained during the development of the crash honeycombs were simultaneously incorporated in the full car body simulation. This iterative procedure was necessary since the single components could affect each other. A final validation was undertaken in the first crash simulations of the car itself. Figure 10 shows the percentage energy absorption of the different components of the Life module. Clearly visible is the contribution made by the crash honeycomb in this load case.

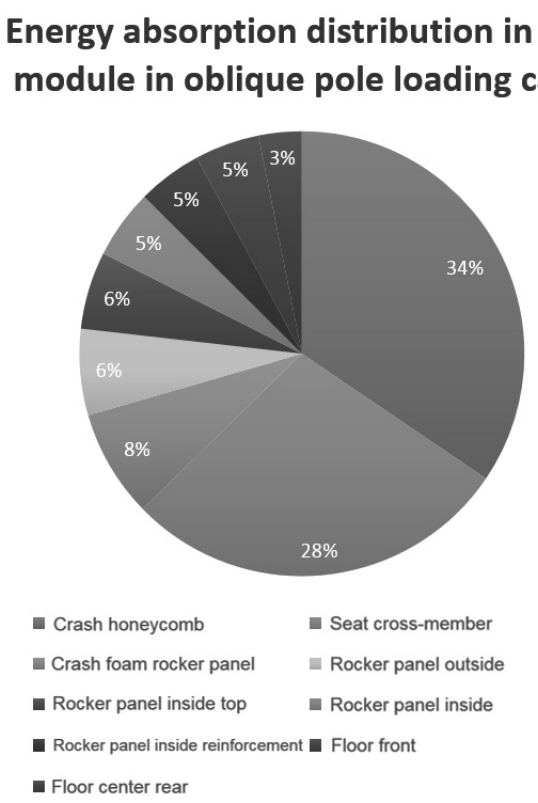

Fig 10: Distribution of energy absorption of the Life module during the pole test

Rheological component considerations and tool layout

The implementation of the geometry was for several reasons a special challenge for the toolmaker. A number of cores only anchored on one side had to offer a uniform temperature distribution on the tool surface but nevertheless have sufficient stability. A flexing of the cores during mold-filling would influence the filling process significantly. Small variations in the flow front directly affect the loading of the relatively delicate cores due to uneven pressure distribution. Great importance was therefore attached to the filling simulation, whose interpretation was challenging. The effects of melt temperature, the steel surface temperature of the cores

and the heat exchange potential of the cores had to be taken into consideration in obtaining a better understanding of the results of the simulations.

If rheological examination did on the one hand provide answers with regard to the mold-filling process, no information was obtained concerning the demoldability of the absorber. With more than 110 single cores each with a length of about 150 mm, the concerns of the toolmaker about the resulting demoulding forces was understandable. In addition the minimal draft angles arising from the energy absorption process did not make tool-making process any easier.
In order to get a better understanding of contraction stresses related to the shrinking process of the material under consideration, results from the filling simulation were later transferred to an ABAQUS equivalent model (see Figure 11).

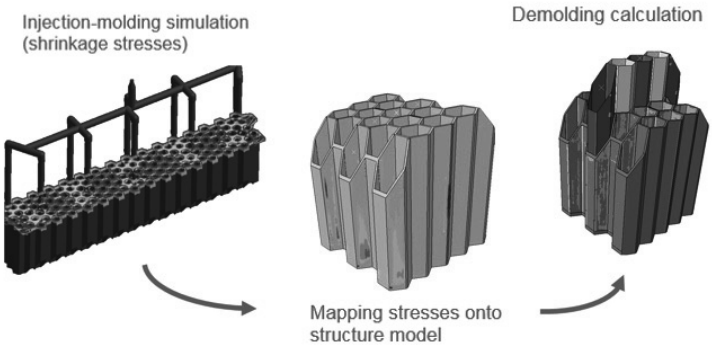

Fig. 11: Demolding simulation – mapping the results of injection-molding simulation onto a structural mechanical model

The molding pressures could then be determined from the stresses. On the basis of the adhesive-friction coefficients of friction obtained from friction tests, extraction forces per core could then be calculated (see Figure 12). The possible compensation for shrinkage forces made possible by the composite was deliberately ignored since only maximum forces were of interest.

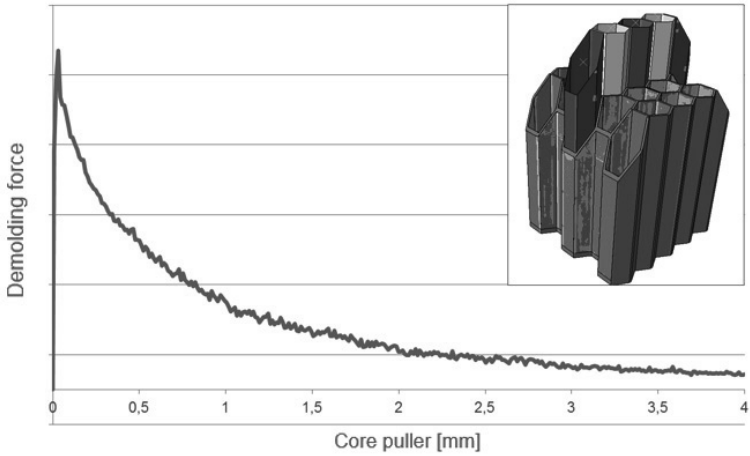

Fig. 12: Simulation of extraction forces at a segment cell

Lessons learned

With the increasing fall in the availability of resources, shorter development times and tighter development budgets, the concentration of know-how and focused collaboration even beyond the company borders offers optimal program development. The development of the crash absorber has positively demonstrated the smooth collaboration of experts in different companies without endangering the spheres of interest of each development partner. Clearly defined gateways allowed the transfer of know-how suitable for the project on the one side but still protected company-specific knowledge. Another benefit related to this procedure was clearly visible during the course of the project. A clear focus, well-defined process steps and bundling of specific knowledge of each development partner guaranteed on-time management of the project without any problems.

As an outcome of the project the collected insights can be used to address energy absorption issues more comprehensively. Even when the requirements profile is different, the gathered knowledge can be transferred into new applications offering a quick and precise evaluation of other absorber structures.

Reference

[1] Thomas Schnaufer; Die Leichtbaustruktur des i3.
Aachener Karosserietage (EuroCarBody) 2013

Local reinforcement in series production

Local reinforcement in series production

Dr. rer. nat. **B. Pfeiffer**, Celanese AG, Sulzbach;
Dipl.-Ing. **S. Tönnies**, Ford Motor Company, Cologne

Abstract

Local continuous-fiber reinforcement – or 'local reinforcement' for short – is ready for series production. A process has been developed at Celanese in which Celstran tapes are inserted by a robot with no tool change and then overmolded with polymer melt. Here, mechanical properties can be increased locally by up to a factor of 6. It was used in series production for the first time in collaboration with the Ford Motor Company in the handle area of the interior door trim of the Ford Transit Courier B460.

1. CELANESE long-fiber- and continuous-fiber-reinforced materials

For more than a decade, CELANESE has been the market and technology leader with its Celstran® LFT long-fiber injection-molding compound. The next leap in innovation in the field of long-fiber reinforcement is continuous-fiber reinforcement. Full fiber impregnation is possible with pultrusion technology.

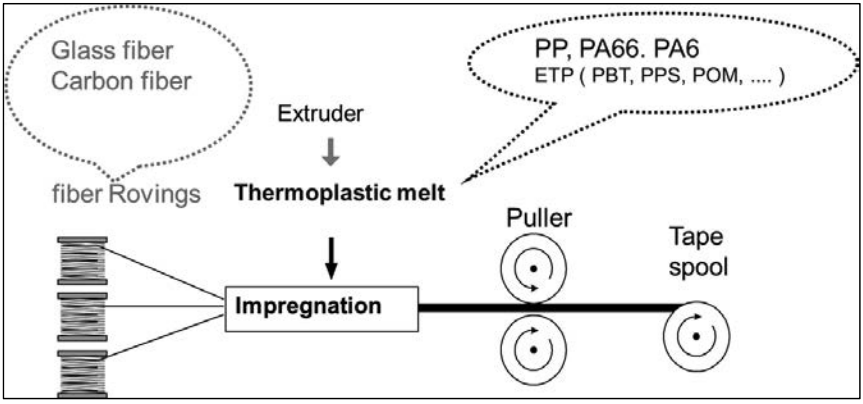

Fig. 1: Pultrusion with Celstran® tapes (source: Celanese process chart)

With Celstran® tapes the pultrudate is not cut into pellets but is wound onto spools [Figure 1]. In this way Celstran® CFR-TP tapes are created (CFR-TP = **C**ontinuous **F**iber **R**einforced **T**hermo**P**lastics), including tapes 305 mm wide, 0.10-0.50 mm thick and with a fiber weight content of 60-70 wt.-%.

In long-fiber injection molding with a polypropylene matrix of **Celstran® PP-GF 30 to PP-GF 50** (glass-fiber content 30-50% wt.-%), tensile strength is 100-130 MPa and the tensile modulus of elasticity 6-12 GPa [1].

A **Celstran® PP-GF 70 tape** has a tensile strength in the fiber direction of 900 MPa and a tensile modulus of elasticity of 34 GPa [2].

2. 'Local reinforcement'

Extremely lightweight construction is possible if the tapes are positioned locally at those places where the highest loads occur. In this case we speak of 'local continuous-fiber reinforcement' or 'local reinforcement' for short. Celanese supplies Celstran® tapes as semi-finished products wound onto spools and also as ready-to-use tape inserts.

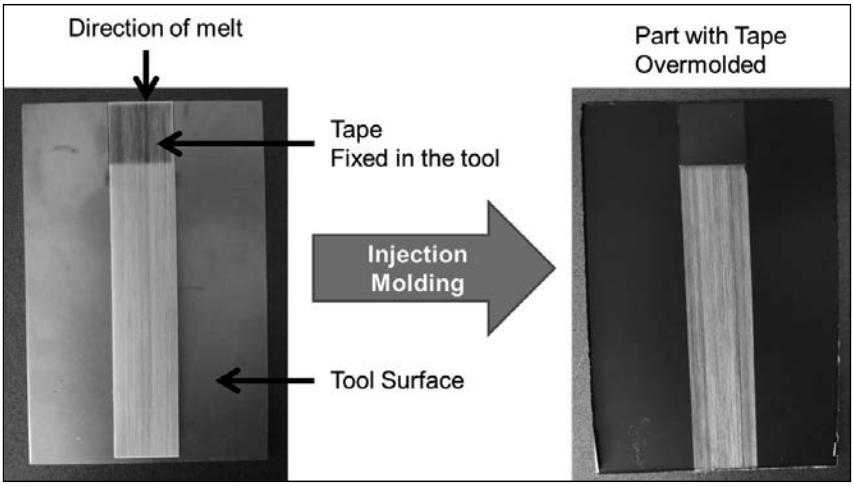

Fig. 2: Celstran® tape secured in the injection mold (held in place by adhesive or magnet) (Source: Celanese Tool Mold Shop)

A low-cost process has been developed at Celanese [Figure 2] in which local insertion and overmolding can be fully automated even in existing tools without tool modification.
A robot removes the inserts from a magazine. The inserts are held by adhesive or magnetic force on the tool surface and overmolded. The inserts do not need to be preheated. The thermal capacity of the injection-molding melt is enough to melt the tapes on sufficiently at the surface. The melt then bonds firmly with the tape.

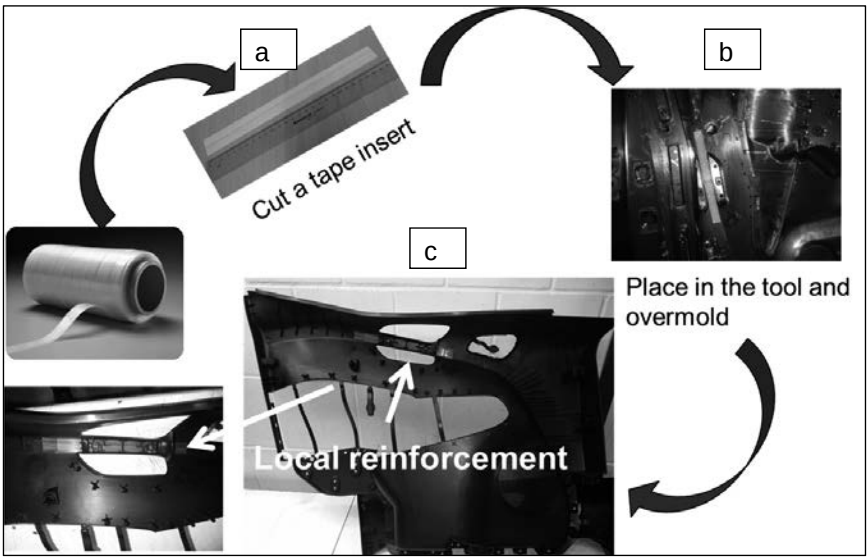

Fig. 3: Greatly simplified process sequence for 'local reinforcement': a. Inserts are cut to size, b. The inserts are positioned on the tool surface, c. The component with local reinforcement is removed from the injection mold. (Source: Celanese internal)

3. Mechanical properties of 'local reinforcement'

For the mechanical characterization of 'local reinforcement' at Celanese, Celstran PP-GF 70 tapes 0.25 mm thick were overmolded in a DIN A4 sheet mold (sheet thickness approx. 2 mm) with Celstran PP and various glass-fiber contents (0 wt.-%, 20-40 wt.-%). Here the

tapes were inserted on the top and bottom sides in the direction of flow and at right angles to it, and test samples taken in the direction of flow and at right angles to it [Figure 4]. The test pieces were taken from the DIN A4 sheets by water-jet cutting.

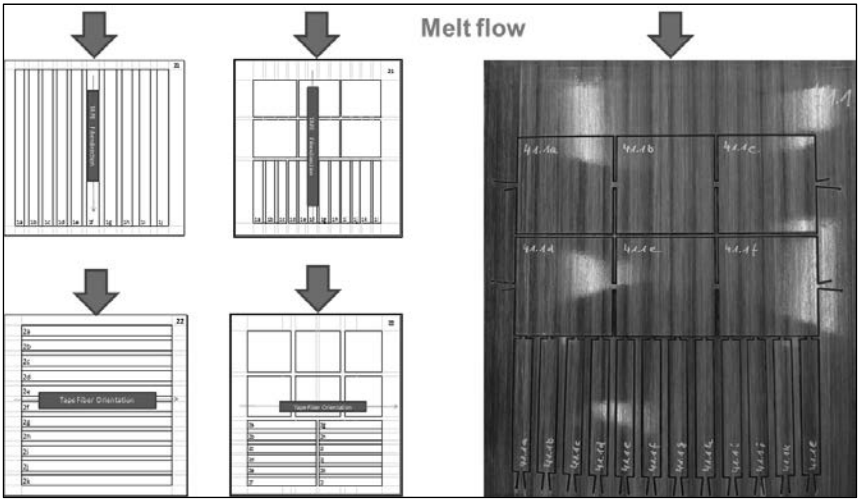

Fig. 4: 'Local reinforcement', mechanical characterization: test pieces were cut out of DIN A4 sheets by water-jet cutting. (Source: Celanese internal)

Results are presented on the following pages [Figures 5-8]. Mechanical information was obtained from tensile, bending, flexural impact and puncture tests.

The tensile and bending tests revealed that strength could be increased by a factor of 1.5, stiffness by a factor of 2, and impact strength (notched Charpy and multiaxial) even by a factor of 6. Particularly in the case of impact strength it was especially advantageous when the tapes were positioned on top at the force application end.

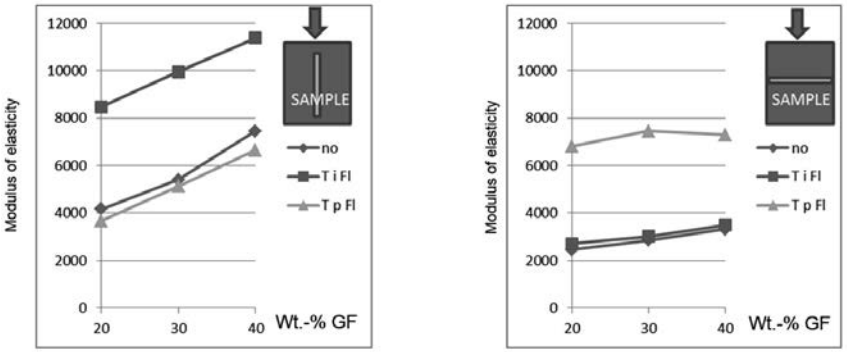

Fig. 5: 'Local reinforcement', mechanical characterization: tensile test ISO 527-1 / -2 – modulus of elasticity (source: Celanese internal)

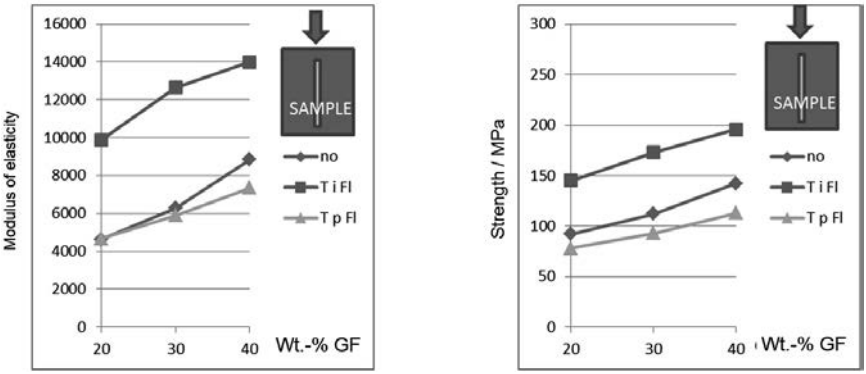

Fig. 6: 'Local reinforcement', mechanical characterization: bending test ISO 178 - flexural modulus and flexural strength. (Source: Celanese internal)

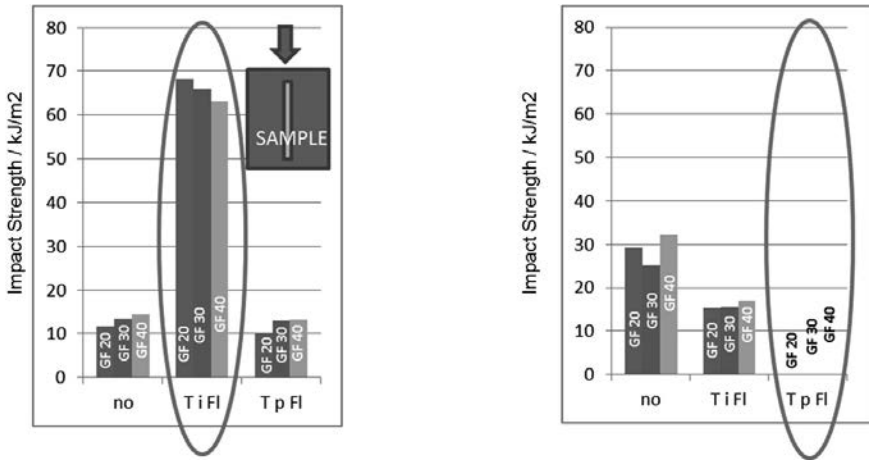

Fig. 7: 'Local reinforcement', mechanical characterization: impact strength, notched Charpy ISO 179-1. (Source: Celanese internal)

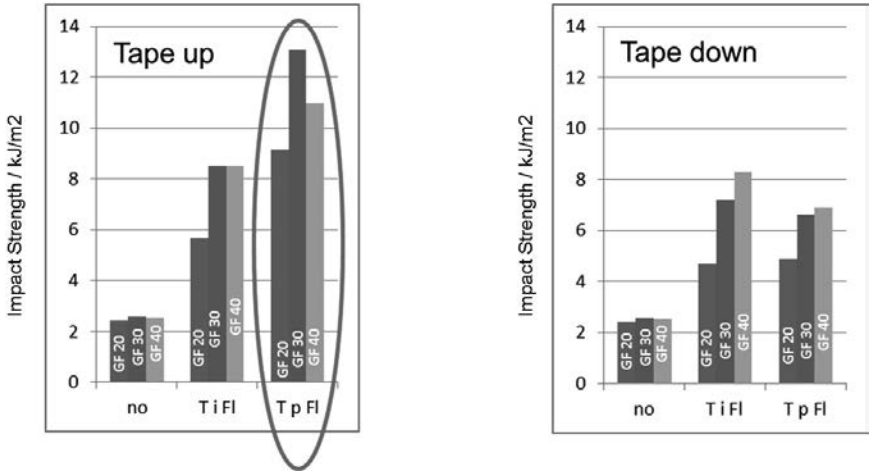

Fig. 8: 'Local reinforcement', mechanical characterization: impact strength, multiaxial ISO 6603-2 (instrumented puncture test). (Source: Celanese internal)

4. Ford Transit Courier inner door trim with 'local reinforcement'

This process was used for the first time in the door trim of the Ford Transit Courier B460 and put into series production.

High stresses occur in the handle area, especially in the case of a crash. Here, local tape reinforcement can mean both cost and weight savings. The presentation covers the series component and the basic principles of the process. A robot inserts tapes into the mold in the handle area, they are fixed onto the tool surface by adhesive or magnetic adhesion and then overmolded with polymer melt [Figure 3]. Figure 8 shows the door trim and the tape on the back of the door trim.

Fig. 8: 'Local reinforcement' in the door trim of the Ford Transit Courier B460 (source: Ford Motor Company)

Due to the great flexibility of this method a wide range of applications is to be expected in the future.

4. Recyclability of continuous-fiber reinforcement

For every future component, legal constraints are imposing ever greater pressure with regard to the recyclability of materials both in production and during the component's life cycle. Here Celanese have also investigated the recyclability of continuous-fiber reinforcement so as to be able to assess the holistic approach. The study shows the possibilities of the recyclability and properties of tape recyclate in combination with Celstran® LFT virgin material. Here the impregnation quality of materials plays a decisive key rôle. With this process Celanese enables the customer to use the materials to the full, and thus offers a great potential for resource conservation and cost savings.

References:

[1] CELANESE brochure: Celstran® LFT brief product information

[2] CELANESE product data sheet: Celstran® CFR-TP PP GF70-13

New manufacturing technology for material-hybrid lightweight solutions: an FRP-metal hybrid floor structure

Dr.-Ing. Dipl.-phys. **O. Täger**, Dipl.-Ing. **F. Häusler**,
Dipl.-Ing. **J. Lohmann**, Volkswagen Group Research, Wolfsburg;
Prof. Dr.-Ing. **N. Modler**, Dipl.-Ing. **T. Weber**, TU Dresden, Dresden

Abstract

This paper looks at how a material-appropriate production technology was developed for hybrid material automotive components made of fiber-reinforced plastics (FRP) and metals, taking an FRP-metal hybrid as an example. Under the aspects of design, process and tool design, the corresponding demonstrator is technically implemented in a pilot-plant environment close to series production.

1 Introduction and motivation

In the conflict arena between steadily increasing demands regarding future mobility and the necessity of reducing greenhouse gases, especially the CO_2 emitted by the internal combustion engine, a high priority continues to be given to body and structure lightweighting as a stimulus for reversing the weight spiral (Figure 1) [1]. Here the material class of fiber-reinforced plastics (FRP) has a great *lightweighting potential*, even beyond low production quantities and small-batch production. In particular, the use of thermoplastic matrix systems in combination with production processes with large-scale production capability makes cycle times possible with which such large-scale production can be implemented [2]. In addition, thermoplastic FRPs offer wide-ranging design possibilities for highly integrative structures such that the cost-effectiveness requirements applicable to higher production quantities can be met by a smaller number of individual parts and thus lower tooling costs. As a large-structure demonstrator a vehicle underbody has been designed as a FRP-metal hybrid structure. It was first produced virtually and then, taking aspects of close-to-series process and tooling design into consideration, was built as a demonstrator in the process and extrusion center of the Institute for Lightweight Engineering and Polymer Technology.

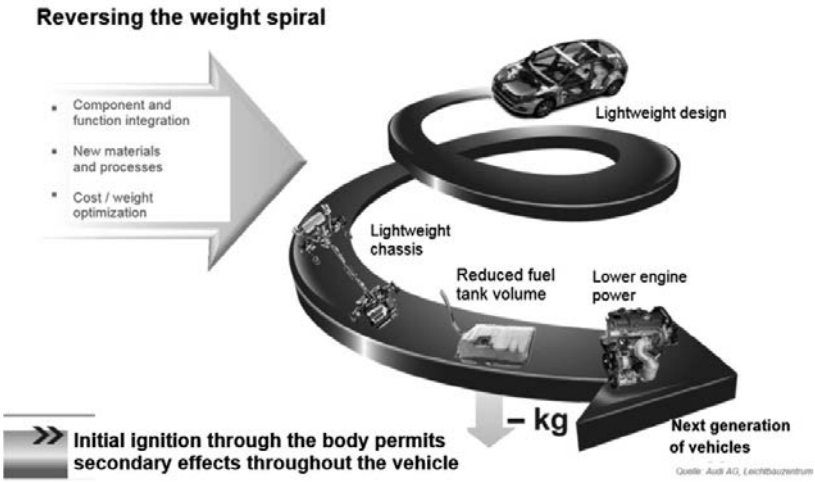

Fig. 1: Reversing the weight spiral: secondary effects and the potential of lightweight body construction

2. Designing an FRP-metal hybrid floor structure

As a basic precondition of using thermoplastic semi-finished products structurally the focus in the constructional design of the selected primary structure is on the loading cases to be satisfied. Furthermore, an added value with regard to conventional *floor structures* should be generated on the basis of the integral design with thermoplastic FRP.

In the design of a car underbody, it is primarily the loads occurring with dynamic and highly dynamic stress conditions which stand at the forefront of investigations. The focus here was primarily on side and frontal impacts as examples. In the case of static loading of the structure, torsional loads were the main subject of examination. In addition to the constraints of the process technology, these main stresses formed the basis for the constructional design process.

Figure 2 shows two stages in the evolution of the design. The concept of a two-shell basic structure is clearly evident here. Evolutionary stage I not only includes the two-shell construction but also the use of rib structures in the most varied forms. The constructive design here includes intensive ribbing particularly in the area of the seat cross-member mountings and in the area of the center tunnel. A further development, which takes production, weight and cost restrictions into account, is shown in Evolutionary Stage 4.

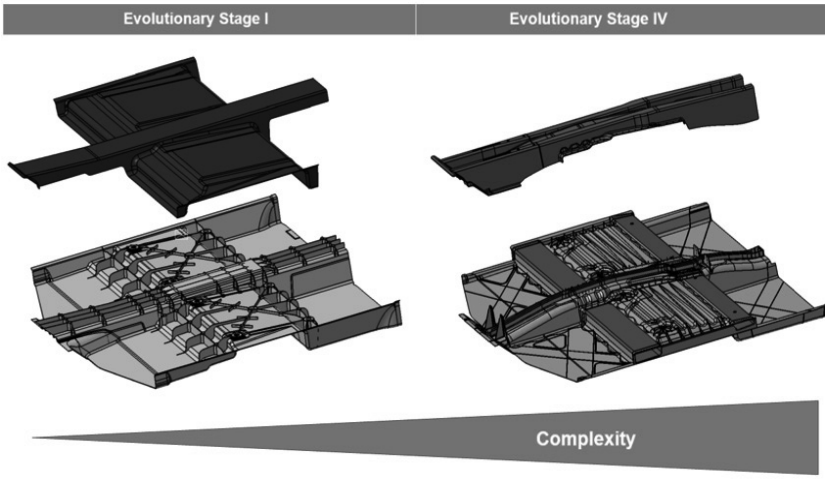

Fig. 2: Comparison of different evolutionary stages

Figure 3 shows the detailed structure of the final design. In order to satisfy a very demanding requirement for a lightweight design at a reasonable cost, a material with a high glass-fiber content formed the basis in selecting a semi-finished product for this underbody structure. Here local inserts oriented with respect to force paths were used to stiffen the overall structure and for local reinforcement both in areas where the seat cross-members are mounted and in the front part of the tunnel.

The basic structure consists of polyamide 6 / glass-fiber (PA6-GF) organic sheets which are used to make up the underbody tray. Due to technical constraints these sheets have to be divided longitudinally along the center tunnel. Here the overlap area is fully covered by glass-mat-reinforced thermoplastic (GMT) molding compound. Transmission of crash loads across the vehicle towards the metal energy absorbers is handled by pre-consolidated polyamide 6 / carbon fiber (PA 6-CF) hollow sections made of unidirectional (UD) semi-finished material whose dominant fiber orientation runs along the y-axis of the vehicle. Here the tube geometry and its layered structure satisfy the requirement for production by the pultrusion method and the associated provision in the form of pre-consolidated semi-finished goods supplied by the meter.

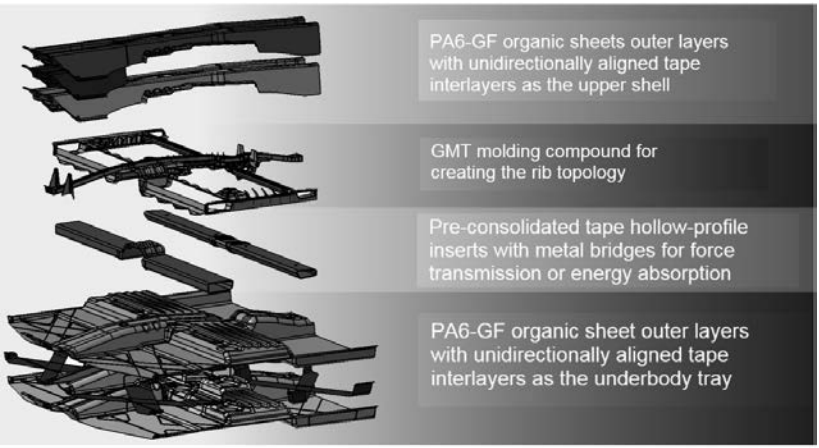

Fig. 3: Detailed structure of the final design.

The design of the rib topology of the fiber-reinforced (GMT, for example) molding compound is on the one hand used here for stiffening the structure by a selective increase in the moment of inertia, and on the other hand thereby implements a functionally integrative construction. As can be seen from Figure 4 the thermoplastic matrix (PA6) serves as an interphase between the different materials in the component (FRP and metal). Furthermore, installation along the center tunnel of the upper shell structure combined with the rib structures creates closed cross-sections which can be used as media conduits (for example, for cables, coolant). The primary area of interest here was the supply air routing to the back of the passenger compartment.

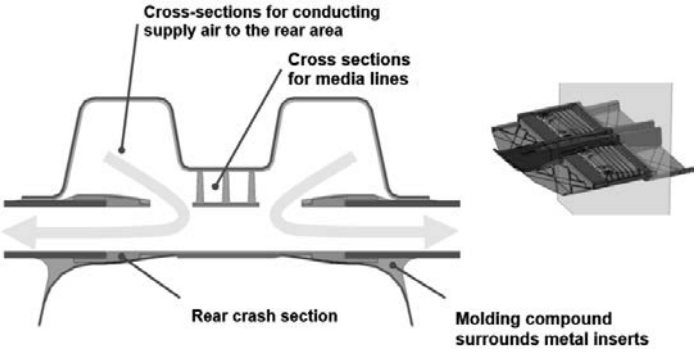

Fig. 4: Synthesis of the ribbing layout for function integration

3. Process development

The highlighted objective of technical process research work was to reproduce an automated production process with series-production capability for semi-finished products or components with the approximate dimensions of 2000 mm x 1600 mm.

The fundamental challenge consisted primarily of securing a robust and reproducible handling of the large and floppy thermoplastic organic-sheet preforms (Figure 6). For this reason the decision was taken at an early stage of the project to have separate preheating and insertion of the semi-finished material.

Figure 5 shows two basic approaches to a separate loading of the mold.

Fig. 5: Feed concepts with one robot (left) and two (right)

In the first place, this means that the handling frame can be smaller and less complex, and therefore conducive to a more accurate positioning of the floppy preform and to robust operation of the feed unit. Secondly, the left-hand and right-hand sheets can be inserted with minimal time delay.

To keep the holding times for the organic sheet in the open mold as short as possible, the molding compound and the organic sheet were brought simultaneously up to temperature and the molding compound, in the form of predefined compound islands, applied to the heated continuous-fiber material in the tool cavity. The use of GMT with a PA6 matrix offers the advantages of precise pre-assembly and partial distribution of the molding compound. Due to the overlap region, molding compound cannot be applied to the two organic sheets in the same way. The so-called robot master system (Figure 7, right) takes over supplying the organic sheet with molding compound for the center tunnel area. This master system then handles control of the so-called slave robot system, which sends signals (area heater temperature, position,

Fig. 6: Dimensions of an organic sheet half

and so on) to the master robot system as criteria for decision-making. Even communication with the press takes place exclusively via the master system.

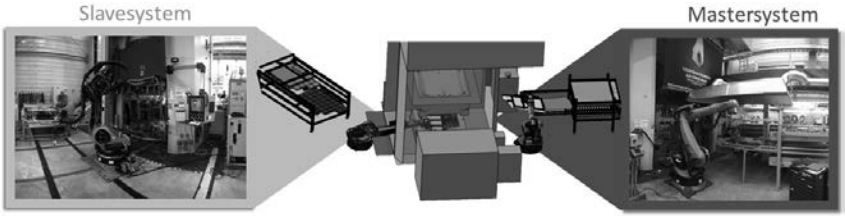

Fig. 7: Overview of the system layout with definition of hierarchies

The remaining GMT molding-compound blanks are distributed evenly over both organic sheets. Here the molding compound is distributed and positioned in such a way that the calculated ribbing pattern is formed and the structural inserts (pre-consolidated hollow sections and metal inserts) can be added by the upper mold.

Figure 8 shows the handling concept for selected positions.
In those areas where the GMT material is exposed due to the two-shell construction, molding-compound grippers with long needles are used. Due to the synchronous loading of the organic sheets and molding compound, open times of less than 20 seconds were reached despite the complexity of the insertion choreography with the rapid-stroke press. Closing forces of approx. 2200 - 2500 t are required for forming the ribs.

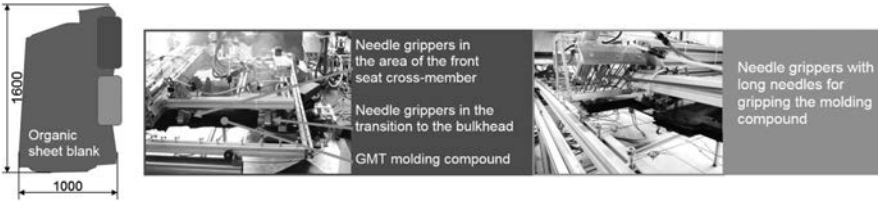

Fig. 8: The handling concept at different positions

With a total cycle time of less than 3 minutes, including demolding (Figure 9), a production quantity of about 100,000 items p.a. can be deduced for a complex structure using the *one-shot production method* for hybrid components.

Fig. 9: Undercuts mean that the component must be demolded laterally

4. Challenges in tooling

A tool design appropriate to both material and process is the basis of the successful implementation of lightweighting with regard to material and production for the hybrid floor structure. The approaches conceived here of a semi-integral construction call for special tooling solutions. The orientation of the ribbing pattern in the bottom mold half means that the necessary adjustment mechanisms must be accommodated in the upper mold half (Figure 10).

Firstly, the hollow structures must be supported to withstand the molding pressure and cannot be placed in their final position until the organic sheets have been inserted and the mold closed. Secondly, the clear space which the package creates under the rear hollow sections results in an undercut which must be supported in the mold. This has the consequence that the rear core mechanism closes on the split mechanism. Since a quick-closing unit (800 mm/s) is used, recourse is made to a purely mechanical contact control function during the positioning of the corresponding mechanisms as the mold closes. Here the solidly formed splits are temperature-controlled since they first come into contact over a large area with the continuous-fiber reinforced semi-finished material and serve simultaneously as draping aids.

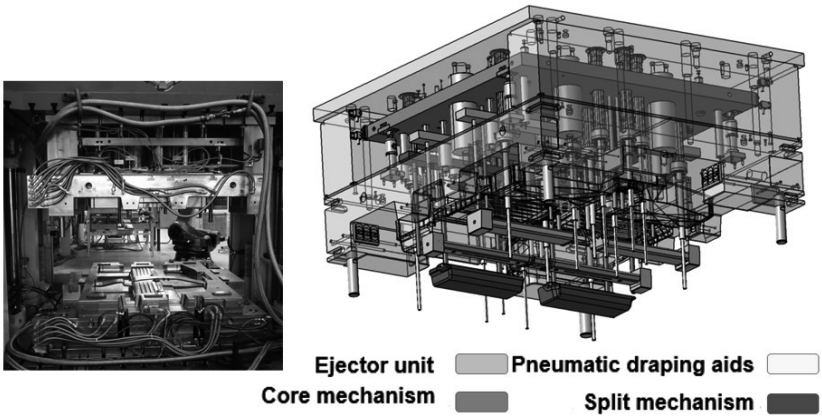

Fig. 10: Underbody press tool and detailed virtual model of the upper mold half

Steel cores without temperature control are used for supporting the hollow sections. They must be withdrawn mechanically at the completion of compression molding. The closed hollow profile has a stabilizing effect inside the rear core structure. In the front core area a single-shell metal structure is used which is designed as a lightweight freeform surface. This is where the holding force is generated by means of pneumatic grippers using weld studs on the metal insert.

The multistage pneumatic draping aids, starting from the center tunnel, grip the organic sheet area in a cascading manner. Here their starting grip at the center tunnel is used for holding in place the two overlapping sheet halves.

Another challenge for the tool design is the use of a positive edge during the closing process. Here the positive edge is closed when the core blocks (Figure 10, green) enter the lower mold half. Figure 11 shows the basic sequence of the mold clamping mechanism.

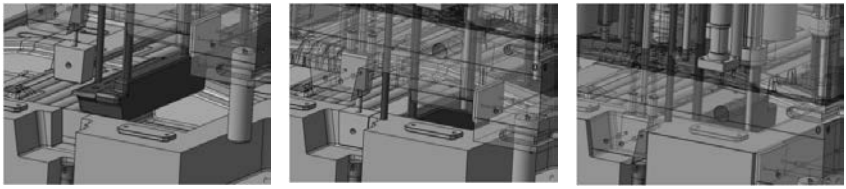

(a) (b) (c)

Fig. 11: Selected stages of the closing process: (a) entry of the split into the lower mold cavity, (b) definition of the core block in the lower mold, (c) mold fully closed

With regard to a cycle-controlled series-production operation, it must be above all possible to control the opening mechanisms hydraulically, especially demolding the cores.

5 Production of demonstrator components

The demonstrator components which have been fabricated are intended to demonstrate the basic feasibility of manufacturing a highly integrated FRP/metal hybrid floor structure under the premise of its utilization appropriate to load paths and stresses.

One of the manufactured hybrid floor structures is shown in Figure 12. Many constructive design approaches were successfully implemented here. However there are currently certain production-related restrictions in relation to the delicately designed ribbing area. Complete filling of the ribbing made it necessary to create additional flow paths for the molding compound and to free further component areas for the compound. This is particularly true of the area beneath the front seats. An additional outer layer of molding compound was required on account of the production constraints we have described and this made it possible for the adjacent rib structure to be filled completely. Another adjustment was made in the area of the core mechanism. To ensure a defined entry of the core leader into the lower mold cavity (in this regard see also Figure 11), cutouts had to be made in the organic sheet in this area.

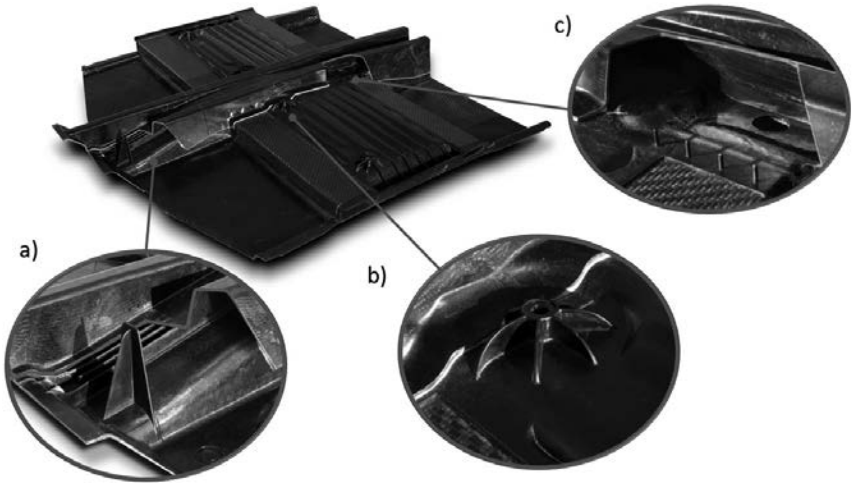

Fig.12: Assembled hybrid floor structure in detail; (a) front incoming air partition and terminating area of center tunnel ribs, (b) rib reinforcement for seat cross-member connection, (c) rear crash structure with insert for supply air ducting.

Since the core blocks move in before the final draping of the floppy inserts, creasing of the continuous-fiber material or jamming of the insert between the lower mold half and core blocking should be prevented in this area. Figure 13 shows the adapted insert blank.

Fig. 13: Adapted organic sheet blank

6 Summary and outlook

The implementation of an FRP/metal hybrid floor structure presented here shows the basic feasibility of producing a lightweighting- and cost-driven primary structure in a multi-material design for larger production quantities. The highly integrative production process based on compression molding technology not only allows a reduction in the number of individual

components but also the integration of additional vehicle-specific functions. The extended compression-molding process with GMT thus emerges as a robust production technology for producing a defined ribbing configuration in combination with continuous-fiber-reinforced base layers. The compression-molding process also stands out by having lower tooling costs in comparison with the structurally analogous injection-molding process although drawbacks have to be accepted with regard to the process-related larger runners and thus lower light-weighting qualities.

In order to establish the use of FRP-intensive hybrid components in the series production process against a background of competing material systems of metal not only must the availability of continuous-fiber-reinforced thermoplastic (glass-fiber-reinforced) semi-finished products be secured at economically attractive prices but above all gaps in the virtual representation of the materials and corresponding production processes must be closed. The simulative representation of the production process must be able to draw reliable conclusions with relation to fiber orientation and distribution on the basis of processing-specific behavior (draping, flow paths, etc.) in order to be able to generate a competitive development process [3, 4]. Furthermore, a properties check of the demonstrators as built must follow, particularly with regard to their dimensional stability under thermal loading.

[1] Friedrich,H.E.: Leichtbau in der Fahrzeugtechnik. Wiesbaden: Springer Vieweg 2013

[2] Eckstein, L., Ickert, L., Goede, M., Dölle, N.: Leichtbau-Bodengruppe mit Verstärkungen aus CFK und GFK, ATZ - Automobiltechnische Zeitschrift (2011), pp. 256-261

[3] Modler N., Adam F., Maaß J., Kellner P., Knothe P., Greuther M., Irmler C.: Intrinsic lightweight steel-composite hybrids for structural components, Materials Science Forum, V. 825-826, pp. 401-408

[4] Sachs U., Akkerman R., Fetfatsidis K., Vidal-Sallé E., Schumacher J., Ziegmann G., Allaoui S., Hivet G., Maron B., Vanclooster K., Lomov S.V.: Characterization of the dynamic friction of woven fabrics: Experimental methods and benchmark results, Composites Part A: Applied Science and Manufacturing, Volume 67, 2014, pp. 289-298

Development of a lightweight instrument-panel support structure

Material and production concept of the instrument-panel support tube made of long-glass-fiber-reinforced partly aromatic polyamide for the BMW M4 GTS

Dipl.-Ing. **R. Krischke**, Dipl.-Ing. **R. Poltrock**, BMW AG, Munich;
Dipl.-Ing. **S. Stein**, BMW AG, Landshut

Abstract

The support structure was originally designed as the carrier for the cockpit integration module and in this main function also contributes to the structural rigidity of the body in the bulkhead area. Mounted on it are instrument panel, glove boxes, airbags, steering column, EE components, and so on.

The component must exhibit a high degree of rigidity over the full temperature range in the passenger compartment and in both vehicle operation and crash situations is subjected to high static and dynamic forces.

Load-bearing structures normally take the form of welded metal constructions (steel, aluminum) or magnesium die castings.

As part of a preliminary development project a support structure made of long-glass-fiber-reinforced thermoplastic was developed which has been developed and industrialized up to readiness for series production for the M4 GTS special series.

The use of a long-glass-fiber-reinforced thermoplastic material meant that a weight saving of approx. 1.6 kg could be saved in comparison with the series component made of steel.

This paper examines not only the component requirements and material selection based on this, supported by mechanical and rheological calculations, but also production aspects.

1. Introduction

In the autumn of 2015, BMW M-GmbH unveiled the M4 GTS whose production has been limited to 700 cars.

The M4 GTS has been designed with pioneering technologies specifically for use on the race track. At the same time it remains unrestrictedly street legal.

The power unit of the M4 GTS is equipped with the innovative water-injection system combined with the M dual-clutch transmission with Drivelogic.
The M-specific 3-way coilovers suspension, front splitter and rear spoiler are manually adjustable, so that the vehicle can be set up individually for a particular race track or for normal use on the roads.
Exclusive carbon components guarantee optimal weight distribution and aerodynamics with variable output. The components in CFRP visual quality include not only the diffuser on the rear spoiler with an adjustable blade and a front splitter, also adjustable, but also the strut brace. The CFRP hood is painted in body color.
The independently molded door and side panels are made of a lightweight material produced from renewable raw materials and weigh only half as much as their series production equivalents. Like the center console with its weight-saving design they also contribute to weight reduction in the M4 GTS in comparison with the series production model.
This paper describes development of the M4 GTS instrument-panel support structure in a long-glass-fiber-reinforced thermoplastic material which made possible a weight reduction of 1.6 kg over the steel production component.

2. Requirements made of the instrument-panel support structure

2.1 General

The support structure is located in the dry interior of the vehicle, laterally mounted directly on the A-pillar nodes, the engine compartment bulkhead and the transmission tunnel. Its primary function is to serve as a connection for the steering column, the instrument panel and other vehicle-specific components such as the HUD (head up-display), air conditioning, and so on.
Secondly, the support structure also has a stiffening function, which should include making a contribution to giving the body sufficient rigidity.

Fig. 1: Lightweight instrument-panel support structure

The special challenge in this project was in the customer-relevant interpretation of requirements over a plastic-specific temperature range.

The graph below shows that the support structure behind the instrument panel heats up to 65 °C – 80 °C during solar simulation for a stationary vehicle (measuring points 88.1 and 102.0 lie directly in the area of solar irradiation).

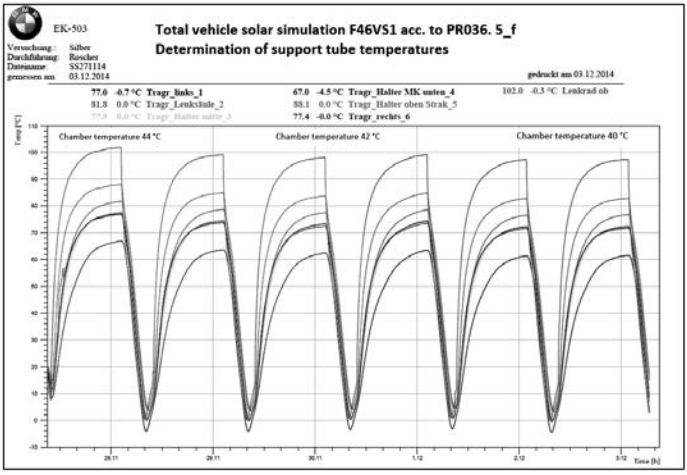

Diagram 1: Temperature analysis of a support structure in the vehicle by means of solar simulation

2.2 Requirements

- Stiffness / corresponding customer-relevant design parameter
    - Vibration comfort steering column / steering wheel ('steering column vibration')
    - Torsional stiffness of the steering column mounting (vehicle-specific)
    - Y-buckling resistance (vehicle-specific, relevant to side crash)
    - Natural frequency of the instrument panel module ('shaker test')
    - Natural frequency of the HUD in the instrument-panel module (vehicle-specific), describes jitter-free image display
    - Steering column and AC acoustics (vehicle-specific)

- Static and dynamic loads
    - Coat straightening test, describes the displacement of the steering wheel under tensile load in -z/ax
    - Vehicle-specific local rigidities, for example, glove box mounting, air conditioning, support areas for airbag systems, and so on
    - Sag of instrument-panel module on automated assembly line

- Crash requirements / consumer protection requirements
    - Crash requirements according to European technical regulations in the context of type approval, UN-R94 and others
    - Euro NCAP
    - Crash requirements in accordance with US technical regulations in the context of type approval, FMVSS 208 and others
    - US NCAP
    - IIHS
    - Further country-specific tests (such as PR China, and others)

All of these requirements are first simulated in the data model and evaluated.

3. Development of the material concept

3.1 General

The material concept was developed on the basis of the requirements applicable to the support structure. The goal of development was to create the component for the installation space available using materials with a thermoplastic matrix.

In contrast to designing components with regard to strength, the focus of this structural component was on a high component rigidity over the entire relevant temperature range as a design criterion.
The stiffness required can only be achieved by using fiber-reinforced materials.
Other requirements – such as good behavior under dynamic stress (crash), heat resistance, chemical resistance, ageing properties, workability and so on – should not of course be ignored here and are influenced not only by the matrix material but also by the reinforcing fibers. In addition, weight and cost targets also have to be met.
At the beginning of the project not only the use of organic sheets for component reinforcement (SpriForm technology) was investigated but also the use of carbon-fiber-reinforced materials. For this reason, the availability of organic sheeting and compatibility with carbon fiber had to be taken into account when selecting the matrix material.

3.2 Matrix material

Once these requirements have been taken into consideration, the polyamide family emerges very quickly as candidates for the matrix material.
(Glass)-fiber-reinforced polyamides are used in vehicles in many highly stressed parts, such as engine compartment components, structural components (engine mounts, transmission cross-member, air-spring piston, and so on).
All polyamides absorb moisture. Moisture absorption up to saturation and the absorption rate differ amongst the different polymer types.
Moisture absorption causes changes in mechanical properties. Moisture makes the components tougher but also reduces strength and rigidity. In vehicle operation a condition of equilibrium sets in which depends on the climatic conditions of the place of operation. In validating polyamide components therefore, not only must the saturated damp state be covered but also the dry, freshly molded state.
The strength and stiffness of fiber-reinforced polyamides with the same fiber content differ only slightly at room temperature. The influence of the matrix material becomes very evident in elongation at break and impact strength. Properties over the temperature and moisture content ranges are dominated by the influence of the matrix.

Table 1:Comparison of the properties of polyamide materials +50%GF from data sheets [1]

Designation	Unit	State	PA6T/6I	PA6T/66	PA66+ PA6I/6T	PA66	PA6
Tensile modulus of elasticity Tensile strength ISO 527	[MPa]	dry damp	18000 17500	17500 17000	18000 17000	17000 12500	17000 11000
Tensile strength ISO 527	[MPa]	dry damp	250 240	250 225	250 220	245 180	245 165
Elongation at break ISO 527	[%]	dry damp	2 2	2 2	2.5 2.5	2.5 3.5	2.5 4.5
Impact strength ISO 179-1eU	[kJ/m²]	dry damp	80 80	85 85	90 90	95 100	90 100
Notched impact strength ISO 179-1eA	[kJ/m²]	dry damp	11 11	13 13	15 15	18 25	15 25
Glass transition temperature	[°C]	dry damp	125 105	95 75	80 60	60 40	60 40
Melting point	[°C]		325	310	260	260	220
Mold temperature range	[°C]		140-160	100-140	80-120	80-100	80–100
Processing temperature	[°C]		330-345	315-340	270-300	280-300	280-300
Density	[g/cm³]		1.65	1.62	1.56	1.56	1.55

It should be noted when designing a structural component with regard to stiffness that the glass transition temperature falls as moisture content rises. The decrease in stiffness over temperature shifts to lower temperatures.

Normally DMA or shear modulus curves are plotted on the logarithmic scale.

Here we may be deceived by the representation selected, since with a logarithmic plot the drop in stiffness to Tg looks much less dramatic than it is in reality, as Diagram 2 clearly shows.

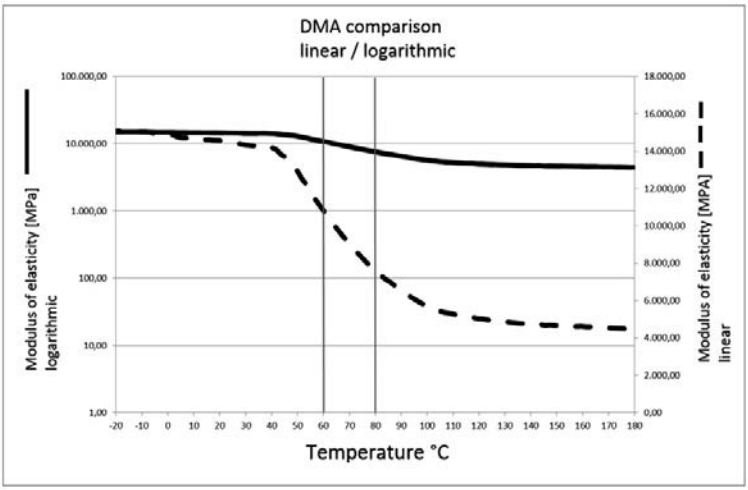

Diagram 2: Comparison of linear / logarithmic DMA plots for a material

Diagram 3 shows the fall in stiffness in the so-called DMA test (dynamic bending test over temperature for different types of polyamide in different conditioning states).

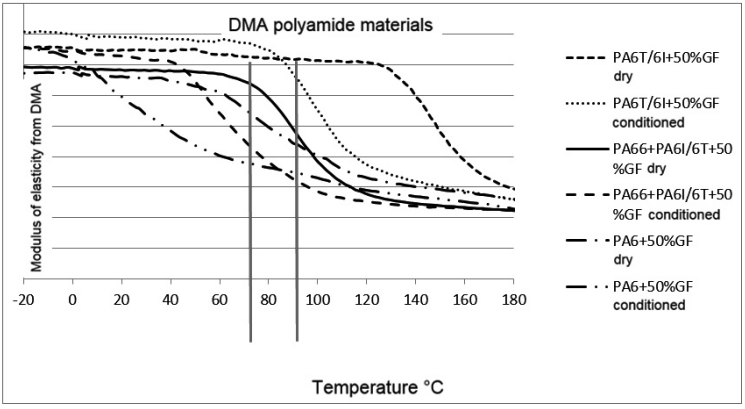

Diagram 3: DMA comparison of polyamide materials, linear plot

Diagram 4 shows the basic course of stiffness plotted against temperature The steep decline begins at approx. 20 ° C before the glass transition temperature (reversal point of the curve). With stiffness remaining as constant as possible up to temperature T, the glass transition temperature must be at least +20 °C.

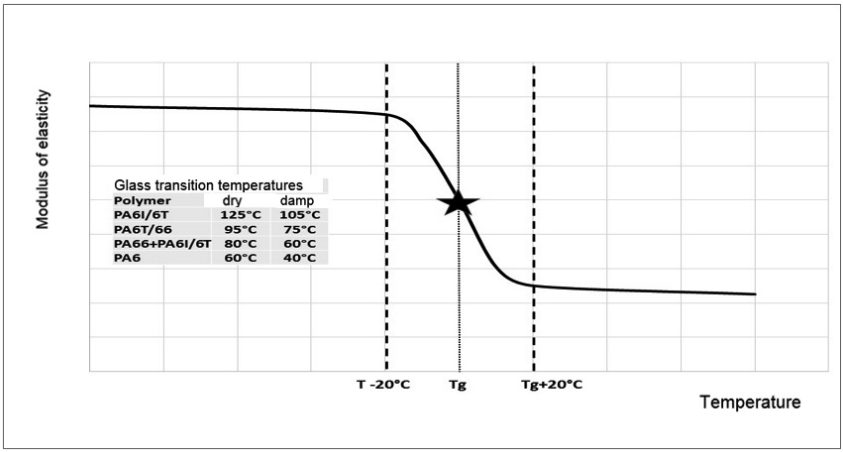

Diagram 4: Stiffness plotted against temperature

3.3 Reinforcing fibers

Glass fibers (GF) are normally used in injection-molding compounds. However, at the beginning of the project carbon fibers (CF) were also at the focus of deliberations.

Table 2 compares the different fiber properties.

Table 2: Mechanical characteristics of reinforcing fibers

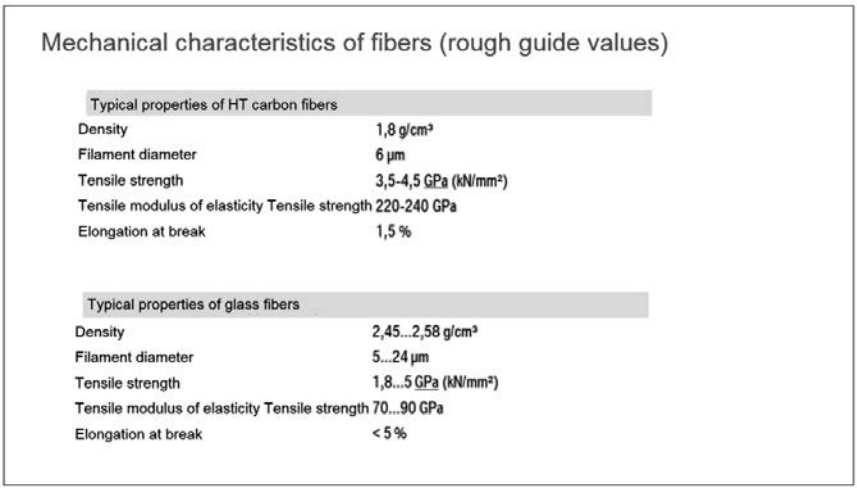

Mechanical characteristics of fibers (rough guide values)

Typical properties of HT carbon fibers	
Density	1,8 g/cm³
Filament diameter	6 µm
Tensile strength	3,5-4,5 GPa (kN/mm²)
Tensile modulus of elasticity Tensile strength	220-240 GPa
Elongation at break	1,5 %

Typical properties of glass fibers	
Density	2,45...2,58 g/cm³
Filament diameter	5...24 µm
Tensile strength	1,8...5 GPa (kN/mm²)
Tensile modulus of elasticity Tensile strength	70...90 GPa
Elongation at break	< 5 %

The advantage of carbon fibers lies in their low density and very high stiffness but with the drawback of a much smaller elongation at break.

Due to previous positive experiences with polyamides as a matrix material for CF-reinforced injection-molding materials, carbon-fiber pellets from production residues were also investigated.

In this stage of development, it was not yet possible to produce sufficient quantities of carbon-fiber pellets from production residues in a cost-effective way. It was however possible to demonstrate in one production process which could yield a maximum production quantity of 10 tonnes per year that only minimally worse mechanical values could be achieved with these recovered materials than those for materials with 'virgin' carbon fibers.

At Fakuma 2014 [2] and the VDI conference Plastics in Automotive Engineering 2015 [3] carbon-fiber pellets from production residues from serial production plants were presented and their properties discussed.

3.4 Selection of materials

Studies with test pieces and sheets and also an experimental mold (Erlangen beam), including in combination with organic sheets, did not supply any clear-cut result for making the final material selection.

For this reason the mold was designed to what is in our opinion the material which is hardest to process, a PPA (PA6T/6I) with 50% long-(glass)-fiber reinforcement.
According to our information, there has not been hitherto any similarly large component in this fiber / matrix combination.
This design (more on this in Section 4) has meant that we have not been restricted on the tooling side and were able to try out different materials in selected substitution tests. *Components were made from materials ranging from PA6 +L(GF/CF), PA66+PPA +(L)GF/CF to PAA+(L)GF/CF* .
Table 3 shows a selection of the materials tested including subjective and objective ratings for production suitability and trials.

Table 3: Material matrix

Designation		Standard	PA6T/6I +40%CFrec	PA6T/6I +50%GF	PA6T/6I +50%LGF	PA66+6I/X +40%CF	PA66+PA6I/X +40%LCF	PA66+PA6I/X +30%LCF	PA66+PA6I/X +50%LGF	PA66+PA6I/X +60%LGF
Tensile modulus of elasticity	[Mpa]	ISO 527	30000	18000	19500	31000	29500	22500	18000	24000
Tensile strength	[Mpa]	ISO 527	265	250	275	260	335	315	260	310
Elongation at break	[%]	ISO 527	1,2	2	1,9	1,5	1,5	1,6	2,2	2,2
Impact strength	[kJ/m2]	ISO 179/1eU	45	80	75	55	75	65	95	120
Notched impact strength	[kJ/m2]	ISO 179/1eA	6	11	30	7	18	16	30	45
Filler content	[%]	EN ISO 1172	40%rCF	50%GF	50%LGF	40%CF	40%LCF	30%LCF	50%LGF	60%LGF
Production suitability / demolding behavior			not OK	OK	OK	OK	OK	OK	OK	OK
Static substitution test			OK	OK	OK	OK	OK	OK	OK	OK
Dynamic substitution test			not OK	not OK	not OK	not OK	not OK	not OK	conditionally OK	OK

The best compromise between stiffness and dynamic behavior proved to be a PA66+PA6I/X + 60%LGF with special long glass fibers.
Although pure PA6T/6I materials have their advantages as regards stiffness and strength, especially at high temperatures, they do however have drawbacks in elongation at break, impact and notched impact strength. These properties are additionally overlaid by the fiber properties.
The disadvantage of CF-reinforced materials can be seen in their dynamic behavior. By contrast, GF-reinforced materials have lower stiffness. Hybrid materials with GF+CF or even toughened CF materials were not able to compensate for the disadvantages of the basic materials.
Long (glass) fibers improve the dynamic behavior of the composite material. Mechanical properties over temperature are shifted towards higher temperatures (Diagram 5).

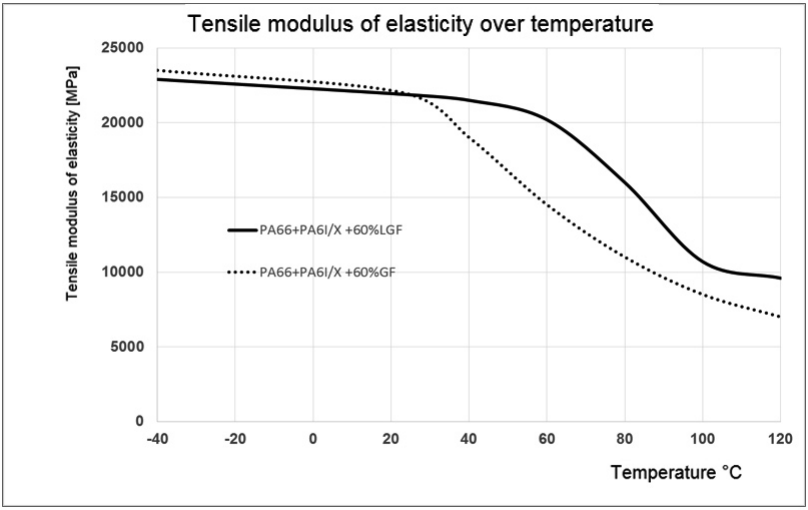

Diagram 5: Tensile modulus of elasticity plotted against temperature in comparison of a short- and a long-glass-fiber-reinforced material

In the case of components made of long-fiber-reinforced injection-molding materials, a fiber 'casting' forms which retains the component shape after incineration of the matrix material (Figure 2).

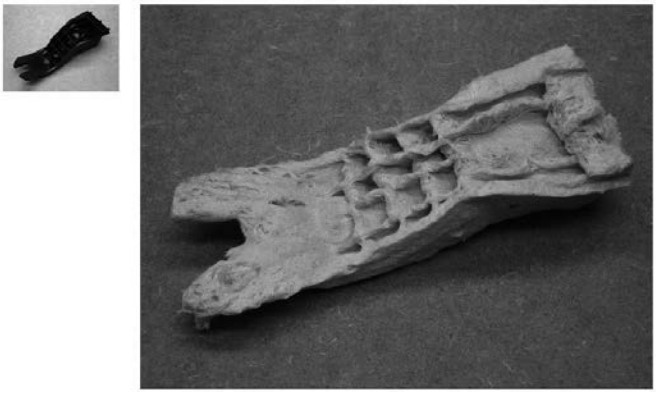

Fig. 2: Glass-fiber 'casting' structure (after incineration) with optimal processing process

Material selection is based in the first step on a materials comparison of injection-molded test pieces but ultimately it is the component which must satisfy all requirements and not the test piece.

3.5 Properties of the selected material in the component

A material card was generated for use in computational validation of the component. The test pieces are machined from injection-molded test sheets in different orientations. Here material characteristic values dependent on the strain rate were measured for different conditioning states and at different temperatures. At present, calculation is still carried out with an averaged characteristic material value without taking fiber orientation into account.

It was difficult to obtain characteristic material values from the component because there are only a few places from where test pieces in compliance with standards can be taken. For this reason a test piece was defined which can be cut out from different locations on the component. These test pieces were subjected to a bending test. This can however only be a destructive test.

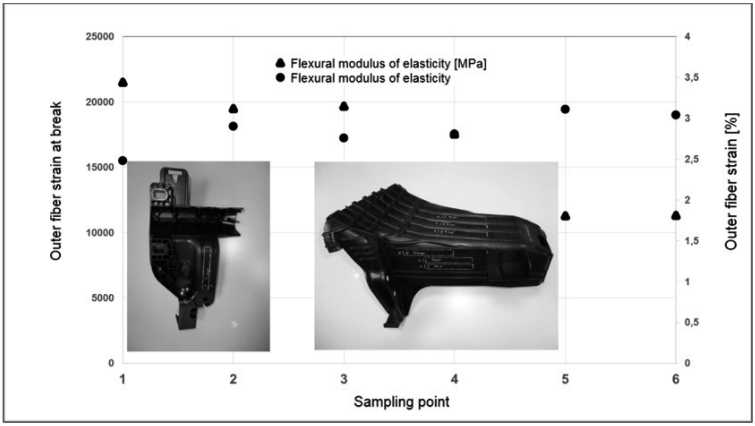

Diagram 6: Characteristic material values from the component

A support required for assembly purposes and also a test piece in accordance with DIN EN ISO 527 were integrated into the cavity of the support tube. Following demolding, the support and the test piece were separated from the support tube. The test piece is used for quality assurance.

3.6 Outlook from the point of view of material

The material properties of the selected material satisfy the requirements made of the component. To develop new components with different geometric constraints or increased stiffness requirements, such as those due to heavier steering columns, it is necessary to develop a material with a higher glass transition temperature while maintaining the elongation at break and the behavior under dynamic loading.

4. Tooling concept

4.1 General remarks

As already mentioned in Section 3, a clear decision had not been made at the time of tooling design as to whether component stiffness and component strength would mean a need for organic sheeting and what material would be the basis for the tooling.

Accordingly, the decision fell in favor of the following design concept for the experimental mold, which was used both for the very lowest production numbers and also as a series-production mold.

1. Straightforward injection-molding variant which was given the higher priority in the designing since an organic sheet was the poorer variant from the point of view of cost.
2. Organic sheet variant, familiar from SpriForm technology, in which a heated organic sheet is inserted into the injection-molding tool, shaped and back-injected.

Fig. 3: Variant 1 - pure injection-molding design

Fig. 4: Variant 2 - organic sheet in transverse combination and back-injected with thermoplastic material

Likewise, it was decided for the mold design that the most critical material from the processing point of view should be used. Here the PA6T/6I with 50% long-glass-fiber content made the highest demands of the tooling concept.
The following design criteria, among others, were thus selected:

- Mold temperature control to 160 °C due to the high glass transition point of PPA material systems.
- Gating system designed for long glass fiber (fiber-protective)
- Melt temperature sensors for monitoring in the hot runner system (2 sensors) on account of the very tight processing window with regard to melt temperature.
- Hot runner volume must be less than the component volume. Long residence times at high melt temperatures must be evaluated extremely critically in the case of PPA material types.
- All hot runner system sections must be completely flushed through in a single injection-molding cycle so as to keep the thermal stress on the material as low as possible.
- Extremely good tool venting due to the burner risk and increased cleaning effort.

4.2 Rheology

An early, rheological analysis of the component ensures avoidance of classic butt weld lines which experience has shown have a negative effect under the high component stresses expected.
Similarly, attention was paid to air entrapments which in PA6T/61 material systems give rise to marked material degradation.
An intelligent positioning of the nozzles has proved a good way of weakening the weld seams in the core area (by further filling with material) so as to maintain system strength.
It can be seen from Figure 5 and 6 that at the time when the main weld lines form no part of the mold is yet 100% filled. This ensures that material continues to flow in the core area and the structure is not weakened such as would occur with a butt weld line.
Care was also taken that close to the main weld lines there was always an additional geometric component outlet such that weld-line weakening is stabilized by the component-related geometry.

Fig. 5: Emergence of major weld lines - 40% mold filling

Fig. 6: Main weld lines closed at the surface, further flushing due to incomplete mold filling → weld lines are shifted in the core.

In addition, safety-relevant connection points such as the steering column connection or the knee airbag connection did not have the corresponding apertures as the component came off-tool but these were milled out in a subsequent step.
This counteracts the high weld-line weakness of long-glass-fiber materials.

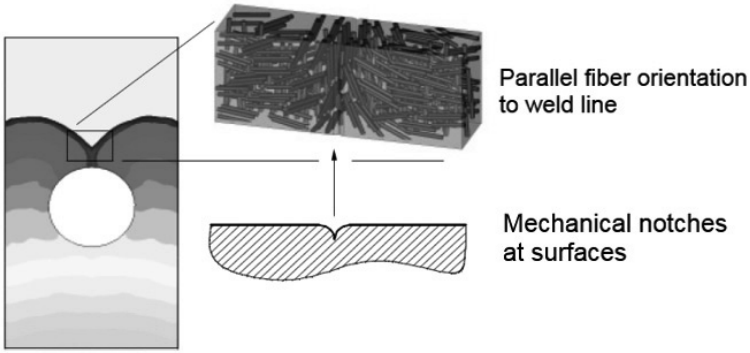

Fig. 7: Classic rheological situation at a through-hole [4]

Another very important aspect of tool design with a PPA material is the factor of residence time in the hot runner.

PPA materials are processed in a very high temperature profile, which permits only a very narrow tolerance window.

The rheological design has been significantly influenced by these two factors (high processing temperature with narrow processing window, and residence times as short as possible).

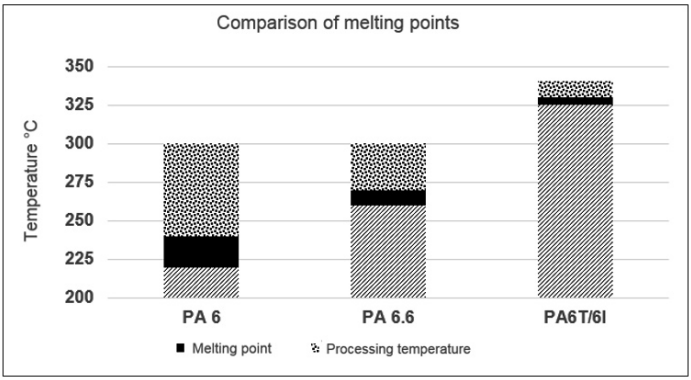

Source: EMS-Chemie, Domat, Switzerland.

Diagram 7: Comparison of melting points of classic polyamides and a PA6T/6I

The following situation thus emerged for the hot runner system design for the support-structure injection mold for the M4 GTS:

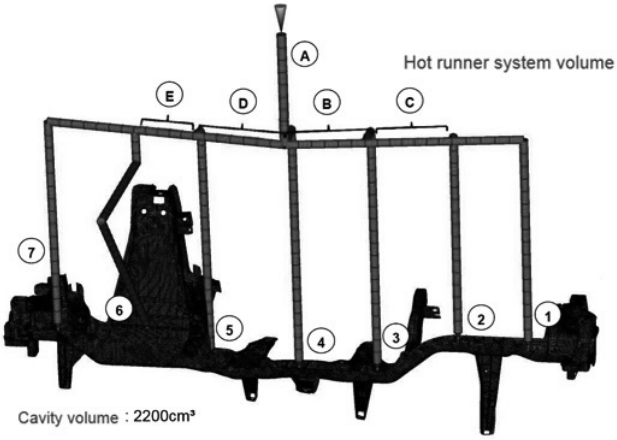

Fig. 8: Hot runner system for the support-structure mold

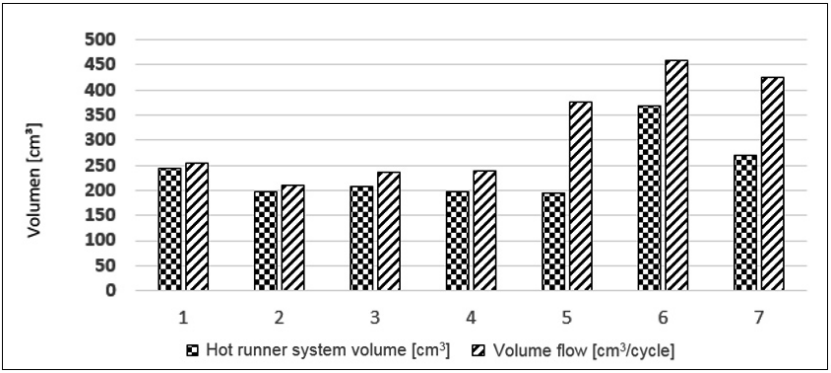

Diagram 8: Hot runner system volume vs. volume flow per cycle. Hot runner segments A to E are included percentually in the hot runner branches.

It can be seen from Diagram 8 that all manifold blocks are completely flushed through with new material during an injection-molding cycle. In this way the very best option in the design of the hot runner system was achieved for a PA6T/6I matrix material.

5. Production concept

A modular production lines was set up at the BMW Landshut plant for the production concept of the M4 GTS special series.

Depending on the quantities demanded, this modular system can be set up within an hour, the week's output of components produced and the system then stowed away to free up the production area for another technology for the M4 GTS.
With this module-based variant the maximum efficiency is achieved for a special series.

The process steps for the M4's thermoplastic support structure can be divided up as follows:

1. Injection molding:

- Production of all serial parts as a group
- Metallic inserts for the A-pillar connection
- Cycle time: 86 sec.

2. Milling:

- Milling all functional and crash-relevant through-holes
- Cycle time: 9.6 min.

3. Inserting rivet bolts:

- Manual insertion blind rivet nuts and bolts via force-controlled setting tools
- Cycle time: 2.8 min.

4. Mounting add-on parts:

- Mounting C clips, spacers, tolerance-compensating systems on the BiW, glove box holders etc.
- Cycle time: 6.4 min.

5. Ultrasonic welding:

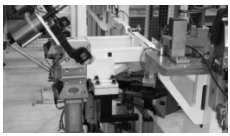

- Ultrasonic welding of tolerance-compensating systems (PA6) to the support structure
- Cycle time: 1.2 min.

6. Component testing

For release of the component, all necessary internal and statutory tests are carried out in accordance with the instrument-panel support structure requirements mentioned in Section 2.

In the component and overall vehicle these include the following tests:

- Creep behavior under load at different temperatures
- Climate shaker
- Airbag bench test
- FMVSS 201 head impact (pendulum tests)
- Sled tests
- EMC testing
- Coat straightening test
- Tapping test to determine steering-column vibrational and acoustic behavior
- HUD jitter in the vehicle
- Front and side collisions

After test driving on both the test site and the roads over the summer and winter periods, component approval was granted for the M4 GTS.

7. Summary

By using a partly aromatic polyamide material (PA66 + PA6I/X + 60% LGF) reinforced with special long glass fibers, with a balanced ratio between rigidity and behavior under dynamic loading, in combination with an optimized tool design and taking rheological conditions into account, it has been possible to obtain a weight reduction of 1.6 kg in the instrument-panel support structure of the M4 GTS.

References:

[1] Data sheets, EMS-Chemie, Domat, Switzerland.

[2] Akro-Plastic brochure, published at Fakuma 2014

[3] Sustainable with carbon, Dr. Stephan Huber, 39th VDI conference Plastics in Automotive Engineering 2015

Consideration of local thicknesses within finite element simulation of injection molded thermoplastics

Dipl.-Ing. **M. Franzen**, Dr.-Ing. **O. Ghouati**, Ford Werke GmbH, Aachen

1 Introduction

Today the automotive industry is challenged by a continuously rising number of demands having a strong influence on the development process. The need for CO_2 reduction and hence the resulting need to reduce the vehicle weight as well as the need to constantly improve occupant and pedestrian protection makes it necessary to fully utilize the deployed materials as efficiently as possible.

In order to be able to meet the increased requirements within the context of shorter cycle times and rising cost pressure, the use of virtual development tools is intensified. For crash simulations the explicit Finite Element Method (FEM) has been applied for a long time. However this process can only be successful when numerical methods are capable and there is a high confidence level.

Within current crash simulations not only the deformation characteristic of a part is of importance but especially assessment of the fracture risk. In 2003 Ford Motor Company R&A in cooperation with external partners therefore started several projects to address these issues. Within these projects the material model MF-GenYld+CrachFEM was developed for various material applications. This material model is capable of accounting for the high degree to which hardening and fracture behavior depend on the load condition and strain rate. This user-defined material model is suitable for the explicit FEM programs LS-DYNA and RADIOSS and is installed on the Ford Motor Company supercomputer cluster, making it applicable to all car-lines within the Ford Motor Company.

To correctly predict the failure risk within Finite Element (FE) crash simulations an advanced material model is only one step in the right direction. Due to the fact that fracture is highly dependent on local thickness, this information must be available as well. In injection-molded thermoplastic parts, however, the local thickness can vary significantly, e.g. in ribs, joints, local reinforcements or attachment points.

Thickness measurements on headlamp lenses showed that in this specific part the local thickness varies significantly. Similar variations have been found in other typical injection-molded parts used in Ford vehicles. It is obvious that ignoring these variations will lead to false simulation results. However current practice is to use 2D mid-plane shell elements with

a uniform thickness of the part or to divide the part manually into sub-areas to account for local thickness changes. This is very time-consuming and not applicable in daily product development. Solid elements are an alternative but this is also not at the moment applicable to full vehicle simulations.

Ford R&A in cooperation with the University of Minho (Portugal) as well as Altair Engineering GmbH (ALTAIR) has therefore developed a tool that automatically calculates the local thickness and transfers it to a Finite Element (FE) mid-plane shell mesh within minutes, even for big models. The tool is implemented into the standard software Hyper Works from Altair which is used by the Ford Motor Company and is globally available for the Ford CAE community. The calculation functionalities as well as the graphical user interface (GUI) are tailored to Ford Motor Company needs worldwide, facilitating the daily use of the tool within product development.

2 Technical approach

For injection-molded parts the local wall thickness is a design feature and this information is therefore included in the CAD data. For blow-molded thermoplastics the thickness is not specified exactly within the CAD data because the final part thickness is a result of the manufacturing process. For this reason the developed method described in this report is only applicable to injection-molded parts. For blow-molded parts a manufacturing simulation must be performed to derive the final local thickness distribution.

The idea of this local thickness measurement and assignment tool called CAD2FE is thus to obtain the local thickness from the CAD data. The basic approach is to calculate the thickness of an FE mid-plane shell element by shooting a ray from this element in both directions. The distance between the origin of the ray and its intersection with the CAD data will then give the local thickness (Figure 1).

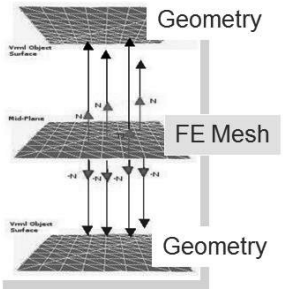

Fig. 1: Basic function of thickness measurement

However in realistic problems the following issues may occur which would significantly impair correct thickness calculation if no countermeasures were applied:

- The FE mesh may not lay parallel within the CAD surfaces, leading to incorrect (too large) thickness calculations.
- The FE mesh may even be outside the CAD surfaces, due to simplifications within the FE models, leading to no thickness measurement at all.
- Within the root of a fin the thickness would not be calculated correctly.

To overcome these limitations the final CAD2FE functionality includes several functionalities for identifying possible incorrect thickness calculation results and applying corrected thickness results. Within the project both the algorithm and the graphical user interface (GUI) were developed by the ALTAIR team. Ford R&A steered the validation procedure as well as the functionalities with the feature.

The final CAD2FE functionality is included in the HyperMesh V13 release and is now a standard feature. The functionality is based on a specification developed by R&A in cooperation with Ford Motor Company development teams all over the world:

- Ford of Europe (FoE)
- Ford North America (FNA)
- Ford of Mexico (FoM)
- Ford of Brazil (FoB)
- Ford of Australia (FoA)
- R&A Europe

The method is applicable to all injection-molded thermoplastics such as:

- Door trim, pillar trim, IP, console, glove box, LLS, GOR, headlamp, cowl, and so on

It can be used in the following attribute simulations:

- Low-Speed Damageability
- Crash
- NVH
- Durability

The tool is currently working for the following FE software tools:

- RADIOSS
- LS-DYNA
- ABAQUS
- NASTRAN

As mentioned before this method is not applicable to blow-molded thermoplastics such as fuel tanks, canisters or gas bottles.

3 Validation examples

Several validation examples have been analyzed at Ford R&A to verify the quality of the CAD2FE functionality as well as to develop best practice and lessons-learned procedures to be applied by Product Development (PD). Some of these validation examples are presented below.

3.1 Headlamp lens

The first validation example is a headlamp lens. The original simulation results in comparison with physical tests can be seen in Figure 2. To identify the variation within the physical parts three physical tests have been performed.

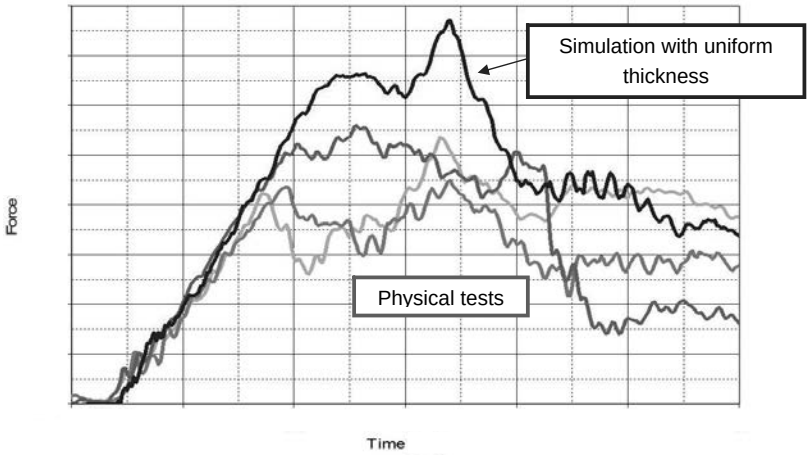

Fig. 2: Crash simulation vs. physical test, impact on lens, uniform thickness

These simulations have been performed with a lens which uses only two different thickness values within the FE simulation, which is a very simple but nevertheless a state of the art approach. In response to this unacceptable deviation between simulation and physical tests a laser scan of a physical lens was carried out to identify the true physical thickness of the parts. An example of such measurements is given in Figure 3.

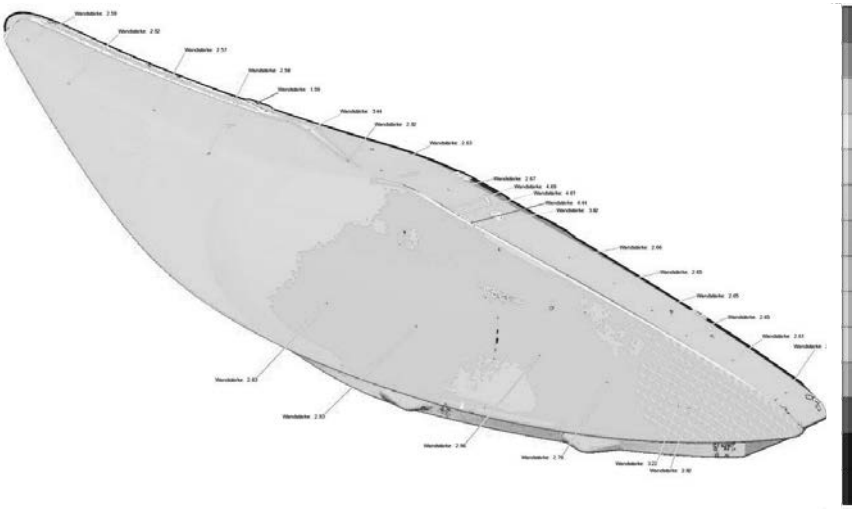

Fig. 3: Physical thickness measurement on a headlamp lens, laser scan

The actual thickness of the lens varies significantly. To validate the CAD2FE functionality the simulation model provided by PD was used to calculate the local thickness values using the HyperMesh-integrated CAD2FE tool. Comparison of the calculated thickness (CAD2FE) and the physical thickness (3D laser scan) is illustrated in Figures 4 and 5 below.

The comparison shows that the CAD2FE functionality is able to calculate the physical part thickness correctly. In particular, extreme thickness values, such as low thicknesses at edges (Figure 5, blue area) as well as very thick areas at edges (Figure 5, red/white areas), are correctly represented. In addition, the transition zone between the two outer edges (Figure 5, arrow) is correctly represented with CAD2FE.

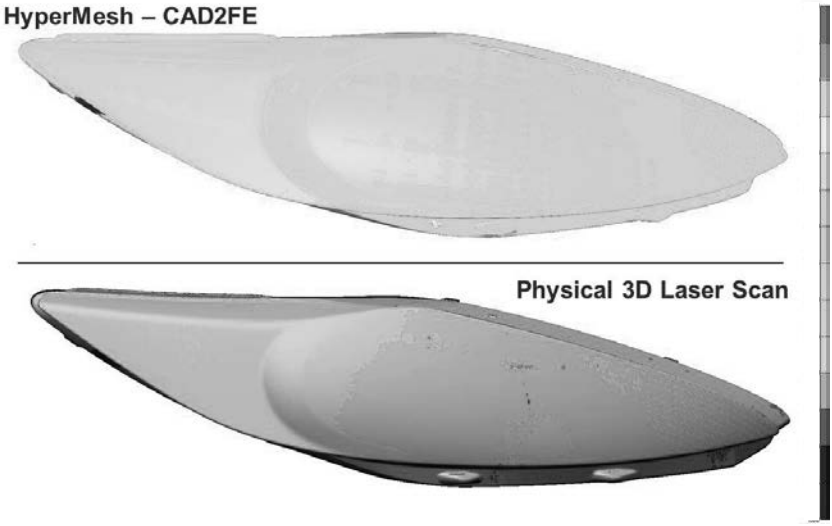

Fig. 4: Comparison between physical thickness measurement and calculated thickness

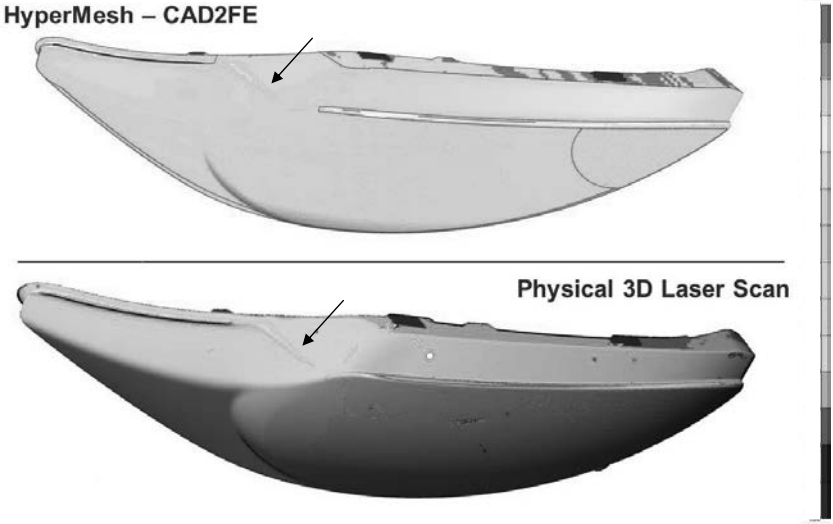

Fig. 5: Comparison between physical thickness measurement and calculated thickness

On the basis of these thickness calculations the simulations were repeated with the same settings, with only the local thickness values calculated by the HyperMesh functionality CAD2FE being added (see Figure 6).

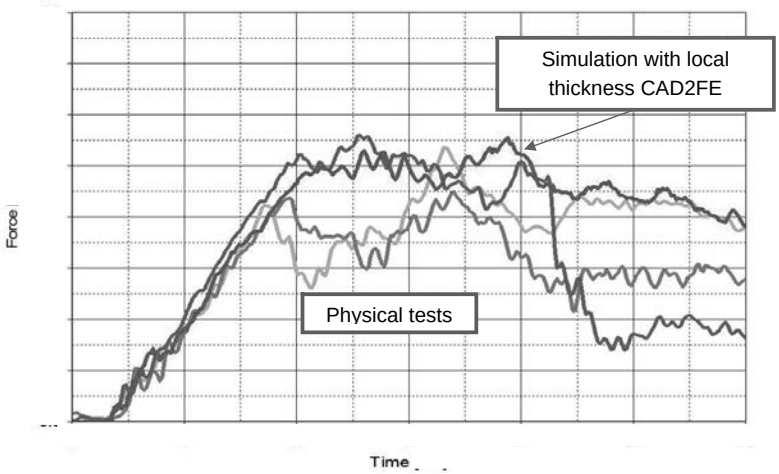

Fig. 6: Crash simulation vs. physical test, impact on lens, CAF2FE thickness

In comparison with the standard uniform thickness simulations (see Figure 2), the simulation quality regarding force-displacement behavior is significantly increased. The simulated forces now fall within the scatter of the test data.

3.2 Armrest

Additional quality checks have been performed with an armrest structure. Within these validations CAD2FE calculations were performed with HyperMesh 13 (see Figure 7), then transferred to the crash mesh and finally 3-point bending simulations were performed. These simulations are then compared with physical tests results as well as simulations with design thickness values. Results are shown in Figure 8.

The armrest simulation results show a significant quality increase when local thickness values are taken into account. The stiffness (elastic range) is represented in a much more accurate manner. The maximum force can now be correctly predicted, giving a quality increase of about 16%. The standard simulation predicts excessively high forces. After the first force drop the physical part exhibits several cracks and local fractures which can also be accurately represented with CAD2FE-based simulations, correctly representing the energy absorption of the part.

Fig. 7: Armrest, CAF2FE calculation results, local thickness

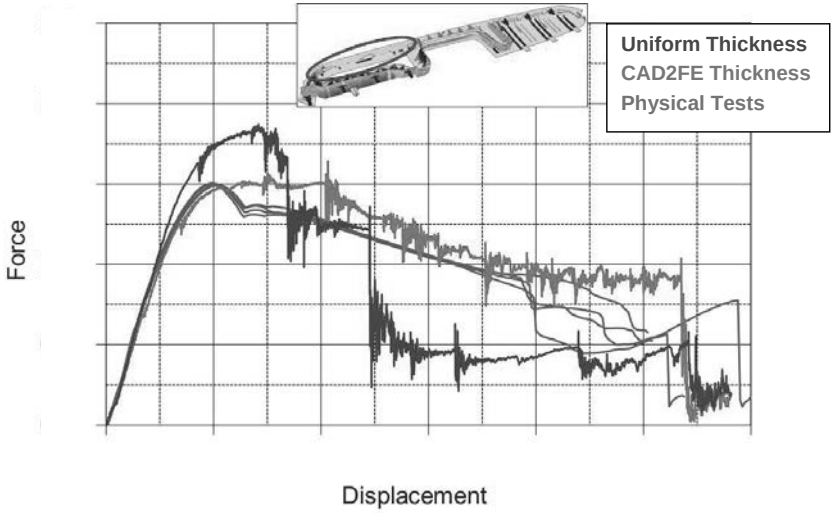

Fig. 8: Armrest 3-point bending test results vs. simulations

These good results are only achievable when the following boundary conditions are met:

- A fine mesh must be used to correctly represent the geometry of the part including all ribs and features.
- An advanced material model must be used to take into account complex deformation and fracture behavior of the thermoplastic (MF-GenYld+CrachFEM).
- The local thickness values must be taken into account (CAD2FE).
- If fiber-reinforced plastics are used then the local fiber orientation must be taken into account (injection simulation mapped onto the crash mesh).

4 Summary

To achieve high-quality simulation results detailed finite-element simulations are required. This includes the detailed definition of local thickness values for injection-molded and cast parts. To be able to take into account the local thickness distribution on an automated basis, Ford R&A together with Altair Engineering GmbH have developed a tool called CAD2FE which has been implemented and integrated into HyperMesh. This tool enables automatic consideration of local thickness values for mid-plane shell meshes within RADIOSS, LS-DYNA, NASTRAN and ABAQUS. The effectiveness and quality of this tool has been verified with several validation parts.

Sensor technology for interconnected injection-molding production: a prerequisite for Industry 4.0

Dr.-Ing. **R. Vaculik**, Kistler Instrumente AG, Winterthur

Abstract

Industry 4.0 is ubiquitous and is currently being implemented in different approaches in industry. The plastics processing industry is also committed to this approach and in numerous demonstrations shows the capabilities of Industry 4.0. Here the goal is to gain synergies by digitizing and networking data within the product life cycle and ultimately to increase profitability. In the field of injection-molding production, sensors within the tool provide a way of monitoring the process and making it more transparent. Monitoring the mold cavity pressure in particular has proved useful since it correlates closely to component quality.

For a long time now, automated monitoring and scrap segregation by means of mold cavity monitoring has been standard in many sensitive branches of industry and enables companies to make considerable cost savings. Furthermore, bringing together the data collected in a virtual production environment offers further possibilities of monitoring and optimizing not only the individual injection-molding cycle but also the entire production sequence.

The basis for this is supplied by sensor technology within the injection mold. This paper describes the current state of tool sensor technology and also future trends in that field and in the further processing of data. This simple, intuitive use of the components and the transparency gained in production act as key factors in the acceptance of the technology and ultimately in the economic advantage achieved.

1. Industry 4.0 - the fourth industrial (r)evolution

The buzzword ‘Industry 4.0’ has finally arrived in plastics processing as well and is currently causing a stir in our industry. This term at this time covers numerous attempts to automate and interconnect production processes as well as to digitize the production environment. As far as automation is concerned, this is not a new approach: back in the 1980s the term CIM (computer-integrated manufacturing) covered numerous approaches to networking production, in most cases with the goal of achieving unmanned production.

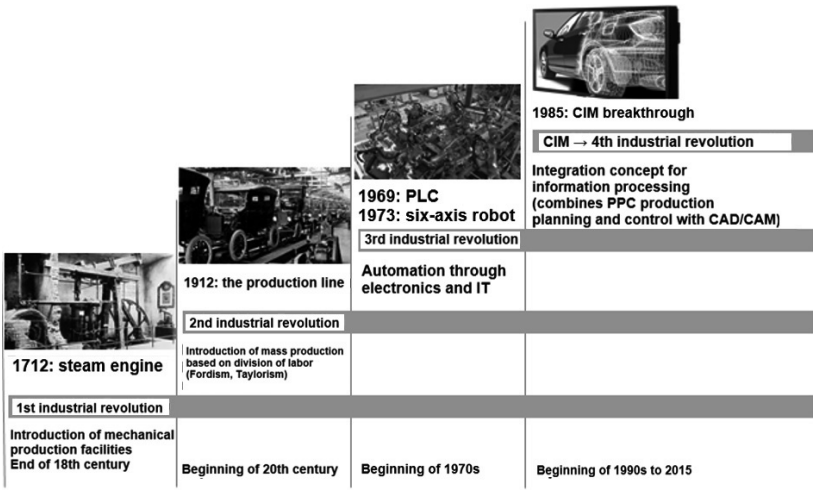

Fig. 1: Stages in the industrial revolution [1;2]

The present-day approaches of Industry 4.0 do however go far beyond this goal. Here the complete life cycle of a product is considered and the individual is now placed at center. Another criterion lies in the collection and systematic use of all data, even those with a relatively remote connection to the product. This relates to the fields of development, production or utilization.

In other words, data acquisition in the process and the correlation with quality and production status play a major rôle for this aspect of Industry 4.0. The Kistler company as manufacturers of sensors and measurement technology offers with its products the basis and also an essential prerequisite for networking data and using it rationally.

The aim of an approach of this kind is, of course, not simply to collect data but rather to use it profitably. Without a strong focus on quality and the economic efficiency of a solution the overall concept will only be implementable with difficulty in our medium-sized companies.

2. Process monitoring with tool sensor technology

Process monitoring of the injection-molding process on the basis of cavity pressure and temperature is a best practice for ensuring quality and cost-saving in the process. As has been known for a very long time, process deviations are reflected very directly in the course taken by the mold cavity pressure curve. Not only variations in the material but also other disturbing influences bring about a characteristic change in the curve. This makes it possible on the basis of a sign of this kind to make a decision as to whether the component produced is a good part or in all likelihood a reject. In the latter case the part is automatically segregated.

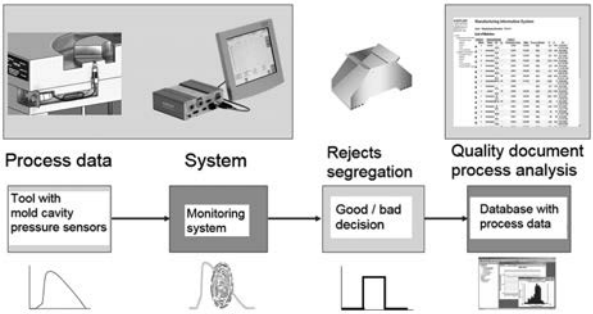

Fig. 2: Measured data acquisition and good/bad decision

The result of all evaluations is saved and becomes available for further evaluations. Curves can be saved to and managed in a central database.

3. Tool sensor technology goes digital

Nowadays, due to the high dynamics and great resilience of the sensors, the mold cavity pressure is measured exclusively by piezoelectric pressure sensors. Here the sensing element creates by the piezoelectric effect a charge separation which is proportional to the pressure or force. The charge must then be transmitted along a very highly insulated cable and connectors to the so-called charge amplifier which converts the charge signal into a voltage signal. The charge amplifier or system monitor is usually firmly mounted on the machine and then delivers a digital or analog signal to the machine control system. This could be the curve history for visualization, a control signal for robot / reject gate, or a direct intervention such as a switching signal or control intervention.

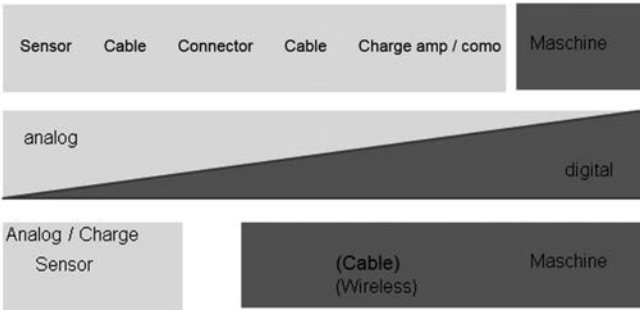

Fig. 3: Digitization of measured value acquisition

During the course of digitizing the entirety of injection-molding production, it is necessary to change over to a standard digital format as far back as possible in the measurement chain. The ideal situation is for the sensor itself to generate a digital signal – in other words, for the charge amplifier to be already integrated in the sensor. This is certainly the long-term goal but in the current implementation comes up against various challenges:

- The progressive miniaturization of sensors. Limits arise simply on account of the size of the connector.
- Temperatures in the mold. Electronic components are normally specified up to approx. 80 °C. However, in some cases considerably higher temperatures prevail in the molds.
- Wiring in general. Supplying the electronics with power and transmitting digital data always requires a multicore cable. In this respect the desire for wireless data transmission within the mold will not be possible in the foreseeable future.

4. Networking process data

The central topic in process data processing is networking and storing the data in a central database. The solution in Kistler's injection-molding segment is the CoMo DataCenter (CDC), which stores the full scope of process and production data on an order-specific basis. The database is structured in a similar way to an MES system but does not go as far in its functionality. The focus is rather on process-relevant data including the full curve histories. This enables the user, by means of a simple filter function, to find specific data records and ana-

lyze them in detail. The evaluation function is thus purposefully limited to the process data and less to the production data.

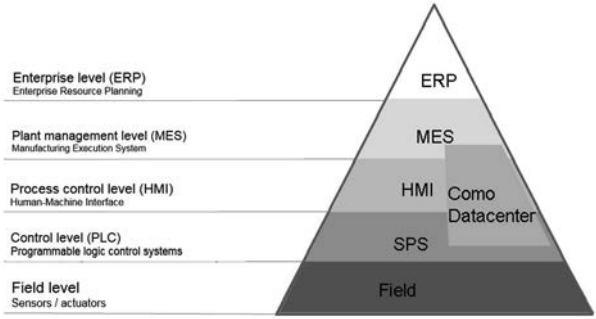

Fig. 4: Communication levels in the production plant

Figure 4 depicts the communication structure between the various control and planning levels in the company. The pyramid is built up on the basic data from sensors and actuators, and aggregates the information up as far as the enterprise control level with the ERP system. The CDC database software is basically to be classified as located on the process control level and communicates with higher levels such as an MES or ERP system.

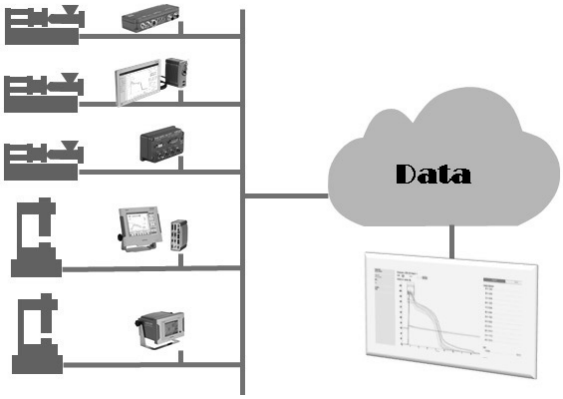

Fig. 5: Networking production resources in injection-molding production

The actual data, that is, measurement curves, good / bad results, and other production data, are fed in by various bus-compatible devices via an Ethernet connection. This makes net-

working possible via a company's internal network or even globally via a secure internet connection. At NPE 2015, for example, five production locations in the USA and Europe were networked together and a virtual, globally interconnected production environment presented as a live demonstration. Since the visualization is also based on web technology, the user is not location- or device-dependent and can access the individual injection-molding processes from anywhere and view in detail the process data.

6. Process analysis

A number of examples are presented below showing how further analyses can be carried out with the process data stored in the central database. This goes beyond evaluating the individual injection-molding cycle and scrap evaluation and enables the evaluation of a process. Currently the user makes an evaluation on the basis of his personal knowledge and experience. However, intelligent algorithms are currently being implemented which are able to identify errors and provide the user with instructions for correcting them.

Figure 6 shows the process data for a smart-card component. In the case of this smart card with a molded-in chip, it is especially important to monitor the maximum pressure range since excessive pressure can damage the chip. The right-hand side of the illustration shows the cavity pressure curves for 2.5 mm pressure sensors (6182A with single-wire technology) close to and away from the gate and also the monitoring windows.
The trend analysis shows the value at which the curve enters the monitoring window. It shows clearly that the process is running with extreme constancy and robustness.

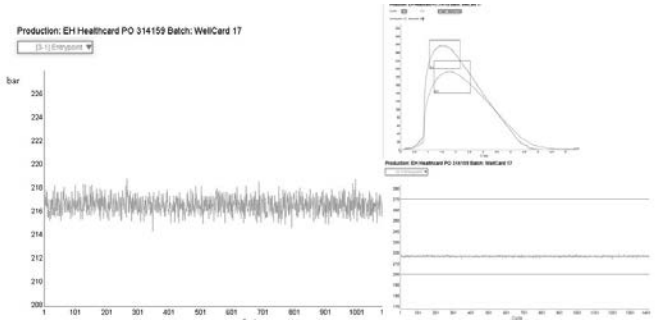

Fig. 6: Process data evaluation in smart-card production

The pressure value being monitored fluctuates only within the range of a few bar and this results in a cpk value greater than 5, which indicates very stable production.

The second example comes from a production case which was recorded as part of the NPE demonstration. It concerns an eight-cavity plug mold. The maximum cavity pressure was monitored as an indicator of an incompletely filled part, a so-called short shot. It can be seen immediately that in this production case, although the monitoring limits were observed with just a few exceptions, various disturbances did occur. The mold is equipped with a hot runner and each cavity contains for monitoring purposes a 1 mm pressure sensor (6183A) positioned close to the gate. For the sake of clarity, only one cavity is shown in this graph. The sinusoidal fluctuation at the start of the process points to a poorly adjusted hot-runner control unit. The control parameters should be optimized, and then this behavior can be prevented. The individual upward or downward extreme maximum pressure values are randomly occurring disturbances which lead to a part being rejected. Falling below the minimum limit indicates a short shot, while exceeding the limit means overpacking.

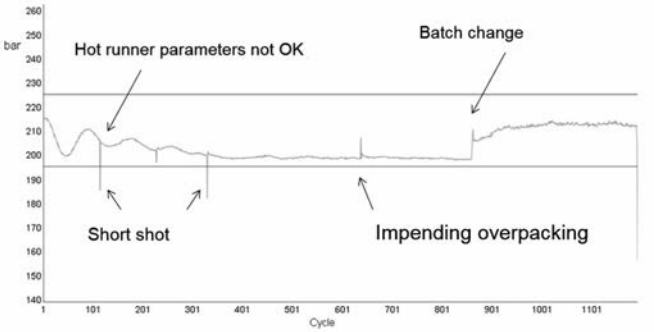

Figure 7: Trend graph of maximum pressure in the case of a connector component

Monitoring by means of a temperature sensor at the same position at the flow path end would not in this case have been able to detect the error and reject the part.

7. Outlook

It has been shown how, with the aid of cavity pressure technology in injection molding, not only the individual cycle can be reliably monitored but also the long-term development of the process. The user is thus already in a position today to monitor his process machine-independently and to avoid waste. Future development will be towards supporting the user in preventing faults and in identifying typical faults. However a fully-automated control of the process is only really feasible in sub-elements. Suggesting to the user that a system so com-

plex as the injection-molding process can be handled with a simple one-dimensional control loop almost as if it were a black box will not be the solution. The individual continues to stand at the central point but it is important to support him in his decisions by simplicity of handling and with intelligent assistance systems.

[1] Illustration analogous to DKKI Report, 2011

[2] Kagermann, Wahlster, Helbig - Promotorengruppe Kommunikation der Forschungsunion Wirtschaft – Wissenschaft: Umsetzungsempfehlungen für das Zukunftsprojekt Industrie 4.0, 2012

Plastic fuel tank systems, energy carriers for future vehicle concepts

Dr.-Ing. **U. A. Karsch**, Kautex Textron, Bonn

Abstract

The majority of today's fuel tank systems around the world are made of plastic, mostly from high-density polyethylene (HDPE) in single- and multi-layer wall construction, manufactured by the blow-molding process. Increasing requirements relating to emissions leakage and, for example, noise production have pushed development onwared from the simple blow-molding process to producing fuel tanks by the half-shell method.

A description is given of how half-shell production works. All necessary tank variants including pressurized tanks for hybrid vehicles can be manufactured with this half-shell technology. The background to pressurized tank development is explained. An all-plastic solution for fuel tanks for hybrid vehicle is possible today thanks to numerous detail developments and adjustments of the tank design.

One major technological change in the manufacturing process has also taken place in tanks for SCR-tank systems in diesel vehicles. Fuel tanks, once blow-molded containers, are nowadays produced with high functional integration by injection molding. Almost all diesel vehicles will be equipped in future with SCR-tank systems for exhaust gas cleaning by nitrogen oxide reduction (NO_x).

Electric mobility will not threaten the plastic tank. Tanks for hybrid vehicles benefit from the further development of the plastic tank. Liquid fuels such as gasoline and diesel fuel continue to have the greatest weight-specific energy density. Plastic tanks are still the preferred energy carriers for these fuels. High-pressure tanks for gaseous fuels as energy sources for alternative drive systems are discussed briefly.

1. State of the art today

In the European and North American markets fuel tank systems are over 90% made of plastic while in the BRIC countries figures of more than 60% are now recorded (Figure 1). Here the first real advance of the plastic fuel tanks into the passenger car sector was with the large-scale production of the VW Passat from 1973 onwards but then with annual percentage growth rates in the double-digit range. This was made possible by the low cost of manufacturing by the blow-molding process, the use of high-density polyethylene (HDPE) and the demands of OEMs for volume-optimized and corrosion-free tanks.

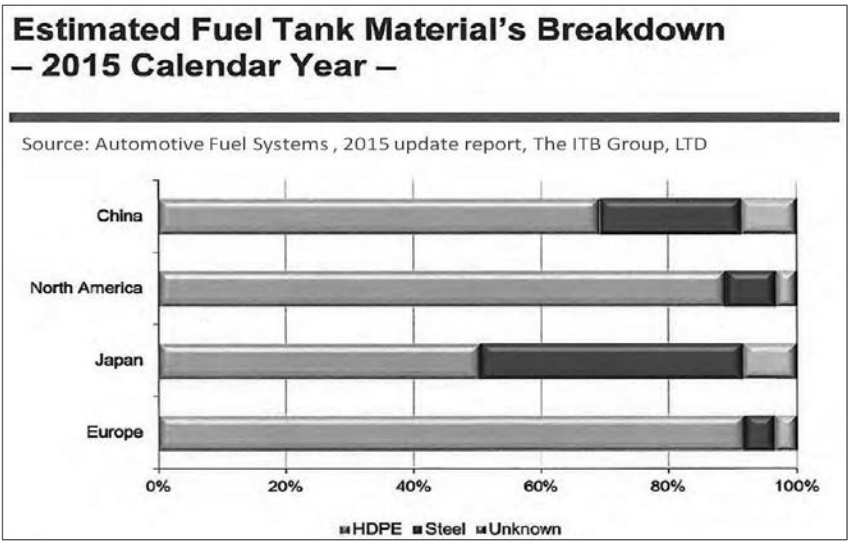

Fig. 1: Plastic fuel tank materials broken down by region

The further development of blow-molding technology and the parallel intensifying demands of the legislature and OEMs have resulted in the present situation where meeting emission requirements has meant an almost complete changeover from the single-layer HDPE mono tank wall structure to a multi-layer co-extruded wall structure (Figure 2). Here a layer of ethylene vinyl alcohol (EVOH) impermeable to fuel molecules is built into the wall structure without this affecting the positive characteristics of the plastic tank ([1], [2]). The two plastics, HDPE and EVOH, cannot be welded together directly so the EVOH layer is incorporated with the help of bonding-agent layers based on a low-density polyethylene (LDPE) modified with maleic anhydride. In this way both the interlayer adhesion and even the mechanical properties of the two heterogeneous plastics are secured. The total thickness of the bonding-agent

layers and the EVOH layer does not exceed 0.5 mm at an average total wall thickness of approx. 4-5 mm. Another layer in the wall system, the so-called regrind layer, consists of reclaimed production waste, the 'flash' which always occurs in the blow-molding process due to the pinched-off edges of the tank. The blow-molding process is thus almost waste-free. An outside layer made of HDPE colored black for cosmetic reasons completes the wall system and gives the tanks their typical black appearance.

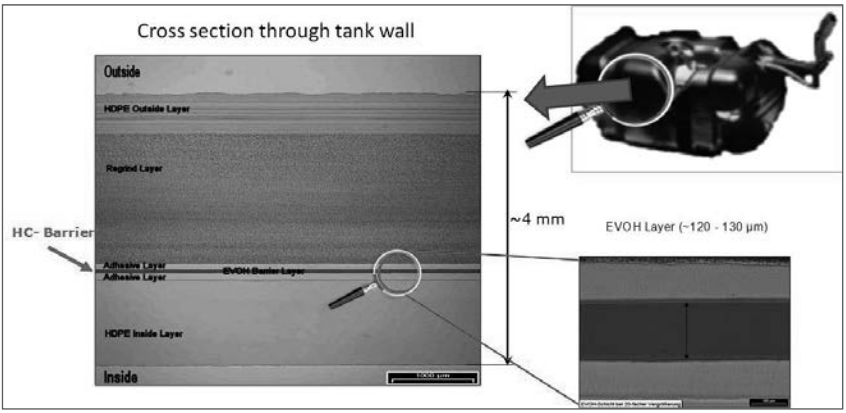

Fig. 2: Cross-section of a six-layer fuel tank wall

The advantages of this plastic fuel tank as it is built today are obvious:
The HDPE plastic allows an almost unlimited design freedom, the tanks are corrosion-free, have a high crash safety due to their toughness and resilience even at low temperatures, are emission-tight due to the co-extruded six-layer structure, are lighter than comparable steel tanks, and have also prevailed for economic reasons since high production quantities are possible with blow molding.

2. Change of production technologies for fuel and SCR systems

(a) Fuel systems

Over time the aforementioned requirements for tank systems have developed further. One demand is a maximum filling volume with the existing installation space in the vehicle; another is optimal refueling and venting behavior under all driving and parking conditions. In addition to this, the increasing level of driving comfort, especially in mid-range and luxury vehicles, makes noise generation in the tank a problem. Passengers should not hear or feel anything from the tank. Sloshing noises at, for example, starting or stopping, are not permissible.

These requirements make it necessary for the valving in the tank to be further optimized – in other words, valves must be placed, for example, only in hard-to-reach corners of a tank. In addition, baffles must also be installed to prevent sloshing sounds in the tank. In other words, numerous components are being added to the tank. One solution is to cut holes in the finished tank body at points where valves or other components, such as baffles, are to be mounted and then weld these components on from outside. For low / zero emissions tanks this method is now no longer practicable. For reasons relating to emissions the welded-on components are complex two-part components (in most cases PA 12 encapsulated in HDPE), firstly because they must be welded onto the HDPE tank, and secondly because they must offer a maximum in emission-tightness. As regards their dimensions, baffles cannot be integrated into a tank via the conventional blow-molding process.

The solution to the above challenges is to integrate the in-tank components into an open tank half-shell. In conventional blow molding, a round tube of melt is extruded from a round-section die, inflated in the mold and then demolded. The result is a closed hollow body (the tank). It is very difficult to include tank installation components in this diameter-limited round tube especially when they are applied over a wide area. It is known that components can be incorporated in open half-shells in the thermoforming process. However, in this method, in which the plastic is in the form of sheets, the sheets have to be heated up twice. The first time is when the plastic is melted during extrusion of the sheets, the second time is when the already extruded pre-dimensioned sheets are once again heated up for the forming operation in the tank half in the thermoforming process. To avoid these two heating steps, the approach is now to produce these sheets in-line for fuel tank production. Here the original round melt tube is divided by a suitable double-acting slot die into two parallel sheet melt flows, each of which case still retains its six-layer wall structure. This principle is shown in Figure 3.
These continuously extruded sheets are then pulled by vacuum into the corresponding tank mold halves of the tank mold which is positioned beneath the slot die. To allow the vacuum to work properly in the mold the sheets are sealed by means of a multipart center tool installed between the sheets.

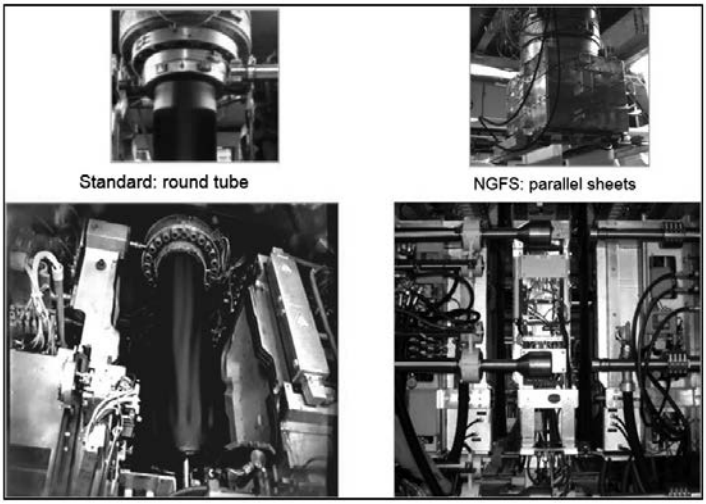

Fig. 3: Conventional extrusion compared with the NGFS® process

The tank installation components, separated by tank upper half and lower half, are positioned in this center tool and, once the tank halves have formed, will be placed in them and attached. The complete unit of mold and center frame is than moved away beneath the wide-slit die so that continuous extrusion of the sheets is not hindered.

The inserted components are secured to the tank wall. The center tool leaves the actual tank mold, which now finally closes and the pinch-off weld forms on the tank. Following a further cooling-down phase in the mold and flushing of the inside of the tank with cold air, the tank is demolded and transported onwards for further processing. With this method the cycle time is equal to the cycle time for producing the tank by the conventional method.

At Kautex Textron this process for in-line molded tank half-shells is referred to as NGFS® (next generation fuel system). Figure 4 illustrates the process in schematic form.

This method for producing in-line molded tank half-shells has been used in high-volume production for about seven years now. When this method was first introduced, there were only a few tank projects involving series production with NGFS®. Table 1 shows the development of this technology at Kautex Textron. In the meantime this process is being rolled out globally by almost all tank manufacturers. From manufacturer to manufacturer

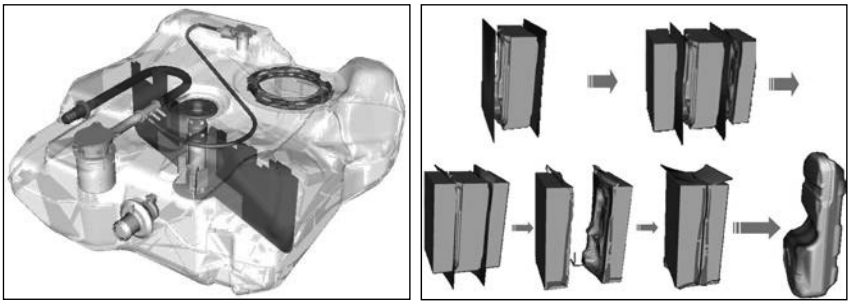

Fig. 4: Schematic of the process sequence (left); see-through diagram of a tank produced in this way, with baffle and other in-tank components (right).

there are very minor differences in the actual procedure; the method even has different names but in each case the tank half-shell principle is used. On the one hand, this speaks for the advantages of the process, which are obvious since tank components can now be installed as desired into the tank before the two half-shells are joined together. On the other hand, the OEM can now continue to use plastic construction for complex tank shapes with equally complex inner workings. The method is particularly suitable for incorporating baffles in the tank to reduce noise levels.

Tabelle 1	2009	2015
Customers	2	7
Projects	2	18
Production locations	2	13
Machines	3	21

In addition to the other standard components such as valves, surge compartments, ejector pumps, baffles and so on (Figure 5), this process is ideally suited for installing in the tank even the stiffening elements which the hybrid tank requires.

Further advantages of this process include the fact that the wall thickness of the extruded sheets can be regulated separately. In this way, weight reductions of up to 8% in the tank can be achieved in comparison with conventional blow molding.

The application of this half-shells procedure for tanks for hybrid vehicles is described in the next section.

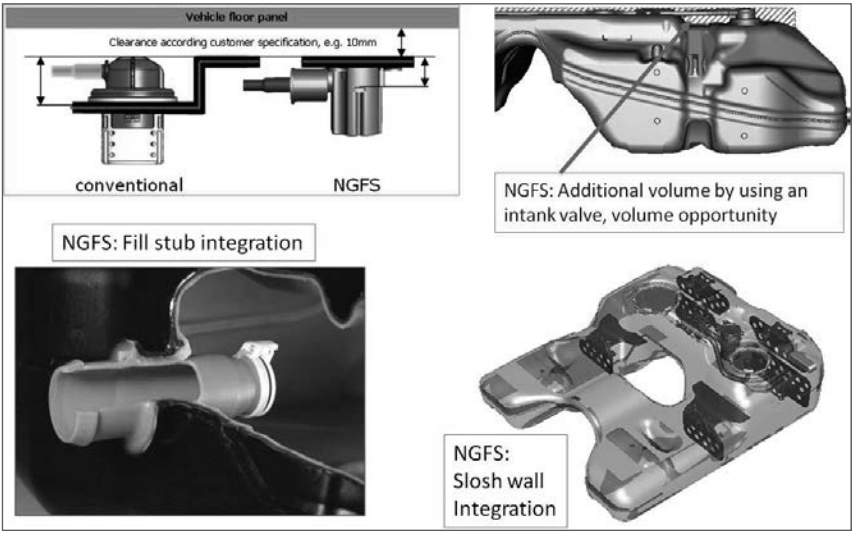

Fig. 5: Comparison of volume gain with NGFS ® and the integration of components

(b) SCR systems

One technological shift with regard to the manufacturing of tanks for SCR systems (Selective Catalytic Reduction) has in recent years taken place in a similar way to the production method for fuel tanks. SCR tank systems are not primarily energy carriers but only indirectly so, since fuel consumption reductions between 4-8% can be achieved by injecting aqueous urea solution into the exhaust line of diesel vehicles. The specific aspects of the SCR technology need not be discussed further here but rather the change in the process used for manufacturing plastic fuel tanks [3].

HDPE is also the preferred material for the SCR tank in diesel vehicles, both for economic and mechanical reasons. The original production technology is also blow molding. However, the requirements applicable to an SCR tank differ from those of the fuel tank. The aqueous urea solution, which consists of 32.5% urea and 67.5% water is best known under the trade name AdBlue®. However, it is also referred to, particularly in the Anglo-American world, as DEF (Diesel Exhaust Fluid) or AUS 32 (Aqueous Urea Solution). This liquid, in contrast to commercial fuels, has some special features which need particular consideration when designing a tank system: freezing point at -11 °C, crystallization at drying, ageing or hydrolytic degradation at elevated temperatures (>40 °C), odoriferous, and emission of gaseous ammonia, chemically aggressive (corrosive) behavior on account of the ammonia content.

In particular, its freezing at -11 °C provided the engineers with new challenges. It was not that there was a fear of the plastic tank being deformed by ice but rather that ice pressure is able to permanently destroy important in-tank components. The design should therefore take this into account and heat the system so that even after a cold start and the correspondingly 'cold' outside conditions liquid AdBlue® is already available after 20 minutes, for example. It can then be injected into the exhaust system whereby a temperature of at least 200 °C must be reached in the exhaust.

Electrical heating systems are used in car fuel tanks. Here, especially in these cold starts, only a limited amount of energy, no more than 120 W, is available. In trucks, heating is implemented by a connection to the coolant circuit.

Furthermore, a high degree of constructional and design freedom is desirable so that in the vehicle package any still unoccupied space can be used optimally for accommodating about 5-20 liters of AdBlue®.

This has meant that the vast majority of first and second generation SCR tanks are manufactured by blow molding. The relatively large radii and wall thicknesses inherent in the blow-molding process rule out an optimal exploitation of the space available in the package. The problem of noise, as already discussed in the fuel tank, is also present in the SCR tanks of mid-range and luxury cars. Even SCR tanks must also be equipped with baffles and this in turn comes up against the limits of the blow-molding technique. Figure 6 shows the stages of evolution in the development of SCR tanks.

The problems described above were solved in the third generation by injection-molding technology. Injection molding can be used with SCR tanks since different mechanical and emission-related requirements apply to these tanks than to the fuel tank. The SCR tank can suffer leaks in the event of a crash but the escaping liquid is not hazardous. In the fuel tank, on the other hand, absolute tightness is required. For reasons relating to emissions, co-extrusion cannot be used either – this would mean considerable challenges in injection molding. In addition, the high-density HDPE grades used for the blow-molding and half-shell process are only suitable with qualifications for injection molding – lack of flowability and a marked tendency to warp being the reasons cited in this regard. For the SCR injection-molded tank special high-density HDPE injection-molding grades are therefore used which have sufficient flowability but nevertheless adequately deliver the mechanical-physical properties of such a tank.

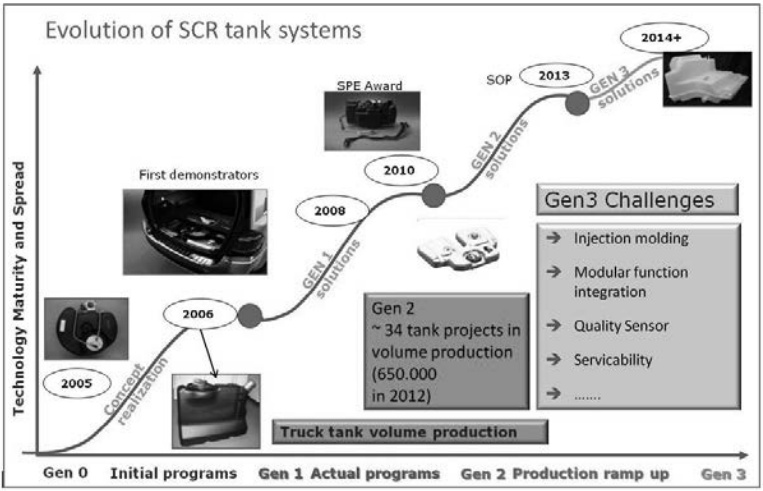

Fig. 6: Evolutionary stages in the development of SCR tank systems

Further advantages of the injection-molding process are uniform wall thicknesses (weight reduction), small radii (volume optimization), functional integration (neck, nipples, clips, baffles, retaining elements, and so on). One drawback is that due to the more complex mold design there must be a relatively early 'design freeze' and changes can only be made with difficulty after this. One mold is needed in each case for the tank's top shell and lower shell (Figure 7). Producing these SCR tank half-shells calls for injection-molding machines with locking forces in the range of 2000 to 2500 tonnes. The technological changeover from blow molding to injection molding has been accomplished for SCR tank systems. Virtually all diesel cars coming into the market in future will have an injection-molded SCR tank. This does not apply to trucks: due to their size (up to 100 liters) these tanks will continued to be manufactured by blow molding or rotational sintering.

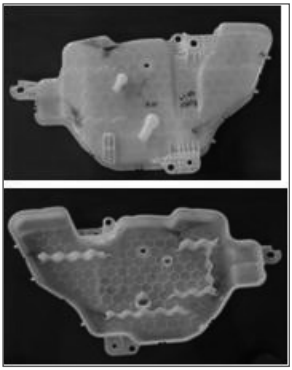

Fig. 7: Injection-molded half-shells for an SCR tank

3. Solutions for hybrid vehicles

The vehicle emission limits for hydrocarbons (HC), carbon dioxide (CO_2) and nitrogen oxides (NO_x) which are constantly becoming stricter throughout the world are the drivers for new technologies and for the development and introduction of hybrid vehicles. In the lead here is the Californian environmental authority CARB (California Air Resources Board) which with its strict environmental laws (ZEV program ZEV = Zero Emission Vehicle, ORVR = On-Road Vapor Recovery) is forcing automobile manufacturers (OEMs) to sell vehicles which comply with this legislation. This legislation concerns emissions from the fuel systems and exhaust and also the required fuel efficiency (CAFE = Corporate Average Fuel Economy). In 2017 a new stage of ZEV regulation comes into force which will give hybrid vehicles a significantly growing share in the total number of vehicles sold (Figure 8). With hybrid vehicles, OEMs are in a position to comply with the strict HC and CO_2 requirements applicable to their fleets. Hybrid vehicles (HEV = Hybrid Electric Vehicle) have an additional electric drive system. In the simple case it is used to support the conventional drive technology. In so-called 'plug-in' hybrid vehicles (PHEV = Plug-in Hybrid Electric Vehicle) it also enables driving on electrical power alone and recharging of the battery afterwards at a power outlet. In this case the conventional drive with a combustion engine may not even be used at all. Currently one special case is still the electric car with a range extender (Rex-EV = Range Extend Electric Vehicle). All of the hybrid vehicle variants we have mentioned still have an internal combustion engine, which has to be supplied with fuel and therefore requires a fuel tank system. Additional requirements concerning high-pressure stability apply to these tank systems and go beyond the tanks so far on the market and described above. The technologies required to meet these pressure stability requirements will be described in more detail below.

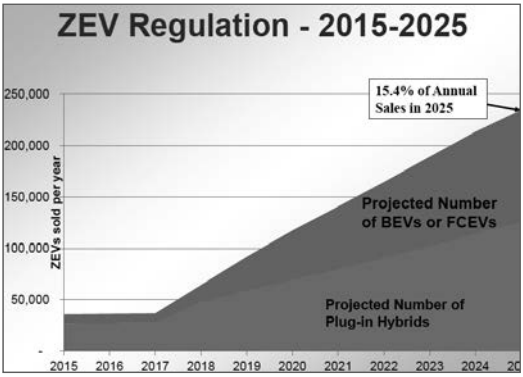

Fig. 8: Share of hybrid / electric vehicles from 2017 in California (source: CARB)

Why do special pressure-stability requirements apply to hybrid vehicles? This requirement applies only to fuel tanks in hybrid vehicles with a gasoline engine; it does not apply to tanks

for hybrid vehicles with diesel engines because of the differences in fuel vapor pressures between gasoline and diesel.
When the vehicle is traveling on electric power the tank is sealed off. Depending on the ambient conditions (temperature), fuel in the tank can then with elevated outgassing deploy its maximum vapor pressure. This leads to an increased internal pressure which, due to the 'open' systems, does not occur in conventional tank systems since the fuel vapors are routed directly into the activated charcoal canister (= ACC) provided for this purpose.
When the hybrid vehicle is in electric mode the carbon canister cannot be flushed since the combustion engine is not running. The result is internal tank pressures in the -15 to +35 kPa range and these are monitored via a so-called FTIV (fuel tank isolation valve).
The FTIV has the task of regulating the pressure in the tank. Basically, the FTIV is controlled via the motor electronics and in the de-energized state is closed. The valve is opened before refueling so that any possible overpressure can be relieved. Approximately 20 seconds must elapse before the driver can open the fuel flap.
In addition, there is the mechanical function in the FTIV which opens the FTV if there is an overpressure in the tank above approx. 30 kPa or an underpressure below approx. -10 kPa. This prevents the tank deforming impermissibly at maximum pressures.
When the FTIV is open, fuel vapors are directed into the carbon canister. These maximum pressures are not normally reached during typical driving conditions or in the statutory emissions tests. It transpires that in practice there is underpressure in the tank when the vehicle is in electric mode. This negative pressure arises from the engine, when operating, taking fuel from the tank.

In the case of the pressure requirements mentioned, plastic tanks made of HDPE in the standard design are very much inclined to deform more strongly, especially at higher temperatures (>40 °C). Here the tank may come into contact with the vehicle body locally and other side effects may also occur, none of which are wanted and are not tolerated by the OEM either. A space of about 10 mm is normally kept free around the tank and in the event of tank deformation can be used in part. Noise reduction is another essential requirement applicable to hybrid tanks. Introduction of the start-stop function in most vehicles and even when they are in electric mode means that no sloshing noises from the tank should be heard in the passenger compartment. Nearly all hybrid tanks are for this reason equipped with baffles (or 'slosh walls').
The first fuel tanks for hybrid vehicles were made of steel with wall thicknesses of approx. 2.5 mm and had, for example, a weight of 31 kg for a 55-liter tank (Toyota RX400h). Since

then some OEMs use suitable 'hybrid pressure tanks' which are mostly made of steel and thus have a weight disadvantage. However, the desire for a lighter plastic hybrid pressure tank clearly exists.

Kautex Textron is the first supplier to have put a plastic hybrid pressure tank on the market and since summer 2012 it has been installed in the US model of the VW Jetta Hybrid (Figure 9).

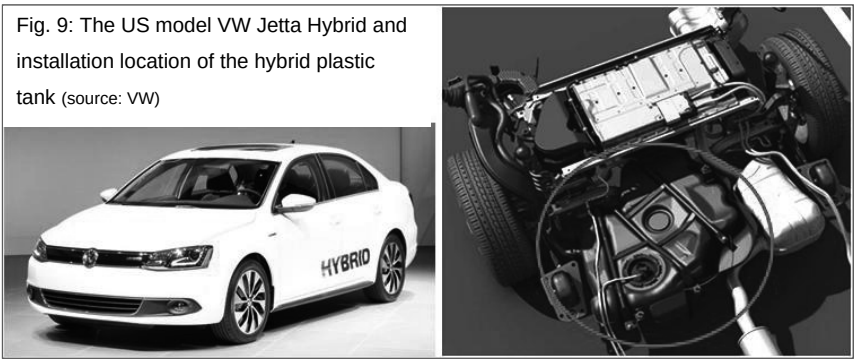

Fig. 9: The US model VW Jetta Hybrid and installation location of the hybrid plastic tank (source: VW)

This tank does however also have an external steel frame to absorb pressure forces and must therefore be considered a 'plastic-steel hybrid tank'. The underpressure requirements are satisfied by means of internal support elements, so-called 'stand-offs'. This solution represents an interim solution on the way to the all-plastic solution for a hybrid tank, as they are already on the market today or will arrive in the next hybrid vehicles.

So how will the pressure requirements be satisfied without a steel corset?

The primary aim of pressure-tank development is to avoid the permissible tank-wall deformations or to reduce them to a minimum. Here the 10 mm space between the tank and the body must not be exceeded if at all possible.

There are various possible approaches to giving the plastic tank the rigidity under pressure desired. Figure 10 provides an overview of the design possibilities discussed below. Over the course of hybrid tank development it has emerged that a connection between the upper and lower sides of the tank is absolutely essential. 'Kissing points' represent such a connection, but have the above-mentioned disadvantages. For this reason, the choice is in-tank connecting elements which were then developed accordingly.

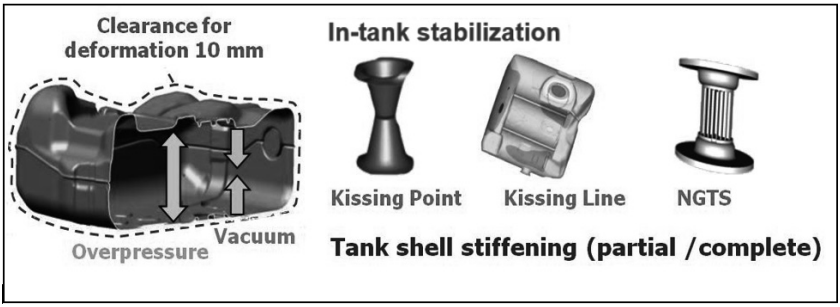

Fig. 10: The fuel tank limits situation and stabilization options

At Kautex Textron these elements are called NGTS (= Next-Generation Tank Stiffeners). Transfer of force between the tank top and tank bottom requires precise calculation of dimensions and positioning, such as of cross-sections and welding surfaces, if forces from the maximum pressure loading are to be transferable. The stiffeners can be attached to the tank wall either by mechanical interlocking or by welding (if the materials are of the same type). In addition, components can be attached to these stiffening elements in the tank such as, for example, pipes, valves, baffles, suction jet pumps.

In-tank connectors are thus the stiffening elements of choice. Depending on the tank design, several of these elements can be used. The optimum positions for the stiffening elements were determined by iterative CAD/CAE simulations. A check was made in a final pressure-loading simulation (example in Figure 11) to see whether the maximum deformations of the tank fell within the permitted installation space limits.

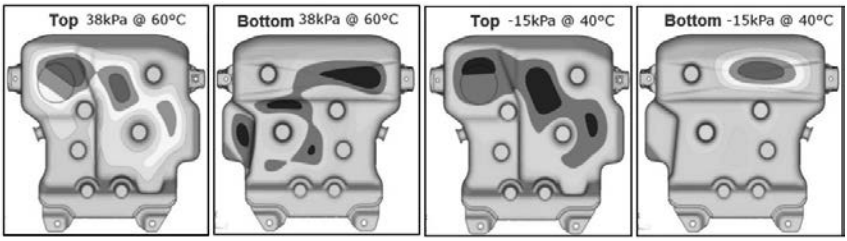

Fig. 11: Example of deformation analysis by CAE simulation for maximum pressures at maximum temperatures for tank tops and bottoms

The design of the support elements only works in the context of the overall design and connection by radii, in a similar way to an arch support such as is found, for example, in cathe-

drals. Figure 12 shows a typical view into the interior of a hybrid pressure tank with supporting elements and baffles.

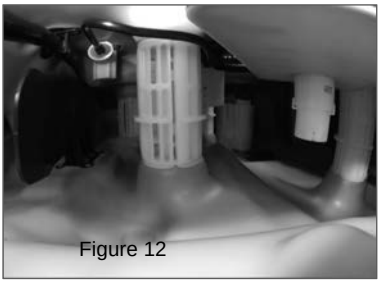

Figure 12

In 2015 Kautex Textron was the first to put on the market two all-plastic pressure tank systems, for the Volvo XC 90 PHEV and the VW Passat GTE PHEV (Figure 13).

Fig. 13: All-plastic tanks for the hybrid vehicles the Volvo XC 90 PHEV (left) and the VW Passat GTE PHEV (right)

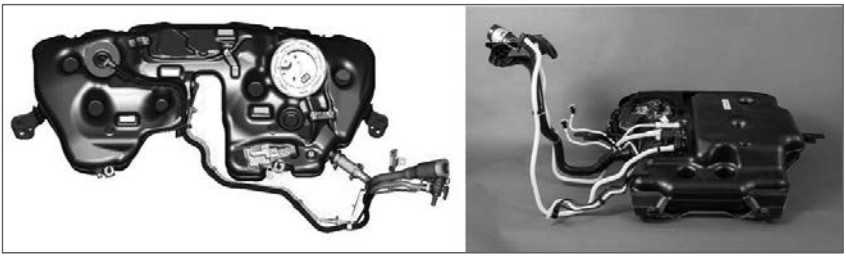

4. Displacement by e-mobility?

In this contribution, the term e-mobility covers purely electric vehicles, either running on batteries or with a fuel cell drive using hydrogen. Given the predicted global production figures of up to 120 million vehicles per year by 2030 (Figure 14), the numbers of hybrid and electric vehicles will also significantly increase but without displacing the conventional gasoline engine drive nor thus the plastic fuel tank. The forecast indicates that from 2020 or so, the share of conventional drives will shift significantly in favor of hybrid vehicles. The number of pressurized plastic tanks will thus also increase markedly. Since manufacturing technology for these tanks has been commercially available since 2015 and numerous tank developments for hybrid vehicles are currently in progress, the proportion of plastic tanks globally will also continue to rise and thus the energy carriers of the future will remain inside the vehicle. In addition to conventional and pressure tanks, Figure 14 also shows high-pressure tanks. These tanks are the future energy stores of natural gas (CNG) up to an operating pressure of 250 bar and, in the case of hydrogen (H_2), 700 bar. For reasons of weight, there will be plastic solutions in future for these tanks too. In the high-pressure nomenclature these tanks are called Type IV tanks. They weigh only approx. 25% of the weight of steel tanks of the same capacity (Type I tanks). The tanks have an inner plastic liner made of thermoplastic material

(HDPE, PA, and also multilayered) which is then wrapped with carbon fiber so as to absorb pressures – in a sense then they are also made of plastic.

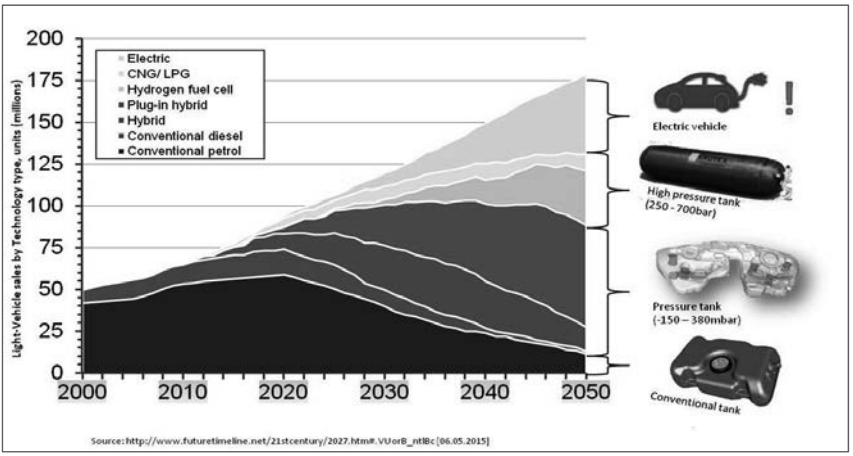

Fig. 14: Forecast of the energy carrier systems for different drive technologies

The carbon fibers are in most cases soaked with liquid resin systems and then wrapped on. Next, the matrix resin is cured in the oven. Alternatively, so-called carbon-fiber thermoplastic tapes are also in development. By means of a suitable heat application method, the tapes are, as they are being wrapped, welded directly to the liner or the preceding layer of tape. A tank wrapped in this way is thus finished when the wrapping process is finished. Which winding technologies will actually prevail in the industrial-scale market will be decided over the next few years. Toyota with its Mirai has gone into the lead here, in a similar way to its Prius hybrid vehicle back around 2000. It has taken almost 10 - 15 years for this technology to become established worldwide. A similar situation is expected with CNG and H_2 drives.

Table 2 *References **Manufacturer's specs	Calorific value kWh/kg	kg/liter	Mass in 50-liter fuel tank [kg]	kWh	Range [km]
Gasoline*	11,6	0,74	37	430	620 (6 l/100km)
Diesel*	11,8	0,83	41,5	490	692 (6 l/100km)
Natural gas CNG* (200bar)	13,9	0,17	8,5	118	
Audi A 4 gtron ** (200bar)			19 spread over 4 tanks	236	500 (3,8kg/100km)
Hydrogen H_2 * (700bar)	33,3	0,04	2	66	
Toyota Mirai** (700bar)			5 spread over 2 tanks	166,5	500
BMW 13 battery**			230 (Battery)	21,6	160
Tesla S battery** (85kWh)			750 (Battery)	85	500

Many factors serve as drivers for the rapid establishment of new drive technologies. For example, electric vehicles are certainly not achieving the figures forecast and postulated by governments. High costs, lack of acceptance, range anxiety are just some of the obstacles in the way of a rapid spread of electric vehicles. Even the high weight of the traction batteries is a factor. As a comparison of current weights and ranges, some figures are given in Table 2: for gasoline and diesel in the example of a 50 liter tank, for natural gas (CNG) and hydrogen current models. At time of going to press the exact weight of the high-pressure tank was not available.

Just as this contribution was in preparation the VW diesel exhaust gas affair occurred. This has and will continue to have a significant impact on the sales figures of diesel vehicles in the USA. Furthermore, due to sinking oil prices the current price of diesel is now less than €1 per liter. A low oil price and thus low fuel prices have always acted as a barrier to the spread and establishment of new technologies on the drive systems market.

It is therefore remains an uncertain and difficult task to make a correct prognosis for new drive technologies such as electric vehicles. The plastic tank as a fuel carrier will therefore stay with us.

References:

[1]. Karsch, U.A.: The fuel tank: a complex system made of plastic, in Plastics in Automotive Engineering conference, Mannheim, 13th/14th April 2002, VDI Technical Division Plastics Engineering, VDI-Verlag Düsseldorf 2002, ISBN 3-18-234245-2

[2]. Karsch, U.A.: Aufbau von aktuellen Tanksystemen für Fahrzeuge des europäischen und amerikanischen Marktes, in conference: Emissionen aus Kraftstoffsystemen von PKW's, 17th/18th April 2002, Haus der Technik, Essen, published in Expert Verlag, Fachbuch Haus der Technik Vol. 15, ISBN 3-8169-2102-7

[3]. Karsch, U.A.: Der blasgeformte SCR-Behälter, Ein weiteres Tanksystem im Fahrzeug, in: Blasformen 2009, VDI-K conference, Baden-Baden, 12th/13th May 2009, ISBN 978-3-18-234299-1

[4]. Karsch, U.A., Gebert, Klaus: Tanks für Hybridfahrzeuge, Eine Herausforderung für Kunststoffe ?, in: Blasformen 2013, VDI Wissensforum conference, Baden-Baden, 5th/6th May 2013, ISBN 978-3-18-234329-5

Study of lightweight applications in truck development

Metal replacement of a headlamp frame by a thermoplastic

A. van den Einden, **P. van der Velden**,
DAF Trucks N.V., Eindhoven, Netherlands

Abstract

New material, process and equipment developments in the field of thermoplastics create opportunities to implement lightweight applications in the truck by replacing metal parts. For this reason a study was started at DAF Trucks with the object of establishing the feasibility of replacing a (complex) structural metal part by a part made of a reinforced plastic. This study was carried out in cooperation with partners SABIC, EDAG and VDL Parree. After a first quick scan of material technologies and applications the aluminum headlamp frame was chosen for this study due to its complexity and high requirements. In this paper a brief overview is given of the analyses and activities required for a successful plastic design to emerge.

Introduction to lightweight applications in trucks

Even in the truck sector, metal replacement in order to reduce weight, integrate functions, create more design freedom and reduce costs is nothing new. For many years now plastics have been used for all kinds of truck applications. Exterior parts made of metal were replaced by thermosets and thermoplastics even more than 30 years ago and more recently plastic applications in the engine such as the valve cover and oil sump have been introduced. DAF trucks have a wide range of plastic exterior parts using thermosets and thermoplastics and in the engine compartment parts which mostly use thermoplastics.

Fig. 1: Exterior parts made of thermoplastics and oil sump

Fig. 2: Thermoplastic valve cover

Due to material, process, tool and machine developments in the field of thermoplastics new opportunities for lightweight constructions in trucks arise. In particular, the development of materials with a high stiffness and a better cold impact resistance create more possibilities for metal replacement. Combinations of materials in hybrid structures such as continuous fiber-reinforced thermoplastic sheets with plastic are also of interest.

For this reason a study was started in cooperation with partners SABIC, EDAG and VDL Parree with the object of establishing the feasibility of replacing a (complex) structural metal part by a thermoplastic part. After a first quick scan of material technologies such as hybrid structures with continuous-fiber-reinforced thermoplastic sheets and long-glass-fiber-filled thermoplastics the choice was made to carry out the study with metal being replaced by long-glass-fibre-filled thermoplastic. The aluminum headlamp frame was chosen as subject for this study due to the high requirements and the fact that it represents a lot of brackets and frames in the current truck design. In addition, the fact that tool life in the aluminum casting process is limited was a driver for an injection-molded plastic part.

Preliminary study on the thermoplastic headlamp frame

For this preliminary study carried out by SABIC the following requirements were taken into account:

- Maximum displacements
- Limited acceleration levels
- Minimum eigenfrequency 35 Hz
- Fatigue (DAF warranty 1,600,000 km)
- Dimensional stability

- Retrocompatible with aluminum part
- Integration into existing package
- Easy integration into current plant process

Injection molding of a thermoplastic part allows the use of more complex geometry, more extensive ribbing patterns and thinner cross-sections.
For a successful conversion from a metal to thermoplastic part it is therefore beneficial to start with identifying the design space available instead of limiting oneself to trying to translate the metal design directly into thermoplastic.
On the basis of requirements such as tensile modulus, strain at stress, chemical resistance to automotive fluids and dimensional stability but also on density and price, the SABIC STAMAX® resin with glass fiber was selected at the start of the preliminary study. This is a polypropylene matrix using long glass fibers as a filler. The use of long glass fibers improves the mechanical performance of the application even at raised temperatures. The presence of long glass fibers in the matrix also results in anisotropic behavior. The glass-fiber orientation is influenced by the injection-molding process. At a later stage in the design process further optimization of the design is possible by linking the fiber orientation from the mold-filling simulations with the mechanical optimization of the part. But since no details of mold filling were available at the time of the preliminary study a quasi-isotropic value is used.

Table 1: Material choice

	PP LGF	PA GF	PA LGF
Tensile modulus @ 80°C	O	O	++
Strain @ stress	O	+	O
Density	+	-	-
Chemical resistance	+	+	+
Dimension stability	+	-	O
Price	+	-	--

Using a topology optimization routine is a good starting point for understanding which structural features are required in the design.
The crucial next step is to convert these solid cross-sections, which are more suitable for cast metal-based solutions, into thin-wall ribbed sections which also meet the requirements but can be successfully injection-molded in long-glass-fiber thermoplastics.
By following these steps, a thermoplastic design concept using SABIC STAMAX® resin was designed for a headlamp bracket. This bracket can meet the requirements while giving an

estimated weight reduction of 30 – 40% as well as the possibility of reducing the number of parts.

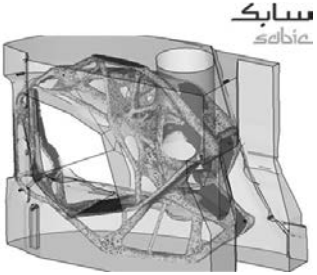

Fig. 3: Topology optimization

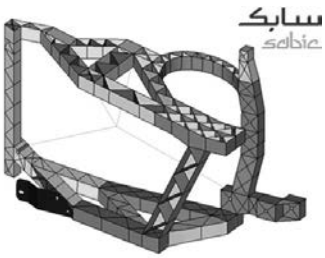

Fig. 4: Result of preliminary study

The result of the preliminary study was the reason for DAF Trucks deciding to continue with the engineering of the lightweight headlamp frame.

Engineering a thermoplastic headlamp frame

For the CAD design the existing, limited package space had to be respected as well as the existing order of assembly and disassembly. Due to the lower material properties of a thermoplastic in comparison with aluminum, stiffness had to be added in the design.

In the FEM and CAE phase of the study the differences from aluminum were taken into account and calculations were carried out. A lot of design iterations were necessary to realize a model which had enough stiffness to meet the requirements concerning eigenfrequency, displacements and acceleration.

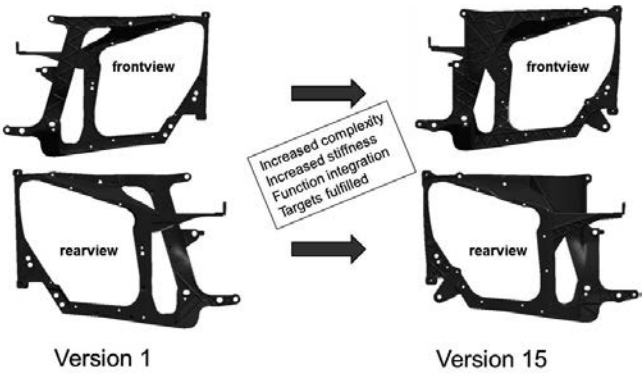

Fig. 5: Design iterations

Moldflow analysis of optimized CAD design

Once the design of the headlamp frame was available, work could start on designing the mold and the gating layout. The number of gates to fill the part, the locations of the gates and the sequence of opening the gates are the main design variables for successfully producing the part. Apart from the necessity of being able to fill the whole mold within the operation window of both material and machine, the gate design also has a significant effect on weld lines and warpage.

Weld lines and warpage also occur in non-filled injection-molded parts but the presence of fibers dominates the effect. At weld lines the fibers mainly lie perpendicular to the weld line with hardly any fibers crossing the weld line. The strength of the part over the weld lines can almost depend only on the strength of the matrix. The aim is therefore to avoid weld lines in highly loaded areas.

The warpage is mainly caused by anisotropic shrinkage of the material during solidification and cooling down. The high stiffness of the fiber means low shrinkage in the fiber direction and higher shrinkage perpendicular to the fiber.

Using the right filling strategy resulted in the right fiber orientation, a minimum of warpage and avoided weld lines at critical locations.

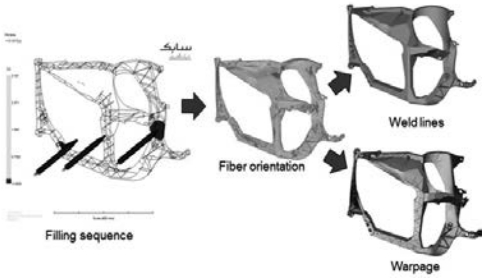

Fig. 6: Mold-filling analysis

After this extensive engineering phase it was decided to build a prototype tool to permit validation of the lightweight headlamp design.

Validation of the lightweight design

For validating the design a prototype tool was prepared and trials carried out at VDL Parree. During the trials the mold filling was carrried out in accordance with the former analysis so as to have the weld lines in non-critical areas. After molding and aging the parts were measured to check dimensional stability. Measurements showed that the warpage is in practice less than previously given by analysis but that the trend is the same. After the measurements a shaker test (road simulation), cobblestone drive and summer drive were carried out. The parts successfully passed all these tests and the calculated displacements due to eigenfrequency were comparable with the measured displacements in the shaker test.

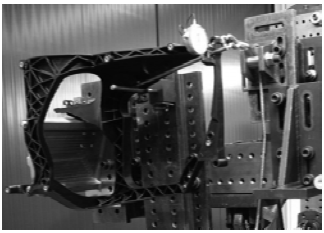

Fig. 7: Shaker test (road simulation)

Results of the study

- The calculated displacements due to eigenfrequency are comparable with the measured displacements in the shaker test and meet the requirements
- The warpage is less than analysed by Moldflow but the trend is the same
- The number of parts is reduced from 3 (+ 4 bolts) to just 1
- The parts are easy to assemble in the existing package
- The weight reduction is approximately 30%
- The cost reduction is approximately 50%

Conclusion

This study proved that it is feasible to replace a complex structural metal part such as the headlamp frame by a lightweight thermoplastic part.

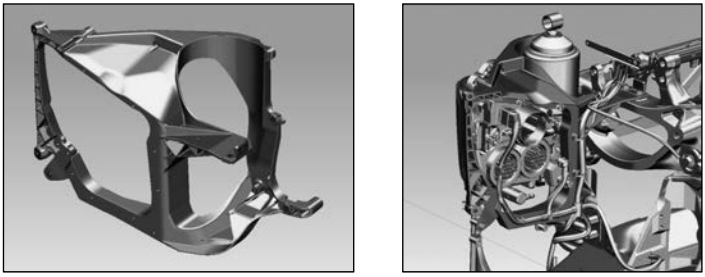

Fig. 8: New lightweight design made of a long-glass-fiber-filled PP

Greenhouse gas footprint of trucks

H. Gräser, MAN Truck & Bus AG, Munich

Abstract

Climate change is one of the biggest challenges for politics, business and society. A significant share of global CO_2 emissions is produced in the transportation sector. A significant contribution to CO_2 reduction is therefore expected in this sector.

Greenhouse gas emissions must be determined over the entire life of a commercial vehicle in order to identify the main control levers. The results show that the largest share of greenhouse gas emissions comes from the provision and use of fuels. Reducing fuel consumption is thus growing in importance as a decisive competitive factor.

Even the manufacture and the end-of-life phase of commercial vehicles generate greenhouse gas emissions. Manufacture includes, among other things, raw material extraction or production, the production of materials, manufacturing processes and energy inputs for the parts and components used. Lightweight design and the selection of materials can accordingly influence the greenhouse gas footprint of a vehicle. With LCA comparisons of different component variants certain requirements must be observed.

Commercial vehicles in CFRP: from prototype to series

Dr.-Ing. **R. Kaiser**, TTT The Team Composite AG

1. Introduction

Since 2003 TTT has been developing innovative commercial vehicles in ultra-lightweight construction and has several prototypes already successfully on the road, a tipping trailer (2004), a mega-curtainsider (2006), three refrigerated semi-trailers (2010/2011), and a 3.5t refrigerated truck (2014), which was designed and built as part of a joint project with Carbon Truck & Trailer GmbH, Volkswagen Commercial Vehicles and COOP CH.

2. Objective: series product

As a prioritized project, the 3.5t delivery truck was further developed first, and primarily the chassis. This can be used not only in in the commercial vehicle segment but also in the motorhome segment. To this end TTT has developed a new chassis concept, the duocoque – in other words, the chassis consists of two identical parts (slim monocoques). The advantage lies not only in an extreme lightweight construction and a reduction in material consumption, but also especially in the reduction of manufacturing costs achieved by using simple structures (preforming) and smaller geometries, as well as lower material consumption and waste. Once this project is finished, the design will be adapted to the 'heavy' commercial vehicles (semi-trailers).

Fig.: Chassis development: from the monocoque (13.6m semi-trailer) to the duocoque (3.5t vehicle)

Lightweight design through multi-material systems

Structural cabin parts made of continuous-fiber-reinforced thermoplastic material with a polyurethane outer skin in Class A quality

A. Spiegel, M.Eng., EDAG Engineering GmbH, Fulda;
Dipl.-Ing. (BA) **S. Schmidhuber**, KrausMaffei Technologies GmbH, Munich;
Dr. **U. Fehrenbacher**, Rühl Puromer GmbH, Friedrichsdorf

Abstract

The aim of the MultiKab research project funded by BMBF was to develop new weight and cost-optimized multi-material systems for commercial vehicle cabins (trucks and agricultural machinery). The focus of the investigations was on a structurally robust, continuous fiber-reinforced thermoplastic carrying structure (organic sheet) which is positively bonded with a fiber-reinforced, duroplastic polyurethane outer skin in Class A quality.

Research was successfully carried out in the project consortium on the materials, manufacturing and joining technologies, and on adapted simulation methods.

To minimize any fiber markings on the visible side of the component, polyurethane systems were developed to create a suitable surface quality for outer skin components. To this end, adapted processing technologies were prepared for PUR-LFI (Long Fiber Injection), IMP (In-Mold Painting) and CCM (Clear-Coat Molding).

In addition, adapted material cards and CAE modeling technologies were developed, and the joins fully characterized with regard to surface texture and interfacial energy.

Finally, a function demonstrator was used to validate the work.

Contact

EDAG Engineering GmbH
Alexander Spiegel, M.Eng.
CC Lightweight Design, Materials & Technologies
Reesbergstr. 1, 36039 Fulda (Germany)
Tel: +49 661 6000-10235
Email: alexander.spiegel@edag.de

CFRP air spring carrier for buses
Feasibility study

Dipl.-Ing. (FH) **S. Rübsamen**, Dipl.-Ing. (FH), Dipl.-Wirt.-Ing. (FH) **N. Elbs**, Dipl.-Ing. (FH) **H. Häberle**, MAN Truck & Bus AG, Munich

Abstract

The product portfolio of MAN Truck & Bus AG covers inter alia trucks for long-distance transport, construction and distribution as well as city and intercity buses and tour buses. Trucks are as a rule used for the transport of goods. In this context the maximum payload of a vehicle is one of the principal factors in the customer's purchasing decision. Realization of this specific customer requirement – taking into account the statutory permissible gross vehicle weight – indicates the need to reduce the vehicle's dead weight. Weight reduction can, for example, be achieved by using lightweight materials. This paper deals with the production of an air spring carrier from a carbon fiber composite (CFC).

The air spring carrier links the rear axle of a tour bus to the body (passenger cell). The feasibility study shows, firstly, that the air spring carrier can be made from fiber composite material under industrial conditions and requirements. Secondly, it gives insight into how the CFC part compares with the steel part used in series production today. The production technology envisaged for the CFC part was braiding followed by a resin transfer molding (RTM) process. The main process requirements set for this highly rigid and safety-relevant part were automated production for thick-walled components, good reproducibility and high process security.

1. Introduction

Commercial vehicles are investment goods and as a rule are used for transportation. The customer's purchasing decision is influenced among other things by the vehicle's carrying capacity and fuel consumption. In this connection the term 'payload' is typically used, and this describes the useful paid-for load. With trucks the payload describes the additional load of goods being carried while with buses the payload refers to the maximum number of passengers plus their baggage.

Statutory regulations currently limit the permissible gross vehicle weight of buses to 18 tonnes for two-axle vehicles and 25 tonnes for three-axle vehicles. The permissible axle load for an undriven front axle is 10 tonnes and for a driven rear axle 11.5 tonnes. The necessity emerges from this of maximizing the payload portion of the permissible gross vehicle weight in order to use the vehicle efficiently. The most obvious way of increasing the payload in buses while leaving comfort unaffected or even improving it is to reduce the dead weight of the vehicle.

As part of a preliminary study, the air spring carrier was identified as a component with great lightweighting potential. It is used in both two-axle and three-axle MAN buses. This study is concerned with applying lightweight design to reduce weight and to optimize components. One estimate forecast a weight-saving potential of at least 50%. By reducing the unsprung mass, an improvement in driving characteristics can also be expected as well as a reduction in wear. On this basis the use of carbon-fiber-reinforced plastic components in the structural area is to be validated at MAN via this component. Since bus and truck chassis are comparable it should be possible to apply the expected results generally to MAN commercial vehicles.

2. The air spring carrier for the rear axle of tour buses and intercity buses

The product portfolio of MAN and NEOPLAN includes two- and three-axle tour buses and intercity buses for various types of duty. Tour buses used for long-distance work are usually configured for about 50 passengers. Between 80,000 and 100,000 km are covered per year and this makes a correspondingly long-lasting and robust design necessary. One example is the MAN Lion´s Coach shown in Fig. 1.

Fig. 1: The MAN Lion's Coach tour bus in operation and the axle load distribution of a two-axle bus

In the tour bus a comparatively high proportion of its dead weight is down to the vehicle's often comfortable interior appointments. The engine and transmission are at the rear and the large overhang thereby resulting means that even in the standard configuration the weight is already significantly concentrated in the rear axle area. The running gear is connected to the chassis by the air spring carrier (Fig. 2). Each rear axle has two air spring carriers for mounting the bus body frame.

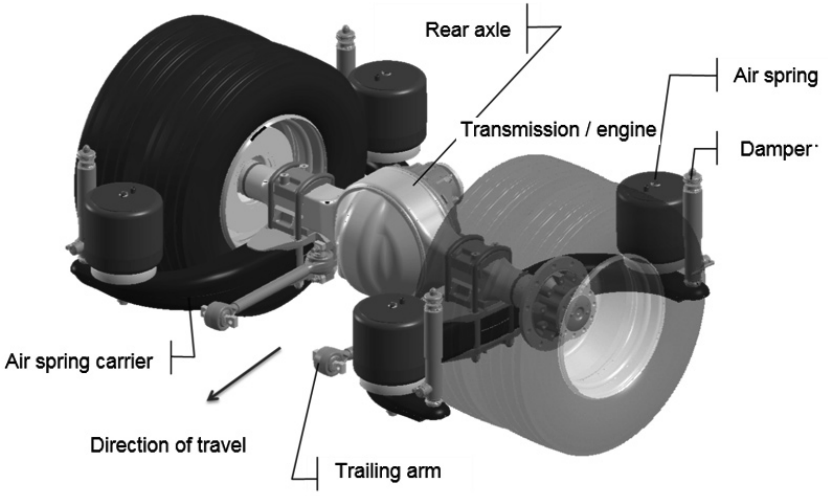

Fig. 2: Tour bus rear-axle area, steel air spring carriers with connection plates

The current series-production air spring carrier, consisting of the supporting structure weighing approx. 53 kg and the steel axle-connection plates, is approx. 1600 mm long and the two arms project by about 600 mm. The air springs and the dampers for the chassis mounting are attached to this supporting structure. The wheels are almost as it were embraced by its curved shape and this makes a wide mounting possible for the bus body frame. The rolling stability is thereby improved and greater travel comfort results.

The current welded steel construction of the supporting structure is to be changed to CFRP hollow profile, thereby enabling a considerable saving in weight. Loads are predominantly introduced vertically into the supporting structure at the connecting points of the air springs and dampers. These create torsional and flexural loads in the component. Firstly, stress behavior can be influenced via the cross-sectional shape and secondly, loads are to be absorbed via the material.

3. CFRP production technology

Basically two demands are made of the CFRP production process. On the one hand, it must be suitable for creating the geometry of the component in question since the supporting structure is designed as a curved, thick-walled hollow component. Fiber orientations of 0° and ±45° are required for the torsional and flexural stresses which occur. On the other hand it must be possible to produce the number of components required – approx. 5000 pcs/year – at an acceptable cost. Satisfactory productivity calls for a high material output coupled with little waste of the expensive carbon fiber. A high degree of automation also appears conducive to ensuring a certain reproducibility, process reliability, and quality. On the basis of the requirements profile the choice of CFRP production technology was for a braided RTM type of design.

3.1. The braiding process

A braiding / RTM process was selected for the hollow profile as an appropriate and near-series production process for fiber composite structures. Munich Composites GmbH of that city is a development partner in this project. This company is able to produce the CFRP hollow structure by means of an automated production process consisting of braiding and resin injection in the RTM process. The circumference of the radial braider is fitted with fiber spools (so-called 'bobbins') (Fig. 3). These bobbins run along the circumference on serpentine paths, passing each other in such a way that the guided rovings coming off the bobbins braid together. Some of the bobbins move clockwise, others anti-clockwise. A third group remains in fixed positions outside the moving bobbins. While the moving bobbins carry out the braiding operation, the fixed bobbins supply the filler yarns which are laid down in the component as 0° fibers. Since the rovings are processed directly, no semi-finished material needs to be made and a process step can be saved with respect to other fiber-processing methods. The dry fibers are guided inwardly to the braiding eye into which the core to be braided is introduced and moved by a robot.

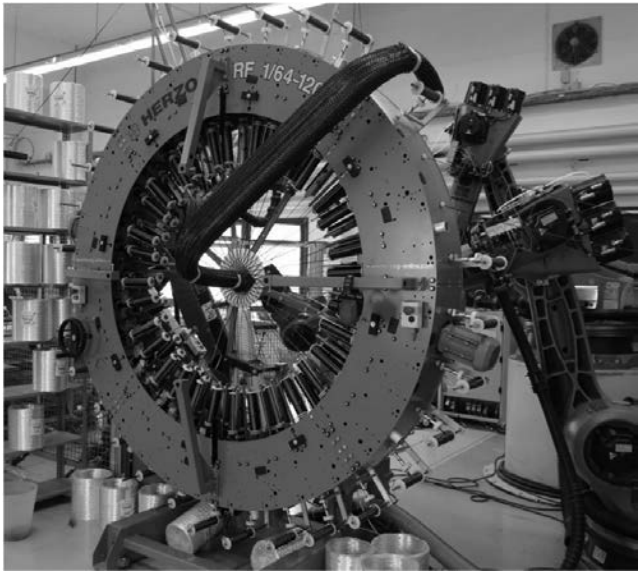

Fig. 3: Radial braider of Munich Composites with the carrier structure preform clamped in place
(source: Munich Composites GmbH)

One special feature of the selected braiding process is that a reusable braiding core developed by Munich Composites is used which is removed once the preform is completed. This core creates the internal component geometry for a component-oriented fiber placement. Each end of the braiding core is held by a robot and the robots guide the component continuously through the braiding eye until all fiber layers have been built up. The fibers are laid down directly via the feed movement of the braiding core. By means of the moving and fixed bobbins a braided dry preform with a triaxial braid is created – in other words, a fiber orientation of 0° and ±45°.

3.2. The RTM process

Resin transfer molding (RTM) is a process for the infiltration of fibrous semi-finished products (preforms). The RTM system used consists of an injection system and a two-part mold. The preform is placed in the mold half. The mold is then closed and vacuum applied. Next, the matrix material, in this case epoxy resin, is injected into the component, generally under

pressure. An even distribution of resin is important here if air entrapments are to be avoided and complete filling of the mold and wetting of the fibers is to be ensured. Injection of the matrix material is the longest process step, especially with thick-walled components. Once curing is completed, the fiber-plastic composite component can be removed.

3.3. Dimensioning and manufacture of the supporting structure

The air spring carrier is loaded with the weight of the entire rear section of the bus. For the purpose of dimensioning an equivalent force was applied at the mounting locations of the air springs. In addition, the CFRP supporting structure should not exceed the installation space of the steel component and should use the existing axle connection via the steel plates. Fig. 4 shows the design concept of the CFRP / steel hybrid air spring carrier with CFRP supporting structure.

The composite material consists of a high-tensile (HT) fiber and an epoxy resin. The triaxial braid absorbs the torsional and flexural loads in accordance with the fiber orientation. Reflecting the load distribution the supporting structure of the CFRP air spring carrier is subdivided on the basis of three wall thicknesses. Starting from the point of load application the wall thickness is about 12 mm, at the component ends it is about 9 mm. The fiber layers are built up layer by layer. Special turning points are envisaged in the component so as to allow continuous production of the braiding layers and wall thicknesses.

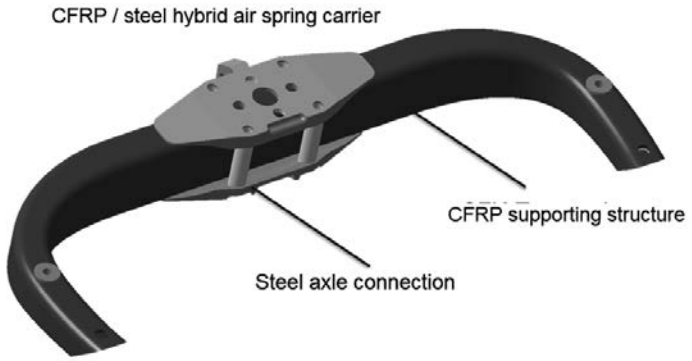

Fig. 4: Design concept of the CFRP / steel hybrid air spring carrier with CFRP supporting structure

The dry preform is taken out of the radial braider and the braiding core removed. In the subsequent series-production process a thin inflatable tubular film for resin injection is inserted into the preform. The preform is inserted into the RTM mold and pressure applied to the tubular film to create the shape of the hollow interior. The resin is then injected into the fiber structure thus formed. The component is left in the mold until it cures, after which it is taken out, any flash is removed manually, and the component is then immediately ready for further use. In contrast, when the feasibility study was carried out, resin injection for the specimen component used the vacuum injection method. In the next step the steel connector elements are glued to the CFRP supporting structure.

4. Findings of the feasibility study - a competitive solution?

The process steps were run through on the basis of a specimen build of the CFRP air spring carrier. The CFRP hollow profile is about 66% lighter than the steel version used in current series production and thus leads to a weight reduction of about 70 kg per bus. This is equivalent to a payload increase of one passenger.

Fig. 5: CFRP / steel hybrid air spring carrier

Creation of the prototype (Fig. 5) showed that the braiding process provides a way of producing this hollow structure. Primarily due to the high raw material price of the carbon fiber the CFRP is as expected considerably more expensive than the steel version. In the direct processing of rovings and the comparatively low wastage of approx. 5% this method contributes to the conservation of resources and to reducing costs.

The technical requirements of production described in Section 3 can be satisfied by the selected braiding / RTM design. The level of automation means that a constant high quality and process reliability can be guaranteed. Although total process times are relatively long, they are nevertheless satisfactory for the annual production quantities required in the tour bus segment. Even though the selected production process appears efficient at first it still has a significant effect on additional costs.

The higher production costs could be justified by the increase in payload. If we take 100,00- km as the average annual mileage of a long-haul bus operator, a simple model calculation shows that carrying one additional passenger can create substantial extra revenue. Furthermore, the weight reduction has a positive effect on fuel consumption and the associated CO_2 emissions.

5. Findings and outlook

The feasibility study can be followed by a systematic development of components which goes more deeply into the component design aspects. Here it is primarily the introduction of loading and the design of the connecting elements which require new approaches in order to enable forces to be introduced in a way appropriate to the load flow. Deficiencies in fiber placement were noted in component samples and these are primarily due to lack of fiber tension. This is attributable to the rectangular cross-section of the carrying structure and could be prevented by a cambered contour. In addition, use of the component in the bus needs to be validated. Strength tests and trials in the vehicle must show what effects environmental influences have and what impact the CFRP component has on driving characteristics.

6. Acknowledgements

We would like to thank the Munich Composites GmbH company, our development partner in this feasibility study, for their support and for releasing the illustrative material.

Potential for weight reduction in commercial vehicles

Air springs with pistons made of glass-fiber-reinforced plastic

Dipl.-Ing. **H. Gawinski**, Dipl.-Ing. **E. Neitzel**, Dipl.-Betriebswirt **D. Bauch**,
ContiTech Luftfedersysteme GmbH, Hannover

Abstract

High demands are made of modern commercial vehicles and buses with regard to transportation efficiency. One approach here is to increase payload while retaining the legally limited axle loads. The key is to substitute plastic for metal. For air springs this route has been pursued consistently for decades. Using the method of integrative computation described in this paper, even air springs for tractors, trucks and buses can be designed with a lightweight construction, with the internal volume of the piston being used to increase driving comfort. It is possible to obtain a more realistic indication of stress in the component by transferring the results of mold flow analysis into the theoretical strength analysis by means of FEM analysis. The result is a much reduced material consumption. Material costs and cycle times in production are minimized. The result is air suspension systems which, compared with the state of the art, deliver a weight saving of up to 15 kg in the case of a four-air-spring drive axle. The reduction in CO_2 emissions resulting from this can be as much as 200 kg over a driven distance of 400,000 km. The corrosion protection inherent in the material also makes a contribution to environmental protection.

1. Motivation

High demands are made of modern commercial vehicles and buses with regard to transportation efficiency (Figure 1). One of the key factors in achieving this objective is a rigorous reduction in the weight of the vehicle. On account of their favorable ratio of payload capacity and mass, air springs are already the optimum suspension element for the chassis in trucks, tractors, buses and trailers. Nevertheless even here the weight of components is to be reduced for future generations of vehicles but without impairing performance.

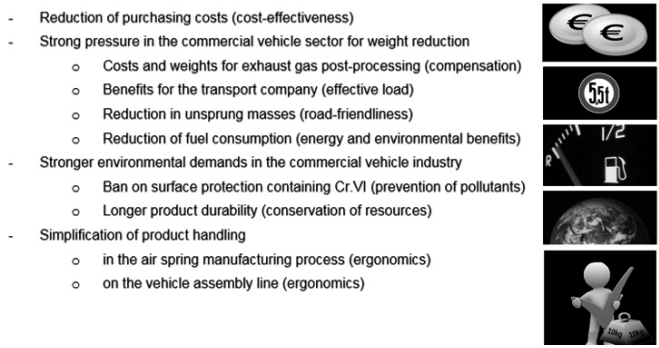

Fig. 1: Motivational factors for the use of plastics in commercial vehicles

2. Requirements for air springs for commercial vehicles

One starting point here is substituting plastic for metal. Here the multifarious requirements applied to air spring modules as regards function and durability must of course be satisfied to the same level (Figure 2).

Fig. 2: Requirements - parameters influencing product durability

A suitable material base for the highly stressed connecting components for frame and axle mounting are short-glass-fiber-reinforced thermoplastics such as polyamide with 30% to 50% glass fiber content.

3. Derivation of load cases

Air suspension systems with plastic connecting components have been in use for decades in driver's cab and seat applications. For about 15 years now, pistons made of glass-fiber-reinforced plastic have been state of the art in the trailer chassis (Figure 3). In these applications it is not necessary to use the volume enclosed by the piston in order to meet rigidity requirements.

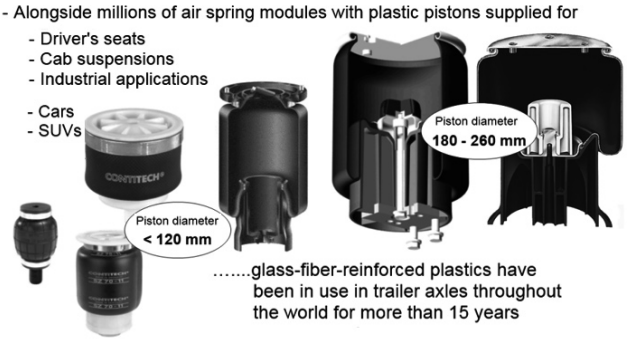

Fig. 3: Plastic: state of the art in various commercial vehicle applications

In tractors, trucks and buses, however, requirements for low spring stiffnesses can only be satisfied by using the internal volume of the piston. The interior of the piston is here at all times under a pressure equal to the internal pressure of the air springs. The stresses on the component resulting from the different operating situations must be taken into account in the structural design. The upward and downward movement of the bellows fold during static lifting and lowering, during loading and unloading, and also with dynamic strings over a wide loading range lead to very different radial and axial loads on the piston surface (Figure 4).
Compliance with the external geometric limits of the installation space and the demand for maximization of the piston's internal volume also compel a minimization of wall thicknesses for the piston, as too the demand for a minimization of material consumption in order to be able via short cycle times to boost cost-cutting potential for material and process costs.

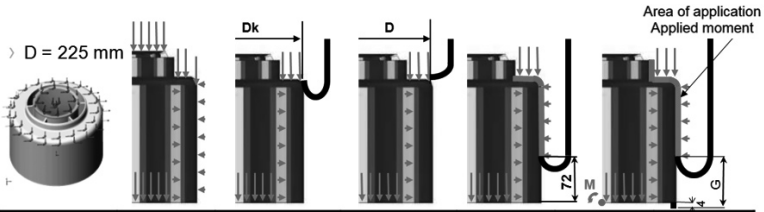

Load case	1	2a	2b	3	4a	4b
Load / running condition	Compressed dynamically at full load	Structure raised at full load	Structure raised at full load	Burst pressure at level location	Rolling on [6°]	Rolling off [-6°]
Temperature	80 °C	80 °C	80 °C	23°C	80 °C	80 °C
Bellows fold (G)		formed	raised	72	26	119
Moment M					165,5 Nm	178,5 Nm
Total force	80 kN	45 kN	45 kN	120 kN	71,2 kN	29,1 kN
Internal pressure	16,0 bar	9,0 bar	p = F/(¼D²π)	24,0 bar	14,3 bar	6 bar
Shoulder force	16,4 kN	9,2 kN	0 kN	24,6 kN	14,4 kN	5,3 kN

Fig. 4: Examples of load cases for an air spring piston without buffering force support

4. Simulation and strength calculation

As a rule pistons without exploitation of the piston volume are produced by injection molding in one piece from a single mold. Here there is greater design leeway for designing the reinforcement ribs and necessary demolding drafts. In many cases an isotropic FEM calculation suffices for providing the theoretical strength verifications. It must however take into account without fail the dependence of material strength on temperature. The product design is deemed to be optimized when the stresses calculated by the isotropic material approach lie below the permissible material stresses for the maximum service temperature of the material (Figure 5).

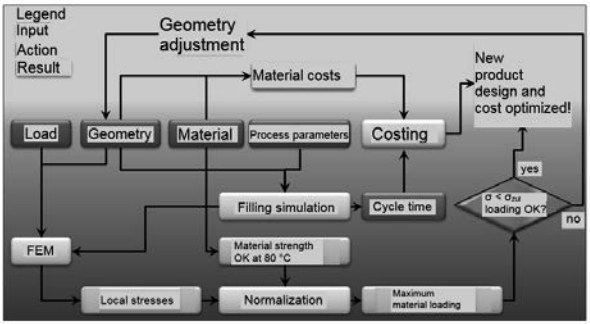

Fig. 5: Design scheme for isotropic calculation

When use is made of the piston volume, the pot-shaped base body is produced first. This carries not only the complex internal ribbing but in most cases the axle-side fastening elements as well. The cover section which has less ribbing and includes the connecting elements on the air-spring side is produced in a second mold. The two components are then joined together in a following step by, for example, rotational friction welding. The smaller wall thicknesses, the complex ribbing and the additional joining zone make it necessary to deploy more complicated calculation methods. The method of integrative computation has proven itself useful here ([1],[2]). In this method the mold-filling process is simulated firstly by a mold-flow analysis while including the mold geometry and injection-molding parameters used in the volume-production process. On the one hand the simulation does deliver important information about mold filling and the formation of the flow fronts which makes it possible to adjust the product and mold geometries to prevent weak points such as weld lines. What is more important however is information about the local fiber orientation which is then input into the component's geometrical model. In a second simulation step the FEM calculation is then carried out taking local fiber orientations into account. To assess whether the component is strong enough, the directed stresses locally present are compared with the performance data of the material for the corresponding degree of fiber orientation. By normalizing to the orientational permissible stress value a key indicator is obtained which provides information about any possible local damage in the component (Figure 6).

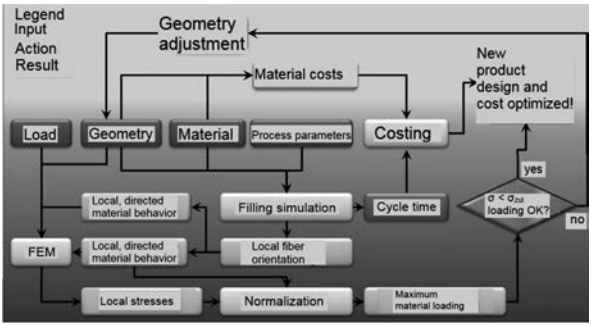

Fig. 6: Design scheme for integrative computation

Optimization is carried out by adjusting the geometry, process parameters and so on until the key indicators show a uniform distribution over the component with a sufficient distance from the damage threshold. With this method not only is an adequate level of strength obtained but also a minimal consumption of materials. Experience gained in high-volume production indicates that applying integrative computation means that up to almost two-thirds of the component weight can be saved when plastic is substituted for steel. Taking the example of a drive axle of a tractor with four air springs, this means a reduction in unsprung masses of up to 15 kg.

5. Weight savings, testing, verification

To underpin the theoretical strength analyses, the load cases are reconstructed in laboratory testing as part of product development (Figure 7).

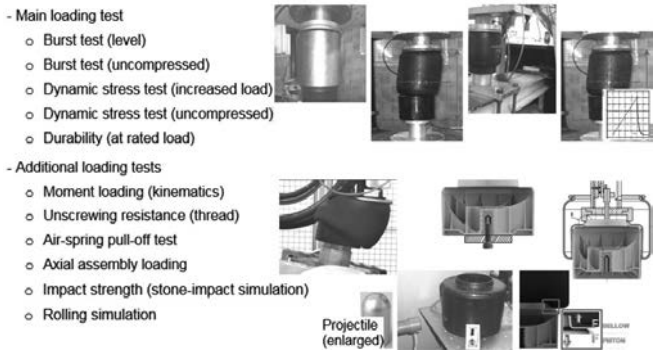

Fig. 7: Testing for verification of design results

What is important here is that the specimens used for testing are close to volume-production specimens – in other words, produced using the same tooling and process data as were used as the basis for the calculation. The reliability of the integrative design method is demonstrated here by the fact that during overload testing the instances of local damage occur at precisely those places in the component which were calculated previously while with the isotropic calculation method there can very well be divergences between the fracture stress and the damage location. The same is usually true of durability tests as well.

6. Summary

To sum up it may be said that by including the integrative computation method, savings in weight and cost even in the chassis area can be achieved by substituting plastic for metal in highly-loaded structural components such as air-spring pistons [3]. This presupposes, of course, a precise knowledge of the load cases from the wide variety of different service conditions in the field. With a 12 kg to 15 kg weight saving for a four-air-spring drive axle, up to 200 kg CO_2 emissions can be saved over a mileage of 400,000 km (Figure 8).

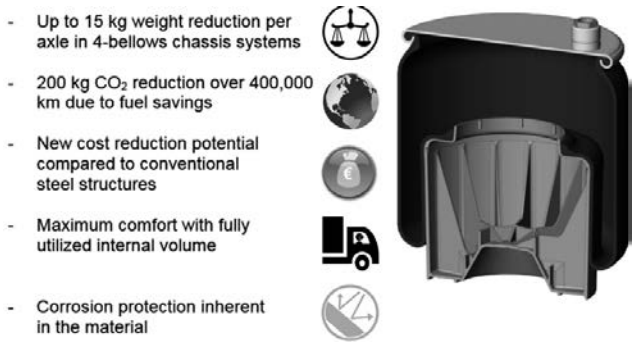

Fig. 8: Benefits of air springs with a plastic piston

These potentials can be exploited here without impairing comfort. At the same time the long service life of the product is ensured without affecting the quality of its visual appearance even under adverse weather conditions by using plastic with its inherent corrosion protection and making any additional surface protection superfluous, together with the environmental pollution associated with this.

[1] Glaser, S.; Wüst, A.; Aumer, B.: Metall ist die virtuelle Messlatte. Kunststoffe 7 (2008), 5 pp. 88-92

[2] Hopmann, C.; Arping, T.; Baranowski, T.: Bauteileigenschaften präzise vorhersagen. Kunststoffe 7 (2011), 5 pp. 44-49

[3] Bauch, D.; Ripamonti, J.; Wolandewich: Damit Trucker und Umwelt sich wohlfühlen. Automotive Special OEM Supplier, 2012, 3 pp. 64-65

Dimensioning and production of leaf springs made of fiber-reinforced plastics for use in heavy-duty commercial vehicles

Special features and challenges

Dipl.-Ing. **H. Kempe**, IFC Composite GmbH, Haldensleben

Abstract

In this contribution the specifics and challenges in dimensioning and producing of highly stressed structures made of fiber-reinforced plastics for heavy duty vehicles are described.

1. Dimensioning and calculation of the fiber-composite springs

The first part will describe the basics of designing the fiber-composite leaf springs while taking kinematic, mechanical, and manufacturing requirements into account. Here the special aspect of the geometry-defining FEM will be outlined, which is then transferred into the constructive implementation. Finally there is a brief examination of tool construction and its special aspects with regard to the production process which follows.

2. Production of the structural components

Taking a front-axle longitudinal leaf spring as an example, a description is given of the production of thick-walled structural components by prepreg hot press molding. Special features of prepreg production are examined, as also the procedure for laying up the prepreg elements.

Finally a description is given of the entire process and also an overview of factors influencing production of the component.

New possibilities for the rapid customizing of mold surface structures

Lasered paint in the mold

Dipl.-Ing. **M. Gehlen**,
Kunststoff-Institut für die mittelständische Wirtschaft NRW GmbH,
Lüdenscheid

Abstract

There are already a number of different ways available today for individualizing mold surfaces such as, for example, erosion, echting or even direct lasering of the cavities. To these we may add a new method in which a surface layer is applied to the mold surface and then cured locally by laser. The processed areas remain in the mold while the remainder of the paint is washed out with water. The principle advantages of this process are in the processing time and also in the fact that the geometry is essentially retained.

Main areas of investigation

Initial investigations at the Kunststoff-Institut Lüdenscheid have shown that the structure is durable and shows no signs of wear even after several shifts of injection molding. In addition, other constraints and issues are of interest and have been investigated. What line widths are minimally feasible, what coating thicknesses are possible or reasonable, what are the surface characteristics on the flat? But questions are also considered such as the effort involved in restoring the original state or removing the cured paint.

Application

Locally lasered paint offers a good alternative to other common structuring possibilities. The process is cost-effective, quickly implementable, and reproducible. With the appropriate data preparation, even 3D components are possible.

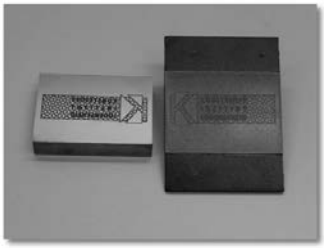

Fig. 1: Structured mold insert

Emission-optimized rubber composites for the treads of retreaded truck tires containing recycled material: EKORUND

Prof. Dr. **M. Beiner**, Fraunhofer IMWS, Halle (Saale)

Improving the energy and resource efficiency of commercial vehicle tires is of great importance to cost-efficiency and ecological compatibility in freight transportation by road. For truck tires, the new EU tire label was therefore introduced with effect from November 1st, 2012. The aim is to encourage cost-effectiveness, environmental compatibility and road safety by means of fuel-efficient, safe and quiet tires. The parameters to be optimized here are rolling resistance, wet grip and external rolling noise. The EU tire label only applies to new truck tires, retreaded truck tires are specifically excluded.

This presentation presents the results of the EKORUND joint project which came under the BMBF program 'KMU innovative'. The aim of the project was to improve the energy and resource efficiency of the retreaded tires of commercial vehicles. In general these already pay due regard to the concept of resource efficiency. Retreading means overhauling old tires and giving them fresh treads. Furthermore, the resource efficiency thus obtained can be given a considerable additional boost by incorporating powdered rubber from tire recyclate into the rubber mixes of new treads.

The specific objective of the EKORUND project was to combine energy and resource efficiency – that is, to research and develop emission-optimized rubber mixes for tire treads with a proportion of fine recyclate of at least 20 m%. Here powdered rubber from well-defined recycled materials was mixed in and used selectively to optimize rolling resistance without significantly impairing the wet grip or service life of the retreaded tires. The state of development achieved is discussed on the basis of indicators from laboratory tests, the results of bench tests on retreaded tires for commercial vehicles, and data from extensive driving tests both on- and off-road. As part of the project, composites containing recyclate were optimized for the treads of different kinds of retreaded truck tires (tractor unit, semi-trailer) and earthmover (ET) tires. It is shown that using them can mean a significant improvement in environmental compatibility, cost-effectiveness and resource efficiency in this important segment of road traffic.

Funded by the Federal Ministry of Education and Research BMBF (KMU innovative 033RK008 A-G).

ISBN 978-3-18-234343-1